CHAPTER ONE
INTRODUCTION

1.1 General Review on Oils and Fats

1.1.1 Fatty Acid

Chemically, a fatty acid is a monocarboxylic acid with long and straight aliphatic tail, which is either saturated or unsaturated. Most natural occurring fatty acids are biosynthesised in two-carbon units and double bonds (in *cis*-configuration) are inserted at the specific positions throughout the chain. Over 1000 fatty acids are known with diverse chain lengths, positions, configurations and degree of unsaturation (Scrimgeour and Harwood, 2007). Nevertheless, only around twenty fatty acids are occurring widely in nature. The examples of common fatty acids and their respective systematic name, trivial name, shorthand name, structure and n-x notation are depicted in Table 1.1.

The systematic nomenclatures are given according to International Union of Pure and Applied Chemistry (IUPAC), which numbers the chain starting from the carbonyl carbon. The ending of -anoic is corresponding to saturated fatty acids, whilst -enoic, -adienoic, -atrienoic, -atetraenoic, -apentaenoic and -ahexaenoic are indicating the presence of one to six double bonds in the fatty acid chain, respectively. In addition, the configurations of double bonds are presented in *Z* or *E*, which is assigned according to the priority rules for the substituents. Yet, *cis*- and *trans*- are also commonly accepted.

Table 1.1 : Systematic, trivial, shorthanded nomenclatures and structure of natural occurring fatty acids

Systematic Name	Trivial Name	Shorthand Name	Structure	*n*-x notation
SFA				
Octanoic	Caprylic	8 : 0	$CH_3(CH_2)_6COOH$	NA
Decanoic	Capric	10 : 0	$CH_3(CH_2)_8COOH$	NA
Dodecanoic	Lauric	12 : 0	$CH_3(CH_2)_{10}COOH$	NA
Tetradecanoic	Myristic	14 : 0	$CH_3(CH_2)_{12}COOH$	NA
Hexadecanoic	Palmitic	16 : 0	$CH_3(CH_2)_{14}COOH$	NA
Octadecanoic	Stearic	18 : 0	$CH_3(CH_2)_{16}COOH$	NA
Eicosanoic	Arachidic	20 : 0	$CH_3(CH_2)_{18}COOH$	NA
Docosanoic	Behenic	22 : 0	$CH_3(CH_2)_{20}COOH$	NA
Tetracosanoic	Lignoceric	24 : 0	$CH_3(CH_2)_{22}COOH$	NA
MUFA				
Z-9-tetradecenoic	Myristoleic	14 : 1 9*c*	$CH_3(CH_2)_3CH=CH(CH_2)_7COOH$	5
Z-9-hexadecenoic	Palmitoleic	16 : 1 9*c*	$CH_3(CH_2)_5CH=CH(CH_2)_7COOH$	7
Z-9-octadecenoic	Oleic	18 : 1 9*c*	$CH_3(CH_2)_7CH=CH(CH_2)_7COOH$	9
E-9-octadecenoic	Elaidic	18 : 1 9*t*	$CH_3(CH_2)_7CH=CH(CH_2)_7COOH$	9
Z-11-octadecenoic	*cis*-vaccenic	18 : 1 11*c*	$CH_3(CH_2)_5CH=CH(CH_2)_9COOH$	7
E-11-octadecenoic	Vaccenic	18 : 1 11*t*	$CH_3(CH_2)_5CH=CH(CH_2)_9COOH$	7
Z-13-docosenoic	Erucic	22 : 1 13*c*	$CH_3(CH_2)_7CH=CH(CH_2)_{11}COOH$	9
Z-15-tetracosenoic	Nervonic	24 : 1 15*c*	$CH_3(CH_2)_7CH=CH(CH_2)_{13}COOH$	9
PUFA				
Z,*Z*-9,12-octadecadienoic	Linoleic	18 : 2 9*c*, 12*c*	$CH_3(CH_2)_3(CH_2CH=CH)_2\ (CH_2)_7COOH$	6
Z,*Z*,*Z*-9,12,15-octadecatrienoic	α-linolenic	18 : 3 9*c*, 12*c*, 15*c*	$CH_3(CH_2CH=CH)_3(CH_2)_7COOH$	3
Z,*Z*,*Z*-6,9,12-octadecatrienoic	γ-linolenic	18 : 3 6*c*, 9*c*, 12*c*	$CH_3(CH_2)_3(CH_2CH=CH)_3(CH_2)_4COOH$	6
Z,*Z*,*Z*,*Z*-5,8,11,14-eicosatetraenoic	Arachidonic	20 : 4 5*c*, 8*c*, 11*c*, 14*c*	$CH_3(CH_2)_3(CH_2CH=CH)_4(CH_2)_3COOH$	6
Z,*Z*,*Z*,*Z*,*Z*-5,8,11,14,17-eicosapentaenoic	Eicosapentaenoic (EPA)	20 : 5 5*c*, 8*c*, 11*c*, 14*c*, 17*c*	$CH_3(CH_2CH=CH)_5(CH_2)_3COOH$	3
Z,*Z*,*Z*,*Z*,*Z*,*Z*-4,7,10,13,16,19-docosahexaenoic	Docosahexanenoic (DHA)	22 : 6, 4*c*, 7*c*, 10*c*, 13*c*, 16*c*, 19*c*	$CH_3(CH_2CH=CH)_6(CH_2)_2COOH$	3

Notes:
SFA, saturated fatty acid; MUFA, monounsaturated fatty acid; PUFA, polyunsaturated fatty acid; NA, not applicable.

Due to lengthy and sophisticated systematic nomenclature, the shorthand and trivial names of fatty acids are in used more generally. The shorthand names are proposed by Farquhar *et al.* (1959). These are given by two numbers separated by a single colon, which are indicating the carbon chain length and number of double bonds in fatty acid acyl chain, respectively. For instance, C18:1 denotes eighteen carbon atoms in the carbon chain length with the presence of one double bond.

The configuration and positions of double bonds are addressed in a number of ways. As mentioned previously, the configuration can be indicated as *cis*-, *trans*-configurations or *Z*, *E*-configurations, whereas for the positions of double bond, it can be stated either starting from the carbonyl carbon, or from the methyl end of the fatty acid chain. The former normally will associate with the *cis*- and *trans*-nomenclature, for instance oleic acid (C18:1 9*c*). However, due to the metabolic relationship between different unsaturated fatty acid families, sometimes it is more useful to number the double bonds in relation to the terminal methyl carbon atom. As an example, eicosapentaenoic acid (EPA), docosahexaenoic acid (DHA) and α-linolenic acid are ω3 polyunsaturated fatty acids as the nearest carbon containing double bond is the third carbon from the methyl end. This type of nomenclature is denoted as *n*-x notation, as illustrated in Table 1.1.

Fatty acids are generally classified into saturated fatty acid (SFA), monounsaturated fatty acid (MUFA) and polyunsaturated fatty acid (PUFA). Among all natural occurring SFA, palmitic acid (C16:0) is the most abundant SFA in animals, plants as well as microorganisms. Although stearic acid is also ubiquitous, its content usually at a lower level compared with palmitic acid (Scrimgeour and Harwood, 2007). In addition, medium chain SFA, namely, caprylic (C8:0), capric (C10:0) and lauric (C12:0), are widespread in coconut and palm kernel oils.

In the context of MUFA, *cis*-monoenes with an even number of carbons are common constituents of oils and fats, whereas the *trans*-counterparts are rare components. The *cis*-configuration is naturally inserted by desaturase enzyme into preformed SFA. The most common MUFA is oleic acid (C18:1 9*c*), while palmitoleic acid (C16:1 9*c*), *cis*-vaccenic (C18:1, 11*c*) and erucic acid (C22:1, 13*c*) generally present as minor components in vegetable oils. In the aspect of their applications, some MUFA are used

as oleochemicals in industry (Scrimgeour and Harwood, 2007). For instance, erucic acid is used as an antislip agent for polythene film after its convertion to amide. Besides, ω-olefins, such as 10-undecenoic acid obtained from pyrolysis of castor oil, are useful oleochemical intermediates (Scrimgeour and Harwood, 2007).

Similar to MUFA, majority of double bonds in PUFA are in *cis*-configuration. Some exmples of PUFA are linoleic acid, α-linolenic, γ-linolenic, EPA and DHA. Linoleic acid is found predominantly in vegetable oils while EPA and DHA are occurred prevalently in marine lipids. Due to the fact that n-6 and n-3 fatty acids cannot be synthesised by humans and therefore they are categorised as essential fatty acids. The n-3 fatty acids, for instance EPA and DHA, are essensial in human growth and development, as well as efficient in decreasing low density lipoprotein (LDL-C) and increasing high density lipoprotein (HDL-C) (Osborn and Akoh, 2002). On top of that, conjugated linoleic acid (CLA) is well-known for its potent applications in inhibiting the growth of cancer cell as well as alleviating the extent of fat deposition (Osborn and Akoh, 2002).

1.1.2 Triacylglycerol

Acylglycerols are esters of glycerol or propane-1,2,3-triol and fatty acids. Partial acylglycerols, namely, monoacylglycerols or diacylglycerols, are essential intermediates in metabolism (Scrimgeour and Harwood, 2007). Nevertheless, triacylglycerols are the main constituents of most naturally occurring oils and fats.

By definition, triacylglycerol contains three acyl chains originated from the fatty acids which are attached to the glycerol moiety. In order to designate the stereochemistry of triacylglycerols, the carbon atoms of glycerol are numbered stereospecifically. In a

Fischer projection, as the glycerol molecule is drawn with the secondary acyl group to the left of the central carbon atom, the carbons are numbered as 1, 2, and 3 from the top to bottom (Figure 1.1). The prefix "*sn*" is being employed which denotes the stereospecific numbering. Therefore, the position distribution of fatty acids in glycerol moiety can be described as *sn*-1, *sn*-2 and *sn*-3 positions. Any triacylglycerol structure will be chiral when the substituents at the *sn*-1 and *sn*-3 positions are different.

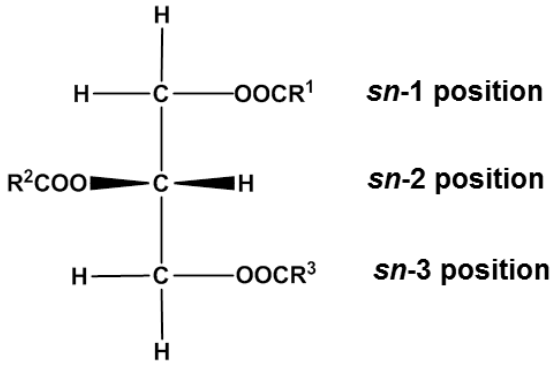

Notes:
R^1, R^2, R^3 are corresponding to alkyl groups attached to the carbonyl carbons at *sn*-1, *sn*-2 and *sn*-3 positions, respectively.

Figure 1.1 : Fischer projection of a triacyl-*sn*-glycerol

1.1.3 Fatty Acid Profile of Triacylglycerols

In most cases, the fatty acid profiles of natural occurring triacylglycerols in oils and fats are defined and exclusive to each plant or animal species. The fatty acids are not in random distribution among the *sn*-1, *sn*-2 and *sn*-3 positions. In general, vegetable oils contain relatively lower content of saturated fatty acids (SFA) compared with animal fats.

As a thumb of rule, fatty acid profile of triacylglycerols can be defined by the means of total fatty acid composition (FAC), triacylglycerol molecular species and fatty acid positional distribution in glycerol moiety. Table 1.2 shows the total FAC of World's

four major edible oils, namely, crude palm oil, soybean oil, sunflower oil and rapeseed oil (canola), determined by the method as described by Christie (1989).

Table 1.2 : Total fatty acid composition (FAC) of World's major edible oils

Fatty acid composition (as % methyl esters)	Crude Palm Oil	Soybean Oil	Sunflower Oil	Rapeseed Oil (Canola)
12 : 0	0.2	ND	ND	ND
14 : 0	1.2	0.1	0.1	0.1
16 : 0	48.5	10.4	6.4	4.2
18 : 0	4.1	4.1	3.6	2.1
20 : 0	0.3	0.4	0.3	0.6
22 : 0	0.1	0.5	0.7	0.3
24 : 0	0.1	0.2	0.2	0.1
Total SFA	54.5	15.7	11.3	7.4
16 : 1*n*-7	0.1	0.1	0.1	0.2
18 : 1*n*-9	35.6	26.1	26.3	63.4
20 : 1*n*-9	0.1	0.3	0.2	1.2
Total MUFA	35.8	26.5	26.6	64.8
18 : 2*n*-6	9.4	52.8	62.0	19.9
18 : 3*n*-3	0.3	5.0	0.1	7.9
Total PUFA	9.7	57.8	62.1	27.8

Notes:
SFA, saturated fatty acids; MUFA, monounsaturated fatty acids; PUFA, polyunsaturated fatty acids; ND, not detected.

Crude palm oil contains significantly higher amount of total SFA content (54.5%) as compared to soybean oil (15.7%), sunflower oil (11.3%) and canola (7.4%). Palmitic acid (C16:0) seems to be the predominant SFA in all of the oils, whilst most abundant monounsaturated fatty acids (MUFA) is oleic acid (C18:1). The most abundant fatty acid in both sunflower oil and soybean is linoleic acid (C18:2), in which their compositions are 62.0% and 52.8% of total fatty acids, respectively. On the contrary, prominent amount of oleic acid (C18:1) is found in rapeseed oil (canola) (63.4%).

Another crucial fatty acid profile for edible oils and fats is the molecular species of triacylglycerol. It describes the relative composition of the molecular species in the oils,

which will result in diverse chemical and physical properties of oils and fats, as well as their nutritional attributes and applications. For instance, several solid fats (palm mid fraction, mango fat, sal fat, shea butter) which are containing major triacylglycerol molecular species of 1,3-dipalmitoyl-2-oleoylglycerol (POP), 1-palmitoyl-2-oleoyl-3-stearoylglycerol (POSt) and 1, 3-distearoyl-2-oleoylglycerol (StOSt), could be potential cocoa butter equivalent (Gunstone and Harwood, 2007). These types of the molecular species are shown in Figure 1.2.

On the other hand, as mentioned in Section 1.1.2, fatty acids are attached to three different *sn*-positions of glycerol backbone to form a triacylglycerol. Therefore, the positional FAC of oils and fats is attainable by using stereospecific analysis and regiospecific analysis.

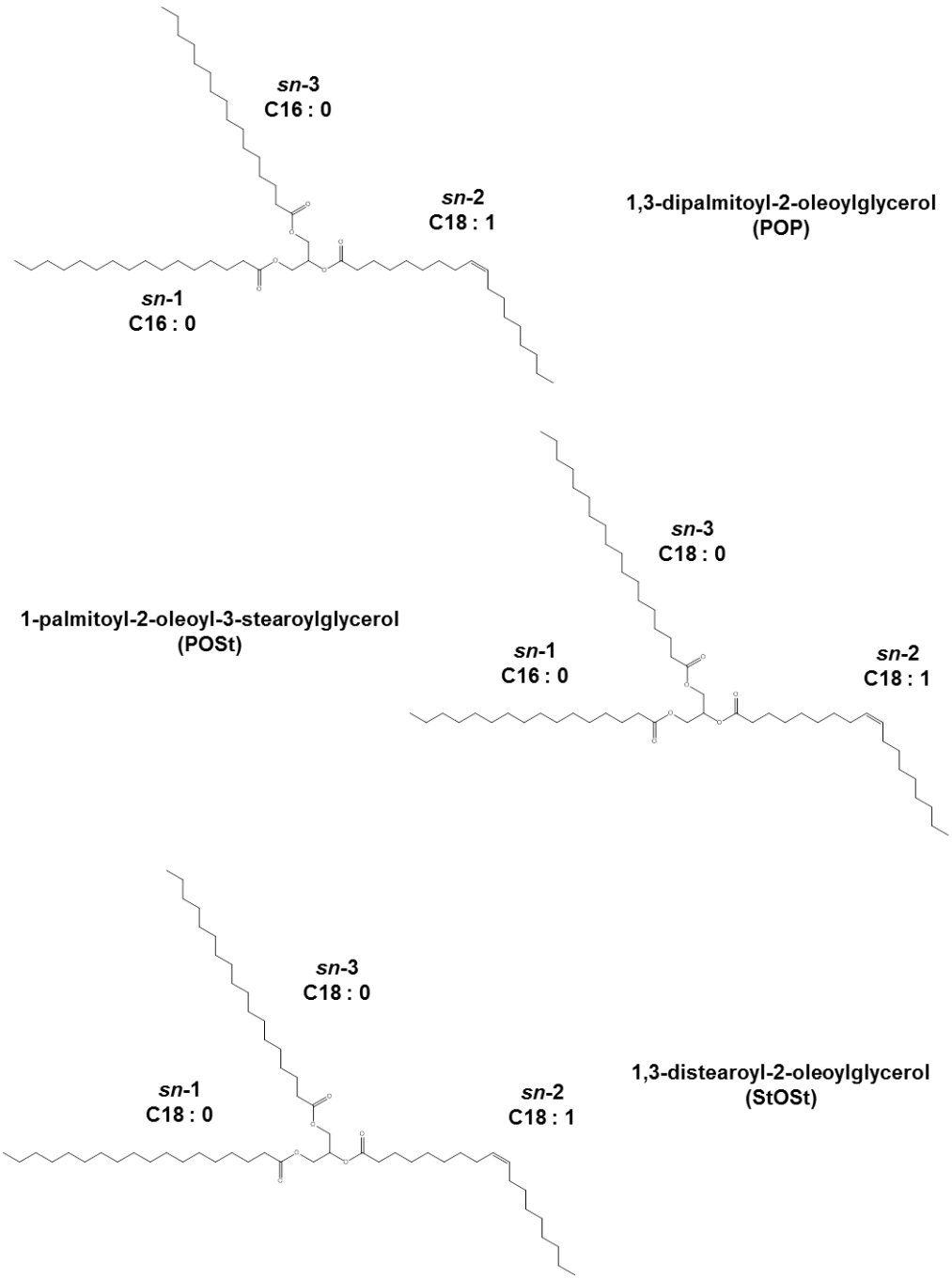

Figure 1.2 : Examples of major triacylglycerol molecular species in cocoa butter equivalent

1.2 Analysis of Positional Distribution of Fatty Acids in Triacylglycerols

When a glycerol molecule is esterified with a mixture of n different fatty acids, the number of possible triacylglycerols that can be formed will be n^3. This complexity,

together with the very similar chemical and physical properties of the various molecules, makes the complete analysis of natural triacylglycerols extremely challenging.

1.2.1 Historical Development of Stereospecific and Regiospecific Analysis Method

A significant effort has been invested in the past decades to develop a quantitative method for determining fatty acid compositions (FAC) at different stereospecific numbering of the glycerol moiety of triacylglycerols in naturally occurring oils and fats. The pioneer work of identification of positional FAC at *sn*-1, *sn*-2, and *sn*-3 positions was developed by Brockerhoff (1965). In the first method, which was referred as the 1,3-diacylglycerols method, deacylation of triacylglycerols was carried out using Grignard reagent, namely, ethyl magnesium bromide. The 1,2(2, 3)-diacylglycerols produced were isolated from the 1,3-diacylglycerols by preparative thin layer chromatography. Next, 1,3-diacylglycerols were further converted to 1,3-diacyl-2-phosphatidylphenol by using phenyl dichlorophosphate. Subsequent treatment with phospholipase A_2 would specifically hydrolyse the *sn*-1 acyl group from a *sn*-2-phosphatide, leaving a lysophosphatide containing the *sn*-3 acyl chain.

In the second method, denoted as the 1,2(2, 3)-diacylglycerols method, triacylglycerols were incubated with pancreatic lipase to give representative 2-monoacylglycerols and 1,2(2, 3)-diacylglycerols. Those 1,2-(2, 3)-diacylglycerols were reacted with phenyl dichlorophosphate to produce a mixture of 1,2-diacyl-3-phosphatidylphenol and 2, 3-diacyl-1-phosphatudylphenol. Subsequent treatment with phospholipase A_2 liberated fatty acids from the *sn*-2 position of the *sn*-3-phosphatide, but left the *sn*-1-phosphatide

unhydrolysed. Separation and fatty acid analysis of the various reaction products permitted the determination of FAC at three stereospecific positions.

On the other hand, Lands *et al.* (1966) used a different approach, which was based on the stereospecificity of diacylglycerol kinase. The initial step was the preparation of 1,2(2, 3)-diacylglycerols by pancreatic lipase and then incubation with diacylglycerol kinase originated from *Escherichia coli*. This will convert the 1,2-diacylglycerols to 1,2-diacyl-3-phosphatide whilst the 2,3-diacylglycerols remained unphosphorylated. After separation using thin layer chromatography, 2-monoacylglycerol and 1,2-diacyl-3-phosphatide were converted into methyl esters and subjected to gas chromatography (GC) analysis.

Both Brockerhoff's and Lands' methods require a few days to perform. Consequently, Dutta *et al.* (1978) presented an on-plate lipase hydrolysis method, in which the enzymatic reaction, extraction of the reaction products and their resolution were performed on the same thin layer chromatography plate without solubiliser or calcium chloride. This method considerably shortened the required time and minimised the loss of products due to transfer. In the following years, Dutta *et al.* (1979) presented a method on the phospholipase A_2 hydrolysis of phosphatidycholine and the separation of the products on a single plate. With this modification, a procedure, which requires a smaller sample size and less time (about 8 hours) to perform, had been developed to analyse stereospecifically the acylglycerol structure of a number of strains of soybeans, oats and palm oil.

Takagi and Ando (1990) proposed a stereospecific analysis of triacylglycerols by chiral phase high performance liquid chromatography (HPLC). The 1-monoacylglycerols and

3-monoacylglycerols which were prepared by Grignard hydrolysis were converted into the 3,5-dinitrophenyl urethane (DNPU) derivatives for subsequent resolution using chiral columns containing a stationary phase with chiral moieties bonded chemically to a base of silica gel. The 3,5-dinitrophenyl moieties of the urethanes contributed to charge transfer interactions with functional groups having *pi* electrons on the stationary phase and thus aided the resolution. The distributions of fatty acids in each of the positions *sn*-1, 2 and 3 could be calculated from the data. By lowering the column temperature and slowing down the flow rate, the method could even be applied to triacylglycerols containing long chain polyunsaturated fatty acids (PUFA), such as eicosapentaenoic (EPA) and docosahexaenoic acids (DHA) in fish oils.

The applications of the methodology of chiral chromatography in the stereospecific analysis of triacylglycerols have recently been reviewed by Kuksis and Itabashi (2005). Generally, the first step of this methodology is similar to that in other methods, that is, the partial hydrolysis of triacylglycerols giving among a mixture of 1,2-diacylglycerols, 2,3-diacylglycerols and 1,3-diacylglycerols. Subsequently, the second step involves in reacting the product with a chiral derivatising agent, (*S*)-(+)-1-(1-naphthyl) ethyl isocyanate, then the purification of resulting diacylglycerol urethane derivatives by chromatography on the solid-phase extraction columns containing an octadecylsilyl phase.

The third and key step which involves resolution of the diacylglycerol urethanes by HPLC on a silica column was proposed by Christie *et al.* (1991). A simple isocratic mobile phase is employed, and the derivatives absorb strongly in the ultraviolet spectrum hence the detection is straightforward. The 1,3-diacylglycerol urethanes elute earlier and is easily recovered. Since the derivatising agent is chiral with single

enantiomer, therefore the 1,2- and 2,3-diacylglycerol urethanes are diastereomers. In normal phase HPLC, the 1,2-diacylglycerol derivatives elute ahead of the 2,3-diastereomers and the two distinct fractions can be collected (Agren and Kuksis, 2002). In a recent study, Petrosino *et al.* (2007) propose a variation of the method in which monoacylglycerol rather than diacylglycerol urethane derivatives were employed.

Due to the nutritional implications of fatty acids at the *sn*-1,3 positions as a whole, as well as the *sn*-2 position, the regiospecific analysis of triacylglycerols is becoming more crucial as compared with the discrete determination of positional FAC at the *sn*-1, *sn*-2, and *sn*-3 positions. In general regiospecific analysis, triacylglycerols were hydrolysed by 1,3-specific lipase to produce a mixture of representative partial acylglycerol intermediates. The partial acylglycerols of interest were then isolated using thin layer chromatography, and subsequently converted to methyl esters prior to FAC analysis by the GC.

In earlier times, pancreatic lipase was employed extensively in the hydrolysis of triacylglycerols during the first step of sample preparation (Mattson and Volpenhein, 1961; Luddy *et al.*, 1964; Brockerhoff, 1965). However, in later years, other 1,3-specific lipases were also being used, for instance, lipase from the strain of *Rhizopus arrhizus* (Arcos *et al.*, 2000), *Rhizopus delemar* (Kosugi *et al.*, 2002), *Mucor miehei* (Foglia *et al.*, 1995; Dourtoglou *et al.*, 2001) and *Rhizopus oryzae* (Foglia *et al.*, 1995). Most highly 1,3-specific lipase were reported as those from genus *Rhizopus*, whilst those lipases originated from *Mucor miehei* and *Pseudomonas fluorescens* were being regarded as regioselective instead of regiospecific (Berger and Schneider, 1991). Triacylglycerol hydrolysis by lipase from *Rhizopus delemar* is illustrated in Figure 1.3.

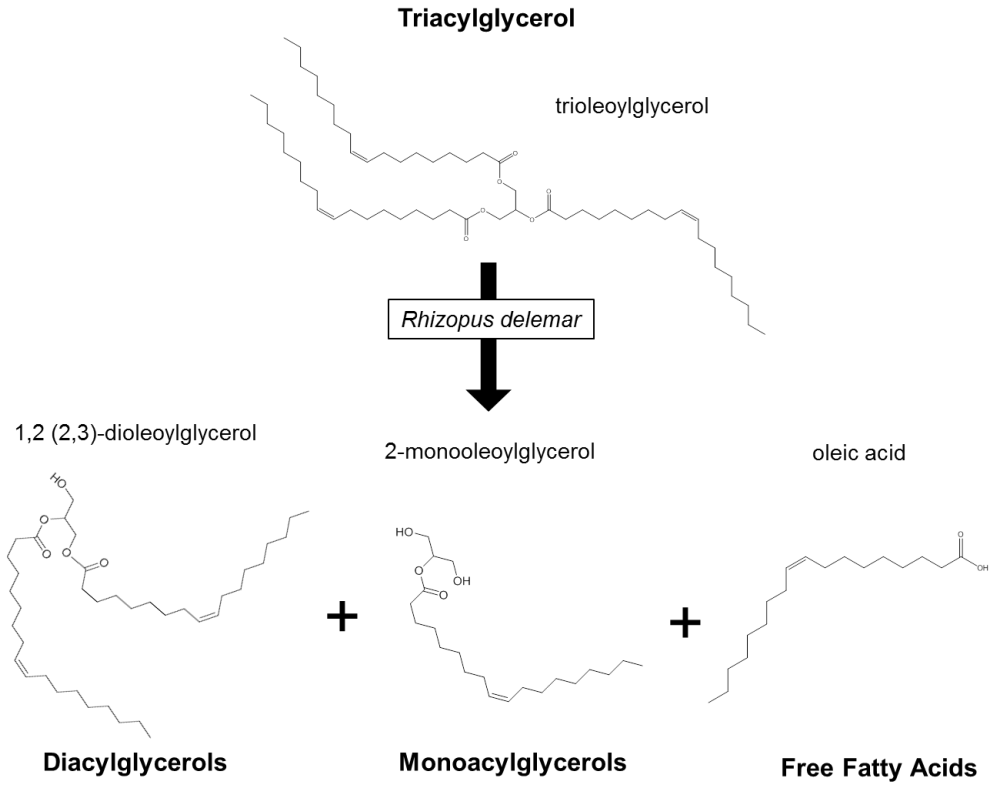

Figure 1.3 : *sn*-1,3 specific lipase from *Rhizopus delemar* hydrolysis of trioleoylglycerol to yield intermediate partial oleoylglycerols

Apart from the utilisation of 1,3-specific lipase, Grignard reagent, specifically ethyl magnesium bromide, also appeared to be a promising hydrolysis agent in regiospecific analysis (Angers and Arul, 1999). By the mean of random chemical degradation which was non-specific towards the positional acyl chain, a wide range of partial acylglycerols, namely, monoacylglycerols (1-monoacylglycerols and 2-monoacylglycerols) and diacylglycerols (1,2-diacylglycerols or 2,3-diacylglycerols and 1, 3-diacylglycerols) could be produced. This is illustrated in Figure 1.4 using trioleoylglycerol (OOO) as an example.

A relatively more reactive Grignard reagent, namely, allyl magnesium bromide, had been introduced by Becker *et al.* (1993). In contrast to ethyl magnesium bromide, allyl magnesium bromide was observed to be efficient in alleviating the problem of acyl

migration from *sn*-2 to *sn*-1,3 positions. This remained as an effort to yield a more representative acylglycerols towards more accurate and precise regiospecific analysis.

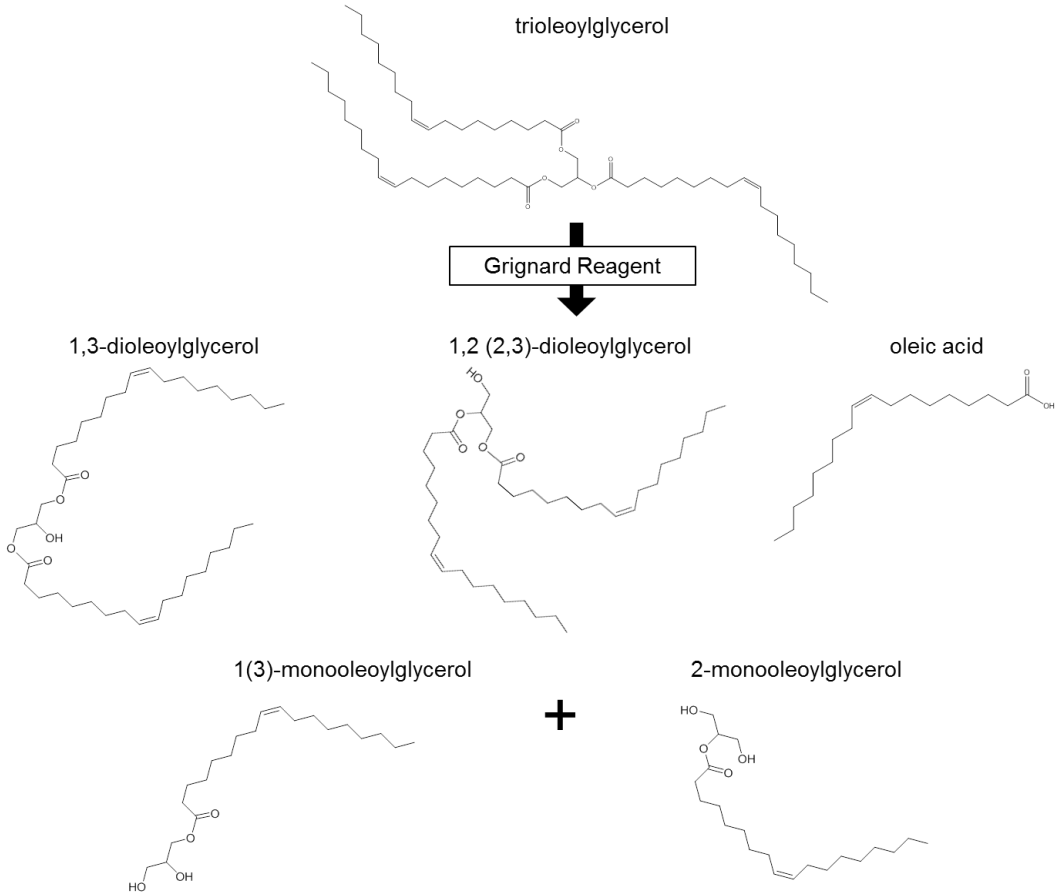

Figure 1.4 : Non-specific Grignard hydrolysis of trioleoylglycerol to yield wide range of partial oleoylglycerols

1.2.2 Shortcomings in Conventional Regiospecific Analysis

In hydrolysis using 1,3-specific enzyme, the lipase assay was reported as not reliable for triacylglycerols which contained substantial amounts of very long chain polyunsaturated fatty acids (PUFA) (Gunstone, 1967). This was caused by the resistance of some PUFA upon hydrolysis by certain lipases (Bottino *et al.*, 1967). On the other hand, although it was observed that the utilisation of ethyl magnesium bromide could be used to obtain more representative mixtures of diacylglycerols (Brockerhoff, 1967; Arcos *et al.*, 2000),

but the high degree of acyl migration during the course of analysis was the major drawback of this approach. The monoacylglycerols are easily isomerised (Figure 1.5) and it is problematic for accurate regiospecific analysis of triacylglycerols.

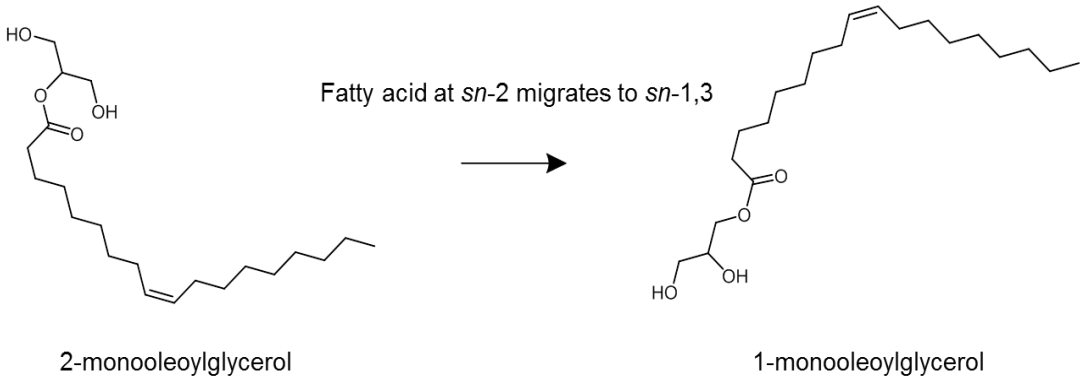

Figure 1.5 : Problem of acyl migration in intermediate monoacylglycerol during sample preparation

Even though the introduction of more reactive allyl magnesium bromide had yielded relatively smaller errors compared with ethyl magnesium bromide (Becker *et al.*, 1993), total elimination of acyl migration is not feasible in both enzymatic and Grignard hydrolysis of triacylglycerols. Besides, several problems related to sample oxidation during derivatisation process as well as with the subsequent separation and identification of methyl esters have been disclosed (Igarashi *et al.*, 2000). On top of the shortcomings stated above, the loss or contamination of sample prior to gas chromatography (GC) analysis, the laborious and time-consuming method for routine basis, has prompted the investigation on more user-friendly, accurate and elegant spectroscopic method for the analysis of positional distribution of fatty acids in triacylglycerol.

1.2.3 ^{13}C NMR Regiospecific Analysis

The resonances of carbonyl carbon of acyl chains in triacylglycerol structure had been shown to give information on the composition of saturated (SFA), monounsaturated (MUFA) and polyunsaturated fatty acids (PUFA) at the *sn*-1,3 and *sn*-2 positions in ^{13}C NMR spectrum of oils and fats (Ng, 1985). The signals of carbonyl resonances were assigned according to the chemical shifts of standard triacylglycerols of known compositions. Theoretically, carbonyl carbons in ester are more shielded (δ 150-180 ppm) as compared with aldehyde and ketone (δ 190-220 ppm). Within the resonances of carbonyl carbons, the group of peaks at δ 173.1 ppm pertains to acyl groups from the *sn*-1,3 positions of triacylglycerol, whereas the group at δ 172.7 ppm belongs to those residing at the *sn*-2 position (Figure 1.6). Chemical shifts for the acyl chains at *sn*-1,3 positions are shifted consistently by 0.39-0.40 ppm at the higher frequencies than those of the corresponding fatty acids attached at the *sn*-2 position, by virtue of their different γ-gauche interaction associated with the steric effects.

Within each region, as the unsaturation occurs closer to the carbonyl carbon, the resonances appear at a higher field compared with the saturated species at the similar position. Electron donation effect of the double bond attenuates the electron withdrawal effect of carboxyl oxygen, causing the carbonyl carbons of unsaturated acyl chain to be more shielded. The difference in chemical shift was found to be greatest if first double bond occurred at the γ-position from the carbonyl carbons. Conversely, those located at the thirteenth carbon and even further from the carbonyl carbon, such difference in chemical shift was undetectable (Bergana and Lee, 1996). On top of that, the separation between *cis*-9-monoene and polyunsaturated acyl chains resonances was only 0.01 ppm. The presence of unsaturation beyond two double bonds, within the identical position of

first double bond, could not be distinguishable in the region of carbonyl carbon resonances (Bergana and Lee, 1996).

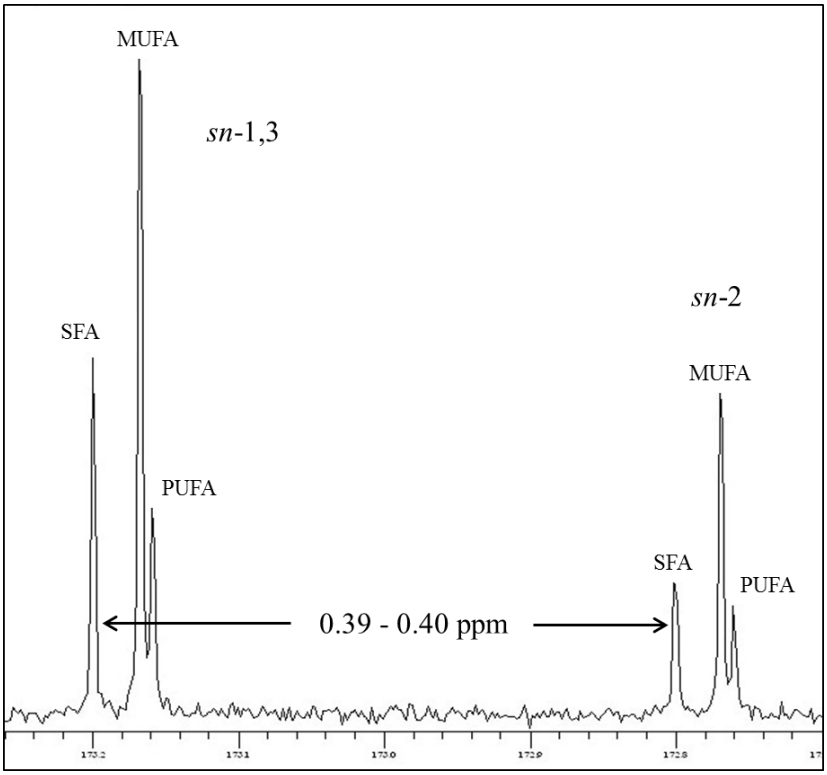

Notes:
SFA, saturated fatty acid acyl chain; MUFA, monounsaturated fatty acid acyl chain (*cis*-9 monoene); PUFA, polyunsaturated fatty acid acyl chain.

Figure 1.6 : ^{13}C NMR spectrum of acyl chain carbonyl resonances of synthetic mixture of triacylglycerols

Regiospecific analysis of triacylglycerols by means of ^{13}C NMR spectroscopy will overcome the aforementioned shortcomings in conventional method (Section 1.2.2). Nonetheless, the major limitation of this method is the indistinguishable saturated acyl chain of different chain lengths. Diversified NMR acquisition and processing parameters had been employed in the similar work (Ng, 1985; Wollenberg, 1990; Vlahov, 1998), which will be further discussed in Chapter 2.

1.3 Positional Fatty Acids and their Health Impact

1.3.1 Lipid Digestion and Absorption

Lipid digestion is expected to initiate in the mouth where a lingual lipase is secreted from the glands (Gurr, 1999). Subsequently, gastric lipase in the stomach participates in the partial breakdown of triacylglycerols before the main digestive site in the small intestine. Most of the hydrolysis takes place in the stomach at pH of 4.5 to 5.5 (Watts *et al.*, 1988). The major products of gastric digestion are the short and medium chain fatty acids. They are absorbed across the gut wall as individual fatty acids into the bloodstream (Watts *et al.*, 1988).

The enzymatic hydrolysis of dietary triacylglycerols is the major activity of digestion, predominantly occurring in the duodenum. The fat emulsion that entering the duodenum from the stomach is mixed with pancreatic juice which is containing bile salts, phospholipids and lipases, as secreted by the pancreas. This lipase is known as pancreatic lipase which catalyses the hydrolysis of triacylglycerols specifically at the *sn*-1 and *sn*-3 positions, and subsequently yields 2-monoacylglyerols and two free long chain fatty acids. Negligible hydrolysis occurs at *sn*-2 position, while there is an insignificant acyl migration to 1-monoacylglycerol being observed previously (Gurr, 1999). This might owing to the body temperature is too low for the isomerisation to occur. On the contrary, Mu and Høy (2004) estimated only 75% conservation of fatty acids at the *sn*-2 position, while the rest had been migrated to *sn*-1 and *sn*-3 positions.

The fat digestion products, particularly 2-monoacylglycerol and long chain fatty acids mix with bile acids forming mixed micelles with non-polar core and an outer shell of amphiphilic constituents (Gurr, 1999). Fatty acid at the *sn*-2 position is absorbed in the form of monoacylglycerols through the intestinal wall, and those which are esterified at

sn-1,3 positions will be absorbed as free fatty acids (Kayden *et al.* 1967). Schulthess *et al.* (1994) suggested that a protein-mediated process is required for the absorption of long chain fatty acids, whilst 2-monoacylglycerol is absorbed by passive diffusion. In some *in vitro* studies with adipocytes, it was found that the fatty acid transport proteins may behave differently on various fatty acids, mainly depending on their chain lengths (Abumrad *et al.*, 1984; Stremmel, 1988). On the other hand, fatty acid at the *sn*-2 position is conserved, *i.e.* as postprandial 2-monoacylglycerols and the re-synthesised triacylglycerols in chylomicron have mainly retained the *sn*-2 positional fatty acid (Tholstrup and Samman, 2004).

1.3.2 Serum Lipid Profile and Blood Cholesterol Level

A person consuming oils and fats does not take in only the fatty acids, but the chemical nature of the triacylglycerols (Ong and Goh, 2002). As mentioned in Section 1.3.1, the positional attachment of fatty acids in the glycerol backbone, determines the final absorption and metabolism in the body.

Upon entry into the enterocyte, the major site of metabolism is the endoplasmic reticulum, at where the triacylglycerols is re-synthesised and subsequently incorporated into chylomicrons. This occurs through the monoacylglycerol pathway, or alternatively by the α-glycerophosphate pathway (Kayden *et al.*, 1967). The 2-monoacylglycerol will serve as a primary backbone for the triacylglycerol re-synthesis in lymph chylomicrons, or gut and liver phospholipid synthesis.

Numerous nutritional studies and reviews reported the significance of the positional distribution of fatty acids at *sn*-1,3 and *sn*-2 positions, in elucidating their behaviour in relation to hypercholesterolemia and the progression of atherosclerotic lesions, instead

of the oil characterisation based on merely total saturation and unsaturation levels (Kritchevsky *et al.,* 1982; Kritchevsky, 1988; Truswell *et al.,* 1992; Choudhury *et al.,* 1995; Renaud *et al.,* 1995; Berry, 2009). Interesterification of oils that alters the positional fatty acids at the *sn*-2 position resulted in different effects on human nutrition and health (Kritchevsky *et al.*, 1982; Kritchevsky, 1988). In a study using rat model, elevated saturated fatty acids (SFA) content at the *sn*-2 position was associated with the increased platelet aggregation and low-density-lipoprotein cholesterol (LDL-C), whereas its reduction was associated with a lower plasma triacylglycerols (Renaud *et al.*, 1995). As a result, a recent review suggested that the dietary oils with high saturation level at the *sn*-2 position were correlated to the cardiovascular diseases (Berry, 2009).

Generally, palm oil is misconceived to behave like saturated fats, namely lard, tallow and other types of fats. Some quarters erroneously implicate palm oil which contains approximately 50% SFA, as one of the causes of prevailing cardiovascular diseases. Ng *et al.* (1992) evaluated the effect of palm olein and olive oil on serum lipids and lipoprotein, and found that the levels of total cholesterol, LDL-C and high-density-lipoprotein cholesterol (HDL-C) were similar for both oils. Similarly, Choudhury *et al.* (1995) reported that diets enriched by palm olein and olive oil showed identical plasma total cholesterol and LDL-C levels in human. This demonstrated that when palmitic acid replaced oleic acid at the *sn*-1,3 positions of triacylglycerols while the *sn*-2 position conserved with oleic acid, the expected increase in LDL-C was not seen. A comparable effect between palm olein and another unsaturated oil, namely rapeseed oil (canola) had also been reported by Truswell *et al.* (1992) and Sundram *et al.* (1995).

In summary, dietary fats with high saturation level at the *sn*-2 position are being more atherogenic and cholesterolemic (Myher *et al.*, 1977; Manganaro *et al.*, 1981; Berry,

2009), while on the contrary, relatively lower fasting total cholesterol was observed in diets with similar fatty acids located at the *sn*-1,3 positions of triacylglycerols (Forsythe *et al.*, 2007). From aforementioned findings, it could be inferring nutritional similarities in terms of serum lipids and lipoprotein among palm olein and other vegetable oils may be due to the comparable fatty acid composition at the *sn*-2 position.

1.3.3 Hypothesis on Obesity

Other than lipid concentration and cholesterol level in blood, obesity has becoming a global epidemic. By definition, obesity means having too much body fat. It is not the same as being overweight, which means weighing too much. A person might be overweight from extra muscle, bone, or water, as well as from having too much fat. There is an extensive body of published works on positional fatty acids of triacylglycerols and their associated effects on serum lipid profile and blood cholesterol level, as mentioned in Section 1.3.2. Yet, to date, there has been little focus on investigating the effect of positional distribution of fatty acids within the glycerol backbone on fat accretion.

During fat digestion, enzymatic hydrolysis of triacylglycerols containing predominantly long chain saturated fatty acids (SFA) at the *sn*-1 and *sn*-3 positions allows for ready absorption of the 2-monoacylglycerols. Conversely, the long chain saturated free fatty acids suffer delayed absorption by virtue of the formation of calcium or magnesium soaps (Ong and Goh, 2002) (Figure 1.7). Therefore, after absorption through the intestinal wall, the amount of re-synthesised triacylglycerols is expected to reduce. Ong and Goh (2002) hypothesise that if the long chain SFA (C16:0 and above) occurs at the *sn*-1 and *sn*-3 position, they generally tend to lower fat deposition, whereas at the *sn*-2 position, they are either neutral or tend to increase fat accretion.

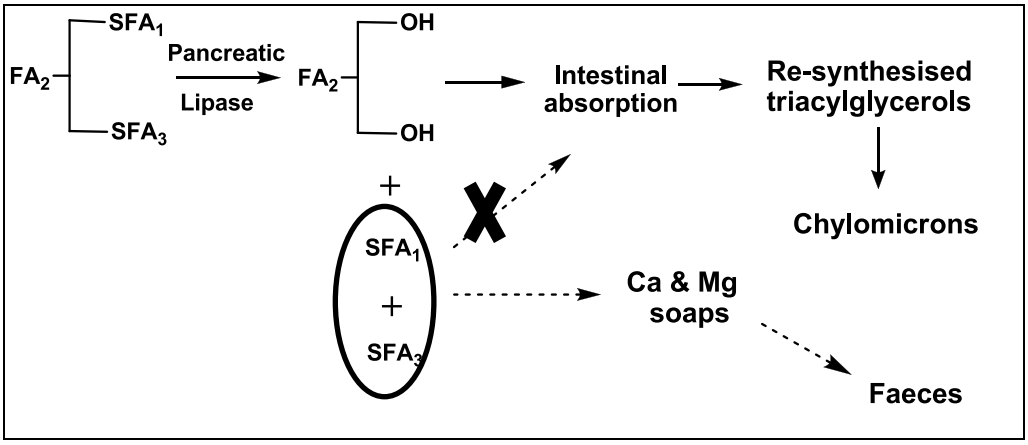

Notes:
FA, fatty acid; SFA, saturated fatty acid; Ca, calcium; Mg, magnesium.

Figure 1.7 : Pathway of free long chain SFA from *sn*-1,3 positions after hydrolysis of pancreatic lipase

Source : Adopted from Ong and Goh (2002)

It is important to find out the obesity risks of various edible or dietary oils, with special reference to its positional fatty acids in the triacylglycerols molecules, not only by the conventional classification of these oils according to their total saturation or total unsaturation levels.

1.4 Structured Lipids

1.4.1 Introduction

The fatty acid profiles of triacylglycerols in natural occurring oils and fats are defined and exclusive to each plant or animal species. In a broad sense, animal fats contain higher content of saturated fatty acids (SFA) compared with vegetable oils. With increasing knowledge of lipid digestion, absorption and metabolism, some innovations on structured lipids have been made possible.

The concept of structured lipids was first introduced by Babayan (1987). By definition, structured lipids consist of the restructured or modified triacylglycerols to alter the fatty acid composition (FAC) and/or their *sn*-position in glycerol moiety by using the chemical or enzymatic reactions. It may provide effective approaches in delivering desired fatty acids or chemical nature of the oils for nutrition or therapeutic purposes (Akoh, 1995). Furthermore, the desired physical properties, for instance solid fat content and slip melting point, can be achieved by designing a suitable structured lipid. Although the physical properties may be achieved by merely blending the oils with different desired properties, yet the simple physical mixture can lead to different hydrolysis and absorption rates as compared with structured lipids, resulting in different metabolic fates (Ikeda *et al.*, 1991; Jensen *et al.*, 1994).

Most published reports on structured lipids deal with medium-chain triacylglycerols which fatty acids with 8–14 carbons are attached to their *sn*-1,3 positions while long chain fatty acids of more than 16 carbons at the *sn*-2 position (Soumanou *et al.*, 1998; Xu *et al.*, 2000; Lee and Foglia, 2000; Nunes *et al.*, 2012). Apart from that, significant efforts are also made in the synthesis of structured triacylglycerols containing conjugated linoleic acid (CLA) (Garcia *et al.*, 1998; Torres *et al.*, 2002; Rocha-Uribe and Hernandez, 2004) and polyunsaturated fatty acid (PUFA) (Lee and Akoh, 1998; Xu *et al.*, 2000). CLA has been reported to show a wide range of nutritional attributes, such as the potent anticancer properties, reduction of atherosclerotic risk and alleviation of body fat accretion (Osborn and Akoh, 2002).

1.4.2 Synthesis of Structured Lipids

Lipids can be tailor-made with any fatty acid in any position on the glycerol moiety. Several chemical or enzymatic reactions, for instance, direct esterification, acidolysis,

transesterification and interesterification can be employed in the synthesis of structured lipids. These technologies provide the opportunity to replace conventional oils and fats in the food products with fully functional and potential healthier lipids. The general scheme of the aforementioned reactions is depicted in Figure 1.8.

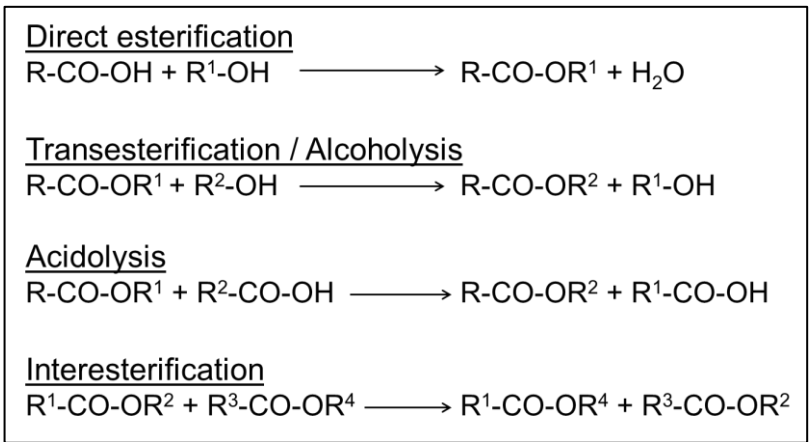

Figure 1.8 : General scheme for common reactions used in synthesis of structured lipids

1.4.2.1 Direct Esterification

Esterification denotes the reaction between carboxylic acid and alcohol, as depicted in Figure 1.8. In the synthesis of tailor-made lipids, this is the reaction between fatty acids and glycerol or partial acylglycerols. Triacylglycerols containing elaidic acids (C18:1 9*t*) at all positions (*sn*-1, *sn*-2 and *sn*-3) had been successfully synthesised using reaction between elaidic acid and glycerol (Adlof and List, 2007). Irimescu *et al.* (2000) synthesised trieicosapentaenoylglycerol from eicosapentaenoic acid (EPA) (C20:5) and glycerol with an immobilised non-regio specific lipase from *Candida Antarctica* (Novozyme™). According to Le Chatelier's Principle, in the effort to increase the oil yield, the co-product, water, which was condensed on the walls of flask during the reaction will be removed by use of a heat gun (Adlof and List, 2007). Upon removing water under reduced pressure, a yield of more than 98% was achieved even at the stoichiometric ratio 1:3 of glycerol and EPA (C20:5). On the other hand, structured lipids containing caprylic acids (C8:0) at the *sn*-1,3 positions and polyunsaturated fatty

acid (PUFA) at the *sn*-2 position can be achieved by esterification between 2-monoacylglycerol and caprylic acids under catalytic action of 1,3-specific lipases (Muñoz *et al.*, 2009).

1.4.2.2 Transesterification/Alcoholysis

In transesterification or alcoholysis, a triacylglycerol molecule is reacted with an alcohol or glycerol in the presence of a strong acid or base (Schuchardt *et al.*, 1998). Transesterification is commonly employed in conjunction with other reactions, namely, acidolysis and interesterification, due to a mixture of partial acylglycerols (monoacylglycerols and diacylglycerols) is produced and they act as the starting materials for the successive reactions. In the preparation of 1,3-dielaidoylglycerol, trielaioylglycerol was reacted with glycerol under sodium methoxide catalysis condition (Adlof and List, 2007). The proposed mechanisms by Eckey (1956) are depicted in Figure 1.9 and Figure 1.10, for base-catalysed and acid-catalysed transesterification, respectively.

Apart from utilising chemical catalysts, some biocatalysts are also being employed in transesterification. In the synthesis of symmetrical triacylglycerols, it was reported that highest yields and purities were achieved in a two-step process, namely, alcoholysis reaction catalysed by *sn*-1,3 specific lipase and subsequently, direct esterification of the 2-monoacylglycerol with desired fatty acids (Schmid *et al.*, 1998; Soumanou *et al.*, 1998). This had been applied in several works. For instance, prior to the esterification with caprylic acid (C8:0), cod liver and tuna oil were subjected to ethanolysis catalysed by Novozyme 435 from *Candida antarctica* to produce 2-monoacylglycerols (Muñoz *et al.*, 2008; Muñoz *et al.*, 2009).

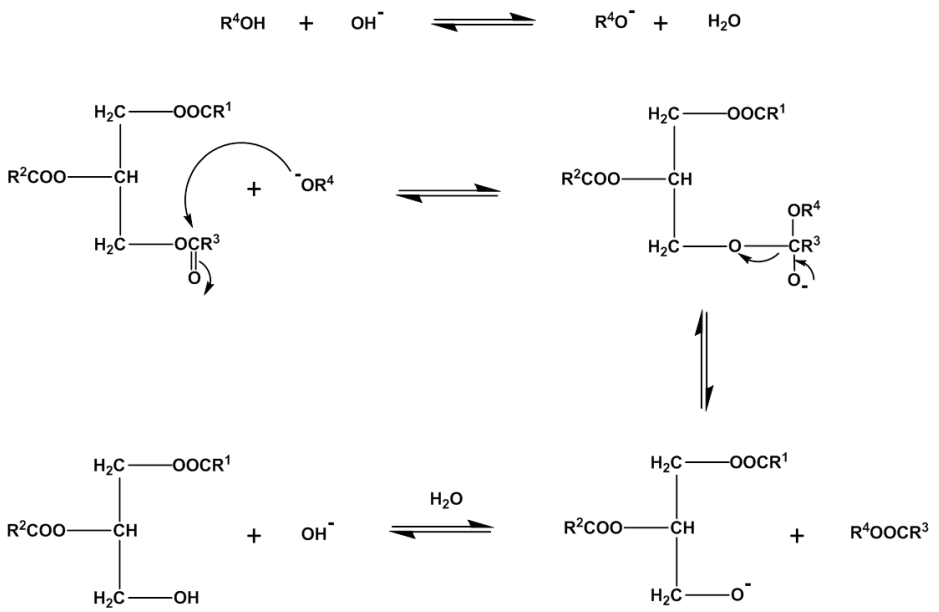

Notes:
R^1, R^2, R^3 are corresponding to alkyl groups attached to the carbonyl carbons at *sn*-1, *sn*-2 and *sn*-3 positions of triacylglycerol, respectively; R^4 is the alkyl group from the alcohol.

Figure 1.9 : Mechanism of base-catalysed transesterification of triacylglycerols (Eckey, 1956)

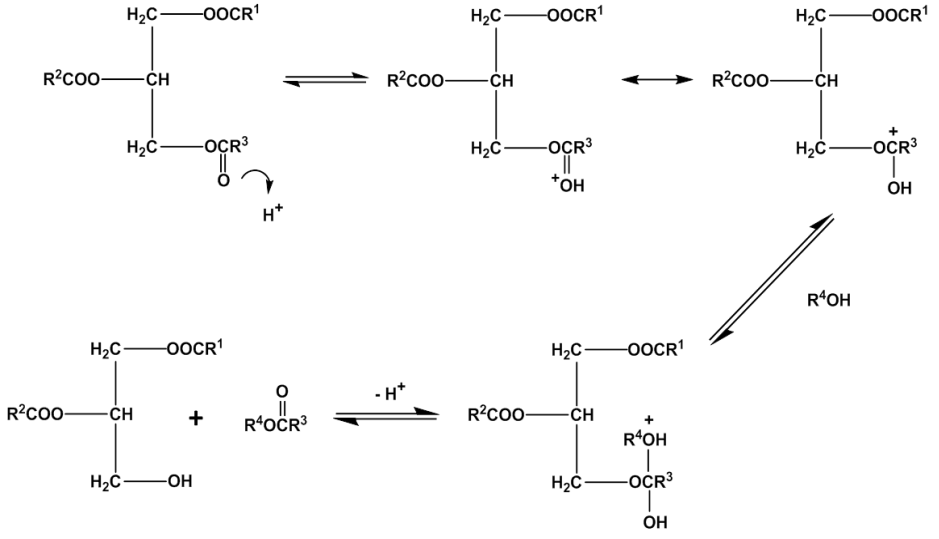

Notes:
R^1, R^2, R^3 are corresponding to alkyl groups attached to the carbonyl carbons at *sn*-1, *sn*-2 and *sn*-3 positions of triacylglycerol, respectively; R^4 is the alkyl group from the alcohol.

Figure 1.10 : Mechanism of acid-catalysed transesterification of triacylglycerols (Eckey, 1956)

The resultant 2-monoacylglycerol was isolated by recrystallisation at cold temperature. The targeted structured triacylglycerol was those containing caprylic acids at the *sn*-1,3 positions and polyunsaturated fatty acids (PUFA) at the *sn*-2 position. Similar approach had been reported by Irimescu *et al.* (2001) in the synthesis of symmetrically structured lipids rich in docosahexaenoic acid at the middle position and caprylic acid (C8:0) at the outer positions of triacylglycerol.

1.4.2.3 Acidolysis

Acidolysis, which is the exchange of acyl group between triacylglycerol and fatty acids, remains an important strategy in designing structured lipids. Acyl exchange is promoted with an excess of fatty acids to substitute the fatty acid residues specifically at the *sn*-1 and *sn*-3 positions by using a 1,3-specific lipase, leaving the fatty acid residues at the *sn*-2 position unchanged. New fatty acids can be introduced to the triacylglycerols in native oils and fats.

Lipases from the strain of *Rhizomucor miehei* was one of the 1,3-regiospecific lipases which had been used extensively in the synthesis of structured lipids by acidolysis (Schmid *et al.*, 1998; Xu *et al.*, 2000; Sellappan and Akoh, 2001; Rocha-Uribe and Hernandez, 2004; Foresti and Ferreira, 2010; Koçak *et al.*, 2011). For instance, Menhaden fish oil and caprylic acid (C8:0) react in the presence of *Rhizomucor miehei* lipase to yield a product with about 30% of caprylic acid (C8:0), 30% of eicosapentaenoic (EPA) (C20:5) and docosahexanenoic acids (DHA) (C22:6) in combination (Xu *et al.*, 2000). Chandler *et al.* (1998) also demonstrated the synthesis of chiral ABC-type structured lipids in a similar way to the chiral AAB-type structured lipid synthesis. The strategy employed was partial stereospecific acidolysis of ABA-type triacylglycerol with a fatty acid, resulting in the ABC-type structured lipid. By the

reaction of 1,3-dipalmitoyl-2-oleoylglycerol (POP) and stearic acid in the presence of *Rhizomucor miehei* lipase, they obtained a mixture of 34.5% of POP (unreacted substrate), 9.0% of 1-palmitoyl-2-oleoyl-3-stearoylglycerol (POSt), 43.4% of 1-stearoyl-2-oleoyl-3-palmitoylglycerol (StOP) and 13.1% of 1,3-distearoyl-2-oleoylglycerol (StOSt). The amount of StOP was 4.8 fold larger than that of POSt.

On the other hand, *Carica papaya latex* acted as a biocatalyst in the modification of chicken fat triacylglycerols by incorporating caprylic acids (C8:0) at the *sn*-1,3 positions (Lee and Foglia, 2000). This is in line with the effort to produce functional structured lipids composed of monounsaturated (MUFA) and medium chain fatty acids. Recently, another lipase from Rhizopus family, namely, *Rhizopus oryzae*, has been utilised in the acidolysis of virgin olive oil with caprylic (C8:0) or capric (C10:0) acids.

Screening of several lipases from *Candida antarctica*, *Mucor miehei*, *Pseudomonas* sp., *Aspergillus niger* and *Candida rugosa* for the incorporation of capric acid (C10:0) into arachidonic and docosahexaenoic acid single cell oils was reported by Hamam and Shahidi (2004). It was observed that the lipase from *Pseudomonas sp.* remained the most effective lipase. On the other hand, incorporation of stearic acid (C18:0) was found higher than that of caprylic acid (C8:0) for all parameters in the synthesis of tailor-made triacylglycerols containing caprylic (C8:0), stearic (C18:0) and linoleic acids (C18:3) using lipase from *Rhizomucor miehei* (Lipozyme IM 60) (Sellappan and Akoh, 2001).

For practical synthesis of chiral/asymmetrical structured lipids, Chandler *et al.* (1998) investigated the stereospecificity of lipases in acidolysis of tripalmitoylglycerol with oleic acid in organic solvent. They found that *Rhizomucor miehei* lipase exhibited a

preference towards the *sn*-1 position over *sn*-3 position to several folds, yielding chiral 1-oleoyl-2, 3-dipalmitoylglycerol. The stereospecificity of enzyme depended on water activity, chain length of the fatty acid and type of the solvent.

1.4.2.4 Interesterification

Interesterification is another prominent method for structured lipids synthesis. Interesterification corresponds to exchange of acyl residues between two triacylglycerols, or between triacylglycerol and alkyl ester, resulting in the production of unique triacylglycerol structure. It allows the intermolecular and intramolecular redistribution of the positional fatty acids within *sn*-1, *sn*-2 and *sn*-3 positions in triacylglycerol structure. The interesterification of triacylglycerol can be carried out either chemically or enzymatically.

Chemical interesterification can be defined as the chemical randomisation of acyl chains among all three stereospecific positions, namely, *sn*-1, *sn*-2, and *sn*-3 positions, either intramolecular, intermolecular or both. In addition, the reaction is completely random if the reaction temperature is above the melting point of the mixture. In the case of lower reaction temperature, some fats with higher melting points will be crystallised, resulted in directed interesterification. The most common catalyst being used is sodium methoxide.

Mechanism proposed by Weiss *et al.* (1961) suggested that the interesterification was initiated by α-hydrogen abstraction from a fatty acid moiety by methanolate anion. The abstraction of α-hydrogen resulted in the formation of an enolate (Figure 1.11). This was further verified by Liu (2004).

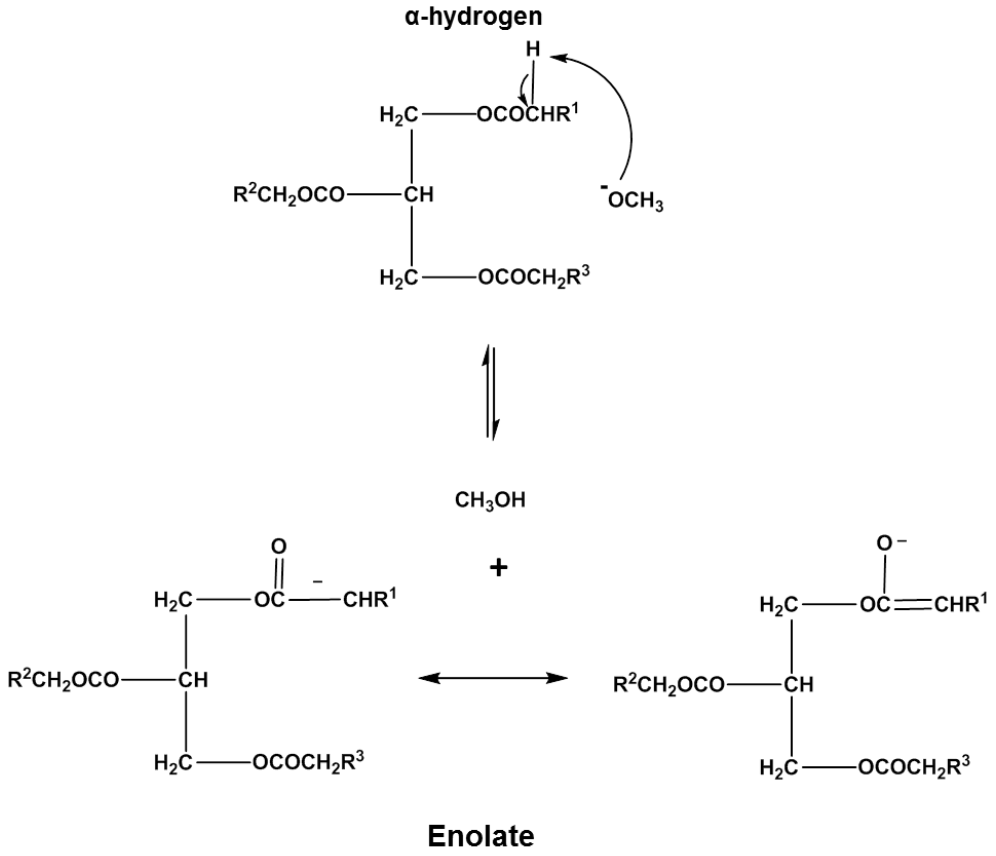

Notes:
R^1, R^2, R^3 are corresponding to alkyl groups attached to the carbonyl carbons at *sn*-1, *sn*-2 and *sn*-3 positions of triacylglycerol, respectively.

Figure 1.11 : Formation of enolate anion and its mesomeric structures (Weiss *et al.*, 1961)

The enolate subsequently attacked the electrophilic carbonyl carbon center, either intramolecular (Figure 1.12) or intermolecular (Figure 1.13), forming a β-keto ester. Interesterification was then likely completed *via* a Claisen condensation mechanism involving the β-keto ester anion as the active intermediate (Liu, 2004). The β-keto ester anion contained electrophilic carbonyl carbons that acted as the active sites for the nucleophilic attack by glycerinate, which would rearrange acyl groups randomly (Figure 1.12 and Figure 1.13). The physical and functional changes have been reported by Laning (1985) using an example of the chemical interesterification of palm, palm kernel and coconut oils.

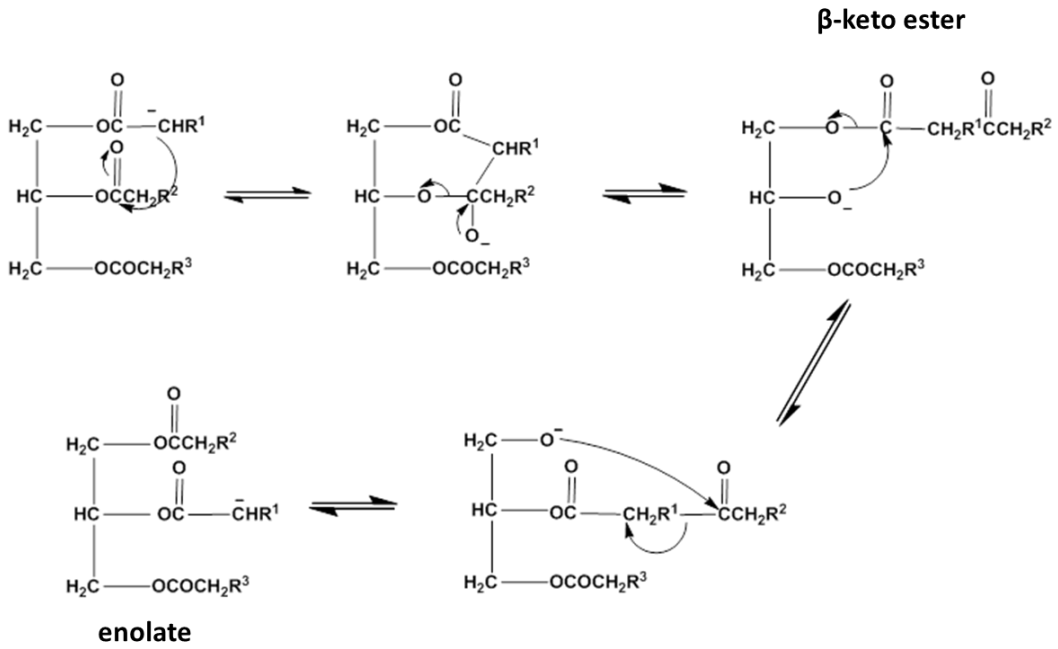

Notes:
R^1, R^2, R^3 are corresponding to alkyl groups attached to the carbonyl carbons at *sn*-1, *sn*-2 and *sn*-3 positions of triacylglycerol, respectively.

Figure 1.12 : Intramolecular rearrangement of the acyl group *via* Claisen condensation (Liu, 2004)

In the context of enzymatic interesterification, similar to acidolysis, a key point for the strategies is the utilisation of lipase in the regiospecific acyl exchange at the *sn*-1,3 positions (lipase from *Rhizomucor miehei*, Lipozyme IM RM 60), as well as the non-specific interesterification (lipase from *Candida Antarctica*). Due to the milder reaction condition requirements, enzymatic interesterification is more preferable than chemical synthesis (Ko çak *et al.*, 2011).

There are generally two forms of substrates reported for enzymatic interesterification, namely, interesterification between triacylglycerol and triacylglycerol (Soumanou *et al.*, 1997; Seriburi and Akoh, 1998; Ibrahim *et al.*, 2008), as well as between triacylglycerol and ethyl ester (Huang and Akoh, 1996). The latter will give mixtures of

triacylglycerols (containing the desired structured lipids) and the remaining ethyl esters. The ethyl esters can be removed after the reaction by molecular distillation (Iwasaki and Yamane, 2000).

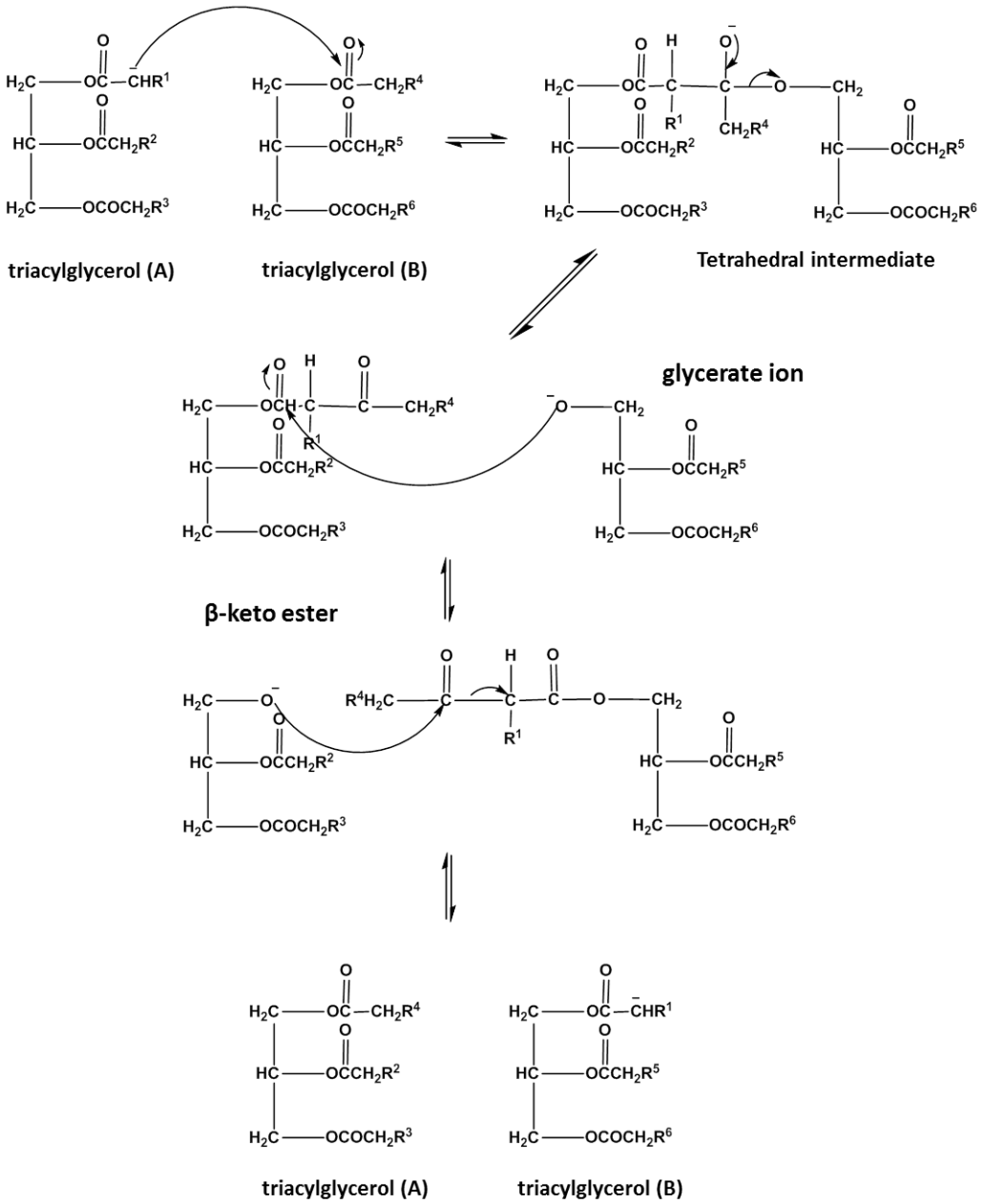

Notes:
R^1, R^2, R^3 are original alkyl groups attached to the carbonyl carbons at *sn*-1, *sn*-2 and *sn*-3 positions of triacylglycerol (A), respectively; R^4, R^5, R^6 are original alkyl groups attached to the carbonyl carbons at *sn*-1, *sn*-2 and *sn*-3 positions of triacylglycerol (B), respectively.

Figure 1.13 : Intermolecular rearrangement of the acyl group *via* Claisen condensation (Liu, 2004)

In a study reported by Soumanou *et al.* (1997), nine commercial lipases were accessed of their ability to hydrolyse pure triacylglycerols as well as some natural oils. Microbial lipases from *Rhizomucor miehei*, *Candida sp.* and *Chromobacterium viscosum* were giving satisfactory results. With the activity similar to *Rhizomucor miehei* lipase, relatively new immobilised *Thermomyces lanuginosa* lipase (Lipozyme IM TL) had been introduced in the 1,3-specific interesterification (Shetty *et al.*, 2011; Yang *et al.*, 2003; Svensson and Adlercreutz, 2011). By using *Thermomyces lanuginosa* lipase-catalysed interesterification between trilaurin and 1,3-dipalmitoyl-2-oleoylglycerol (POP), the effect of acyl migration was investigated (Svensson and Adlercreutz, 2011). It was found that by varying the reaction time, different triacylglycerol mixtures could be obtained in structured lipids, as prolonged interesterification will lead to complete randomisation. The combination of lipases from *Rhizomucor miehei* and *Thermomyces lanuginosa* was reported to generate a positive synergistic effect at all mixing ratios in enzymatic interesterification of palm stearin and coconut oil (Ibrahim *et al.*, 2008).

Mangos *et al.* (1999) reported that the prospective plant-derived lipase, *Carica papaya latex* found in the exudate of *Carica papaya* is known for its short-chain acyl group specificity, *sn*-1,3 regioselectivity and *sn*-3 stereoselectivity. Consequently, it has been employed to synthesise low caloric short and long chain triacylglycerols through the interesterification between triacetin and hydrogenated soybean oil.

In contrast to all high specificity and selectivity lipase, immobilised *Candida Antarctica* lipase, SP435, was found to be non-specific when catalysing the interesterification of triolein and tristearin (Lee and Akoh, 1997; Seriburi and Akoh, 1998; Fomuso and Akoh, 1998). Goli *et al.* (2008) also demonstrated the application of similar lipase in the

interesterification between structured lipids containing conjugated linoleic acid (CLA) and palm stearin for prospective margarine production.

Generally, the synthesised tailor-made lipids can be characterised by their triacylglycerol molecular species by High Performance Liquid Chromatography (HPLC), solid fat content (SFC) by pulse-NMR, melting and crystallisation behaviour by Differential Scanning Calorimetry (DSC), and also their distribution within the *sn*-1,3 and *sn*-2 positions of glycerol backbone.

1.4.3 Applications of Structured Lipids

The targeted nutritional benefits of structured lipids are wide-ranging. For instance, absorption of essential polyunsaturated fatty acids (PUFA), namely, docosahexaenoic acid (DHA) and eicosapentaenoic acid (EPA), can be improved by incorporating the fatty acids into *sn*-2 position. Besides, some structured lipids are designed to provide energy which is not deposited in adipose tissue and subsequently reduce the risk of obesity. An example of commercially available reduced-energy structured triacylglycerols is Salatrim (Finley *et al.*, 1994). The *sn*-2 position is predominantly occupied by the short chain fatty acids (C2:0-C4:0), whereas the long chain saturated fatty acid, namely, stearic acid (C18:0), resided at the *sn*-1,3 positions. The structured triacylglycerols still give the fat properties in terms of taste and mouth-feel, but provide reduced energy.

Medium chain triacylglycerols offer several health benefits and have been studied extensively in the field of medicine as well as nutrition. Structured lipids containing medium chain fatty acids at the *sn*-1,3 positions of triacylglycerol are more readily absorbed and oxidised for energy as compared with long chain triacylglycerols

(Jandacek *et al.*, 1987). Consequently, this has been used to treat fat absorption abnormalities in premature infants or in patients with malabsorption syndrome (Gupta *et al.*, 2003). They are burned rapidly for energy and consequently not deposited in adipose tissue (Chan *et al.*, 1998).

Apart from the medical and nutraceutical applications, functional structured lipids can also be tailor-made for various food applications. *Trans*-free margarine can be produced by acidolysis of stearic acid and high-laurate canola oil (Formuso and Akoh, 2001) as well as interesterification of stearic methyl ester and triolein (Seriburi and Akoh, 1998). On the other hand, chemical interesterified structured lipids from butterfat and canola oil can improve the spreadability of butter at cold temperature (Rousseau *et al.*, 1996).

Availability of cocoa butter, which consequently affects its cost, has prompted the research on the discoveries of cocoa butter equivalent for chocolate and confectionery coatings. The most typical cocoa butter equivalents are palm mid fractions, illipe fat, shea butter, sal fat, mango fat and kokum butter (Osborn and Akoh, 2002). Foglia *et al.* (1993) suggested that beef tallow can also be employed as base fat for the synthesis of structured lipids as cocoa butter equivalent.

As a general rule, in the aspect of physical quality, oils and fats are modified to attain certain functionalities, *viz.* improved spreadability, physical appearance, melting behaviour, solid fat content, thermal and crystallisation characteristics. On top of that, the improved chemical properties of structured lipids will result in better stability and their nutritional attributes.

1.5 Objectives of Present Study

The contribution of dietary fat to daily calorie intake has long been recognised. Dietary fat is efficiently stored, being an important factor in the growing problem of obesity. However, all fats may not be partitioned for storage with similar efficiency. In line with the growing prevalence of morbid obesity, the ultimate objective of present study is to investigate the relationship between different types of triacylglycerol structure and obesity.

There is an extensive body of published works on the positional fatty acids of triacylglycerol and their associated effects on serum lipids profile and blood cholesterol level. These reported findings show the nutritional attributes of the positional fatty acids, particularly at the *sn*-2 position on blood lipids profile, compared with mere total saturation and unsaturation levels. On the contrary, there is a paucity of information relating to their accompanying effects on fat accretion. Literature review on the subject has revealed that fatty acids at different *sn*-position are subjected to different rates of intestinal absorption. This is a clue that the degree of fat deposition might be correlated to the positional distribution of fatty acids in triacylglycerol.

Current study will be executed using several animal studies, as the groundwork for the potential testing in future clinical trials. Prior to the *in vivo* studies, an accurate and precise regiospecific analysis of oils and fats is needed. Yet, the conventional methods for analysis of positional fatty acids are laborious and time consuming. It involves several steps, *viz.* chemical or enzymatic hydrolysis, purification on thin layer chromatography, derivatisation of methyl esters and the separation on gas chromatography. As a consequence, it is hardly to be employed as a routine analytical tool. Moreover, sample loss or acyl migration during preparation might subject the

quantitative results to indiscernible errors. Therefore, the development of a more elegant, user-friendly and rapid regiospecific analysis is worthwhile. This is essential for nutritionist to correlate their clinical findings with the positional fatty acids within glycerol moiety.

On the other hand, outcomes of the *in vivo* testing will be used as a guideline in the synthesis of structured lipids which aims to associate with fat-alleviating effect. In the effort to achieve sustainable chemistry, biological catalyst, namely 1,3-specific lipase will be employed in the interesterification of oils and fats. It will be conducted in the solvent-free condition as to minimise the use of hazardous substances during the course of synthesis. The newly synthesised structure lipids will be subjected to aforementioned regiospecific analysis and chromatography analysis of triacylglycerol molecular species.

In summary, it is the objective of the present study to develop a rapid and direct analysis of fatty acid compositions at the *sn*-1,3 as well as *sn*-2 positions of glycerol moiety, and thereafter the elucidation of the effects of positional fatty acid compositions on body fat accretion. The findings from the *in vivo* studies will provide useful information for the synthesis of prospective healthier structured lipids for preserving a healthy and relatively lower obesity rates.

CHAPTER TWO
REGIOSPECIFIC ANALYSIS OF TRIACYLGLYCEROLS USING ^{13}C NMR

2.1 Background

Quantitative ^{13}C NMR (qCNMR) even though is not widely used for regiospecific analysis, it has been used as an appealing technique to determine the positional distribution of fatty acids in glycerol backbone of triacylglycerols in various edible oils and fats. Specifically for qCNMR regiospecific analysis, carbonyl carbons in the triacylglycerols are the main carbon nuclei of interest. Due to the absence of a directly attached proton, carbonyl carbons exhibit lengthy spin-lattice relaxation times (T_1) as compared to other types of carbons (methyl, methylene and methine carbons). In addition, relatively low natural abundance of carbon-13 (1.1%) also pose significant challenge to achieve an optimum signal-to-noise (S/N) ratio and peak resolution in a reasonable experimental time for accurate and precise quantitative results.

There is no clear guideline and consistency on data acquisition and processing parameters that can be attained from prior reports on qCNMR regiospecific analyses (Ng, 1985; Wollenberg, 1990; Vlahov, 1998; Aursand *et al.*, 1995; Standal and Axelson, 2009; Suarez *et al.*, 2010). Conversely, there are several assumptions being employed. A considerable number of parameters, *viz.* pulse sequence, pulse angle, pulse delay, temperature as well as the processing of NMR analysis differed immensely for similar work (Ng, 1985; Vlahov, 1998). This has resulted in diverse experimental time per analysis which is ranging from the fastest 58.5 minutes (Vlahov, 1998) to the lengthiest 206 minutes (Ng, 1985). Due to lengthy experimental time, a semi

quantitative analytical approach was preferred in the analysis of fish oils (Aursand *et al.*, 2007; Standal *et al.*, 2009). Moreover, the quantitative data will be subjected to indiscernible errors owing to the inappropriate use of NMR parameters during the data acquisition and processing. Consequently, this would complicate the comparison of analytical results acquired from different laboratories or with different NMR instrumentations. On the other hand, a rather complicated HSQC-TOCSY NMR analysis has been demonstrated on a synthetic mixture of pure triacylglycerols to analyse the positional distribution of palmitoyl and oleoyl acyl chains (Simova *et al.*, 2003).

The basic acquisition for qCNMR experiment follows the general relaxation-excitation-acquisition scheme. Each part plays a key role in the quantitative experiments. As aforementioned, the affecting NMR data acquisition parameters in qCNMR are pulse sequence, repetition time, spectral width, data points, acquisition time, pulse angle, and temperature. As required for all high resolution NMR work, proper shimming of the oil sample to achieve good line shape, high peak resolution with optimum S/N ratio is clearly an important prerequisite. However, iterative shimming of various axial (Z^1, Z^2, Z^3, Z^4, Z^5 and Z^6) and radial (X, Y, XY, XZ, YZ, X^2-Y^2) shims may be time-consuming and tedious for routine work. The degree of difficulty depends on the condition of spectrometer, the concentration of sample, working temperature as well as the type of experiment need to be carried out. For most routine works, it is sufficient to adjust axial shims, especially Z^1 and Z^2, and employ sample spinning during measurement. While both manual and automated shimming methods are optional, gradient shimming is found to be more efficient in producing better line shape in a relatively shorter time.

On the other hand, dissolved oxygens are paramagnetic species which may contribute greatly to the spin relaxation through dipole-dipole interaction between the nuclear spin and unpaired electron. This phenomenon leads to the broadening of the lines, and subsequently, causes the loss of vital resolution in NMR spectrum. For that reason, degassing is an important sample pretreatment step for NMR analysis. It can be done by bubbling inert nitrogen gas or subjecting ultrasonication through the sample, or perform the freeze-pump-thaw cycle on the sample several times. Elimination of the dissolved oxygen is also crucial due to its deleterious effect as an oxidising agent, particularly for biological sample.

Conventional ^{13}C NMR experiment uses broadband proton decoupling pulse sequence to suppress the coupling between carbon and proton for higher sensitivity in the resultant spectrum. The sensitivity of carbon-13 is enhanced by Nuclear Overhauser Enhancement (NOE) evolved during proton decoupling which results from the internuclear dipole-dipole interaction between proton and carbon-13. It is particularly important in structure elucidation and conformational analysis in organic chemistry. Yet the NOE affects carbon intensities in different extents, mainly depends on the degree of protonation of the carbon. Therefore, instead of broadband decoupling, the inverse gated decoupling pulse sequence is preferred in qCNMR in an effort to quench the NOE on carbon intensities. The major drawback of this strategy is that the required experiment times will be longer for reasonable S/N ratios in order to ensure accuracy of integration.

By definition, the delay before excitation is usually referred as the repetition time. It is the total period of acquisition time and pulse delay prior to the application of successive pulse. In order to achieve peak area that is proportional to the number of nuclei responsible for that resonance, all longitudinal magnetisation (M_z) has to be returned to

equilibrium magnetisation (M_o) during repetition time. Pulsing too rapidly, that is, using very short repetition times relative to T_1, will lead to a substantial decrease in signal intensity. In the extreme case, magnetisation has insufficient time to recover and eventually no signal can be observed. This phenomenon is known as saturation.

By adjusting spectral width of the spectrum, the observation frequency range can be set wide enough to encompass all peaks of interest, notwithstanding too wide setting will eventually result in reduced digital resolution and excessive noise. A wider qCNMR spectral width should be utilised for determining the exact chemical shifts of the peak of interest, prior to the adjustment of specific width for resolution enhancement. Peaks which fall outside the spectral width will be partly or completely filtered by the spectrometer filters, and may appear folded or aliased into the spectrum. Thus, judicious consideration must be taken during the selection of suitable spectral width. The attenuation of the intensity of desired signal and appearance of folded signals must be avoided.

One of the critical acquisition parameters, namely data points, is the extent of digitisation of the resultant NMR spectrum upon Fourier transformation. If the number of data points is too low, there will not be sufficient points to accurately define each resonance. Consequently, it leads to truncation of time domain signal and hence, formation of “ripples” or “wiggles” in the frequency domain of NMR spectrum. Nonetheless, excess of data points will increase the noise-rich tail of Free Induction Decay (FID). Therefore, S/N of the resultant spectrum is diminished.

As mentioned earlier, acquisition time is part of the repetition time prior to the next scan. It is the time required for digitising the FID. According to the Nyquist theorem

(Derome, 1987; Claridge, 1999), the acquisition time is directly proportional to the total digitised data points, but inversely proportional to the spectral width. It must be sufficiently long to allow the FID to decay and avoid truncation artifacts to ensure full spectral resolution.

In the context of flip angle, instead of the 90 ° pulse, Ernst angle (Pauli *et al.*, 2005) and those smaller than 90 ° (Vlahov *et al.*, 2010) have been introduced in quantitative solution state NMR analysis. These have been claimed to shorten total experimental time by decreasing the repetition time needed to allow the recovery of equilibrium magnetisation before applying a new pulse. Notwithstanding the reduced repetition time, pulse angle smaller than 90 ° will yield an attenuated S/N, which needs a higher number of transients for the compensation. This compromise warrants the investigation of the practical and optimum pulse angle for a rapid regiospecific analysis using qCNMR.

Apart from the data acquisition, the data processing parameters that will be included in the current investigation are zero filling, apodisation, smoothing algorithm and integration method. Prior to the Fourier transformation of FID, zero filling is usually being employed to enhance the resolution of spectrum in the frequency domain, by adding a string of zeroes to the tail of FID in the time domain. In quantitative NMR analysis, zero filling was reported to have no effect on the precision of peak integration (Nadjari and Grivet, 1991). Yet in the other study of systematic errors due to the integration of NMR spectra, one level of zero filling was found to be sufficient for reducing the systematic integration error, provided a 1% integration limit is used (Mcleod and Comisarow, 1989). In contrast, it was reported that no zero filling should be done in order to ensure unbiased quantitative information obtained from

experimental data (Abildgaard *et al.*, 1988). All the data points of the real and imaginary part of the spectrum were uncorrelated, as long as zero filling and exponential apodisation were omitted (Abildgaard *et al.*, 1988). Consequently, judicious consideration should be applied in qCNMR regiospecific analysis where accuracy is highly required.

By definition, apodisation is the process of multiplying the FID prior to Fourier transformation by a mathematical or window function. Generally, there is a variety of window functions available in NMR data processing software, for instance exponential, trapezoidal, Gaussian, Blackman Harris, shifted sine-bell and sine-bell squared. The type of window function applied depends upon the enhancement required, as for cosmetic value: the S/N ratio can be improved by applying an exponential window function with certain values of line broadening factor, whilst the resolution can be improved by the functions of sine-bell family. Since all FID are supposed to decay exponentially with time, the exponential tends to be the most suitable window function in data processing of qCNMR. Under the exponential window function, line broadening factor can be utilised to enhance the S/N ratio, but at the cost of peak resolution.

In contrast to the line broadening of exponential window function in the time domain, smoothing is another alternative for S/N ratio enhancement in frequency domain. Some of the common signals smoothing algorithms used in NMR data processing are simple moving average and Savitzky-Golay. Both algorithms use different mathematical approaches to calculate central point as the new smoothed data points. The drawback of this approach is decrement of peak resolution if excessive smoothing algorithm is being employed.

The conventional integration methods used in quantitative NMR are based on digital summation and interpolation procedures. Digital summation gives a fairly crude approximation of the total area under the curve by combined areas of a set of triangles, whereas interpolation method combines areas of a set of trapezoids consisting equal width. Simpson's rule is one of the interpolation schemes of the latter method. However, both methods are sensitive to inaccuracies arising from non-Lorentzian line shapes, phasing errors, and the low digital resolution (Sotak *et al.*, 1984). To solve this, deconvolution or curve fitting, a logical extension of interpolation method, can be used to fit all the data points within a peak to an appropriate function. It can be employed to partially overlapping line shape to determine the areas of individual signals contained within the composite profile. Deconvolution leads to far smaller relative errors in the estimation of peak areas compared with the numerical integration, as long the peak shapes that are Lorentzian or nearly Lorentzian (Weiss and Ferretti, 1983). Ideally, Lorentzian function (L(x)) (Equation 2.1) represents most of the NMR line shapes, notwithstanding the function can be modified into mixture of Lorentzian and Gaussian functions (G(x)) (Equation 2.2) in order to approximate the real experimental line shape adequately. This hybrid function (M(x)) is shown in Equation 2.3, as follows:

$$L(x) = \frac{h}{1+\left[\frac{x-x_0}{\frac{w}{2}}\right]^2} \tag{2.1}$$

$$G(x) = h\, e^{-\frac{2(x-x_0)^2}{w^2}} \tag{2.2}$$

$$M(x) = (2.0 - \alpha) \cdot L(x) + (\alpha - 1.0) \cdot G(x) \tag{2.3}$$

where h is the peak height, x_0 is the centre position of the peak, w is the full width taken at the half-height of the peak and α is the coefficient of mixing which lies in the range of 1.0-2.0.

2.2 Optimisation of NMR Data Acquisition Parameters

2.2.1 Materials

Triacylglycerol standards (minimum purity of 99%), namely, tripalmitoylglycerol (PPP), trioleoylglycerol (OOO) and trilinoleoylglycerol (LLL) were obtained from Sigma Chemical Company (St. Louis, Missouri). Crude palm oil was a gift from Malaysian Palm Oil Board Experimental Mill, Labu, Negeri Sembilan, Malaysia. Refined, bleached and deodorised (RBD) palm olein (iodine value, IV 56), shea butter, cocoa butter and mango olein were obtained from Intercontinental Specialty Fats Sdn. Bhd., Dengkil, Selangor, Malaysia. RBD soybean oil, rapeseed oil (canola), grapeseed oil, corn oil, rice bran oil, sunflower oil and olive oil were commercial samples obtained from local supermarkets. Mango fat and *Jatropha* oil were obtained using hexane extraction. Deuterated chloroform (minimum purity of 99.8%) was purchased from Merck (Darmstadt, Germany).

2.2.2 Sample Preparation

A synthetic mixture of triacylglycerol standards was prepared by mixing 99.9 mg of tripalmitoylglycerol (PPP), 248.8 mg of trioleoylglycerol (OOO) and 52.0 mg of trilinoleoylglycerol (LLL) and diluted with 1.0 mL of deuterated chloroform to produce a 2:5 (m/v) sample/solvent ratio. The molar percentages of PPP, OOO and LLL were 26.7, 60.6, and 12.7 mol%, respectively. Naturally occurring oil samples were preheated at 60 ℃ for 10 minutes to ensure sample homogeneity and then 0.2 g of the oil were dissolved in 0.5 mL of deuterated chloroform. All samples were degassed for 5 minutes by purging with inert nitrogen gas and lastly ultrasonicated for 1 minute. The volume of sample used in NMR analysis was set at 0.5 mL for achieving the best resolution.

2.2.3 Statistical Analysis

Results were expressed as means ± standard deviation. The spectroscopic data related to Nuclear Overhauser Enhancement (NOE) factors were analysed statistically by one-way analysis of variance (ANOVA). T_1 was subjected to two-way repeated-measures ANOVA with oil type and positional distribution of acyl chains as between-subject factors. Significant difference was deduced at P values of ≤ 0.05.

2.2.4 Instrumentation

All ^{13}C spectra were recorded at a spectrometer frequency of 100.40 MHz fitted with a 5-mm-i.d. dual probe. Free induction decay (FID) was processed in exponential window. No zero-filling and artificial cosmetic valued apodisation were employed during the processing of NMR data. A coefficient mixture ratio of 1:1 between Lorentzian and Gaussian functions was used in deconvolution, and subsequently optimised by a nonlinear least-square procedure to achieve the optimal values of the line shape parameters. All spectra were processed using Standard JEOL ALICE processing software. In the study of individual parameters, the other influencing acquisition parameters were set at the optimum condition.

2.2.4.1 Pulse Sequence

Both broadband decoupling and inverse gated heterodecoupling pulse sequences were employed for comparisons. JEOL LA-400 MHz spectrometer was utilised for the acquisition of ^{13}C NMR spectra of triacylglycerol standards, palm oil, soybean oil and olive oil, whereas JEOL ECA-400 MHz was employed for the measurement of soybean oil sample only. The ratio of peak intensities obtained under full Nuclear Overhauser Enhancement (NOE) to the NOE suppressed represented the NOE enhancement factors $(1 + \eta)$.

2.2.4.2 Repetition Time

^{13}C spin-lattice relaxation times (T_1) were measured using inversion recovery pulse sequence, by changing the τ values from 60.0 s to 0.1 s. The test oils were synthetic mixture of triacylglycerol standards, *Jatropha* oil, mango fat, grapeseed oil, olive oil, palm olein iodine value (IV) 56, soybean oil, rice bran oil, canola and sunflower oil.

2.2.4.3 Spectral Width

Regiospecific analysis on crude palm oil was conducted under the spectral widths of 18000 Hz (full spectrum) and 1500 Hz. A full spectral width was utilised for determining the exact chemical shifts of carbonyl carbons, prior to subsequent adjustment of narrower specific width. Once the spectral width was set, the transmitter offset frequency was positioned in the centre of the selected observation range.

2.2.4.4 Temperature

The study was performed on rapeseed oil (canola) at various experimental temperatures of 20, 30, 40 and 50 ℃. At temperature of 40 ℃, both manual and automated shimmings were employed to study the actual influencing factor on the peak width. The *cis*-9 monounsaturated carbonyl carbon resonance at the *sn*-1,3 positions was selected as the standard for multiple comparisons.

2.2.4.5 Other Acquisition Parameters

To obtain the optimum pulse angle, ^{13}C NMR spectra of rapeseed oil (canola) were recorded using 30 ° and 90 ° pulse angles, which corresponded to the pulse widths of 3.50 and 10.50 μs, respectively. On the other hand, NMR spectra of soybean oil were acquired by 4096, 8192 and 16384 data points for the multiple comparison. The time-domain signal, which is also known as free induction decay (FID) was observed.

Meanwhile, the effects of acquisition time on the resultant NMR spectrum were investigated using soybean oil at 5.4 s and 10.8 s. In order to obtain the ideal number of scans for a high-resolution NMR spectrum, the NMR spectra of rapeseed oil (canola) were recorded for 64, 128 and 256 transients.

2.2.5 Results and Discussion

2.2.5.1 The Effect of Pulse Sequence Selection

Numerous studies recommended that broadband decoupling pulse sequence, under full Nuclear Overhauser Enhancement (NOE) conditions, could be applied in the regiospecific analysis of triacylglycerols with the advantage of higher signal-to-noise (S/N) ratio in the resultant spectra (Vlahov, 1998; Vlahov *et al.,* 2010). This was accompanied by assumption that the intensities of carbonyl carbon resonances were being affected by proton decoupling to the same extent (Ng, 1985; Wollenberg 1990; Vlahov, 1998). Nevertheless, the reported NOE factors for the *sn*-1,3 positions were in the range of 1.73–1.78, whereas for the *sn*-2 position was in the range of 1.67-1.77 (Vlahov, 1998). Statistical analysis shows that the peak intensities at both positions brought by NOE are significantly different (P=0.05). Furthermore, our quick calculation shows that the intensity brought by such enhancements for both positions can differ up to 6%. On the other hand, due to the nature of quaternary carbons, carbonyl carbons in triacylglycerols experienced only weak NOE through space with protons in the closest vicinity during proton decoupling. Theoretically, the enhancement of S/N was not apparent.

Even though it is particularly important to engage heteronuclear NOE for S/N ratio improvement, it is not suitable for the current work. NOE was expected to be different for carbonyl carbons originated from the *sn*-1,3 and *sn*-2 positions due to the different

number of protons in closest vicinity (≤ 5 angstroms), as illustrated in Figure 2.1. Due to the slightly different chemical environment and the number of protons in closest vicinity, the heteronuclear NOE experienced by the carbonyl carbons at both *sn*-1,3 and *sn*-2 positions are expected to be different during proton irradiation.

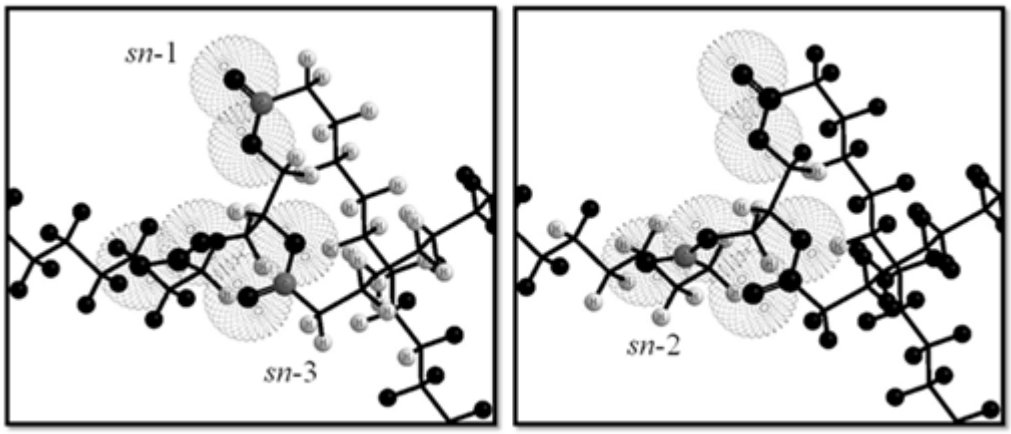

Notes:
Carbon-labelled atoms are carbonyl carbons at the *sn*-1, *sn*-2 or *sn*-3 position. Hydrogen-labelled atoms are protons located within 5 angstroms from the nearest carbonyl carbons. Total numbers of labelled protons are 29 and 15 for the *sn*-1,3 and *sn*-2 positions, respectively.

Figure 2.1 : Three dimensional illustration of carbonyl carbons in tripalmitoylglycerol (PPP)

Table 2.1 shows the NOE factors for four samples, namely, the synthetic mixtures of triacylglycerol standards, palm olein, rapeseed oil (canola) and soybean oil. The results show that the NOE factors for carbonyl carbons at the *sn*-1,3 and *sn*-2 positions differ significantly ($P<0.007$), whereas there is no significant difference found for the diverse degree of unsaturation in the acyl chain, oil source and also spectrometer at the similar magnetic field ($P>0.05$). Moreover, the NOE differs significantly ($P<0.04$) for different oils in conjunction with the distribution of fatty acids at different *sn*-positions (Table 2.1). Furthermore, NOE has very versatile behaviour depending on the temperature, magnetic field strength, solvent viscosity and molecular tumbling rate. These are the factors affecting the NOE throughout the experiment. Consequently, the actual NOE

factors may vary in different experiments and subjected to the condition of instrument or sample used, especially when the experimental temperature is not well-controlled. Thus, it might subject in indiscernible errors.

Table 2.1 : NOE (1+ η) factor for carbonyl carbons of triacylglycerols in selected oils

Oil Source	*sn*-1,3			*sn*-2		
	Saturated	Monounsaturated	Polyunsaturated	Saturated	Monounsaturated	Polyunsaturated
Triacylglycerol standards [a]	1.16	1.35	1.28	1.35	1.36	1.17
Palm oil [a]	1.36	1.33	1.11	1.50	1.29	1.24
Olive oil [a]	1.30	1.37	1.26	NA	1.13	1.05
Soybean oil [a]	1.27	1.56	1.39	NA	1.41	1.33
Soybean oil [b]	1.18	1.37	1.27	NA	1.01	1.05

Notes:
NA, not applicable; NOE factors are significantly differed between the *sn*-1,3 and *sn*-2 positions (P<0.007).
[a] Measurements were done by JEOL LA-400 MHz spectrometer.
[b] Measurement was done by JEOL ECA-400 MHz spectrometer.

As a result, inverse gated decoupling pulse sequence (Figure 2.2) is recommended in the current work of regiospecific analysis of triacylglycerols in order to quench the NOE. Additionally, it has an additional advantage of minimising sample heating and thus, suppressing the broadening effect to avoid loss of peak resolution, since the absence of proton irradiation during pulse delay will allow thermal equilibrium to be re-established before the next acquisition.

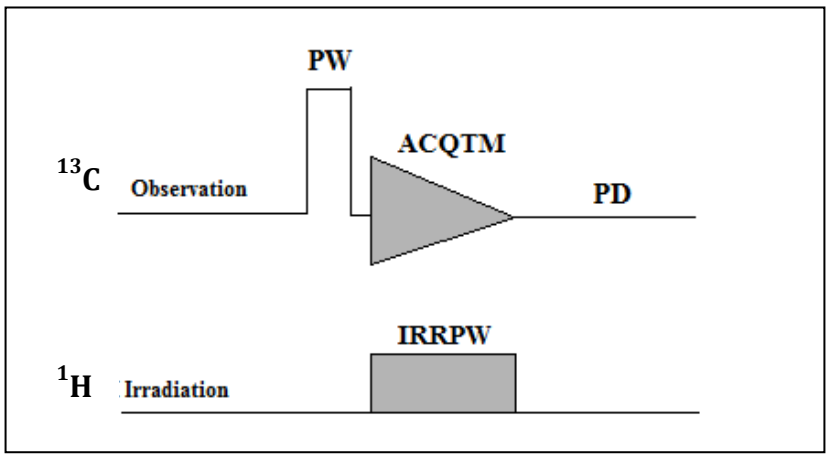

Notes:
NOE = Nuclear Overhauser Enhancement, ACQTM = acquisition time, PD = pulse delay, PW = observation pulse width, IRRPW = irradiation pulse width

Figure 2.2 : Pulse sequence of Single Pulse with Inverse Gated Heteronuclear Decoupling. ^{1}H decoupler was turned on during acquisition time only to suppress NOE

2.2.5.2 The Effect of Repetition Time

In the effort to achieve peak area which is proportional to the number of corresponding nuclei, all longitudinal magnetisation (M_z) has to be returned to equilibrium magnetisation (M_o) within the repetition time. The relationship between M_z, M_o, spin-lattice relaxation time (T_1), repetition time *t*, and pulse flip angle θ, is given in Equation 2.4.

$$\frac{M_z}{M_o} = \frac{1-exp^{-\frac{t}{T_1}}}{1-exp^{-\frac{t}{T_1}}cos\,\theta} \qquad (2.4)$$

An optimum repetition time was established by having the T_1 pre-determined through the inversion recovery pulse sequence. Therefore, the experimental data of T_1 for carbonyl carbons in triacylglycerol standards and various types of oils are determined and presented in Table 2.2. In a broad sense, carbonyl carbon, which is being grouped as quaternary carbon, is having relatively longer T_1 than any other protonated carbons

(primary, secondary and tertiary carbons), by virtue of the absence of a directly attached proton. Due to the higher mobility of carbon nuclei at the *sn*-1,3 positions, they possess significantly longer T_1 (P<0.01) as compared to that of the *sn*-2 position. There is no significant difference for the T_1 of carbonyl carbons at the same stereospecific numbering (P=0.07). The insignificant difference is also true even for different type of oils (P=0.10) (Table 2.2). The T_1 of carbonyl carbons reported in previous study (Vlahov, 1998) were slightly higher than T_1 measured here, since a higher magnetic field strength is employed in the present study. The chemical shift anisotropy, which is the major mechanism of spin lattice relaxation of carbonyl carbons, is field-dependent. It is expected that at higher field, T_1 of the carbonyl carbons will be shorter and therefore, the experiment can be repeated more rapidly.

Table 2.2 : T_1 relaxation times for carbonyl carbons of triacylglycerol in different type of oils and fats

Sample	T_1 (s)		
	Acyl chain	*sn*-1,3[b]	*sn*-2[b]
Triacylglycerol standards	Saturated	3.93 ± 0.20	2.90 ± 0.10
	Monounsaturated	3.64 ± 0.30	2.84 ± 0.21
	Polyunsaturated	3.52 ± 0.04	2.64 ± 0.05
Sunflower oil	Saturated	3.74 ± 0.33	NA
	Monounsaturated	3.60 ± 0.45	2.74 ± 0.04
	Polyunsaturated	4.18 ± 0.32	3.38 ± 0.10
Rapeseed oil (canola)	Saturated	4.32 ± 0.24	NA
	Monounsaturated	3.67 ± 0.31	3.02 ± 0.16
	Polyunsaturated	4.03 ± 0.20	3.02 ± 0.09
Rice bran oil	Saturated	3.62 ± 0.18	NA
	Monounsaturated	3.60 ± 0.03	2.81 ± 0.19
	Polyunsaturated	3.96 ± 0.09	3.38 ± 0.18
Soybean oil	Saturated	4.11 ± 0.22	NA
	Monounsaturated	3.90 ± 0.33	3.10 ± 0.17
	Polyunsaturated	4.62 ± 0.44	2.89 ± 0.09
Grapeseed oil	Saturated	4.26 ± 0.42	NA
	Monounsaturated	3.82 ± 0.30	3.10 ± 0.38
	Polyunsaturated	4.01 ± 0.48	3.32 ± 0.22
Palm olein IV56	Saturated	4.33 ± 0.12	2.96 ± 0.18
	Monounsaturated	3.97 ± 0.55	3.03 ± 0.15
	Polyunsaturated	4.62 ± 0.02	2.89 ± 0.35

Table 2.2, continued

Sample	T_1 (s)		
	Acyl chain	*sn*-1,3[b]	*sn*-2[b]
Mango fat	Saturated	4.33 ± 0.26	NA
	Monounsaturated	4.04 ± 0.10	2.74 ± 0.20
	Polyunsaturated	3.75 ± 0.11	2.60 ± 0.05
Olive oil	Saturated	3.90 ± 0.05	NA
	Monounsaturated	3.82 ± 0.06	3.05 ± 0.17
	Polyunsaturated	4.33 ± 0.33	2.89 ± 0.11
Jatropha oil	Saturated	4.18 ± 0.02	NA
	Monounsaturated	4.04 ± 0.51	2.86 ± 0.04
	Polyunsaturated	4.33 ± 0.29	3.18 ± 0.28

Notes:
NA, not applicable; IV, iodine value; Accuracies of T_1 are quoted as standard deviation of the mean of three replicates. T_1 are significantly differed between *sn*-1,3 and *sn*-2 positions (P<0.01).

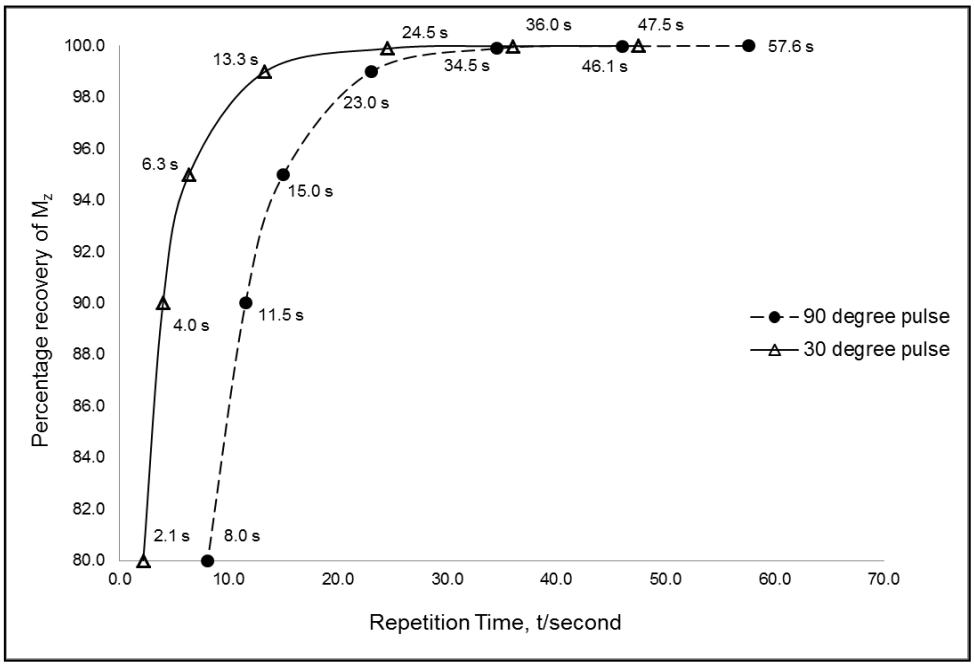

Notes:
Triangles and circles correspond to experiments with 30 ° and 90 ° pulse angle, respectively. The longest T_1 of carbonyl carbons is set at 5.0 seconds.

Figure 2.3 : Relationship between targeted accuracy and the minimum required repetition time, *t*

In Table 2.2, the longest T_1 was found to be 4.62 seconds in palm olein at 9.4 Tesla. Hence, 5.0 seconds is chosen as the longest T_1 for more general regiospecific analysis. With the aid of Equation 2.4, a correlation graph between the ratio of M_z/M_o and

repetition time, *t*, is plotted to illustrate the minimum repetition time required for achieving equilibrium at a given accuracy (Figure 2.3).

As depicted in Figure 2.3, in order to achieve 99% recovery of M_z after excitation by 90 ° pulse, the minimum repetition time must be at least 23.0 seconds (4.6 times of longest T_1). This figure will increase tremendously to 34.5 seconds (6.9 times of longest T_1) and 46.1 seconds (9.2 times of longest T_1) if targeted accuracies are set at 99.9% and 99.99% recovery of M_z, respectively. After the acquisition time, the sample also needs sufficient interval to achieve thermal equilibrium to prevent additional line broadening of resonances. Thus, adequate pulse delay is required to minimise unfavourable sample heating effects due to the proton decoupling during acquisition time (Pauli *et al.*, 2005; Pauli *et al.*, 2007). This also allows the complete suppression of Nuclear Overhauser Enhancement (NOE) which is evolved during the decoupling of protons. As a result, a repetition time of 34.5 seconds which is corresponding to 99.9% recovery, is recommended for a routine and practical regiospecific analysis of triacylglycerols by quantitative ^{13}C NMR (qCNMR) at 9.4 Tesla.

2.2.5.3 The Effect of Pulse Angle Selection

In quantitative NMR spectroscopy, 90 ° pulse is usually employed as it gives the maximum signal-to-noise (S/N) ratio. The major drawback is the lengthy repetition time required for the equilibrium magnetisation state to be re-established before the application of subsequent pulse. Consequently, Ernst angle (Pauli *et al.*, 2005) and flip angle smaller than 90 ° (Vlahov *et al.*, 2010) have been introduced in the quantitative solution state NMR analysis. In order to elucidate the optimum pulse angle for the current work, a comparison between 90 ° pulse and 30 ° pulse has been made.

As shown in Figure 2.3 (Section 2.2.5.2), repetition delays are required to achieve 99.9% recovery of longitudinal magnetisation (M_z) in equilibrium for 90 ° pulse and 30 ° pulse are 34.5 seconds and 24.5 seconds, respectively. For accumulation of 128 scans, the total experiment time will be 73.6 minutes using 90 ° pulse, whereas the analysis time is reduced to 52.3 minutes for 30 ° pulse. Within the expectation, the repetition time is dramatically reduced using a smaller pulse angle. However, such reduction is found to cause significant attenuation in the S/N. S/N ratios for the resultant spectrum acquired using 90 ° (Figure 2.4) and 30 ° pulses (Figure 2.5) are found to be 153:1 and 83:1, respectively.

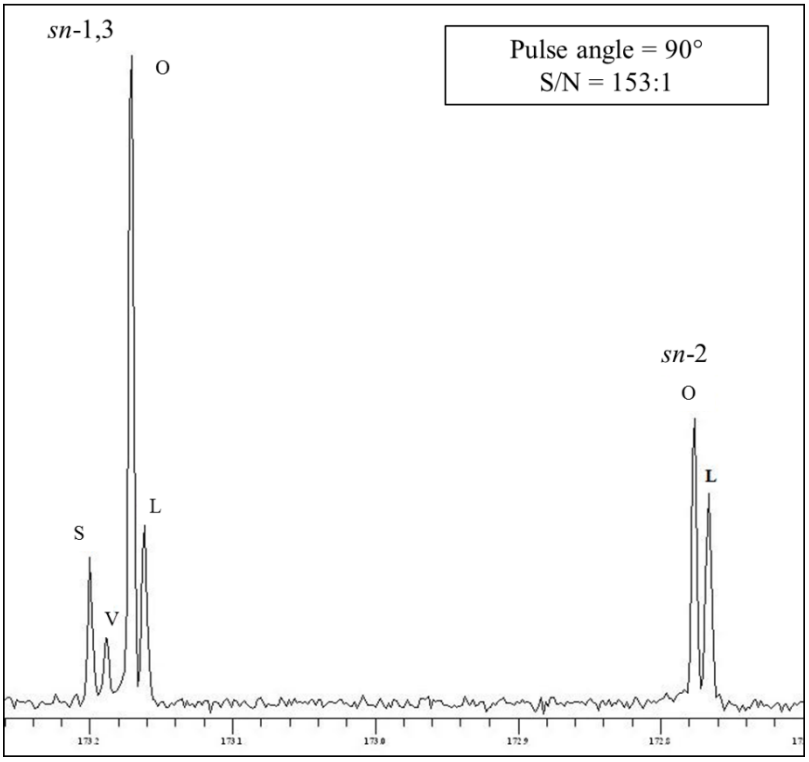

Notes:
S, saturated fatty acid acyl chain; V, *cis*-11 monoene fatty acid acyl chain; O, *cis*-9 monoene fatty acid acyl chain; L, polyunsaturated fatty acid acyl chain; S/N, signal-to-noise ratio.

Figure 2.4: ^{13}C NMR spectrum of carbonyl carbon resonances of triacylglycerols in canola (Pulse angle = 90 °)

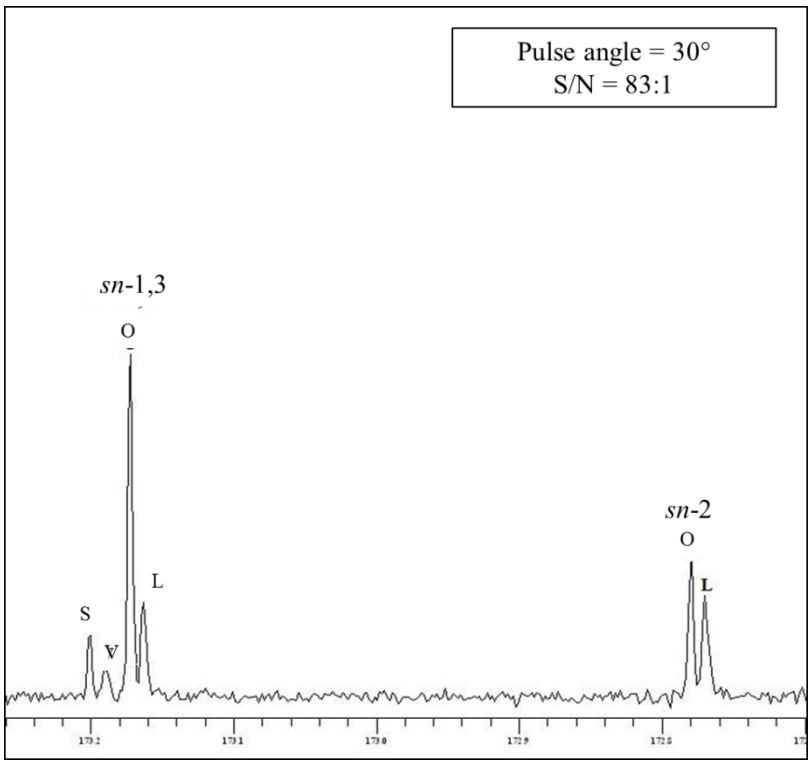

Notes:
S, saturated fatty acid acyl chain; V, *cis*-11 monoene fatty acid acyl chain; O, *cis*-9 monoene fatty acid acyl chain; L, polyunsaturated fatty acid acyl chain; S/N, signal-to-noise ratio.

Figure 2.5 : ^{13}C NMR spectrum of carbonyl carbon resonances of triacylglycerols in canola (Pulse angle = 30 °)

The equilibrium magnetisation M_o and transverse magnetisation M_y are related by

$$M_y = M_0 \sin\theta \exp^{-\frac{t}{T_2}} \quad (2.5)$$

T_2 is the spin-spin relaxation time. According to Equation 2.5, if the pulse angle is 30 °, the M_y detected is only 0.5 times of M_o, whereas for 90 °pulse angle, all of the initial M_o is converted into the detected M_y. Henceforth, the S/N ratio with 90 ° pulse is twice of that obtained with 30 °pulse, in which it is further affirmed in Figure 2.5. Therefore, for the experiment under employment of 30 ° pulse, the number of scans needs to be quadrupled since the increment of S/N is correlated by the square root of the number of signals taken. As a result, the total experiment time using 30 ° pulse will be 209.2 minutes, 2.8 times longer than that required by 90 °pulse.

Other researchers suggested the utilisation of Ernst angle in quantitative NMR in an effort to reduce the total experiment duration (Pauli *et al.*, 2005; Pauli *et al.*, 2007). Yet, this angle is maximising steady-state signal in a shorter repetition time, instead of achieving fully recovered magnetisation in equilibrium. The effort in obtaining a fully relaxed magnetisation during repetition time is not taken into consideration. For this reason, Ernst angle, which is usually smaller than 90 °, is favoured for structural elucidation, but not in quantitative ^{13}C NMR (qCNMR) regiospecific analysis.

2.2.5.4 The Effect of Spectral Width

A suitable spectral width can ensure the improvement of signal-to-noise (S/N) ratio, easier phasing and more accurate integration values. Figures 2.6 and 2.7 show the NMR spectrum acquired under spectral widths of 18000 Hz (full spectrum) and 1500 Hz, respectively. When the radio frequency excitation covered all types of carbon frequency range of triacylglycerols, the peak at δ172.76 ppm which pertained to polyunsaturated acyl chains at the *sn*-2 position could not be resolved from the resonance of *cis*-9-monoene acyl chain at δ172.77 ppm, as depicted in Figure 2.6. To solve this, a narrower spectral width of 1500 Hz (15 ppm) is set from 165 ppm to 180 ppm where the carbonyl carbons of acyl chains resonate (172-173 ppm), to ensure the better resolution (Figure 2.7).

In addition, the ideal spectral width should cover additional 7 ppm at a higher and lower field from the carbonyl carbon resonances so they will fall within 80% of the central part of filter bandwidth to prevent signal attenuation. The transmitter offset frequency is also positioned close to the position of signals of interest, so that the resonances will not experience a reduced flip angle, resulting in a smaller observed signal. Thus, the pulse

off-resonance and the signal attenuation by digital or analogue filter at the edges of the spectrum can be avoided.

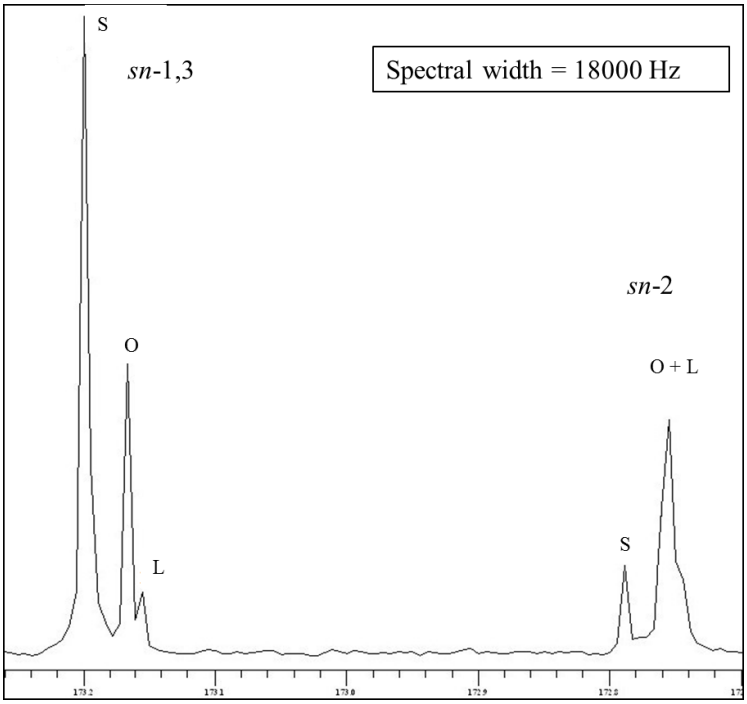

Notes:
S, saturated fatty acid acyl chain; O, monounsaturated fatty acid acyl chain (*cis*-9 monoene); L, polyunsaturated fatty acid acyl chain. A shoulder peak which was corresponding to the resonance of polyunsaturated acyl chain at *sn*-2 was observed.

Figure 2.6 : ^{13}C NMR spectrum of carbonyl carbon resonances of triacylglycerols in crude palm oil (Spectral width = 18000 Hz)

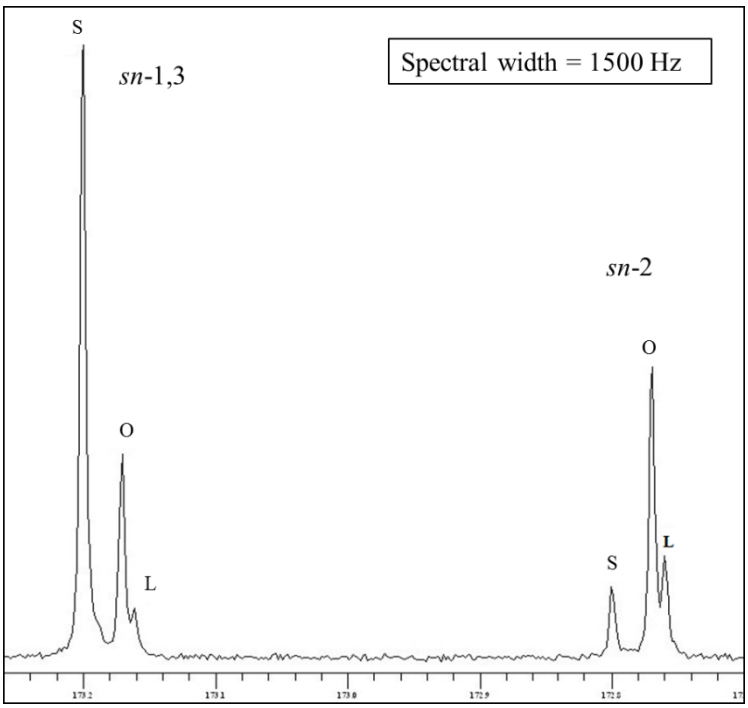

Notes:
S, saturated fatty acid acyl chain; O, monounsaturated fatty acid acyl chain (*cis*-9 monoene); L, polyunsaturated fatty acid acyl chain. Monounsaturated (*cis*-9-monoene) and polyunsaturated acyl chain resonances were well resolved.

Figure 2.7 : ^{13}C NMR spectrum of carbonyl carbon resonances of triacylglycerols in crude palm oil (Spectral width = 1500 Hz)

2.2.5.5 The Effect of Data Points

Data points are the extent of digitisation of the resultant NMR spectrum upon Fourier transformation. Figure 2.8(a), 2.8(b) and 2.8(c) show the Free Induction Decay (FID) obtained under data points of 4096, 8192 and 32768, respectively.

In Figure 2.8(a), data points of 4096 are shown to be insufficient for the fully decayed FID. This is further illustrated in frequency-domain signals of the resultant spectrum (Figure 2.9), in which the resonance corresponding to *cis*-11-monoene at the *sn*-1,3 positions totally diminished.

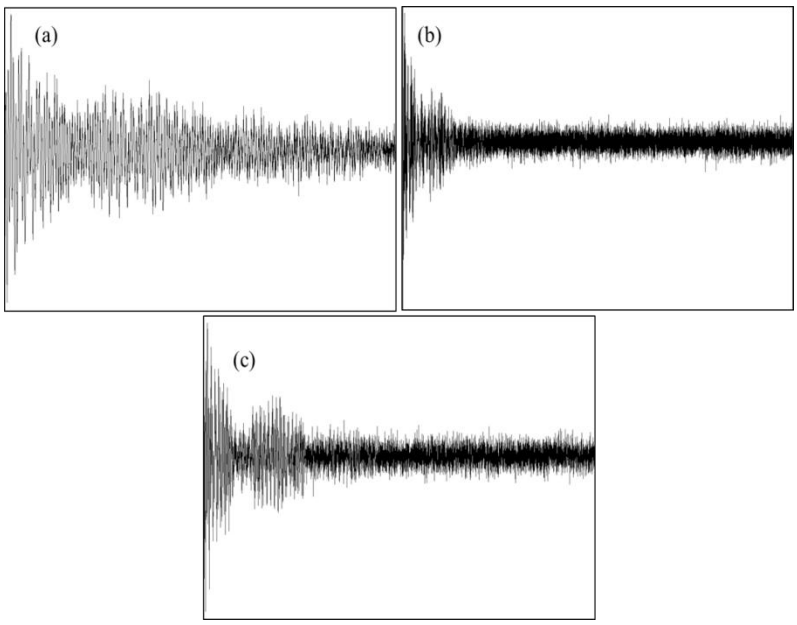

Figure 2.8 : Time-domain signals of ^{13}C NMR regiospecific analysis of soybean oil. The number of data points as varied as follows (a) data points = 4096, (b) data points = 16384 and (c) data points = 8192

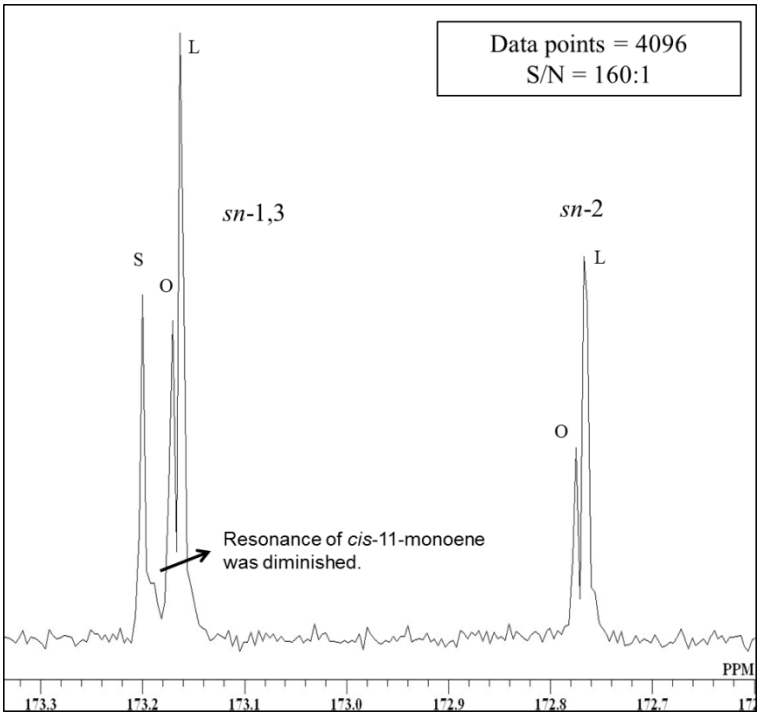

Notes:
S, saturated fatty acid acyl chain; O, *cis*-9 monoene fatty acid acyl chain; L, polyunsaturated fatty acid acyl chain; S/N, signal-to-noise ratio.

Figure 2.9 : ^{13}C NMR spectrum of carbonyl carbon resonances of triacylglycerols in soybean oil (Number of data points = 4096)

On the other hand, as depicted in Figure 2.8(b), excessive data points (16384 points) increased the noise-rich tail of the FID. As a result, signal-to-noise (S/N) ratio of the resultant spectrum dropped tremendously to 41:1 (Figure 2.10). Eventually, 8192 data points are being utilised as it is adequate for the FID to be fully decayed, while it will not yield excessive points for the development of undesirable noise (Figure 2.11). As the measurement is done under a narrower spectral width (1500 Hz) with lower number of points, the same resolution can still be attained compared with much wider spectral width and higher number of data points.

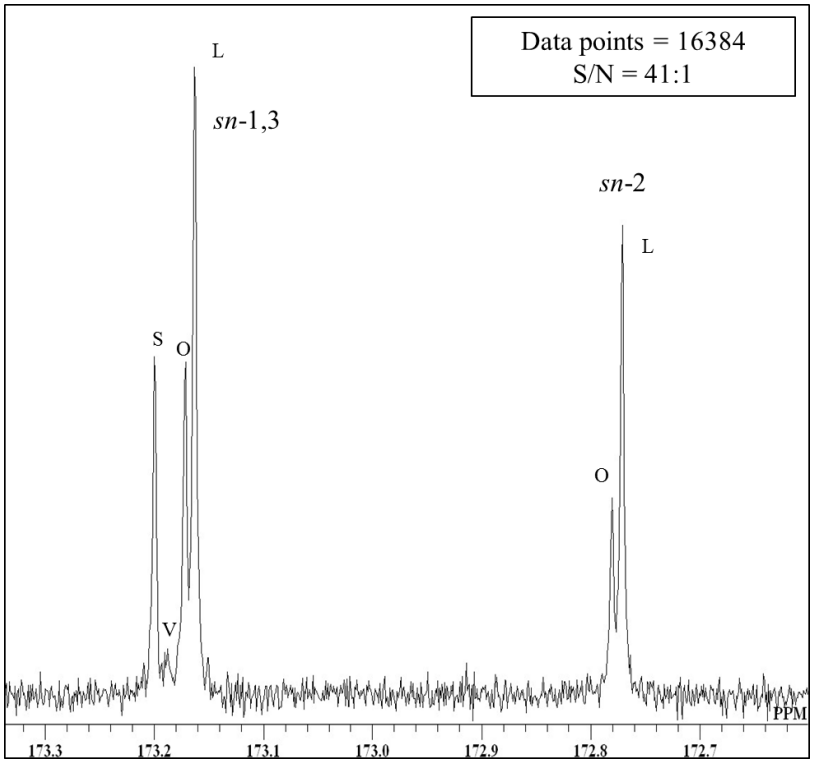

Notes:
S, saturated fatty acid acyl chain; V, *cis*-11 monoene fatty acid acyl chain; O, *cis*-9 monoene fatty acid acyl chain; L, polyunsaturated fatty acid acyl chain; S/N, signal-to-noise ratio.

Figure 2.10 : ^{13}C NMR spectrum of carbonyl carbon resonances of triacylglycerols in soybean oil (Number of data points = 16384)

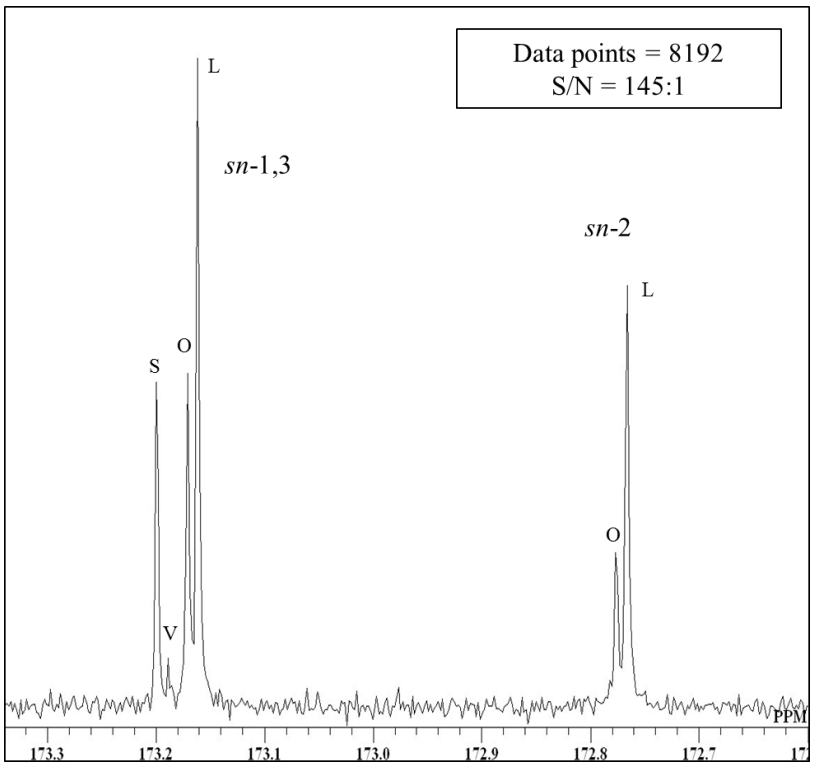

Notes:
S, saturated fatty acid acyl chain; V, *cis*-11 monoene fatty acid acyl chain; O, *cis*-9 monoene fatty acid acyl chain; L, polyunsaturated fatty acid acyl chain; S/N, signal-to-noise ratio.

Figure 2.11 : ^{13}C NMR spectrum of carbonyl carbon resonances of triacylglycerols in soybean oil acquired under optimum number of data points (8192)

2.2.5.6 The Effect of Acquisition Time

Due to the optimum setting of data points (8192) and spectral width (1500 Hz), the acquisition time is automatically being adjusted to 5.4 s. Previous study suggested that a longer acquisition time of 14.7 s was needed to achieve sufficient resolution (Vlahov, 1998). Thus, the influence of acquisition time was investigated in the present study and the results are given in Figure 2.12 and Figure 2.13.

Longer acquisition time (10.8 s) results in attenuation of signal-to-noise ratio (S/N) (135:1) and there is no improvement in resolution likely due to the collection of excessive noise and sample heating by decoupling over a longer period (Figure 2.12). Therefore, a short yet adequate acquisition time is highly recommended. When the

repetition time of single scan is reduced, the total experimental time of the carbonyl carbon resonances will also reduce. This is reflected by the reduction of 11.5 minutes in the total experimental time, when 5.4 s, instead of 10.8 s, is used as the acquisition time. With the selected acquisition time, digitisation of 0.18 Hz suffices to resolve the carbonyl carbons of triacylglycerols under different chemical environment. It is sufficiently long to allow the Free Induction Decay (FID) to decay and avoid truncation artefacts to ensure full spectral resolution.

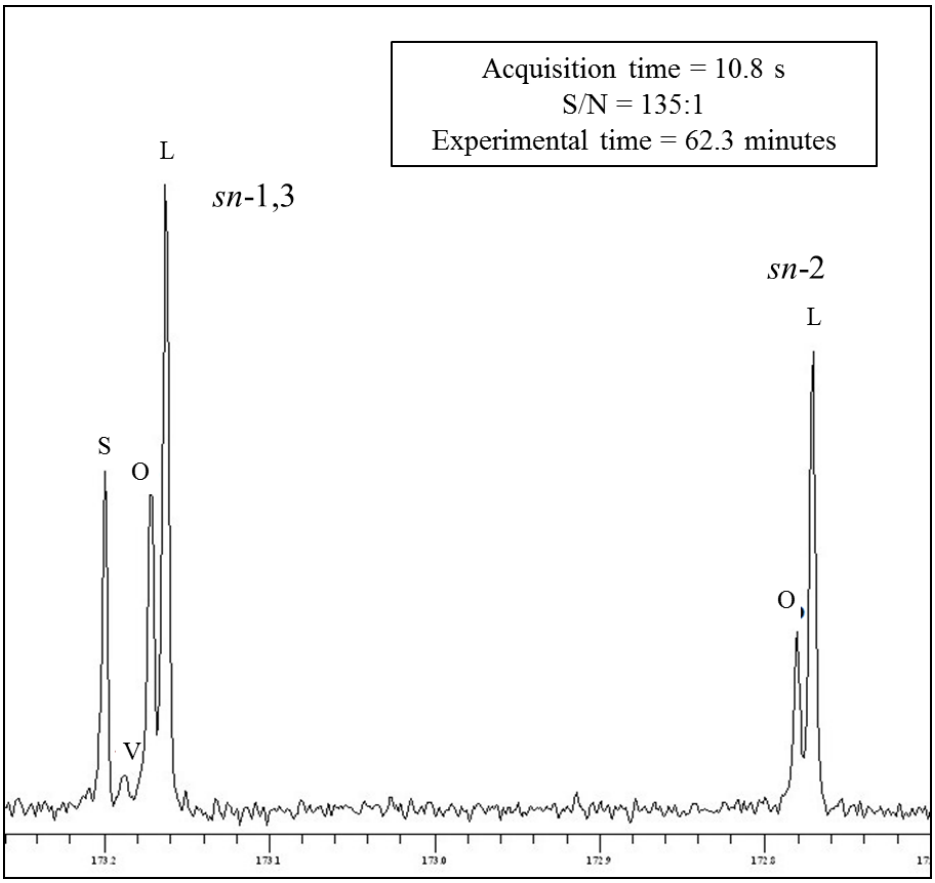

Notes:
S, saturated fatty acid acyl chain; V, *cis*-11 monoene fatty acid acyl chain; O, *cis*-9 monoene fatty acid acyl chain; L, polyunsaturated fatty acid acyl chain; S/N, signal-to-noise ratio.

Figure 2.12 : ^{13}C NMR spectrum of carbonyl carbon resonances of triacylglycerols in soybean oil (Acquisition time = 10.8 s)

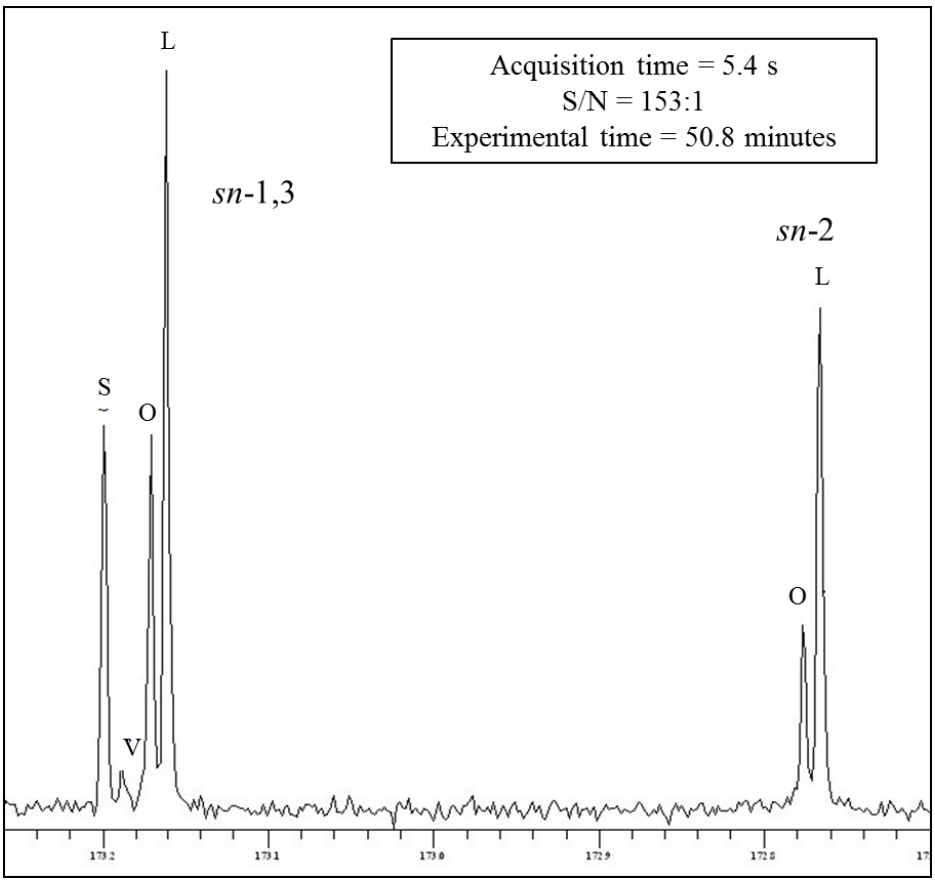

Notes:
S, saturated fatty acid acyl chain; V, *cis*-11 monoene fatty acid acyl chain; O, *cis*-9 monoene fatty acid acyl chain; L, polyunsaturated fatty acid acyl chain; S/N, signal-to-noise ratio.

Figure 2.13 : ^{13}C NMR spectrum of carbonyl carbon resonances of triacylglycerols in soybean oil (Acquisition time = 5.4 s)

2.2.5.7 The Effect of Experimental Temperature

Oil sample is generally viscous, especially at a higher sample concentration. Prior study suggested that high experimental temperature (50 ℃) was necessary to achieve good resolution in the resultant spectrum of carbonyl carbons (Ng, 1985). In an ideal case, when the temperature is elevated, the molecular motion will be faster and then it shortens the correlation time and consequently the relaxation becomes slower. Since line width is inversely proportional to spin-spin relaxation times (T_2), narrower lines are expected at higher temperature.

Yet in the present investigation using *cis*-9 monounsaturated carbonyl carbon resonance of rapeseed oil (canola) for multiple comparisons, there is no significant difference observed in peak width and signal-to-noise (S/N) ratio of the resultant spectrum when the experimental temperature was being elevated, as shown in Figure 2.14. The line width of the resonance was measured at half height of the corresponding peak. As the experimental temperature is elevated from 20 ℃ to 50 ℃, the S/N ratios remain comparable (153:1), while the smallest peak widths are found at 20 ℃ (0.31090 Hz) and 40 ℃ (0.31663 Hz). Nonetheless, the differences are not significant to cause any improvement. The resolution enhancement at a higher temperature (50 ℃) which was disclosed previously (Ng, 1985), is not observed in the present study.

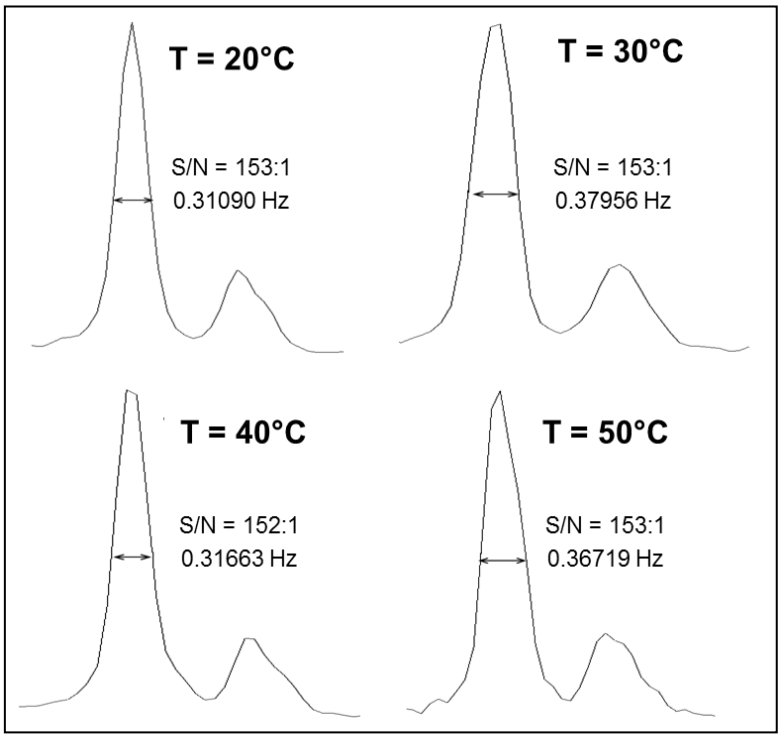

Notes:
S/N, signal-to-noise ratio.

Figure 2.14 : Effect of experimental temperature (T = 20 ℃, 30 ℃, 40 ℃ and 50 ℃) on peak width and S/N ratio of *cis*-9 monoene acyl chain carbonyl resonances of triacylglycerols in rapeseed oil (canola)

On the contrary, an increment of 0.16 Hz on the peak width and a depreciation of S/N ratio from 153:1 to 140:1 have been observed under automated shimming (Z1 and Z2 axial shims) instead of manual shimming, as depicted in Figure 2.15. The results suggest that the variation of peak width is dominated by the quality of shimming, but not dependent on the experimental temperature.

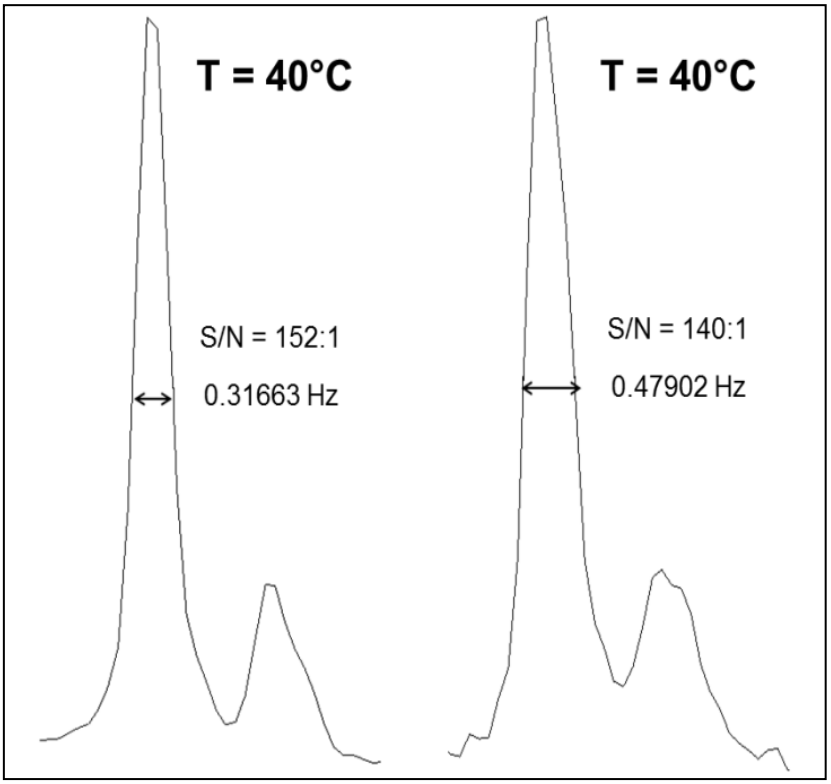

Notes:
Manual shimming is shown on the left whereas automatic shimming (Z1 and Z2 axial shims) is shown on the right. S/N, signal-to-noise ratio.

Figure 2.15 : Effect of shimming quality on peak width and S/N ratio of *cis*-9 monoene acyl chain carbonyl resonances of triacylglycerols in rapeseed oil (canola) at 40 ℃

In the event of measurement at an elevated temperature, substantial waiting time is mandatory prior to the sample shimming as to achieve desired temperature and thermal equilibrium. As a result, the experimental time is further delayed. On top of that, the superconducting magnet is more difficult to shim at higher temperature, especially at the temperature near the boiling point of deuterated solvent. In summary, the ^{13}C NMR

regiospecific analysis of triacylglycerols at room temperature, 25℃ (298 K), with the aid of temperature control, is preferred for routine measurement.

2.2.5.8 The Effect of Number of Scans

It is crucial to generate spectra that have high signal-to-noise (S/N) ratio to ensure precise measurements for quantitative analysis. Sensitivity of NMR spectrum is highly related to the concentration of sample. Consequently, a reasonably concentrated oil sample in deuterated chloroform (2:5 (m/v)) was used for all measurements. In the present study, the number of scans is optimised by varying the settings from 64, 128 to 256 scans, using a 400 MHz magnet and a 5 mm i.d. room-temperature probe of direct geometry.

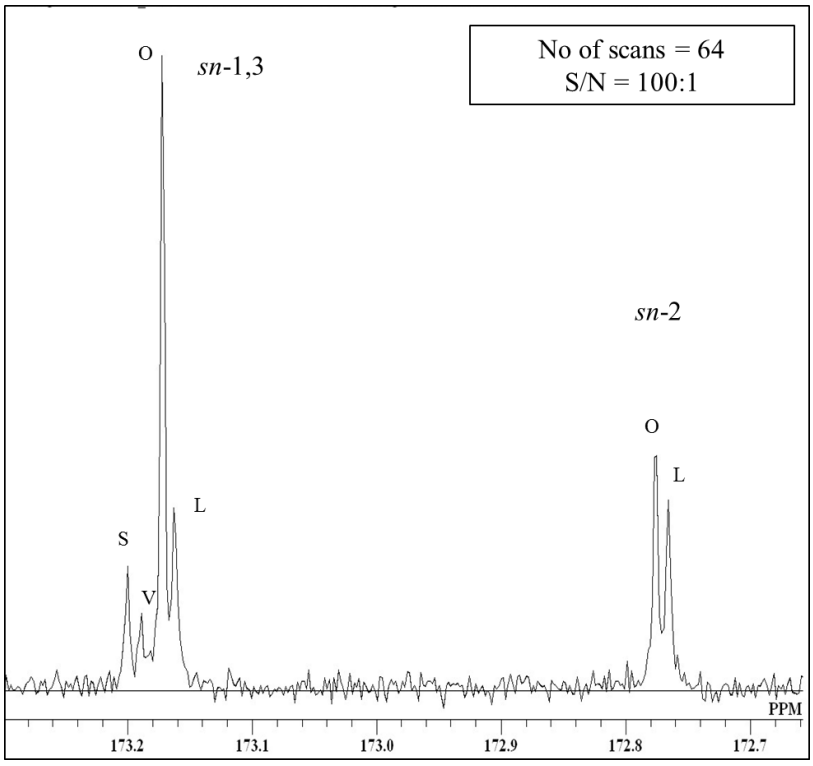

Notes:
S, saturated fatty acid acyl chain; V, *cis*-11 monoene fatty acid acyl chain; O, *cis*-9 monoene fatty acid acyl chain; L, polyunsaturated fatty acid acyl chain; S/N, signal-to-noise ratio.

Figure 2.16 : ^{13}C NMR spectrum of carbonyl carbon resonances of triacylglycerols in canola (Number of scans = 64)

As depicted in Figure 2.16, the S/N obtained after 64 scan times is shown to be 100:1. By increasing the scan times to 128 scans, there is a significant increment of S/N to 150:1 (Figure 2.17). In other words, the S/N ratio is enhanced 0.5 times of its initial value after increasing the scan times doubly. However, the S/N ratio does not increase greatly from 128 scans to 256 scans, *i.e.* the increment is found to be only 13.3% (Figure 2.18). Consequently, 128 scans are sufficient to achieve S/N of nearly 150:1 for a rapid and accurate regiospecific analysis as routine basis. Moreover, four steady state pulses (dummy scans) are preceded prior to the actual free induction decay (FID) data accumulation in order to establish an equilibrium condition throughout the NMR experiment.

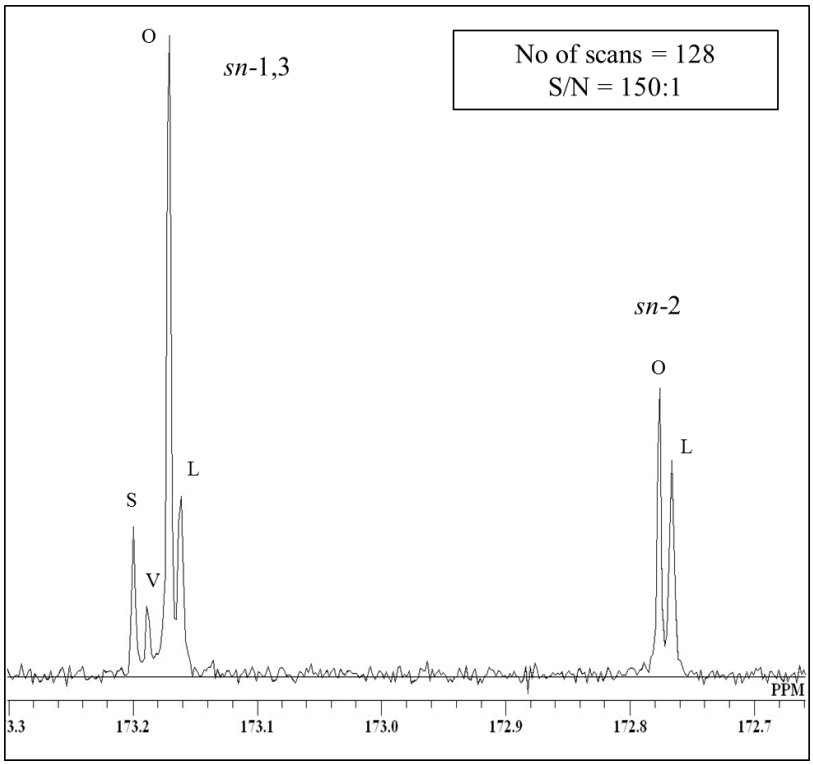

Notes:
S, saturated fatty acid acyl chain; V, *cis*-11 monoene fatty acid acyl chain; O, *cis*-9 monoene fatty acid acyl chain; L, polyunsaturated fatty acid acyl chain; S/N, signal-to-noise ratio.

Figure 2.17 : ^{13}C NMR spectrum of carbonyl carbon resonances of triacylglycerols in canola (Number of scans = 128)

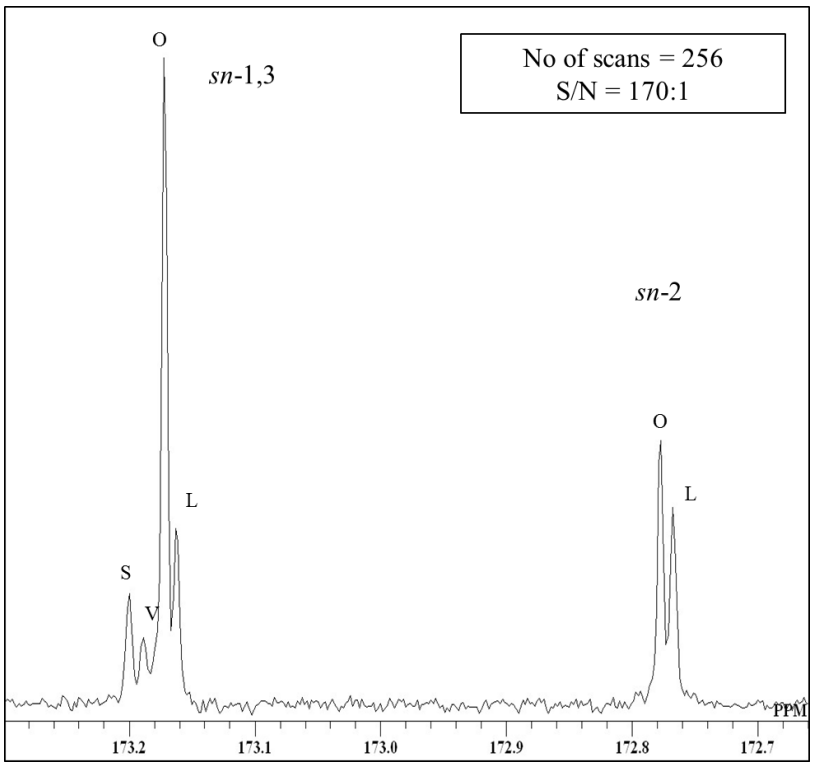

Notes:
S, saturated fatty acid acyl chain; V, *cis*-11 monoene fatty acid acyl chain; O, *cis*-9 monoene fatty acid acyl chain; L, polyunsaturated fatty acid acyl chain; S/N, signal-to-noise ratio.

Figure 2.18 : ^{13}C NMR spectrum of carbonyl carbon resonances of triacylglycerols in canola (Number of scans = 256)

2.3 Optimisation of NMR Data Processing Parameters

2.3.1 Sample

All lipid samples were prepared according to Section 2.2.2. Rapeseed oil (canola) was used as the test oil for the determination of smoothing algorithm, while the synthetic mixture of triacylglycerol standards was employed for the optimisation of remaining processing parameters.

2.3.2 Instrumentation

All NMR acquisition parameters were set at the optimum conditions, as described in Section 2.2. Standard JEOL ALICE processing software was used for all post-

processing. In the study of individual parameter, the other influencing processing parameters were set at the optimum condition, as described in the following sections.

2.3.2.1 Zero Filling

^{13}C spectrum was subjected to with and without zero filling. The accuracies of results were examined by comparing with the known composition of synthetic triacylglycerol mixture. This investigation was done in five replications to eliminate standard errors.

2.3.2.2 Apodisation

Free induction decay (FID) was processed in exponential window. By varying the broadening factors at 0.0 Hz, 0.1 Hz, 0.2 Hz and 0.4 Hz prior to the Fourier transformation, the accuracies of results were accessed by comparing to the known composition of synthetic triacylglycerol mixture. This investigation was done in five replications.

2.3.2.3 Smoothing Algorithm

The carbonyl carbon region in ^{13}C NMR spectrum of rapeseed oil (canola) was used to study the effect of smoothing algorithm on the quality of resultant spectrum. A 9-point weighted Savitzky-Golay signal smoothing was used for comparisons.

2.3.2.4 Integration Method

Deconvolution/curve fitting had been employed to quantify the individual resonances of carbonyl carbons of triacylglycerol standards by pure Lorentzian function, pure Gaussian function as well as hybrid function of Lorentzian and Gaussian functions at 1:1 ratio. The accuracy of the integration methods were accessed by the known composition of synthetic mixture of triacylglycerol standards.

2.3.3 Results and Discussion

2.3.3.1 The Effect of Zero Filling

Due to aforementioned prior literature (Nadjari and Grivet, 1991; Mcleod and Comisarow, 1989; Abildgaard *et al.*, 1988), concrete justification need to be done in the practical regiospecific analysis of triacylglycerols by quantitative ^{13}C NMR (qCNMR). In the analysis of synthetic mixture of triacylglycerols (Table 2.3), one level of zero filling is found to yield low repeatability and precision, as indicated by the wide-ranging standard deviation (0.8 mol% – 2.6 mol%), compared with those obtained in the absence of zero filling (0.3 mol% – 0.8 mol%). This artificial data processing has caused greater systematic errors and unrepeatability. On condition that the data points are sufficient for Free Induction Decay (FID) to be fully decayed, zero filling should be omitted.

Table 2.3 : Study of the effect of zero filling on the accuracy and precision of qCNMR regiospecific analysis of synthetic triacylglycerol mixture

Carbonyl carbon signals	Composition (mol%)		
	Without zero filling	After one level of zero filling	Actual (by synthetic mixing)
sn-1,3			
Saturated	26.2 ± 0.8	27.0 ± 1.3	26.7
Monounsaturated	61.1 ± 0.3	59.3 ± 2.6	60.6
Polyunsaturated	12.7 ± 0.8	13.7 ± 1.8	12.7
sn-2			
Saturated	25.5 ± 0.2	27.0 ± 1.0	26.7
Monounsaturated	60.2 ± 0.5	60.0 ± 1.4	60.6
Polyunsaturated	14.3 ± 0.7	13.0 ± 0.8	12.7
Overall			
Saturated	26.0 ± 0.6	27.0 ± 1.1	26.7
Monounsaturated	60.8 ± 0.3	59.5 ± 2.2	60.6
Polyunsaturated	13.2 ± 0.8	13.5 ± 1.4	12.7

Notes:
Values are mean of five replicates ± standard deviation on the same free induction decay (FID).

2.3.3.2 The Effect of Broadening Factor in Exponential Apodisation

By definition, apodisation is the process of multiplying the time-domain signal or Free Induction Decay (FID) by a mathematical or window function prior to the Fourier transformation. As all FID are supposed to decay exponentially with time, the exponential tends to be the ideal window function in the data processing of quantitative ^{13}C NMR (qCNMR).

Under the exponential window function, line broadening factor can be utilised to enhance the signal-to-noise (S/N) ratio, but at the expense of peak resolution. Too large line broadening factor (*e.g.* 1 Hz or more) will not permit the observation of individual resonances. Table 2.4 shows the errors in the results of the synthetic mixture of triacylglycerols with known composition, which are caused by different extent of line broadening. After the application of line broadening, the standard deviations fall in the range of 0.7 – 4.8 mol%. Apart from the depreciation of the precision, the accuracy also dropped tremendously if a higher extent of line broadening was employed. This is observed in the composition of mono- and polyunsaturated carbonyl carbon resonances, compared with the actual values in the synthetic mixture. Under 0.2 Hz and 0.4 Hz factors of line broadening, the mono- and polyunsaturated carbonyl carbon resonances are poorly resolved, which subsequently reduced the accuracy of quantitative results (deviation about 10 mol%). As a consequence, artificial data processing methods which aim to improve spectral resolution or S/N ratio are highly recommended to be fully omitted for an accurate regiospecific analysis of triacylglycerols. The alteration of peak area or resolution must be minimised in order to maintain the originality and unbiased quantitative information.

Table 2.4 : Study of the line broadening effect on the accuracy and precision of qCNMR regiospecific analysis of synthetic triacylglycerol mixture

Carbonyl carbon signal	Composition (mol%)				
	LB factor 0.0 Hz	LB factor 0.1 Hz	LB factor 0.2 Hz	LB factor 0.4 Hz	Actual (by synthetic mixing)
sn-1,3					
Saturated	26.2 ± 0.8	25.7 ± 3.5	26.7 ± 3.4	26.4 ± 3.0	26.7
Monounsaturated	61.1 ± 0.3	62.4 ± 2.6	59.5 ± 3.3	53.2 ± 3.1	60.6
Polyunsaturated	12.7 ± 0.8	11.9 ± 1.5	13.8 ± 1.1	20.4 ± 2.5	12.7
sn-2					
Saturated	25.5 ± 0.2	29.5 ± 2.1	28.4 ± 0.7	26.1 ± 2.0	26.7
Monounsaturated	60.2 ± 0.5	60.0 ± 1.5	54.5 ± 2.9	50.2 ± 3.0	60.6
Polyunsaturated	14.3 ± 0.7	10.5 ± 0.8	17.1 ± 2.5	23.8 ± 4.8	12.7
Overall					
Saturated	26.0 ± 0.6	26.9 ± 2.2	27.1 ± 2.4	26.3 ± 2.7	26.7
Monounsaturated	60.8 ± 0.3	61.6 ± 1.8	58.0 ± 2.6	52.2 ± 2.2	60.6
Polyunsaturated	13.2 ± 0.8	11.5 ± 0.9	14.8 ± 1.4	21.5 ± 2.9	12.7

Notes:
LB, line broadening; Values are mean of five replicates ± standard deviation on the same free induction decay, which was processed in exponential window function.

2.3.3.3 The Effect of Smoothing Algorithm

Figures 2.19 and 2.20 show the ^{13}C NMR spectra obtained before and after application of 9-point weighted Savitzky-Golay signal smoothing, respectively. As shown in Figure 2.20, artefact peak is found adjacent to the *cis*-9 monoene resonance at the *sn*-2 region, whereas the distortion of peak areas are noted severely at the *sn*-1,3 resonances, after the application of data smoothing using data processing software. The removal of some important data points in such process is unavoidable, causing the loss or distorted quantitative data. As a result, smoothing algorithm should not be applied in the processing of quantitative data even if the signal-to-noise (S/N) ratio of the spectrum can be enhanced.

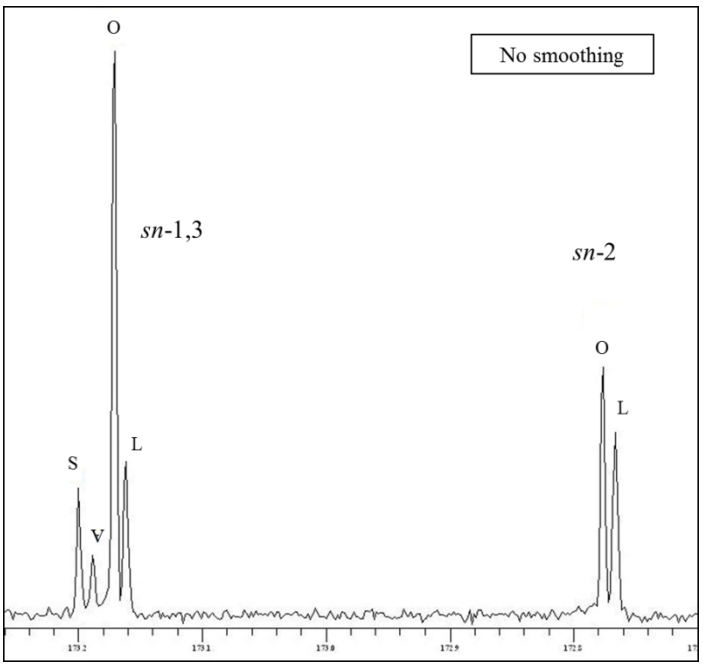

Notes:
S, saturated fatty acid acyl chain; V, *cis*-11 monoene fatty acid acyl chain; O, *cis*-9 monoene fatty acid acyl chain; L, polyunsaturated fatty acid acyl chain; S/N, signal-to-noise ratio.

Figure 2.19 : ^{13}C NMR spectrum of carbonyl carbon resonances of triacylglycerols in rapeseed oil (canola) (No smoothing)

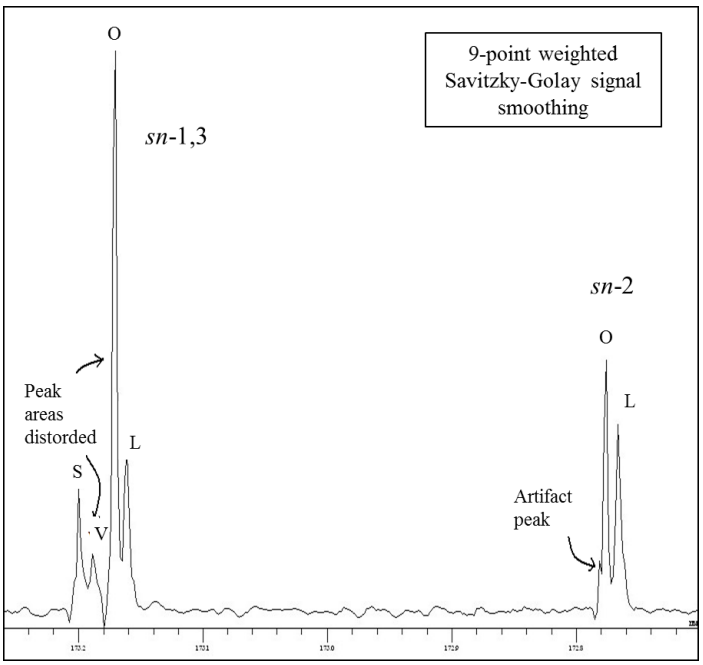

Notes:
S, saturated fatty acid acyl chain; V, *cis*-11 monoene fatty acid acyl chain; O, *cis*-9 monoene fatty acid acyl chain; L, polyunsaturated fatty acid acyl chain; S/N, signal-to-noise ratio.

Figure 2.20 : ^{13}C NMR spectrum of carbonyl carbon resonances of triacylglycerols in rapeseed oil (canola) (after 9-point weighted Savitzky-Golay signal smoothing)

2.3.3.4 The Effect of Waveform Function in Deconvolution

In the present method, deconvolution or curve fitting, a logical extension of the interpolation method, is used to fit all data points within a peak according to an appropriate function (Figure 2.21). It can be employed to separate partially overlapped line shape to determine the areas of individual signals contained within the composite profile, as shown in the separation waveform (Figure 2.21). When the theoretical line-shape function (synthetic waveform) is deviated from the observation waveform, a general nonlinear least-squares optimisation procedure is required to find the optimal values of the line-shape parameters, namely, the height, width and centre position of peak. As shown in the same figure, the difference waveform is kept as minimum as possible during the optimisation process.

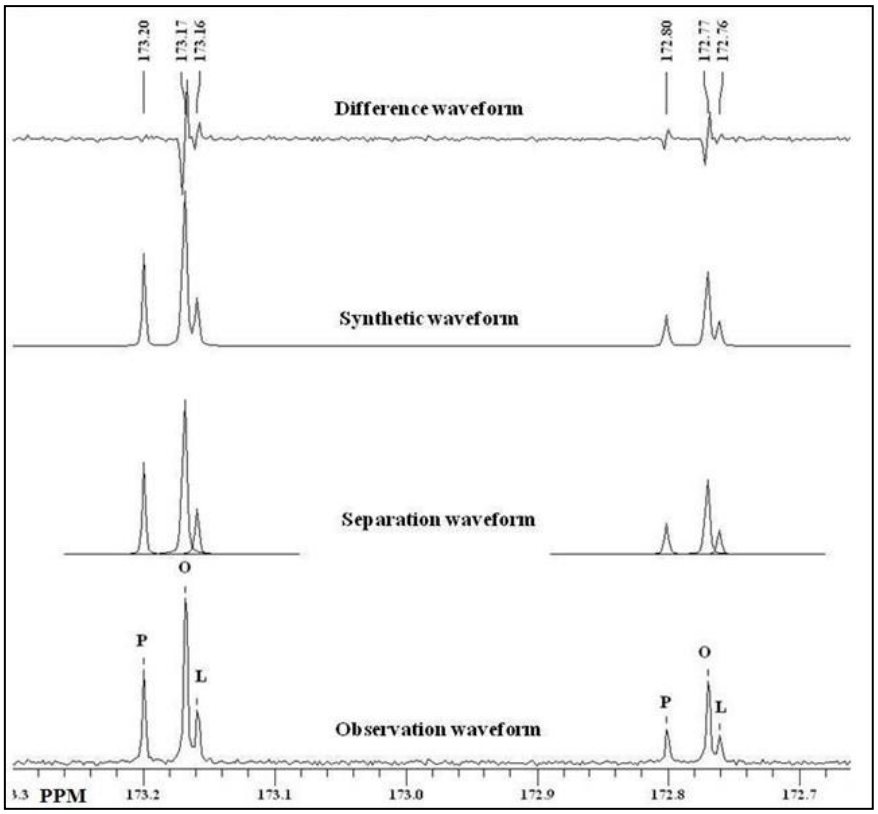

Notes:
P, palmitoyl fatty acid acyl chain; O, oleoyl fatty acid acyl chain; L, linoleoyl fatty acid acyl chain.

Figure 2.21 : ^{13}C NMR spectrum of acyl chain carbonyl resonances of synthetic triacylglycerol mixture. Curve fitting was used as the integration method

In the present study, a ratio of 1:1 mixture of Lorentzian and Gaussian function is found to produce the most accurate data in the analysis of the known concentration of synthetic triacylglycerol mixtures, with errors below 0.5 mol%. Figure 2.22 illustrates the different waveforms produced by pure Lorentzian, pure Gaussian and hybrid function between Lorentzian and Gaussian in 1:1 ratio. It is noted that the actual observation spectrum deviated from the ideal NMR Lorentzian line shape. The above-mentioned deviation leads to errors up to 4.3 mol%, whereas pure Gaussian function is found to yield errors from 2.3 to 7.0 mol%, as shown as in Table 2.5. By engaging the hybrid function, regiospecific results obtained within the same Free Induction Decay (FID) data display a high repeatability of less than 1% error.

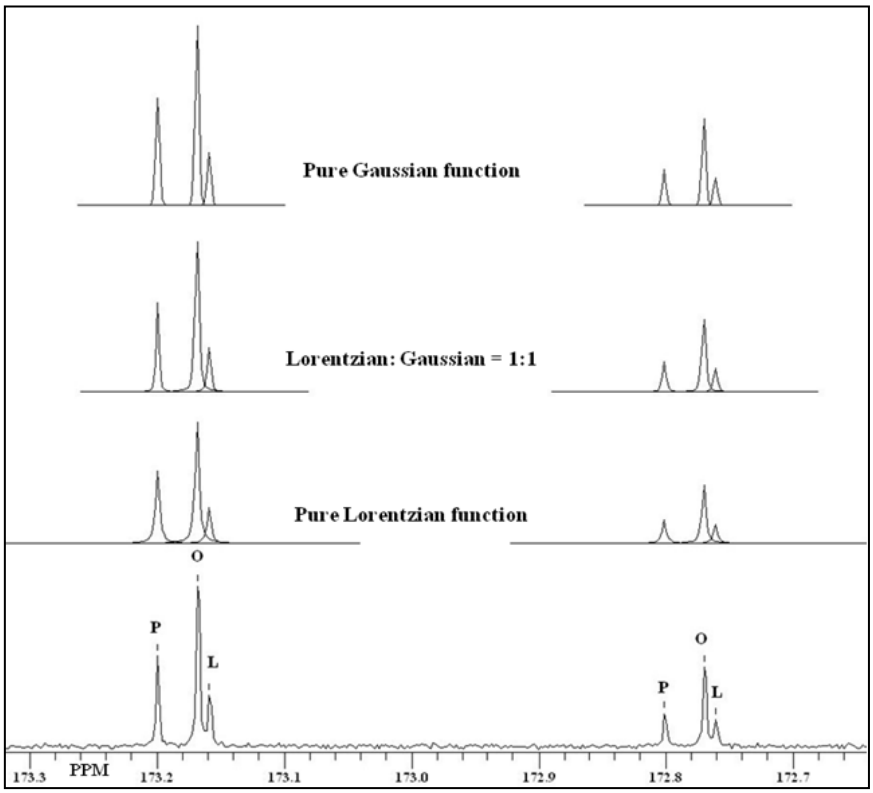

Notes:
P, palmitoyl fatty acid acyl chain; O, oleoyl fatty acid acyl chain; L, linoleoyl fatty acid acyl chain.

Figure 2.22 : Waveforms produced by using different curve fitting function in deconvolution of carbonyl carbon resonances of synthetic triacylglycerol mixture

Table 2.5 : Comparison of different curve fitting function in processing of regiospecific data of synthetic triacylglycerol mixture

Function	Acyl group	Composition (mol%)			
		Experimental (measurement using ^{13}C NMR)			Actual (by synthetic mixing)
		sn-1,3	*sn*-2	*sn*-1,2,3	
Pure Lorentzian	Palmitoyl (C16:0)	22.4 ± 0.1	22.9 ± 0.1	22.6 ± 0.1	26.7
	Oleoyl (C18:1)	63.3 ± 0.3	63.1 ± 0.8	63.2 ± 0.5	60.6
	Linoleoyl (C18:2)	14.3 ± 0.4	14.0 ± 0.2	14.2 ± 0.2	12.7
Lorentzian : Gaussian Mixing ratio 1:1	Palmitoyl (C16:0)	26.5 ± 0.1	26.2 ± 0.9	26.4 ± 0.4	26.7
	Oleoyl (C18:1)	60.9 ± 0.7	61.1 ± 0.4	61.0 ± 0.4	60.6
	Linoleoyl (C18:2)	12.6 ± 0.8	12.8 ± 0.6	12.7 ± 0.7	12.7
Pure Gaussian	Palmitoyl (C16:0)	23.0 ± 0.6	22.1 ± 0.3	22.7 ± 0.4	26.7
	Oleoyl (C18:1)	57.6 ± 0.2	58.3 ± 0.1	57.8 ± 0.2	60.6
	Linoleoyl (C18:2)	19.4 ± 0.1	19.7 ± 0.1	19.5 ± 0.1	12.7

Notes:
Values are mean of five replicates ± standard deviation on the same free induction decay.

2.4 Application on Naturally Occurring Oils and Fats

2.4.1 Experimental

2.4.1.1 Materials

Crude palm oil was a gift from Malaysian Palm Oil Board Experimental Mill, Labu, Negeri Sembilan, Malaysia. Refined, bleached and deodorised (RBD) high-oleic sunflower oil, shea butter, cocoa butter, mango fat and mango olein were obtained from Intercontinental Specialty Fats Sdn. Bhd., Dengkil, Selangor, Malaysia. RBD sal stearin was obtained from Mewah Oil Sdn. Bhd., Pulau Lumut, Selangor, Malaysia. RBD

peanut oil, sesame oil, Avogadro oil, walnut oil, flaxseed oil, coconut oil, soybean oil, rapeseed oil (canola), corn oil, rice bran oil, sunflower oil and olive oil were commercial samples obtained from the local supermarkets. Moringa oil and *Jatropha* oil were obtained using Soxhlet extraction while Menhaden fish oil was procured from Sigma Chemical Company (St. Louis, Missouri). Deuterated chloroform (minimum purity of 99.8%) was purchased from Merck (Darmstadt, Germany).

2.4.1.2 Sample Preparation

Naturally occurring oil samples were preheated at 60 ℃ for 10 minutes to ensure sample homogeneity. All oil samples were then diluted with deuterated chloroform to produce a 2:5 (m/v) sample/solvent ratio, degassed for 5 minutes and eventually subjected to 1-minute ultrasonication. The volume of sample used in NMR analysis was set at 0.5 mL.

2.4.1.3 ^{13}C NMR Spectroscopy

^{13}C NMR spectra were recorded using a JEOL LA-400 MHz spectrometer fitted with a 5-mm-i.d. dual probe ^{13}C/^{1}H carefully tuned at the recording frequency of 100.40 MHz. The proton decoupled ^{13}C spectra were acquired using the inverse gated heterodecoupling sequence. A spectral width of 1500 Hz in the region of acyl chain carbonyl carbon resonances was employed. 8192 data points, 90 ° pulse and 5.4 s acquisition times were used. Total repetition delay was set at 34.5 s. All spectra were acquired with 128 scans at 298.15 K. Free induction decay (FID) was processed in exponential window. No zero-filling and artificial cosmetic valued apodisation were employed. A coefficient mixture ratio of 1:1 between Lorentzian and Gaussian functions was used in deconvolution, and subsequently optimised by a nonlinear least-square procedure. Standard JEOL ALICE processing software was used for all post-

processing. All the above measurement parameters and data processing methods are established from studies presented in previous section.

2.4.1.4 Gas Chromatography

Total fatty acid compositions of oils and fats were conducted using gas chromatography (GC). All oils and fats samples were derivatised to methyl esters in accordance with a method reported by Christie (1989). A 50 mg of oil sample was weighed and dissolved in dry toluene (1 mL) into a 50 mL round bottom flask. Then, 2 mL of 0.5 M sodium methoxide in anhydrous methanol was added into sample, and the mixture was maintained at 50 ℃. After 20 minutes of reaction, 0.1 mL of glacial acetic acid and 5 mL of water were added in sequence to quench the reaction. The required methyl esters were extracted into hexane, and then pure methyl esters could be obtained after the removal of solvent under reduced pressure.

Methyl esters sample (1 μL) was injected into GC (Shidmadzu, GC-2010A series) equipped with a flame ionisation detector and a BPX70 capillary column of 30 m x 0.32 mm i.d.. An initial temperature of 140 ℃ was held for 2 minutes, which was then increased at 8 ℃ per minute to 220 ℃. The column was held at the final temperature for another 5 minutes. The oven, injector and the detector ports were set at 140 ℃, 240 ℃ and 260 ℃, respectively. The carrier gas was helium with column flow rate of 1.10 mL per minute at a 50:1 split ratio.

2.4.2 Results and Discussion

2.4.2.1 Application on Oils with Distinctive Fatty Acid Profile

In contrast to the synthetic triacylglycerol mixture, naturally occurring oils and fats are generally complex matrixes consisting of minor components, such as tocopherols,

tocotrienols, phospholipids, sphingolipids, squalene, carotenoids and chlorophyll (Gunstone and Harwood, 2007). The peak resolution and signal-to-noise (S/N) ratio of ^{13}C NMR spectrum will be affected by this complexity. On the other hand, the applicability and repeatability of NMR regiospecific analysis may be questionable for different types of oils and fats due to their different physical appearance. However, it is pleasantly found that the current developed NMR parameters are highly versatile and definitely not 'a tailored-made" conditions for the synthetic mixture but can be applied to oil samples with diverse unsaturation and saturation levels. Three major fatty acid profiles in triacylglycerols will be illustrated in the present study, namely, unsaturated-unsaturated-unsaturated (UUU), saturated-unsaturated-saturated (SUS) and saturated-saturated-saturated (SSS).

Figure 2.23 shows the carbonyl carbon region in ^{13}C NMR spectrum of canola with fatty acid profile of UUU. Canola contains only 11.1 mol% of saturated fatty acids at the *sn*-1,3 positions, and none at the *sn*-2 position. Due to the nature of high unsaturation content, canola exists as highly liquefied oil at room temperature regardless of the duration of storage. Consequently, this nature does not impose any complications on the liquid-state ^{13}C NMR analysis. Besides that, ^{13}C NMR had an advantage over gas chromatography (GC) method in the isolation of *cis*-11-monoenes, mainly *cis*-vaccenic (11*c*-18:1) and eicosenoic acid (11*c*-20:1) (Ng & Koh, 1988; Scano *et al.*, 1999), from other *cis*-9-moenes due to its steric interactions with the glycerol carbons and the linear electric field effect of the double bond. *Cis*-vaccenic was a common fatty acid in the microorganisms and animal tissues, notwithstanding its presence in vegetable oils had not been well investigated due to its relatively low abundance and limitation of the conventional analytical procedures. From the current analysis, we show that canola

contains about 5.5 mol% of *cis*-11-monoene at the *sn*-1,3 positions of triacylglycerols, as illustrated in Figure 2.23.

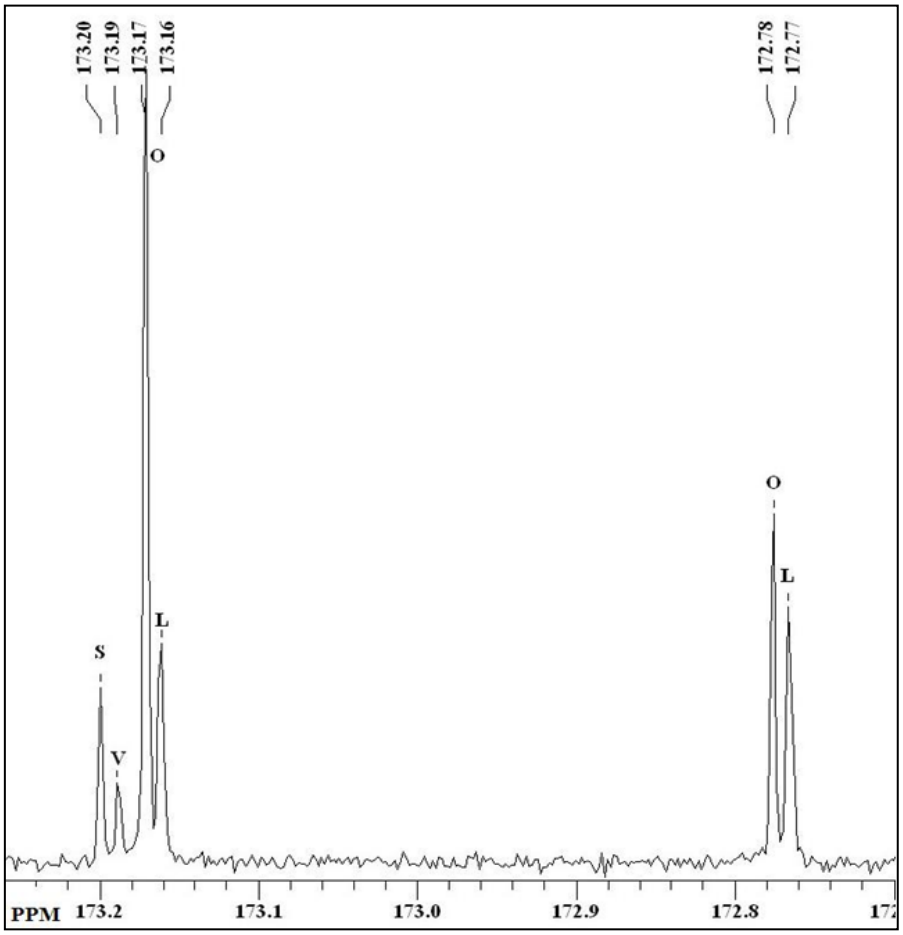

Notes:
UUU, unsaturated-unsaturated-unsaturated triacylglycerol profile; S, saturated fatty acid acyl chain; V, *cis*-11 monoene fatty acid acyl chain; O, *cis*-9 monoene fatty acid acyl chain; L, polyunsaturated fatty acid acyl chain.

Figure 2.23 : ^{13}C NMR spectrum of acyl carbonyl resonances of triacylglycerols in canola (Fatty acid profile UUU)

In contrast, mango fat, which is having the fatty acid profile of SUS, exists in solid state at room temperature (25 ℃). The major saturated fatty acid is stearic acid (C18:0), which is responsible for the high melting behaviour of mango fat. Hence, mango fat and other solid fats must be preheated at 60 ℃ for 10 minutes to ensure sample homogeneity prior to dissolution in deuterated solvent. As depicted in Figure 2.24, saturated fatty

acids occurred solely at the *sn*-1,3 positions, while the *sn*-2 position resided by the mono- and polyunsaturated fatty acids. Similar S/N ratio and peak resolution are observed between Figure 2.23 and Figure 2.24, suggesting that the current NMR regiospecific analysis is applicable regardless of the physical state of lipids at room temperature.

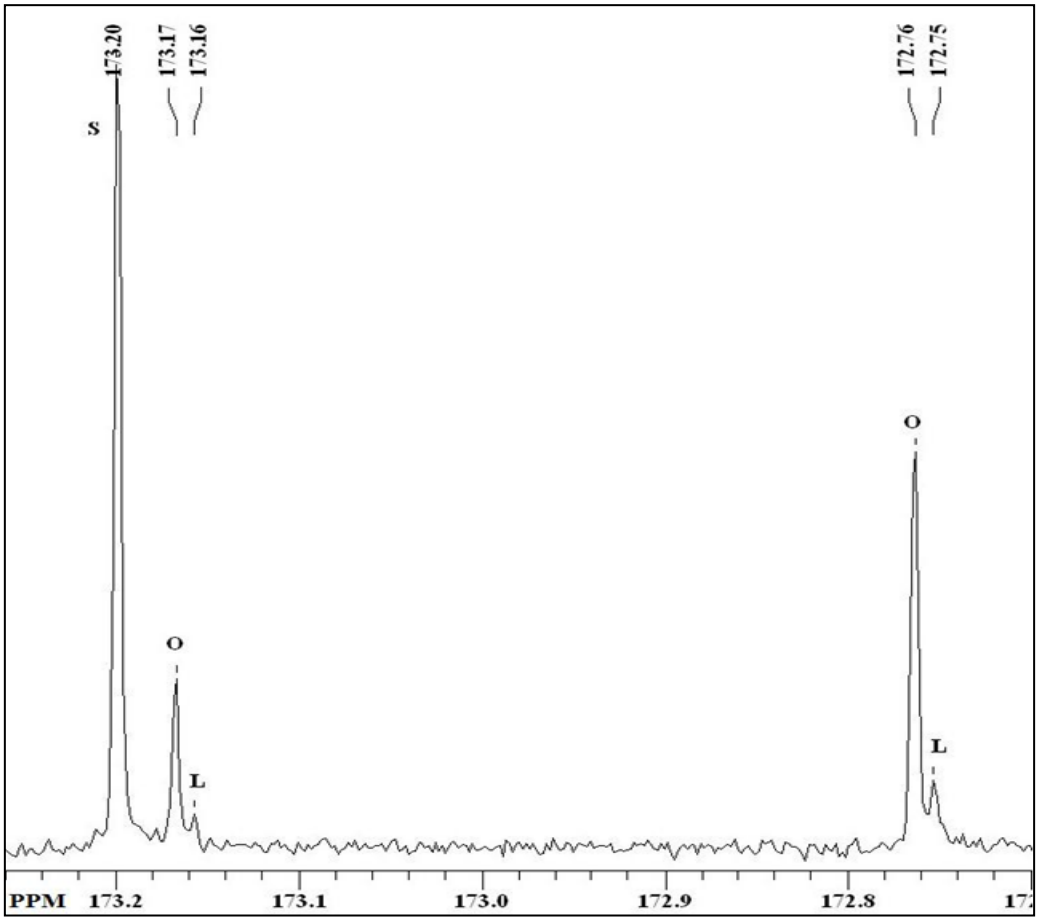

Notes:
SUS, saturated-unsaturated-saturated triacylglycerol profile; S, saturated fatty acid acyl chain; O, *cis*-9 monoene fatty acid acyl chain; L, polyunsaturated fatty acid acyl chain.

Figure 2.24 : ^{13}C NMR spectrum of acyl carbonyl resonances of triacylglycerols in mango fat (Fatty acid profile SUS)

Apart from that, the current method has also been applied to analyse the positional distribution of fatty acids in coconut oil. In contrast to mango fat and other conventional solid fats, coconut oil contains mainly medium chain saturated fatty acids, namely,

caprylic (C8:0), capric (C10:0) and lauric (C12:0) acids. Consequently, the physical state of coconut oil remains liquefied at room temperature despite their extraordinary high saturation. Figure 2.25 shows the ^{13}C NMR spectrum of acyl carbonyl resonances of triacylglycerols in coconut oil. It is demonstrated that the fatty acid profile of coconut oil is SSS and the fatty acid composition remained identical at both *sn*-1,3 and *sn*-2 positions. The low content (0.7 mol% – 1.3 mol%) of polyunsaturated fatty acids in coconut oil is identified with the aid of the difference in chemical shift between both regions and also the deconvolution integration method, as discussed in Section 2.3.4.4.

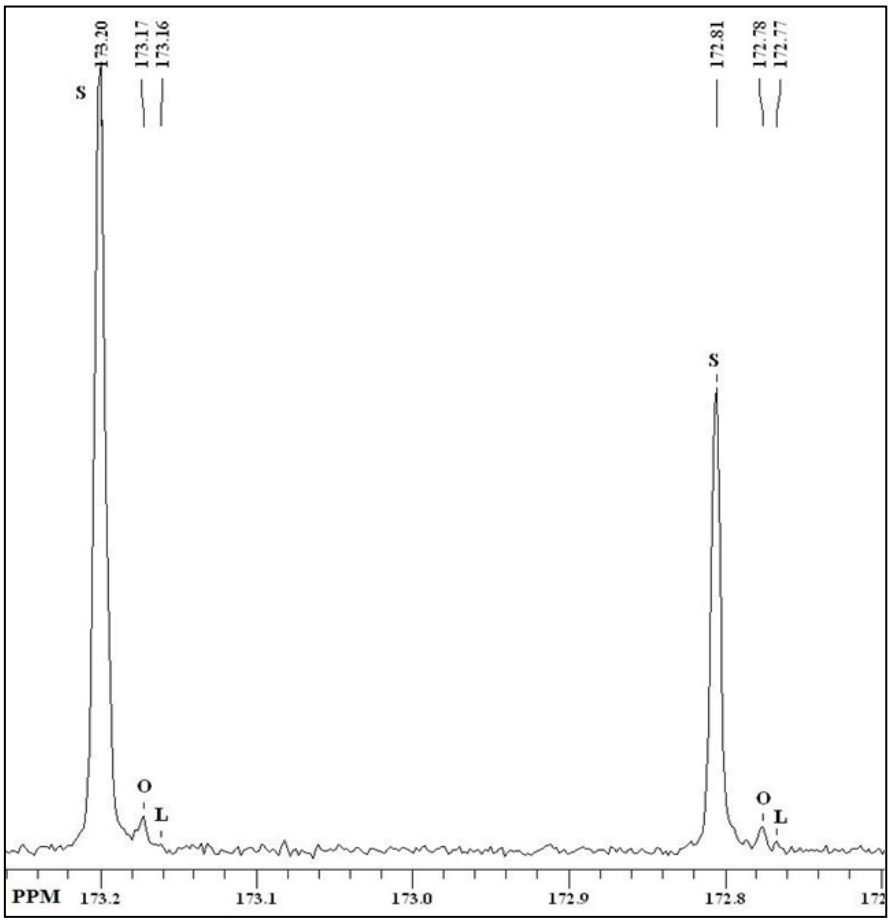

Notes:
SSS, saturated-saturated-saturated triacylglycerol profile; S, saturated fatty acid acyl chain; O, *cis*-9 monoene fatty acid acyl chain; L, polyunsaturated fatty acid acyl chain.

Figure 2.25 : ^{13}C NMR spectrum of acyl carbonyl resonances of triacylglycerols in coconut oil (Fatty acid profile SSS)

2.4.2.2 Regiospecific Analysis of World's Four Major Vegetable Oils

The current optimised ^{13}C NMR regiospecific analysis had been demonstrated successfully on the World's four major vegetable oils, namely, crude palm oil, sunflower oil, soybean oil, and rapeseed oil (canola) and the data is given in Table 2.6. The total fatty acid compositions (FAC) of vegetable oils determined by ^{13}C NMR and gas chromatography (GC) are comparable, with the maximum differences up to 1.7 mol%. It suggests that the total area under the carbonyl carbon resonances in NMR spectrum is proportional to the number of nuclei that gives rise to that resonance, with high accuracy and precision.

In spite of the identical total FAC, there are discrepancies in the positional fatty acid composition obtained through the current developed method and those from the conventional enzymatic or chemical methods. By investigating the trend in these discrepancies (Table 2.6), it is noticed that the quantitative ^{13}C NMR (qCNMR) has always yielded higher saturation content at the *sn*-1,3 positions and lower at the *sn*-2 position, compared with those reported results by conventional methods (Renaud *et al.*, 1995; Neff and List, 1999; Gunstone and Harwood, 2007). Therefore, it is postulated that the unsaturated acyl groups in the intermediate diacylglycerols are having higher tendency to migrate from the *sn*-2 position to the *sn*-1,3 positions after the enzymatic or chemical hydrolysis. It is a consequence of the *cis*-conformation of the long chain acyl groups, which cause higher extent of steric hindrance in the structure. This postulated phenomenon is illustrated in Figure 2.26.

Table 2.6 : Regiospecific analyses of four major vegetable oils by experimental (by ^{13}C NMR) and literature values (by conventional method)

Sample	Composition (mol%)				
	sn-position	Saturated	Monounsaturated		Polyunsaturated
			cis-11-monoene	*cis*-9-monoene	
Crude Palm Oil	1,3	75.2 ± 0.8 (67.5)	ND (ND)	21.3 ± 0.6 (27.2)	3.5 ± 0.3 (5.3)
	2	14.8 ± 0.3 (25.7)	ND (ND)	66.3 ± 0.3 (57.3)	18.9 ± 0.6 (17.0)
	1,2,3	55.1 ± 0.3 (53.6)	ND (ND)	36.3 ± 0.4 (36.0)	8.6 ± 0.2 (9.2)
	FAC	54.5 ± 0.3	35.9 ± 0.5		9.7 ± 0.5
Soybean Oil	1,3	26.3 ± 0.6 (21.3)	2.0 ± 0.4 (ND)	23.4 ± 0.9 (25.9)	48.4 ± 0.2 (52.8)
	2	ND (ND)	ND (ND)	23.8 ± 0.5 (24.6)	76.2 ± 0.5 (75.5)
	1,2,3	17.5 ± 0.4 (14.2)	1.3 ± 0.3 (ND)	23.5 ± 0.6 (25.4)	57.7 ± 0.1 (60.4)
	FAC	15.9 ± 0.5	26.5 ± 0.2		57.7 ± 0.3
Sunflower Oil	1,3	18.6 ± 0.4 (12.7)	0.6 ± 0.2 (ND)	27.2 ± 0.6 (28.3)	53.6 ± 0.3 (57.7)
	2	ND (6.6)	ND (ND)	26.9 ± 0.3 (27.9)	73.1 ± 0.3 (65.0)
	1,2,3	12.4 ± 0.3 (10.6)	0.4 ± 0.1 (ND)	27.1 ± 0.3 (28.2)	60.1 ± 0.2 (60.7)
	FAC	11.3 ± 0.2	27.0 ± 0.1		61.7 ± 0.1
Rapeseed Oil (Canola)	1,3	11.1 ± 0.3 (9.4)	5.5 ± 0.8 (ND)	66.0 ± 0.9 (60.9)	17.4 ± 0.3 (23.3)
	2	ND (2.1)	ND (ND)	55.2 ± 0.3 (52.7)	44.8 ± 0.3 (43.2)
	1,2,3	7.4 ± 0.1 (6.8)	4.0 ± 0.1 (ND)	61.7 ± 0.8 (58.1)	27.0 ± 0.7 (31.0)
	FAC	7.4 ± 0.2	64.7 ± 0.2		27.9 ± 0.1

Notes:
ND, not detected; FAC, fatty acid composition. Values are mean of three replicates ± standard deviation. Literature data for palm oil (Renaud et al., 1995), soybean oil (Neff and List, 1999), sunflower oil and canola (Gunstone *et al.*, 2007) are in parentheses.

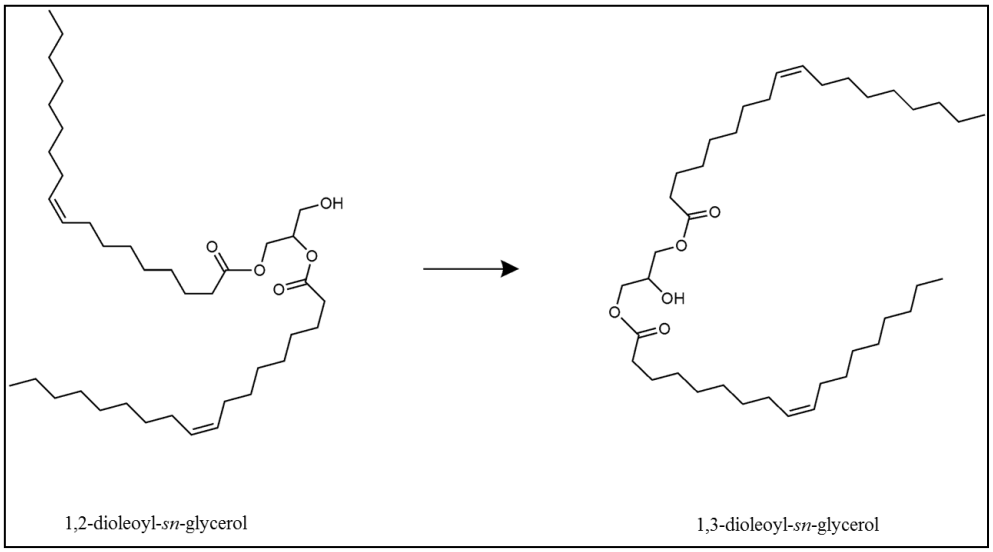

Notes:
Proposed higher extent of steric hindrance in the 1,2-dioleoyl-*sn*-glycerol intermediate, due to the *cis*-conformation of long chain *cis*-unsaturated acyl chain.

Figure 2.26 : Probable acyl migration of oleoyl acyl chain (*cis*-9-monoene) from *sn*-2 to *sn*-1 or *sn*-3 position in intermediate diacylglycerols

2.4.2.3 Regiospecific Analysis of Other Naturally Occurring Oils and Fats

Quantitative ^{13}C NMR (qCNMR) has been applied to determine the positional fatty acid compositions in other naturally occurring oils and fats, ranging from the relatively liquefied *Jatropha*, rice bran, flaxseed, Avogadro, corn, Moringa oil, to the highly solidified shea, cocoa butter, mango fat and sal stearin, which do not have any regiospecific data reported up-to-date. The results are as depicted in Table 2.7. These new regiospecific analysis data will be useful to offer more insights into their inherent effects on human nutrition and the value-added downstream applications.

Coconut oil, also known as lauric oil, contains high compositions of saturated fatty acids at both *sn*-1,3 (93.4 mol%) and *sn*-2 positions (96.0 mol%). As seen from its common nomenclature, the most abundant saturated fatty acid is the medium chain lauric acid (C12:0). Nevertheless, the nutritional value of coconut oil remained controversial. Some researchers claimed that medium chain triacylglycerols tend to

increase high-density lipoprotein cholesterol (HDL-C) level and help to protect against the prevalence of arteriosclerosis (Kaunitz, 1986). On the contrary, some investigators reported that the consumption of foods containing coconut oil would be a risk factor for coronary heart disease and thus, it should not be used on a regular basis (Pehowich *et al.*, 2000). In line with this finding, it was also reported that palm oil causes remarkably lower cholesterol concentrations than the coconut oil (Sundram *et al.*, 1991; Katan *et al.*, 1994).

Table 2.7 : Regiospecific analyses data of selected oils and fats by ^{13}C NMR

Sample	Composition (mol%)				
	sn-position	Saturated	Monounsaturated		Polyunsaturated
			cis-11-monoene	*cis*-9-monoene	
Cocoa butter	1,3	95.0 ±0.8	ND	5.0 ±0.7	ND
	2	7.8 ±0.6	ND	92.2 ±0.5	ND
	1,2,3	65.4 ±0.7	ND	34.6 ±0.7	ND
Coconut Oil	1,3	95.1 ±0.1	ND	4.2 ±0.3	0.7 ±0.8
	2	94.3 ±0.1	ND	4.4 ±0.2	1.3 ±0.7
	1,2,3	94.8 ±0.1	ND	4.3 ±0.2	0.9 ±0.8
Rice Bran Oil	1,3	34.7 ±0.1	0.8 ±0.1	40.2 ±0.2	24.4 ±0.3
	2	ND	ND	44.8 ±0.2	55.3 ±0.2
	1,2,3	22.9 ±0.1	0.5 ±0.1	41.8±0.1	34.9 ±0.1
Olive Oil	1,3	28.4 ±0.2	3.6 ±0.8	57.5 ±0.4	10.5 ±0.5
	2	ND	ND	76.2 ±0.9	23.8 ±0.9
	1,2,3	18.9 ±0.2	2.4 ±0.6	63.7 ±0.4	14.9 ±0.6
Jatropha Oil	1,3	36.3 ±0.7	ND	38.6 ±1.8	25.2 ±1.8
	2	ND	ND	44.6 ±1.3	55.5 ±1.3
	1,2,3	24.9 ±0.7	ND	40.5 ±1.9	34.6 ±1.6
Corn Oil	1,3	25.6 ±0.8	ND	30.8 ±0.4	43.7 ±0.4
	2	ND	ND	29.8 ±0.7	70.2 ±0.7
	1,2,3	17.1 ±0.6	ND	30.5 ±0.5	52.5 ±0.1
Shea Butter	1,3	51.8 ±1.7	ND	37.7 ±1.7	10.5 ±0.1
	2	ND	ND	73.2 ±1.4	26.8 ±1.4
	1,2,3	33.9 ±1.5	ND	49.9 ±1.3	16.1 ±0.5
Mango Fat	1,3	78.3 ±0.6	ND	17.9 ±0.8	3.8 ±0.6
	2	ND	ND	86.6 ±0.7	13.4 ±0.7
	1,2,3	52.1 ±0.8	ND	40.9 ±0.8	7.0 ±0.6
Mango Olein	1,3	48.7 ±0.9	ND	45.5 ±0.4	5.8 ±0.7
	2	ND	ND	82.1 ±0.9	17.8 ±0.9
	1,2,3	32.8 ±0.9	ND	57.8 ±0.7	9.4 ±0.4

Table 2.7, continued

Sample	Composition (mol%)				
	sn-position	Saturated	Monounsaturated		Polyunsaturated
			cis-11-monoene	*cis*-9-monoene	
Sal Stearin	1,3	93.7 ±0.2	ND	4.6 ±0.7	1.7 ±0.7
	2	ND	ND	100.0 ±0.0	ND
	1,2,3	62.4 ±0.2	ND	36.5 ±0.4	1.1 ±0.7
High-oleic Sunflower Oil	1,3	11.6 ±	2.6 ±	73.9 ±	11.9 ±
	2	ND	ND	86.5 ±	13.5 ±
	1,2,3	7.8 ±	1.7 ±	78.1 ±	12.4 ±
Peanut Oil	1,3	30.0 ±0.3	4.9 ±0.4	52.9 ±0.2	12.2 ±0.1
	2	ND	ND	65.4 ±0.1	34.6 ±0.1
	1,2,3	20.4 ±0.3	3.4 ±0.3	56.9 ±0.2	19.3 ±0.1
Walnut Oil	1,3	13.9 ±0.6	2.1 ±0.3	15.8 ±0.2	68.2 ±1.1
	2	ND	ND	19.2 ±0.2	80.8 ±0.2
	1,2,3	9.3 ±0.5	1.4 ±0.2	16.9 ±0.2	72.4 ±0.9
Flaxseed Oil	1,3	12.7 ±0.5	ND	16.5 ±0.1	70.8 ±0.5
	2	ND	ND	21.0 ±0.4	79.0 ±0.4
	1,2,3	8.3 ±0.2	ND	18.1 ±0.2	73.6 ±0.2
Moringa Oil	1,3	32.8 ±0.6	19.0 ±0.2	40.7 ±0.4	7.6 ±0.1
	2	ND	ND	86.1 ±1.1	13.9 ±1.1
	1,2,3	22.6 ±0.5	13.1 ±0.3	54.8 ±0.3	9.6 ±0.4
Avogadro Oil	1,3	27.1 ±0.9	8.1 ±0.1	55.3 ±1.2	9.6 ±0.4
	2	5.1 ±0.1	ND	67.6 ±0.6	27.2 ±0.6
	1,2,3	19.8 ±0.6	5.4 ±0.1	59.4 ±1.0	15.4 ±0.5
Sesame Oil	1,3	22.6 ±0.3	1.1 ±0.2	35.6 ±0.1	40.7 ±0.5
	2	ND	ND	40.6 ±0.1	59.4 ±0.1
	1,2,3	15.0 ±0.1	0.7 ±0.1	37.3 ±0.1	47.0 ±0.2

Notes:
ND, not detected. Values are mean of three replicates ± standard deviation.

As the positional fatty acids data for coconut oil was not available yet, most nutritional investigations were conducted and discussed in terms of the total saturation levels as well as the carbon chain length of fatty acids, rather than from the perspective of positional distribution of fatty acids in the glycerol backbone. From the regiospecific analysis data of coconut oil in Table 2.7, the difference in terms of saturated contents at the *sn*-2 position between palm olein and coconut oil is 88 mol%. Therefore, the regiospecific data obtained using the current developed method has the potential to further elucidate some previous nutritional evidences.

By comparing between Table 2.6 (Section 2.4.2.2) and Table 2.7, the saturated fatty acids in mango fat, mango olein, shea butter, sal stearin, cocoa butter and crude palm oil predominantly reside at the *sn*-1,3 positions whereas the *sn*-2 position mostly contains mono- and polyunsaturated fatty acids. All of them are having the similar saturated-unsaturated-saturated (SUS) fatty acid profile. Mango fat has been known as one of the blending components with other edible oil in the food industry to achieve desirable fatty acid composition (Gunstone and Harwood, 2007). Furthermore, fractionated mango fat has been reported to be a good partial substitute for cocoa butter (Baliga and Shitole, 1981). The availability of positional fatty acid profile reported herein is deemed to be useful for practical application in the food industry, particularly in the enzymatic interesterification process.

A substantial number of animal and clinical nutrition studies had demonstrated that the rice bran oil behaved as effective as other vegetable oils, for instance canola, in lowering the plasma cholesterol levels notwithstanding limited reason was being offered (Lichtenstein *et al.*, 1994; Rukmini and Raghuram, 1991). This observation was reported even though the total saturation in rice bran oil is 22.9 mol% (Table 2.7), which is approximately three times of that in canola (7.4 mol%) (Table 2.6, Section 2.4.2.2). One of the probable attributes may be the undetected saturated fatty acid content at the *sn*-2 position of triacylglycerol in both oils. Thus, the similar nutritional attributes are expected for flaxseed oil, sesame oil, Moringa oil, peanut oil and walnut oil, owing to the absence of saturated content at the *sn*-2 position (Table 2.7).

It is predominantly vital to verify the exact degree of saturation with minimum errors, particularly at the *sn*-2 position, due to the aforementioned nutritional importance. Isomerism or acyl migration from the *sn*-2 position to the *sn*-1,3 positions must be

avoided during the course of sample preparation. Henceforth, ^{13}C NMR regiospecific analysis reported herein provides a direct analysis method with negligible sample pre-treatment, such as derivatisation or extraction, therefore eliminates the possibility of sample loss or contamination prior to the GC analysis. With the exception of indistinguishable saturated fatty acids, it provides not only comparable results as the conventional methods, the current method is less time-consuming with results available more rapidly, *i.e.* the total experimental duration is 44 minutes (at least six times shorter than the conventional methods). Error of less than 2.0 mol% can be achieved coupled with high repeatability and versatility on the analysis of oils and fats from diverse sources.

2.4.2.4 Regiospecific Analysis of Fish Oil

The presence of long chain polyunsaturated fatty acids in fish oils, namely, stearidonic acid (C18:4), eicosatetraenoic acid (C20:4), eicosapentaenoic acid (C20:5), docosapentaenoic acid (C22:5) and docosahexaenoic acid (C22:6), has the potential to cause complications on the assignment of carbonyl carbon resonances. Due to the lengthy experimental time, a semi quantitative approach was chosen in the analysis of fish oils (Aursand *et al.*, 2007; Standal *et al.*, 2009). Therefore, present quantitative ^{13}C NMR (qCNMR) regiospecific analysis has been applied to study the positional fatty acids in menhaden fish oil. The NMR spectrum is demonstrated in Figure 2.27 while the corresponding positional fatty acid compositions are tabulated in Table 2.8.

The signal assignments of carbonyl resonances are in agreement with previous works (Aursand *et al.*, 2007; Standal *et al.*, 2009; Suárez *et al.*, 2010). It is interesting to note that the chemical shift is highly influenced by the position of the first double bond from carbonyl carbon, instead of the total number of double bonds in the acyl chain. As

illustrated in Figure 2.27, when the unsaturation occurs closer to the carbonyl carbon, *viz.* from Δ9-fatty acid to Δ4-fatty acid, the resonances are shifted to higher field. Due to the high electron density of double bond, it tends to exert shielding effect on the electron-withdrawing carbonyl group, causing the carbon resonance to appear at a lower frequency. The newly developed method presents the first approach with the employment of a narrower spectral width (1500 Hz at which the carbonyl carbon resonates) in qCNMR regiospecific analysis on fish oil, targeting to provide full quantitative data in much shorter analysis.

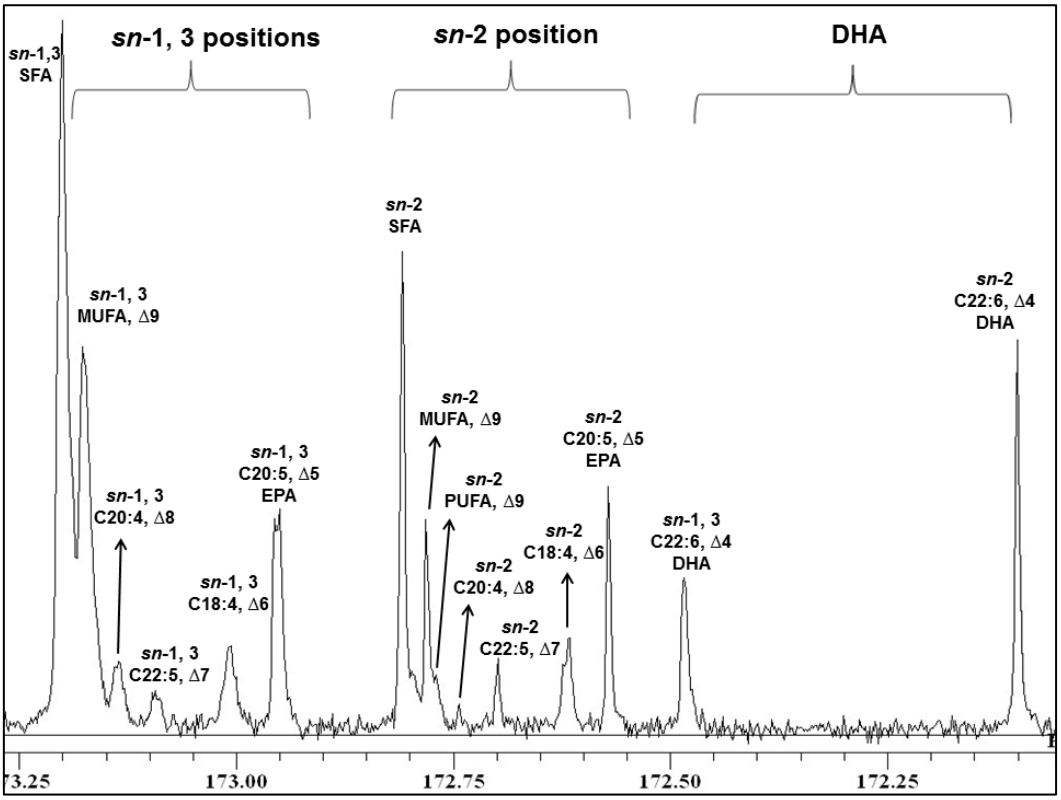

Notes:
SFA saturated fatty acids, MUFA monounsaturated fatty acids, PUFA polyunsaturated fatty acids, EPA eicosapentaenoic acid, DHA docosahexaenoic acid.

Figure 2.27 : 400 MHz ^{13}C NMR spectrum of acyl chain carbonyl resonances (spectral width = 1500 Hz) of triacylglycerols in menhaden fish oil

Table 2.8 : Regiospecific analyses data of menhaden fish oil by ^{13}C NMR

Acyl chain [a]	Composition (mol%) [b]		
	sn-1,3	*sn*-2	Total
Saturated	42.9 ± 1.9	32.7 ± 0.6	38.2 ± 0.9
Monounsaturated, Δ9	21.8 ± 0.7	11.3 ± 0.8	16.9 ± 0.1
Polyunsaturated, Δ9	ND	2.6 ± 0.4	1.2 ± 0.2
C20:4, Δ8	3.5 ± 0.2	1.3 ± 0.2	2.5 ± 0.1
C22:5, Δ7	2.3 ± 0.1	4.0 ± 0.4	3.1 ± 0.2
C18:4, Δ6	5.2 ± 0.2	6.7 ± 0.6	5.9 ± 0.2
C20:5, Δ5	15.6 ± 0.5	15.7 ± 0.3	15.6 ± 0.4
C22:6, Δ4	8.7 ± 0.3	25.7 ± 0.8	16.6 ± 0.8

Notes:
[a] The acyl chains are presented according to the sequence of their resonance from higher to lower frequency.
[b] ^{13}C NMR results are mean of three replicates ± standard deviation.
*ND = Not detectable

2.5 New Regiospecific Data on Palm Oil and Kernel Oil Fraction

2.5.1 Experimental

2.5.1.1 Materials

Refined, bleached and deodorised (RBD) palm oil, palm olein iodine valued (IV) 56, palm olein IV 57, palm olein IV 59, palm olein IV 65, palm olein IV 67, palm stearin IV 20, palm stearin IV 32, palm kernel oil, palm kernel olein, palm kernel stearin and palm mid fraction were obtained from Intercontinental Specialty Fats Sdn. Bhd., Dengkil, Selangor, Malaysia.

2.5.1.2 Methodology

Oil samples were pre-treated and prepared in a similar way as described in Section 2.2.2 prior to the NMR analysis. All NMR acquisition and processing parameters were set at the optimum conditions, as described in Section 2.2 and Section 2.3, respectively. JEOL LA-400 MHz spectrometer at the recording frequency of 100.40 MHz was employed in the acquisition of NMR data, while standard JEOL ALICE processing software was used for all post-processing.

2.5.2 Results and Discussion

Although the information for total fatty acid composition (FAC) and triacylglycerol molecular species are generally established for the palm fractions (Gunstone and Harwood, 2007), the regiospecific data is not yet available. By using the current established ^{13}C NMR regiospecific analysis, the positional distribution of fatty acids in palm fractions, ranging from the palm stearin, palm mid fraction, palm olein to the palm kernel fractions, have been analysed and tabulated in Table 2.9.

Palm olein fractions (IV 56-65) display significantly lower saturated content at the *sn*-2 position (5.3 mol% – 7.9 mol%), whereas the *sn*-1,3 positions are mainly resided by long chain saturated fatty acids (SFA). Commercially available palm cooking oil (palm olein IV 56) contains only 7.9 mol% saturated content at the *sn*-2 position (Table 2.9). It further elucidates why the palm olein behaves as healthy as olive oil in human (Choudhury and Truswell, 1995) despite the 47.3 mol% saturation in palm olein compared with the highly unsaturated olive oil (total saturation level is only 18.9 mol%).

Cocoa butter equivalents are fats rich in symmetrical triacylglycerols, *viz.* those possess fatty acid profile of saturated-unsaturated-saturated (SUS), and subsequently behave alike cocoa butter in all aspects. Palm mid fraction, which contains high amounts of 1,3-dipalmitoyl-2-oleoylglycerol (POP) is the excellent candidate for the formulation with other SUS fats for the production of chocolate products (Berger, 1981). In Table 2.9, the saturated content at the *sn*-1,3 positions and unsaturated content at the middle position of palm mid fraction IV 47 are 78.3 mol% and 10.0 mol%, respectively. It resembles closely to the fatty acid profile of SUS. In addition, cocoa butter equivalents can also be

formulated with interesterified palm stearin/palm kernel olein (25:75) or palm stearin/palm kernel olein/palm kernel oil (25:37.5:37.5) (Noor Lida *et al.*, 2002).

Table 2.9 : New regiospecific analyses data of palm fraction by ^{13}C NMR

Sample	Composition (mol%)				
	sn-position	Saturated	Monounsaturated		Polyunsaturated
			cis-11-monoene	*cis*-9-monoene	
Palm stearin IV 20	1,3	90.7 ±0.7	ND	8.1 ±0.9	1.2 ±0.1
	2	69.4 ±0.8	ND	25.7 ±0.5	4.9 ±0.3
	1,2,3	83.6 ±0.6	ND	14.0 ±0.7	2.4 ±0.1
Palm stearin IV 32	1,3	87.4 ±0.1	ND	11.3 ±0.1	1.3 ±0.0
	2	43.1 ±0.7	ND	46.3 ±0.6	10.5 ±0.1
	1,2,3	73.6 ±0.1	ND	22.2 ±0.1	4.2 ±0.1
Palm mid fraction IV 47	1,3	78.3 ±2.0	ND	18.2 ±2.0	3.5 ±0.0
	2	10.0 ±0.9	ND	73.6 ±1.6	16.3 ±0.7
	1,2,3	54.6 ±3.0	ND	37.4 ±3.0	8.0 ±0.0
Palm olein IV 56	1,3	68.6 ±0.4	ND	26.6 ±0.3	4.8 ±0.3
	2	7.9 ±0.9	ND	68.6 ±0.9	23.4 ±0.2
	1,2,3	48.3 ±0.4	ND	40.6 ±0.5	11.1 ±0.2
Palm olein IV 57	1,3	69.6 ±0.0	ND	26.4 ±0.3	4.0 ±0.3
	2	5.6 ±0.0	ND	76.3 ±0.3	18.0 ±0.3
	1,2,3	49.3 ±0.2	ND	42.3 ±0.1	8.5 ±0.1
Palm olein IV 59	1,3	67.2 ±0.4	1.1 ±0.1	27.0 ±0.4	4.6 ±0.1
	2	5.7 ±0.0	2.8 ±0.0	72.9 ±0.0	18.6 ±0.1
	1,2,3	46.5 ±0.6	2.0 ±0.1	42.1 ±0.5	9.4 ±0.1
Palm olein IV 65	1,3	59.1 ±0.2	2.0 ±0.4	32.6 ±0.2	6.3 ±0.1
	2	6.0 ±0.3	2.1 ±0.0	65.8 ±0.1	26.1 ±0.2
	1,2,3	42.3 ±0.2	2.0 ±0.3	43.2 ±0.1	12.6 ±0.0
Palm olein IV 67	1,3	52.9 ±1.6	2.0 ±0.0	39.0 ±1.8	6.1 ±0.1
	2	5.3 ±0.1	2.3 ±0.2	65.7 ±0.2	26.7 ±0.1
	1,2,3	37.7 ±0.7	2.1 ±0.1	48.1 ±0.8	12.1 ±0.2
Palm kernel oil	1,3	90.1 ±0.2	ND	8.2 ±0.1	1.7 ±0.1
	2	76.1 ±0.2	ND	20.4 ±0.3	3.5 ±0.2
	1,2,3	85.4 ±0.0	ND	12.3 ±0.1	2.3 ±0.1
Palm kernel olein	1,3	86.6 ±0.1	ND	11.1 ±0.1	2.3 ±0.0
	2	65.7 ±0.1	ND	27.7 ±0.2	6.6 ±0.0
	1,2,3	79.5 ±0.2	ND	16.7 ±0.1	3.7 ±0.1
Palm kernel stearin	1,3	96.3 ±0.1	ND	2.9 ±0.1	0.8 ±0.0
	2	92.1 ±0.1	ND	7.9 ±0.1	ND
	1,2,3	94.9 ±0.1	ND	4.6 ±0.1	0.5 ±0.0

Notes:
ND, not detected. Values are mean of three replicates ± standard deviation.

With the high amounts of SFA, palm stearin fraction is used extensively as the hard stock for the enzymatic interesterification reaction with other softer oils, for instance soybean oil, sunflower oil and canola. This remains one of the production route for *trans*-fat-free products, *viz.* margarine, shortening and vanaspati (Lin, 2002). The positional distribution of fatty acids in palm stearin fractions are given in Table 2.9. Moreover, other *trans*-free formulations can also be attained with ternary blends of palm oil/palm stearin/palm olein or palm oil/palm stearin/palm kernel oil. There are a wide variety of suitable formulations for food products can be tailor-made along with various fractions of palm oil. These products exhibit characteristics and melting behaviour similar to those of the hydrogenated counterparts.

Palm kernel fractions share close resemblance in some food applications with palm stearin fractions, especially in the manufacture of margarine, creamer, ice cream and specialty fats. Yet, the predominant SFA found in palm kernel fractions are caprylic (C8:0), capric (C10:0) and lauric acids (C12:0), while palm stearin consists mainly by palmitic (C16:0) and stearic acids (C18:0). As discussed in previous section, the medium chain SFA behaved differently in their digestion and metabolism pathway in human body (Harwood, 2007). These fatty acids are easily absorbed in the digestive tract and being used as energy sources in the body immediately. Consequently, the problem of excessive storage of fatty acids in the adipose tissue will be alleviated (Pantzaris and Basiron, 2002).

It is well-known that medium chain SFA presents abundantly in coconut and palm kernel oils, and therefore, they are named as ‘lauric oils’. Apart from that, coconut oil (Table 2.7) and palm kernel stearin (Table 2.9) exhibit comparable fatty acid distribution at the *sn*-1,3 and *sn*-2 positions. The only remarkable difference is found for

the amount of *cis*-9-monoene at the *sn*-2 position (consists mainly of oleic acid), which is 7.9 mol% and 4.4 mol% in palm kernel stearin and coconut oil, respectively.

On the other hand, it is noteworthy that the content of *cis*-11-monoene is only detectable in the olein fractions of palm oil, ranging from the palm olein IV 59 until palm olein IV 67 (Table 2.9). These fatty acids occur randomly at both *sn*-positions of triacylglycerols at the composition ranging from 1.1 mol% to 2.8 mol%. This is in line with the earlier report which disclosed the presence of *cis*-vaccenic acid in palm oil sample (Ng and Koh, 1988).

In an effort to observe the correlation between the fatty acid profiles of palm fractions and their respective IV more explicitly, the total FAC, positional FAC at the *sn*-1,3 and *sn*-2 positions have been plotted against IV and as depicted in Figure 2.28, Figure 2.29 and Figure 2.30, respectively.

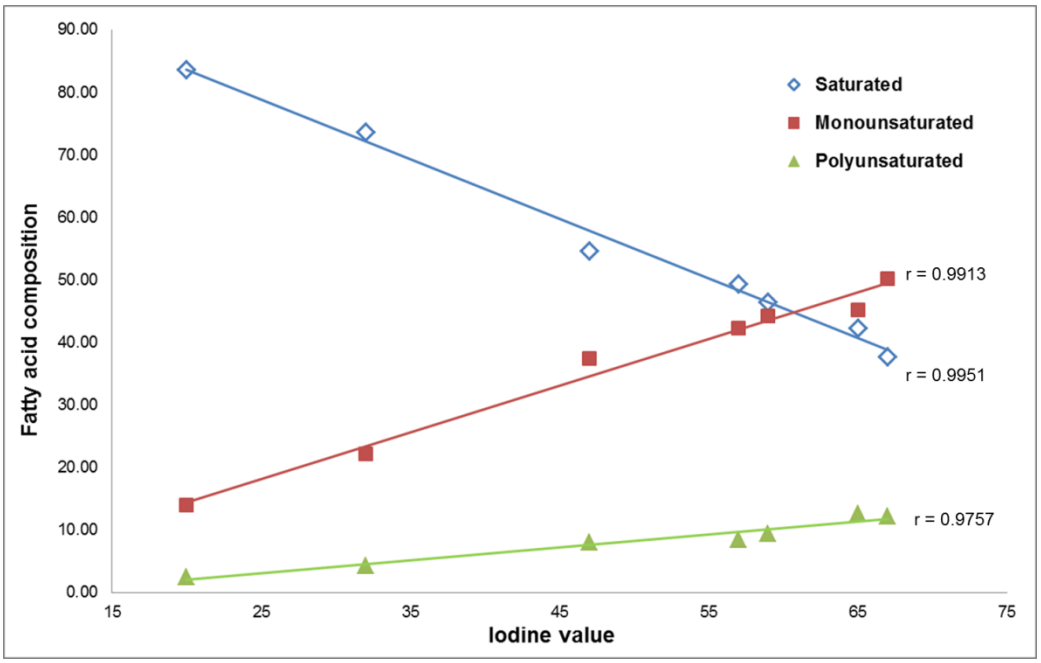

Figure 2.28 : Relationship between total fatty acid composition (FAC) and iodine values of palm oil fraction

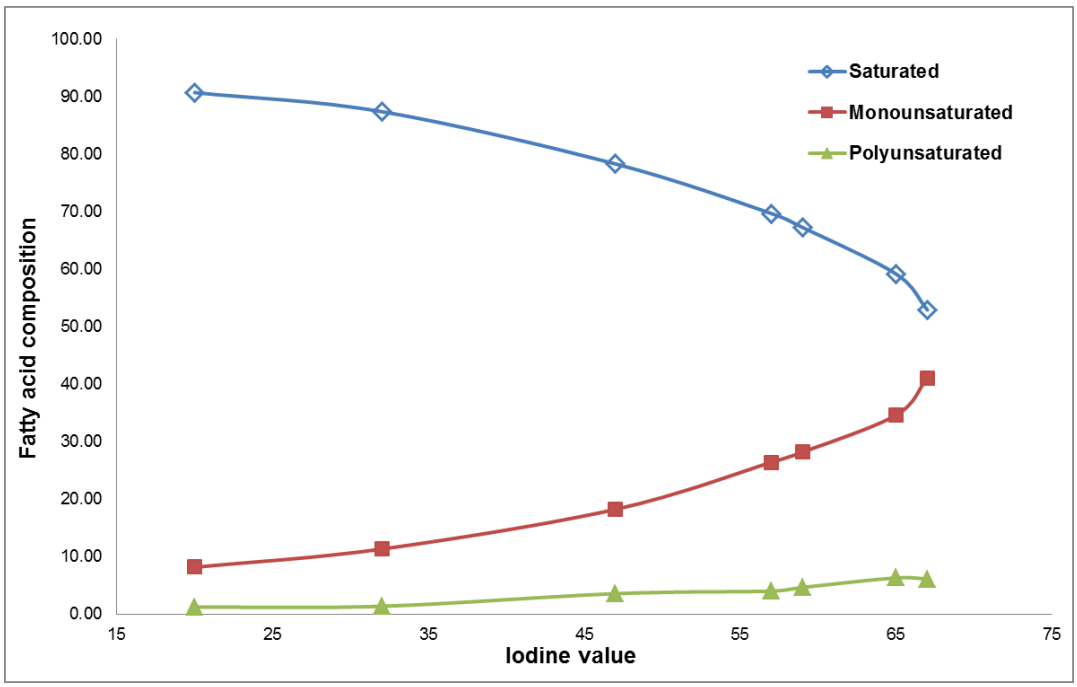

Figure 2.29 : Correlation between fatty acid composition (FAC) at *sn*-1,3 positions of triacylglycerols and iodine values of palm oil fraction

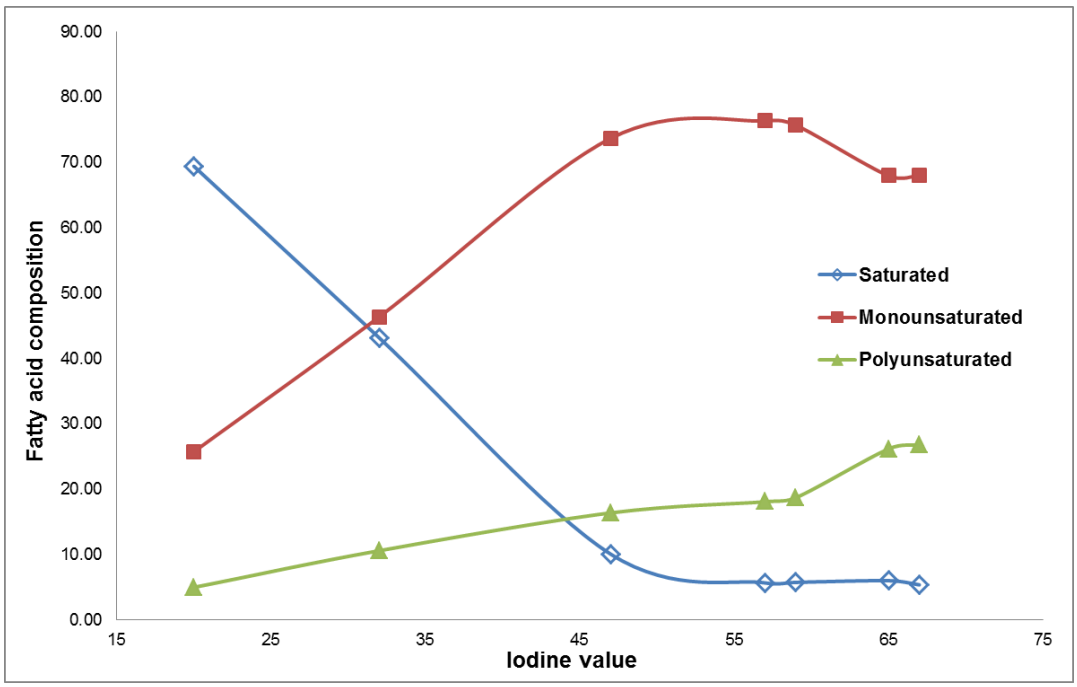

Figure 2.30 : Correlation between fatty acid composition (FAC) at *sn*-2 position of triacylglycerols and iodine values of palm oil fraction

Within expectation, the correlations between the total compositions of saturated, monounsaturated and polyunsaturated fatty acids in palm oil fractions and their associated IV are in an exceptional linear relationship (correlation coefficients, r=0.9757 – 0.9951) (Figure 2.28). The saturated content at the *sn*-1,3 positions drops dramatically from IV 20 to IV 67 (Figure 2.29). This is accompanied by the increment of monounsaturated fatty acid (MUFA) content. In contrast, the composition of polyunsaturated fatty acid (PUFA) does not vary significantly throughout the IV.

As mentioned beforehand, the SFA content at the middle position of triacylglycerols exerts significant nutritional implication in human, particularly in the blood lipid profile and cholesterol level. As shown in Figure 2.30, the saturated content at the *sn*-2 position decreases vividly from palm stearin IV 20 to palm mid fraction IV 47, and continues to stay near-identically throughout the olein fractions of palm oil (5.3 mol% – 7.9 mol%). This is concomitant with the trend of MUFA composition at the *sn*-2 position. Nevertheless, there is a drop of MUFA content after IV 59, and subsequently replaced by the increment of PUFA. In contrast to the identical PUFA content at the *sn*-1,3 positions, there is an increment of this type of fatty acid at the *sn*-2 position throughout a diverse range of IV. With the trends demonstrated in Figure 2.29 and 2.30, the positional distribution of fatty acids in palm oil fractions with given IV can be estimated.

The unique feature of palm oil is its balanced range of saturated and unsaturated fatty acids, which allows fractionation into various fractions for different food uses. As a conclusion, instead of the total fatty acid composition, regiospecific data provides the detailed information for positional distribution of fatty acids in the *sn*-1,3 and *sn*-2

positions, which is relatively more crucial in the elucidation of nutritional attributes of edible oils and fats.

2.6 Conclusion

With careful selection of data acquisition and processing parameters in quantitative ^{13}C NMR (qCNMR), a more elegant, rapid, accurate and less laborious regiospecific analysis of triacylglycerols has been established and can be used in a cook book approach. Inappropriate NMR data acquisition and processing methods as reported in earlier works have been shown to yield bias quantitative results. This is due to probable acyl migration during the conventional regiospecific analysis is fully omitted. The regiospecific data of edible oils and fats that was obtained previously using conventional methods were reviewed and analysed using the current established qCNMR technique. Thus, the present study provides insights to help nutritionist and to further support the understanding of their clinical findings.

Apart from application in regiospecific analysis, the current methodology can be extended as a reaction monitoring tool, particularly for the transesterification and interesterification reactions by analysing the positional distribution of fatty acids for intermediate products. Furthermore, it can be considered as a cookbook approach for other qCNMR experiments, for instance in the quantitative analysis of olefinic carbons in triacylglycerols or other types of compounds, and even be further applied to other types of nuclei, namely quantitative ^{15}N, ^{29}Si and ^{31}P NMR spectroscopy.

CHAPTER THREE
INVESTIGATION OF THE EFFECT OF POSITIONAL FATTY ACIDS IN TRIACYLGLYCEROLS ON OBESITY

3.1 Background

Obesity is a cardiovascular risk factor which is also related to the substantial increases in the prevalence of hypertension, type 2 diabetes and the disorder of lipoprotein metabolism. The incidence continues to be a major health threat to human, as a result the World Health Organisation (WHO) has termed obesity as alarming 'globesity'. Among factors promoting obesity, the diet that we consumed daily remains the main culprit. According to the Oil World Annual 2012, the average consumption of oils and fats per capita has grown progressively every year from a level of 18.9 kg in year 2001 to 25.2 kg in year 2011. Henceforth, it is crucial to investigate attributes dietary oils and fats to obesity in human.

Substantial efforts have been directed to establish the relationship between obesity and edible oils and fats, yet the reported results seem to be contradicting. In previous studies on the adipogenic effect of oils using rodents (Ikemoto *et al.*, 1996; Stachon *et al.*, 2006), highly unsaturated soybean (84.4% unsaturation) and sunflower oil (89.7% unsaturation) have been shown to cause higher body fat content compared with palm oil and lard. Nevertheless, this observation is not parallel with other studies using broiler chicken (Sanz *et al.*, 2000; Newman *et al.*, 2002) and rat models (Shimomura *et al.*, 1990; Matsuo *et al.*, 2002), in which it was observed that sunflower oil significantly lowers fat accretion compared with beef tallow which was used to represent the saturated fats.

Recently, it was found that fat accumulation at subcutaneous and visceral cavities were highest in mice fed with lard-enriched diet compared to those fed with olive, canola and sunflower oil (Catta-Preta *et al.*, 2012). In general, intake of saturated fats has been perceived to exert deleterious effects on fat deposition (Hariri *et al.*, 2010). However another saturated fat, cocoa butter, which consists of 63% total saturation, is reported to be able to prevent weight gain more efficiently than olive oil and safflower oil (Timmers *et al.*, 2011).

In the context of differential effects of individual fatty acids, saturated fatty acid (SFA) is accounted for the higher rates of weight gain (Larson *et al.*, 1996), while polyunsaturated fatty acid (PUFA), such as linoleic acid (C18:3*n*-6), does not induce obesity in C57BL/6J mice model (Ikemoto *et al.*, 1996). In addition, it has been shown that excessive intake of monounsaturated fatty acid (MUFA) gives deleterious effects comparable to that caused by diet enriched with SFA (Catta-Preta *et al.*, 2012). A recent study using rat model shows a negative correlation between carcass fat and dietary linoleic acid (C18:3*n*-6) contents, whereas positive correlations are observed for palmitic (C16:0), stearic (C18:0) and oleic acids (C18:1) (Matsuo *et al.*, 2002).

The effect of *n*-6 PUFA, particularly linoleic acid (C18:3*n*-6), on fat deposition has always been controversial. Linoleic acid (C18:3*n*-6) is reported to cause pro-obesity effects in rodents (Jen *et al.*, 2003; Stachon *et al.*, 2006), yet Matsuo *et al.* (2002) postulated that *n*-6 PUFA is the most effective fatty acids in limiting accretion of fat. The review article by Czernichow *et al* (2010) states that the role of *n*-6 PUFA in obesity remains unclear as no conclusive inference can be deduced from the available epidemiological evidence. Moreover, *n*-3 PUFA (Okuno *et al.*, 1997; Newman *et al.*, 2002; Micallef *et al.*, 2009) is also claimed to reduce fat deposition, however no

decisive results can be attained by recent systematic review of the effect of *n*-3 PUFA on body weight gain (Martinez-Victoria *et al.*, 2012).

Since most researchers are focussing predominantly on the relationship between obesity and different dietary oils based on their total saturation levels, there is no consistent conclusion can be obtained. On the other hand, there is a paucity of information concerning the positional fatty acids of triacylglycerols and their associated effects on fat accretion. The effect of different rates of fat absorption owing to the different positional attachment of fatty acids in the triacylglycerol has been given limited consideration.

As described, fatty acids at the different *stereospecific numbering* (*sn)*-position were not subjected to similar rate of absorption. An individual consuming oils and fats does not take in only the individual fatty acids, or saturation as a whole, but the chemical nature of the triacylglycerol (Ong and Goh, 2002). The positional attachment of the fatty acids on glycerol backbone is the key determinant of fat digestion and absorption (Small, 1991; Ong and Goh, 2002). As demonstrated in Figure 3.1, fatty acid at the *sn*-2 position is absorbed in the form of monoacylglycerols through intestinal mucosa after the action of 1,3-specific pancreatic lipase, while those are esterified at the *sn*-1,3 positions will be absorbed as free fatty acids (Kayden *et al.*, 1967; Small, 1991).

Literature shows that long chain SFA in free-form suffers delayed absorption due to the formation of insoluble calcium or magnesium soaps after enzymatic hydrolysis (Mattson *et al.*, 1979; Brink *et al.*, 1995; Innis *et al.*, 1997). The physicochemical state of lipid in the intestinal lumen during lipid digestion is that of a micellar phase. Consequently, the stability of the equilibrium between oil and aqueous phase, as well as

the rate in which the free fatty acids establish the equilibrium, are important in elucidating the fatty acid absorption (Freeman, 1969). Poor diffusion of fatty acid from oil to aqueous phase may inhibit enzymatic action by blocking the interface. Moreover, the solubility of fatty acids in aqueous will be impaired by the high concentration of divalent cations, namely, the calcium and magnesium ions. As an instance, the distribution of very long chain SFA (having carbon number 18 and above) in the micellar phase becomes restricted in the presence of calcium ions above a critical concentration (Nenzonana and Desnuelle, 1968). Under such circumstance, they may react with divalent cations to form poorly soluble soaps.

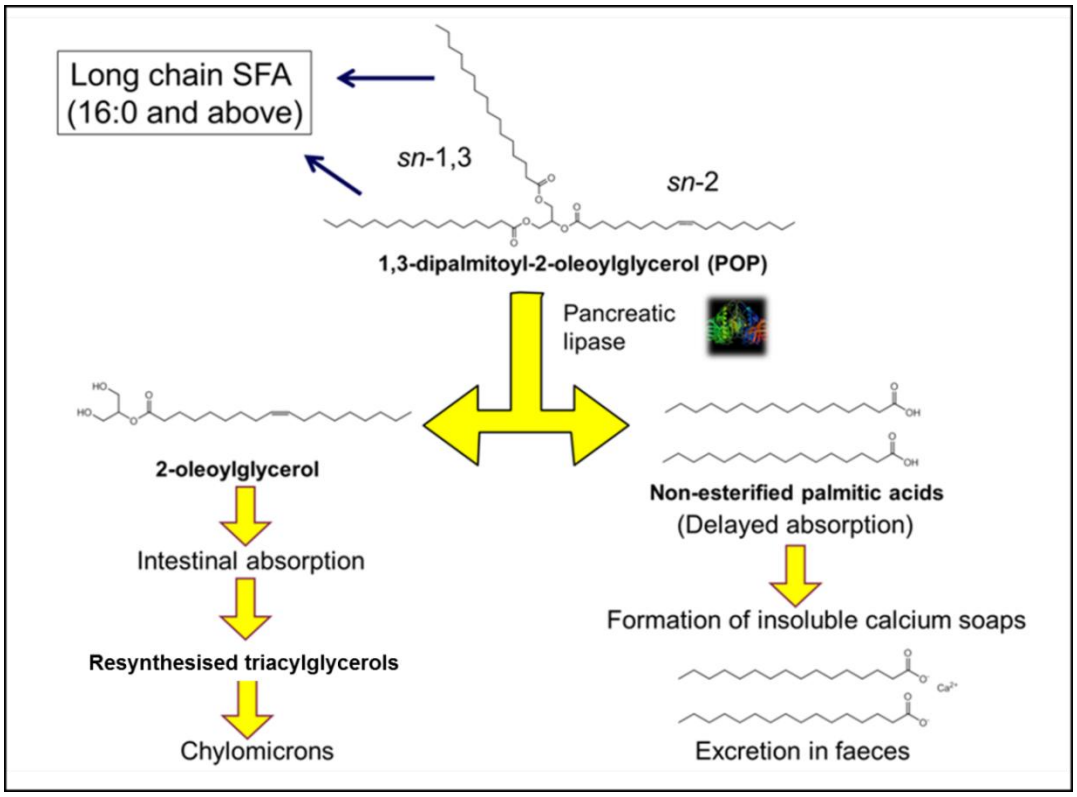

Figure 3.1 : Enzymatic hydrolysis and fat absorption in intestine as illustrated by 1,3-dipalmitoyl-2-oleoylglycerol (POP)

Using 1, 3-dipalmitoyl-2-oleoylglycerol (POP) for illustration (Figure 3.1), after cleavage by 1, 3-specific pancreatic lipase, 2-monooleoylglycerol will be absorbed

through intestine mucosa, whereas palmitic acids in free-form will suffer delayed absorption due to formation of calcium soaps, and eventually being excreted in faeces. As a consequence, the amount of resynthesised triacylglycerols is reduced, affecting their incorporation in lipoproteins (chylomicrons) and subsequent metabolism, their distribution into tissues and eventually the extent of fat deposition. Furthermore, prior literature disclosed that the SFA excretion was directly related to the fatty acid chain length, that is, stearic acid (C18:0) was shown to exhibit greater excretion index compared with palmitic acid (C16:0) (Lien *et al.*, 1993). A further alleviation of fat deposition might be expected if stearic acids (C18:0) reside mainly at the *sn*-1,3 positions of triacylglycerols.

In the present study, two *in vivo* studies were designed and conducted. *In vivo* study 1 was designed to investigate the effect of positional fatty acids on fat deposition and obesity, by using refined, bleached and deodorised (RBD) palm olein (POo), chemical interesterified RBD palm olein (IPOo) and RBD soybean oil (SOY) which differ in the degree of saturation levels at the *sn*-1,3 positions of triacylglycerols. Meanwhile, *in vivo* study 2 aimed to examine the effect of different common long chain SFA, namely palmitic (C16:0) and stearic acid (C18:0), at the *sn*-1,3 positions of triacylglycerols on obesity, using RBD cocoa butter (COB), RBD sal stearin (SAL), RBD palm mid fraction (PMF) and RBD high-oleic sunflower oil (HOS) as test oils. In addition, C57BL/6 mice were chosen as this strain was reported as a robust and efficient animal model for human obesity and type 2 diabetes, as well as these mice remained lean if the fat content of the diet was limited (Surwit *et al.*, 1988; Surwit *et al.*, 1995; Winzell and Ahrén, 2004).

3.2 *In Vivo* Study 1: Different Saturation Levels at the *sn*-1,3 Positions of Triacylglycerols on Fat Deposition

3.2.1 Experimental

3.2.1.1 Diets

Refined, bleached and deodorised (RBD) palm olein with iodine value (IV) 56 (POo) was a generous gift from Intercontinental Specialty Fats Sdn. Bhd., Selangor, Malaysia. The chemical interesterified palm olein IV 56 (IPOo) was prepared from POo using sodium methoxide as catalyst, according to previous published method (Lo and Handel, 1983). RBD soybean oil (SOY) was obtained from Soon Soon Oil Mills Sdn. Bhd., Selangor, Malaysia. Autoclavable standard pellet feeds (digestible energy 14.0 MJ/kg) were purchased from Specialty Feeds, Glen Forrest, West Australia. It was used as the diet for control group without further fortification, while the other three test diets were fortified with POo, IPOo and SOY at oil composition of 150 g/kg diet. All test diets are isoenergetic (20 MJ/kg). The nutritional values of the autoclavable standard pellet feeds for mice are shown in Table 3.1.

Total fatty acid composition (FAC) and positional fatty acids at the *sn*-1,3 and *sn*-2 positions of test oils (POo, IPOo and SOY) are given in Table 3.2 and Table 3.3, respectively. POo and IPOo share the similar total FAC, but differ in positional distribution of fatty acids within glycerol moiety. Oil fortification was done manually in the laboratory by mixing the pulverised standard diet pellets thoroughly with test oil and thereafter pelleted to the original shape. The diets were then left to dryness at 30 ℃ overnight and stored at 4 ℃ in fridge.

Table 3.1 : The composition of the autoclavable standard pellet feeds for mice

Nutrients	Composition (per kg diet)
Crude protein	194 g
Fat	48 g
Polysaccharides	151.3 g
Crude fibre	51 g
Digestible energy	14.0 MJ
Total Vitamins	
Vitamin A (Retinol)	19500 IU
Vitamin B1 (Thiamine)	80 mg
Vitamin B2 (Riboflavin)	30 mg
Vitamin B6 (Pryridoxine)	28 mg
Vitamin B12 (Cyancobalamin)	150 µg
Vitamin C (Ascorbic acid)	20.0 mg
Vitamin D (Cholecalciferol)	2000 IU
Vitamin E (α-Tocopherol acetate)	110 mg
Vitamin K (Menadione)	20 mg
Niacin (Nicotinic acid)	145 mg
Pantothenic acid	60 mg
Biotin	410 µg
Folic acid	5.0 mg
Choline	1600 mg
Amino Acid	
Valine	8.7 g
Leucine	14.0 g
Isoleucine	8.0 g
Threonine	7.0 g
Methionine	3.0 g
Cystine	3.0 g
Lysine	9.0 g
Phenylanine	9.0 g
Tyrosine	5.0 g
Tryptophan	2.0 g
Fatty Acid Composition	
Myristic acid	0.3 g
Palmitic acid	5.0 g
Stearic acid	1.4 g
Palmitoleic acid	0.1 g
Oleic acid	19.0 g
Gadoleic acid	0.3 g
Linoleic acid	13.0 g
α-Linolenic acid	3.0 g
Arachadonic acid	0.1 g
Eicosapentaenoic acid (EPA)	0.2 g
Docosahexaenoic acid (DHA)	0.5 g
Total Minerals	
Calcium	7.80 g
Phosphorous	7.00 g
Magnesium	2.00 g
Sodium	2.00 g
Potassium	7.00 g
Sulphur	2.00 g

Table 3.1, continued

Nutrients	Composition (per kg diet)
Iron	590 mg
Copper	24 mg
Iodine	0.5 mg
Manganese	115 mg
Cobalt	1.0 mg
Zinc	90 mg
Molybdenum	1.2 mg
Selenium	0.4 mg
Cadmium	0.04 mg

Notes:
All nutritional parameters of the diet meet or exceed the National Research Council (NRC) guidelines for mice. A fixed formula using the following ingredients: Wheat, barley, lupins, soya meal, fish meal, mixed vegetable oils, canola oil, salt, calcium carbonate, dicalcium phosphate, magnesium oxide and a Vitamin and trace mineral premixed with cereal grain based diet. Information was provided by Specialty Feeds, Glen Forrest, West Australia.

Table 3.2 : Total fatty acid composition (FAC) of dietary oils and fats for *in vivo* study 1

Acyl chain	Fatty acid composition (as % methyl esters)		
	POo	IPOo	SOY
12 : 0	0.26	0.27	ND
14 : 0	1.00	1.01	0.07
16 : 0	39.30	39.54	10.54
18 : 0	4.36	4.37	4.28
20 : 0	0.38	0.37	0.35
22 : 0	0.04	0.07	0.38
Total SFA	45.30	45.63	15.62
16 : 1*n*-7	0.16	0.17	0.08
18 : 1*n*-9	42.70	42.48	23.84
20 : 1*n*-9	0.15	0.13	0.21
Total MUFA	43.01	42.79	24.13
18 : 2*n*-6	11.47	11.36	53.47
18 : 3*n*-3	0.22	0.22	6.77
20 : 2*n*-6	ND	ND	ND
Total PUFA	11.68	11.58	60.25

Notes:
POo, palm olein; IPOo, chemical interesterified palm olein; SOY, soybean; SFA, saturated fatty acids; MUFA, monounsaturated fatty acids; PUFA, polyunsaturated fatty acids; ND, not detected.

Table 3.3 : Positional fatty acid composition of dietary oils for *in vivo* study 1

Sample	Composition (mol%) *								
	sn-position	SFA		MUFA				PUFA	
				cis-11-monoene		*cis*-9-monoene			
		Mean	SD	Mean	SD	Mean	SD	Mean	SD
POo	1, 3	71.0	0.4	ND	ND	26.1	0.3	2.9	0.3
	2	7.4	0.9	ND	ND	74.3	0.9	18.3	0.2
	1, 2, 3	50.3	0.4	ND	ND	41.8	0.5	7.9	0.2
IPOo	1, 3	49.6	0.6	ND	ND	39.9	0.8	10.5	0.6
	2	49.0	0.8	ND	ND	41.0	0.7	10.0	0.7
	1, 2, 3	49.2	0.8	ND	ND	40.5	0.8	10.3	0.6
SOY	1, 3	26.3	0.6	2.0	0.4	23.4	0.9	48.3	0.2
	2	ND	ND	ND	ND	23.8	0.5	76.2	0.5
	1, 2, 3	17.5	0.4	1.3	0.3	23.5	0.6	57.7	0.1

Notes:
SFA, saturated fatty acids; MUFA, monounsaturated fatty acids; PUFA, polyunsaturated fatty acids; POo, palm olein; IPOo, chemical interesterified palm olein; SOY, soybean oil; ND, not detected. Values expressed as mean and standard deviation, SD.
* ^{13}C NMR results are mean of three (3) replicates.

3.2.1.2 Animal Experiment

Thirty-two weaned male C57BL/6 mice (Monash University, Selangor, Malaysia) were randomly distributed into four groups of eight mice each and caged individually. The average body mass of mice after randomisation did not differ significantly (P=0.945) and for control, palm olein (POo), interesterified palm olein (IPOo) and soybean oil (SOY) dietary groups were 17.4 ± 0.9 g, 17.9 ± 1.0 g, 17.3 ± 1.4 g and 17.5 ± 1.0 g, respectively. The mice were kept in a room with adequate ventilation at 23 ± 2 ℃ and a relative humidity of 60% with a 12-h light:dark cycle. Mice were given *ad libitum* access to food and water.

The food and water consumption were determined on a daily basis, whereas the body mass of mice was recorded weekly. The actual food intake was corrected for spilled food after separated from faeces. Fresh faeces were collected daily, pooled and stored at

-20 ℃ for faecal analysis, starting from week 3 until week 15. At the end of the study, mice were sacrificed by dislocation of the neck. Subsequently, the subcutaneous and visceral fats were removed, weighed and kept frozen at -80 ℃. All protocols for the mice experiments were approved by the Animal Care and Use Committee (ACUC), Faculty of Medicine, University of Malaya, Kuala Lumpur, Malaysia (ethic no: KIM/23/03/2011/CSF (R)).

3.2.1.3 Lipid Extraction

Extraction of fatty acids from faeces and adipose tissues were carried out by using a modified method (Folch *et al.*, 1957). A 300 mg of faeces was extracted with 15 mL of chloroform-methanol mixture (2:1 v/v) containing 10 ppm of butylated hydroxytoluene. After overnight extraction, the solution was filtered and mixed with 4 mL of 0.9% sodium chloride. It was then shaken and left overnight at 4 ℃ in order to remove aqueous impurities. Lower phase containing lipids was evaporated under reduced pressure on the subsequent day.

3.2.1.4 Lipid Analysis

Total fatty acid composition (FAC) was determined as described by Christie (1989): Test oils as well as the extracted fatty acids from faeces and adipose tissue were derivatised to fatty acid methyl esters by sodium methoxide-catalysed and sulphuric acid-catalysed transesterification, respectively. Methyl ester sample (1 µL) was injected into gas chromatography (GC) (GC-2010A series, Shidmadzu) equipped with a flame ionisation detector and a BPX70 capillary column of 30 m x 0.32 mm i.d. An initial temperature of 140 ℃ was held for 2 minutes and then was increased to 220 ℃ at the rate of 8 ℃ per minute. The column was held at the final temperature for another 5 minutes. The oven, injector and the detector ports were set at 140 ℃, 240 ℃ and 260 ℃,

respectively. The carrier gas was helium with column flow rate of 1.10 mL per minute at a 50:1 split ratio. The excretion index for each fatty acid in faeces was computed by the ratio of the FAC in faeces to the composition of the corresponding fatty acids in the dietary oils (Table 3.2, Section 3.2.1.1).

Regiospecific analysis of test oils and extracted lipids from adipose tissue were conducted, as established and described in Chapter 2. Briefly, ^{13}C NMR measurements were performed using a JEOL ECA-400 MHz NMR spectrometer operating at 9.4 T. Manual shimming was employed. A spectral width of 1500 Hz at where the acyl chain carbonyl carbons resonate, 8192 data points and 90 ° pulse excitation were applied. Experimental temperature was set at 298.15 K while repetition time of 34.5 s was chosen. Total scans per analysis were 128 times. Deconvolution was used as the integration method to separate the overlapped peak and calculate its area. Standard ALICE processing software was employed.

In order to determine the absolute amount of free fatty acids, extracted free fatty acids from faeces were transferred into a 2 mL auto-sampler vial. Into this vial, 0.5 mL of N,N-Bis(trimethylsilyl)trifluoroacetamide (BSTFA) solution (4.5 mL of BSTFA in 10 mL dichloromethane) was added accurately by using a micropipette. The vial was shaken well and then heated for four hours at 60 ℃ - 70 ℃ for silyllation process. For the calibration graph (Figure 3.2), standard fatty acids, namely, palmitic, stearic and oleic acids (0.1 mg, 1 mg, 5 mg, 7 mg, and 10 mg in 10 mL dichloromethane) were prepared in the same manner as sample prior to GC injection.

The sample (1 µL) was injected into GC (Shidmadzu, GC-2010A series) equipped with a flame ionisation detector and a BPX5 capillary column of 30 m x 0.25 mm i.d. An

initial temperature of 100 ℃ was held for 1 minute, and subsequently was increased to 360 ℃ at the rate of 10 ℃ per minute. The column was held at the final temperature for another 15 minutes. The oven, injector and the detector ports were set at 100, 245 and 370 ℃, respectively. The carrier gas was helium with column flow rate of 2.0 mL per minute.

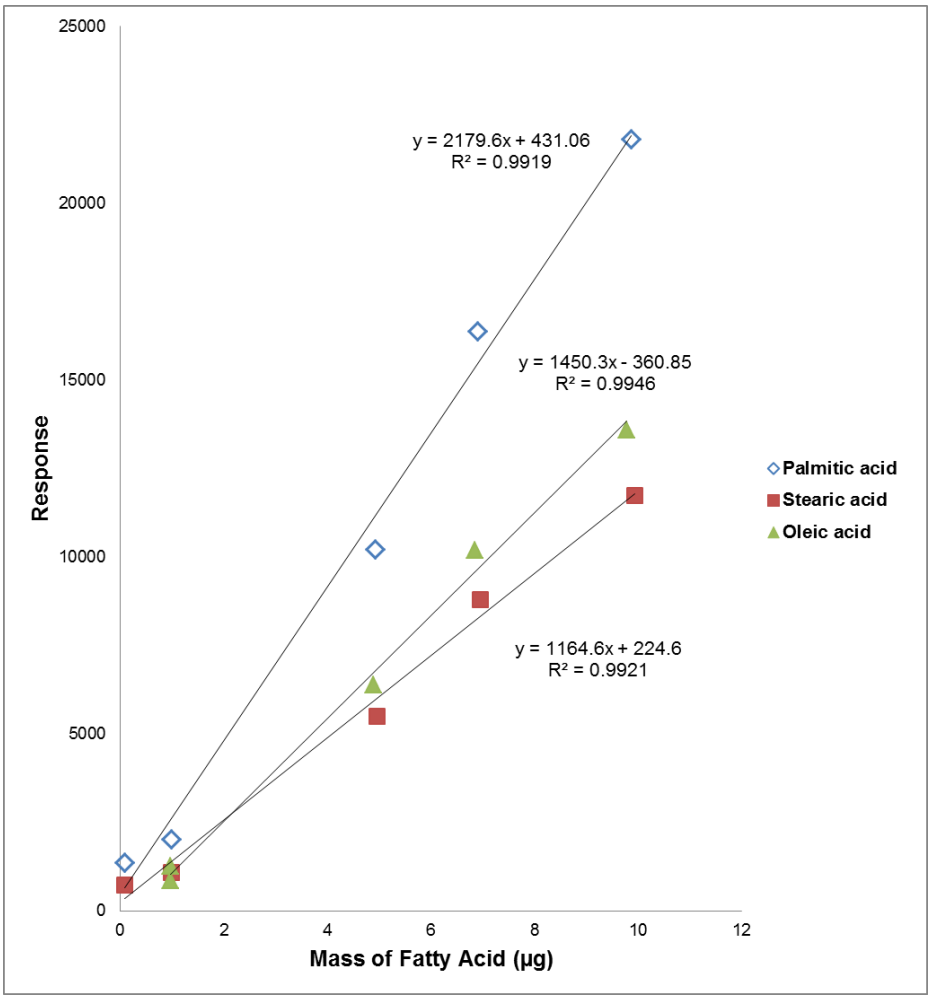

Figure 3.2 : Calibration graph for palmitic, stearic and oleic acids in the determination of the absolute amount of faecal fatty acids

3.2.1.5 Statistical Analysis

IBM SPSS Statistic 20 (SPSS Inc. Chicago, IL, USA) was employed for the statistical analysis of data. The significance level of differences among the dietary groups was

assessed by one way analysis of variance (ANOVA). When significant differences were found, pair wise comparisons between groups were executed by Fisher's Least Significant Difference (LSD) test. *P* values lower than 0.05 were considered significant.

3.2.2 Results

3.2.2.1 Food Consumption

As presented in Table 3.4, all mouse groups showed similar total food consumption in 15 weeks, except for the control group. Mice fed with control diet which was in the absence of test oils, served as a baseline. The weekly food consumption throughout the experimental period is depicted in Table 3.5. For all dietary groups, the food consumptions were the highest during Week 1, and then remained comparable from Week 2 until Week 15.

Table 3.4 : Total food consumption of C57BL/6 mice over 15 weeks (*In vivo* study 1)

	Control		POo		IPOo		SOY	
	Mean	SEM	Mean	SEM	Mean	SEM	Mean	SEM
Food consumption* (g)	357.79^{a}	10.66	327.01^{b}	2.79	315.92^{b}	7.18	322.01^{b}	5.81

Notes:
POo, palm olein; IPOo, chemical interesterified palm olein; SOY, soybean oil. Values expressed as mean and standard error of the mean, SEM.
^{a,b} Mean values within a row with unlike superscript letters were significant different ($P<0.05$)
* Food consumption was calculated as the total food intake for each mouse in 15 weeks and then averaged for each group (n=8).

Table 3.5 : Weekly food consumption of C57BL/6 mice from different dietary groups (*In vivo* study 1)

Week	Food Consumption (g)							
	Control		POo		IPOo		SOY	
	Mean	SD	Mean	SD	Mean	SD	Mean	SD
1	26.48	2.97	26.40	1.27	24.92	1.01	25.33	1.03
2	23.49	2.14	21.75	1.45	21.06	1.63	22.20	1.75
3	23.04	1.33	19.33	0.81	20.00	1.80	21.15	1.19
4	23.57	2.03	19.83	1.02	20.16	1.17	20.46	1.40

Table 3.5, continued

Week	Food Consumption (g)							
	Control		POo		IPOo		SOY	
	Mean	SD	Mean	SD	Mean	SD	Mean	SD
5	23.76	2.72	20.59	0.96	20.71	1.35	20.58	1.70
6	23.09	2.60	20.97	1.08	20.57	1.52	21.25	1.19
7	23.61	1.96	21.76	0.90	20.47	1.99	21.33	1.46
8	23.09	1.75	21.53	1.05	20.52	1.62	21.48	1.82
9	23.03	1.91	21.12	1.12	20.64	1.33	21.31	1.42
10	21.98	1.90	21.05	1.03	20.66	2.09	20.66	1.51
11	24.92	2.72	21.69	1.15	21.18	0.90	21.35	1.48
12	25.84	3.36	23.81	1.07	22.75	1.97	22.79	1.59
13	24.17	2.81	22.72	0.68	21.46	1.20	21.03	2.49
14	24.28	2.15	22.61	0.87	19.98	1.95	20.92	1.44
15	23.44	1.97	21.85	1.86	20.84	1.95	20.17	1.98

Notes:
POo, palm olein; IPOo, chemical interesterified palm olein; SOY, soybean oil. Values expressed as mean and standard deviation, SD.

3.2.2.2 Body Mass Gain

Different dietary oils exerted comparable effect on mice body mass gain, feed efficiency (body mass gain per gram feed consumed) and fat-free body masses (Table 3.6). As mentioned earlier, mice fed with control diet which was in the absence of test oils, served as a baseline. The weekly body mass gain throughout the experimental period is shown in Table 3.7. For all dietary groups, the gain of mice body mass were the highest during Week 1, and then remained comparable from Week 2 until Week 15.

Table 3.6 : Body mass of C57BL/6 mice over 15 weeks (*In vivo* study 1)

	Control		POo		IPOo		SOY	
	Mean	SEM	Mean	SEM	Mean	SEM	Mean	SEM
Body mass gain (g)	12.85^{a}	1.06	18.55^{b}	0.86	18.96^{b}	0.59	19.61^{b}	1.14
Body mass gain/feed ($x10^{-2}$ g/g)	3.57^{a}	0.21	5.67^{b}	0.23	6.00^{b}	0.13	6.07^{b}	0.27
Fat-free body mass (g)	29.34^{a}	0.99	33.55^{b}	0.91	32.54^{b}	0.57	33.16^{b}	0.86

Notes:
POo, palm olein; IPOo, chemical interesterified palm olein; SOY, soybean oil. Values expressed as mean and standard error of the mean, SEM.
[a,b] Mean values within a row with unlike superscript letters were significant different (P<0.05)

Table 3.7 : Weekly body mass gain of C57BL/6 mice from different dietary groups (*In vivo* study 1)

Week	Body Mass Gain (g)							
	Control		POo		IPOo		SOY	
	Mean	SD	Mean	SD	Mean	SD	Mean	SD
1	2.18	1.61	3.09	1.40	3.33	1.01	3.38	1.71
2	0.66	0.54	0.94	0.75	1.53	0.50	1.48	0.72
3	1.66	0.79	1.42	0.61	1.63	0.47	1.67	0.28
4	1.17	0.61	1.09	0.52	0.99	0.35	1.29	0.50
5	1.15	0.50	1.56	0.28	1.45	0.34	1.34	0.77
6	0.80	0.29	1.57	0.43	1.47	0.38	1.65	0.52
7	0.51	0.25	1.14	0.55	1.05	0.43	1.45	0.46
8	1.21	0.37	1.61	0.65	1.61	0.43	1.76	0.55
9	0.42	0.27	0.61	0.65	0.69	0.35	0.76	0.67
10	0.60	0.40	0.82	0.39	0.80	0.68	0.94	0.90
11	0.18	0.49	0.18	0.49	0.28	0.59	0.04	0.39
12	0.11	0.37	0.82	0.27	0.61	0.39	0.65	0.63
13	0.64	0.75	1.54	0.42	1.49	0.32	1.27	0.54
14	1.00	0.30	1.61	0.56	1.18	0.51	1.15	1.14
15	0.56	0.37	0.55	0.51	0.85	0.53	0.78	0.33

Notes:
POo, palm olein; IPOo, chemical interesterified palm olein; SOY, soybean oil. Values expressed as mean and standard deviation, SD.

3.2.2.3 Fat Deposition

Mice fed with soybean oil (SOY)-enriched diet gained significantly higher mass of subcutaneous fat (P=0.011) and total fat (P=0.013) than those receiving palm olein (POo)-enriched diet (Table 3.8). Chemical interesterified palm olein (IPOo) group exhibited non-significant difference in terms of fat deposition compared to SOY and POo groups.

In order to eliminate the effect of differential amount of fat intake per mouse, the mass of total fat deposited was further subjected to normalisation with total food consumption, shorthanded as fat/feed. Visceral fat/feed in POo fed group was significantly lower (P=0.044) than mice fed with SOY-enriched diet (Table 3.8), while no difference was found when compared with IPOo group. In the context of total fat/feed, all groups differed significantly (P=0.012, Table 3.8). SOY group was accounted for the significantly higher subcutaneous fat/feed (P=0.006) and total fat/feed (P=0.003), after compared to mice receiving POo-enriched diet. It is noteworthy that, chemical interesterification was associated with higher subcutaneous fat/feed and total fat/feed (P=0.049 and 0.013, respectively) as exhibited in mice fed with IPOo-enriched diet as compared to those fed with POo-enriched diet (Table 3.8).

When the fat/feed ratios (subcutaneous, visceral and total) were correlated to the saturated fatty acid (SFA) contents at the *sn*-1,3 positions of triacylglycerols, a negative linear correlation was observed (Figure 3.3a), and it is accompanied by a positive linear correlation between fat/feed and total unsaturated fatty acid content at the similar positions (Figure 3.3b). The correlation coefficients, r, were in the range of 0.9076 to 0.9686. On top of that, all correlation coefficients in Figure 3.3a were statistically significant with P values in the range of 0.033 to 0.038.

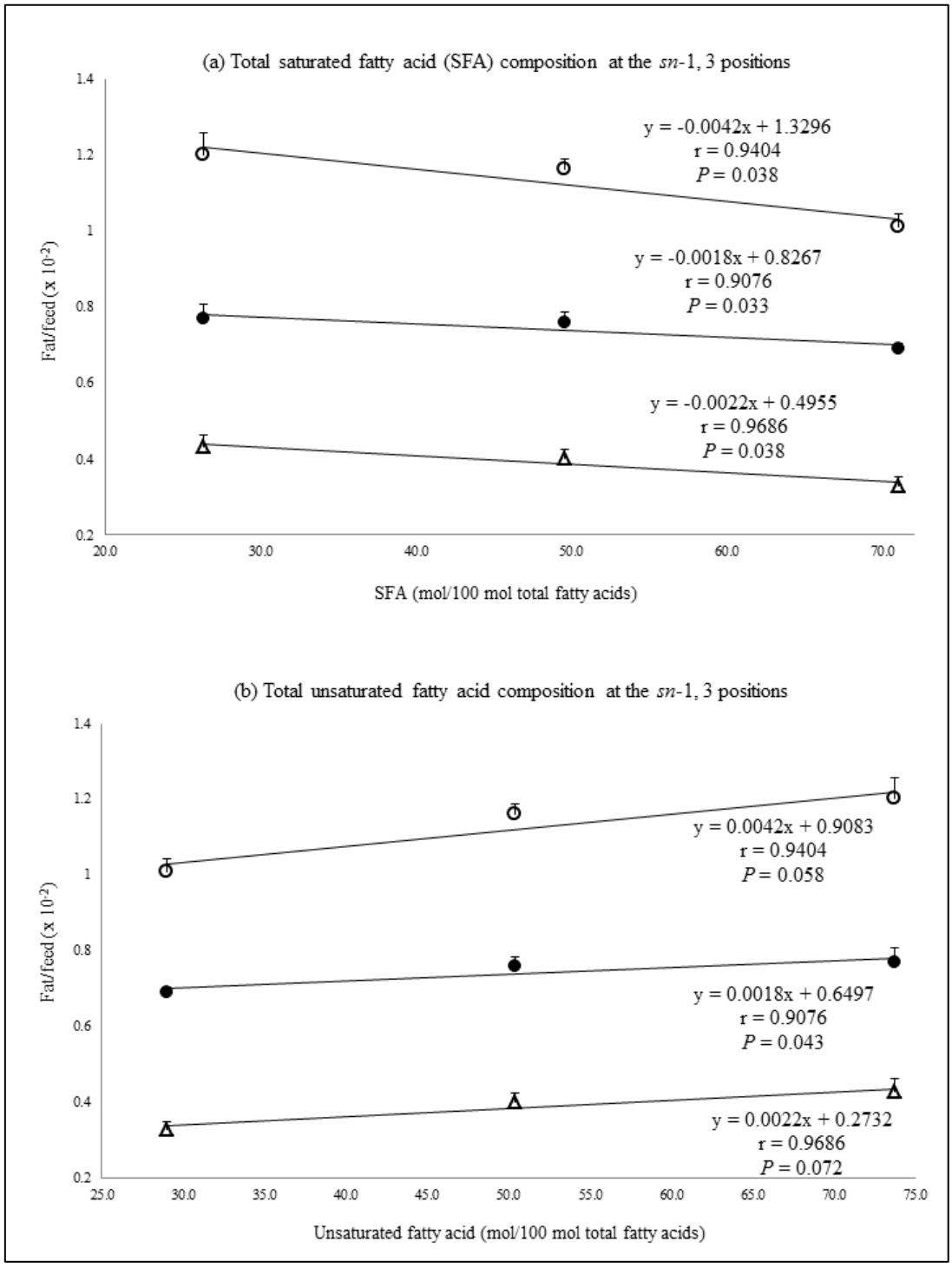

Notes:

Total fat/feed (○, *n* 8), visceral fat/feed (●, *n* 8) and subcutaneous fat/feed (Δ, *n* 8) varied with (a) total saturated fatty acid composition at *sn*-1,3 positions and (b) total unsaturated fatty acid composition at *sn*-1,3 positions. Values are mean with their standard error represented by vertical bars. Correlation coefficients with *P* values < 0.05 were considered as significant.

Figure 3.3 : Effect of total saturation level at the *sn*-1,3 positions of triacylglycerols on fat deposition (mass of fat deposited/total feed consumed)

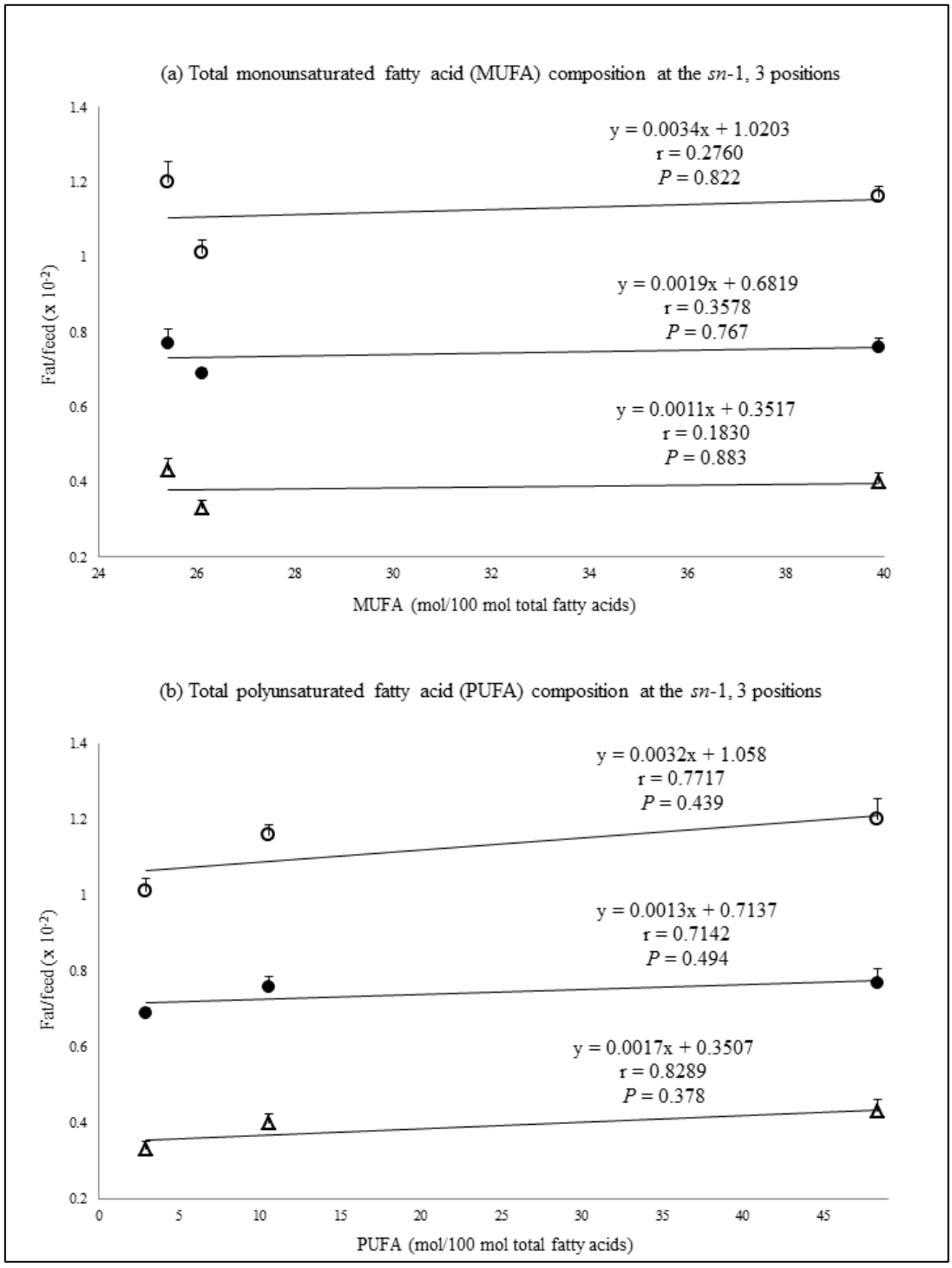

Notes:

Total fat/feed (○, *n* 8), visceral fat/feed (●, *n* 8) and subcutaneous fat/feed (Δ, *n* 8) varied with (a) total monounsaturated fatty acid composition at *sn*-1,3 positions and (b) total polyunsaturated fatty acid composition at *sn*-1,3 positions. Values are mean with their standard error represented by vertical bars. Correlation coefficients with *P* values < 0.05 were considered as significant.

Figure 3.4 : Effect of different extent of unsaturation at the *sn*-1,3 positions of triacylglycerols on fat deposition (mass of fat deposited/total feed consumed)

Conversely, poor regressions were found for monounsaturated fatty acids (MUFA) (r = 0.1830-0.3578) (Figure 3.4a) and polyunsaturated fatty acids (PUFA) (r = 0.7142-0.8289) (Figure 3.4b) at the same positions. All the correlation coefficients in Figure 3.4 were insignificant as the *P* values were greater than 0.05.

Table 3.8 : Fat deposition in C57BL/6 mice over 15 weeks (*In vivo* study 1)

	Control		POo		IPOo		SOY	
	Mean	SEM	Mean	SEM	Mean	SEM	Mean	SEM
Mass of fat								
Subcutaneous (g)	0.43^{a}	0.04	1.07^{b}	0.07	1.25^{bc}	0.07	1.38^{c}	0.12
Visceral (g)	0.39^{a}	0.09	2.25^{b}	0.06	2.41^{b}	0.10	2.49^{b}	0.15
Total (g)	0.82^{a}	0.10	3.32^{b}	0.13	3.66^{bc}	0.11	3.87^{c}	0.22
Mass of fat/feed								
Subcutaneous fat/feed ($x10^{-3}$ g/g)	1.20^{a}	0.13	3.28^{b}	0.21	3.97^{c}	0.24	4.29^{cd}	0.33
Visceral fat/feed ($x10^{-3}$ g/g)	1.14^{a}	0.29	6.87^{b}	0.15	7.62^{bc}	0.26	7.70^{c}	0.38
Total fat/feed ($x10^{-3}$ g/g)	2.34^{a}	0.33	10.14^{b}	0.35	11.59^{c}	0.28	11.99^{cd}	0.56

Notes:
POo, palm olein; IPOo, chemical interesterified palm olein; SOY, soybean oil. Values expressed as mean and standard error of the mean, SEM.
^{a,b,c,d} Mean values within a row with unlike superscript letters were significant different ($P<0.05$)

3.2.2.4 Faecal Fatty Acids

Composition of free fatty acids excreted in the faeces of mice is given in Table 3.9. The content of linoleic acid (C18:2*n*-6) excreted in the faeces was significantly higher in mice fed with soybean oil (SOY)-enriched diet, as compared with both palm olein (POo) ($P<0.00001$) and chemical interesterified palm olein (IPOo) fed groups ($P=0.00001$). This outcome was subsequently reflected in the total amount of polyunsaturated fatty acids (PUFA) excreted by mice receiving SOY-enriched diet, which accounted for a 63.1% of total fatty acids. Furthermore, it is crucial to note that the content of α-linolenic acid (C18:3*n*-3) excreted in the faeces of mice fed with SOY-

enriched diet differed remarkably relative to those fed with POo-enriched diet (*P*=0.023), however no difference was found in mice fed with IPOo-enriched diet. Total excretion of monounsaturated fatty acids (MUFA) and saturated fatty acids (SFA) were significantly lower in SOY group, in comparison with POo (*P*=0.0007 and 0.00002, respectively) and IPOo (*P*=0.0001 and 0.00005) fed groups.

Table 3.9 : Composition of free fatty acids in the faeces of mice from each test group (*In vivo* study 1)

	Faecal fatty acid composition (as % methyl esters)							
	Control		POo		IPOo		SOY	
Acyl chain	Mean	SD	Mean	SD	Mean	SD	Mean	SD
12 : 0	ND	ND	0.09	0.13	ND	ND	ND	ND
14 : 0	2.26^{a}	0.16	1.24^{b}	0.05	1.13^{b}	0.08	0.75^{b}	0.04
16 : 0	24.98^{a}	1.41	52.97^{b}	0.95	44.92^{c}	1.29	14.43^{d}	1.82
18 : 0	8.06^{a}	0.31	10.91^{b}	0.28	10.23^{b}	0.38	6.12^{c}	0.38
20 : 0	1.45	0.01	1.57	0.22	1.96	0.41	0.92	0.07
22 : 0	1.58	0.09	1.05	0.44	1.92	0.23	0.92	0.10
Total SFA	38.34^{a}	1.98	67.83^{b}	0.20	60.17^{c}	2.23	23.15^{d}	1.01
16 : 1*n*-7	ND	ND	0.19	0.27	ND	ND	0.10	0.01
18 : 1*n*-9	27.04^{a}	0.79	20.70^{b}	0.70	24.65^{c}	1.22	13.29^{d}	0.05
20 : 1*n*-9	0.90^{a}	0.07	0.53^{b}	0.10	0.70^{ab}	0.15	0.35^{b}	0.12
Total MUFA	27.94^{a}	0.86	21.41^{b}	0.86	25.35^{c}	1.06	13.75^{d}	0.08
18 : 2*n*-6	30.48^{a}	0.92	9.81^{b}	0.93	13.19^{b}	1.10	61.26^{c}	2.35
18 : 3*n*-3	3.25^{a}	0.20	0.95^{b}	0.13	1.29^{bc}	0.07	1.84^{c}	0.43
Total PUFA	33.72^{a}	1.12	10.76^{b}	1.06	14.48^{b}	1.17	63.10^{c}	2.79

Notes:
POo, palm olein; IPOo, chemical interesterified palm olein; SOY, soybean; SFA, saturated fatty acids; MUFA, monounsaturated fatty acids; PUFA, polyunsaturated fatty acids; ND, not detected. Values expressed as mean and standard deviation, SD.
^{a,b,c,d} Mean values within a row with unlike superscript letters were significant different ($P<0.05$).

In spite of being fed with diets containing comparable total fatty acid composition (FAC), mice fed with POo-enriched diet exhibited greater excretion of SFA (*P*=0.019) compared with mice in IPOo dietary group. The composition of palmitic acid (C16:0) was significantly higher (*P*=0.021) in POo group, yet no significant difference was observed for stearic acid (C18:0) content. On the contrary, there was a substantial higher amount (*P*=0.008) of MUFA, which predominantly comprised of oleic acid

(C18:1), being excreted by the mice fed with IPOo-enriched diet compared with those in POo dietary group. Similar increment was also noted for PUFA excretion in IPOo group, but the difference was not significant. The absolute amount of free fatty acids in the faeces of mice from different dietary groups are depicted in Table 3.10. Total amount of free fatty acids in the faeces from mice fed with POo-enriched diet is significantly higher than those fed with IPOo-enriched (P=0.046) and SOY-enriched diets (P=0.030).

Table 3.10 : The absolute amount of free fatty acids in the faeces of mice from different dietary groups (*In vivo* study 1)

Fatty acid *	Absolute amount of free fatty acids (μg /1 g of faeces)		
	POo	IPOo	SOY
16 : 0	5.52	3.83	0.91
18 : 0	1.03	0.75	0.49
18 : 1*n*-9	1.95	1.81	0.94
18 : 2*n*-6	0.92	0.97	3.97
Total	9.42[a]	7.36[b]	6.31[b]

Notes:
POo, palm olein; IPOo, chemical interesterified palm olein; SOY, soybean.
[a,b] Mean values within a row with unlike superscript letters were significant different (P<0.05)
[*] The analyses were done on major fatty acids (more than 5g/100 g total fatty acids in the composition).

Mice fed with POo-enriched diet displayed greater excretion index for both major SFA (excretion indices of 1.35 for palmitic acid and 2.50 for stearic acid) in the pair wise comparison with IPOo group (1.14 for palmitic acid and 2.34 for stearic acid) (Table 3.11). This trend was subsequently mirrored in the excretion index for total SFA (1.50 for POo and 1.32 for IPO dietary groups). It is worth mentioning that the SFA excretion of longer chain was greater than those with a shorter chain length. Within the similar pair wise comparison, IPOo group was responsible for the concomitant increment of excretion indices for total MUFA (18.0% greater) and PUFA (35.9% greater). In general, the rate of fatty acid excretion in all the dietary groups was in the following order: SFA > PUFA > MUFA.

Table 3.11 : The excretion indices for each fatty acid in the faeces of mice from different dietary groups (*In vivo* study 1)

Fatty acid	Excretion index			
	Control	POo	IPOo	SOY
12 : 0	ND	0.34	ND	ND
14 : 0	2.22	1.24	1.12	1.06
16 : 0	1.75	1.35	1.14	1.37
18 : 0	2.58	2.50	2.34	1.43
20 : 0	3.32	4.10	5.24	2.60
22 : 0	3.16	26.23	28.57	2.45
Total SFA	2.05	1.50	1.32	1.48
16 : 1*n*-7	ND	1.16	ND	1.32
18 : 1*n*-9	0.79	0.48	0.58	0.56
20 : 1*n*-9	1.33	3.56	5.19	1.68
Total MUFA	0.80	0.50	0.59	0.57
18 : 2*n*-6	0.75	0.86	1.16	1.15
18 : 3*n*-3	0.61	4.40	5.99	0.27
Total PUFA	0.73	0.92	1.25	1.05

Notes:
POo, palm olein; IPOo, chemical interesterified palm olein; SOY, soybean; SFA, saturated fatty acids; MUFA, monounsaturated fatty acids; PUFA, polyunsaturated fatty acids; ND, not detected.

3.2.2.5 Adipose Tissue

In a broader sense, by observing the fatty acid composition (FAC) of the diets (Table 3.2, Section 3.2.1.1) and those deposited in adipose tissues (Table 3.12 and Table 3.13), the composition of saturated fatty acid (SFA) were decreased after deposition. The content of palmitoleic acid (C16:1) was increased vastly by 28.9 to 40.3-fold in adipose tissues compared with those in the diets. This is concomitant with the major decrement of the saturated counterpart, namely, palmitic acid (C16:0). In addition, several polyunsaturated fatty acids (PUFA) were found in adipose tissue, yet they were absent in the diets. The instances of PUFA were eicosatrienoic acid (C20:3*n*-6), arachidonic acid (C20:4*n*-6) and docosahexaenoic acid (C22:6*n*-3).

In summary, the deposition trend was followed according to a greater degree of fatty acid deposition for monounsaturated fatty acids (MUFA), then by PUFA and the least

deposited SFA. By comparing the FAC between subcutaneous and visceral adipose tissues, no significant difference was found.

Table 3.12 : Fatty acid composition of the extracted lipids from subcutaneous adipose tissue of mice (*In vivo* study 1)

	Fatty acid composition (as % methyl esters)							
	Control		POo		IPOo		SOY	
Acyl chain	Mean	SD	Mean	SD	Mean	SD	Mean	SD
12 : 0	0.06	0.02	0.09	0.01	0.06	0.04	ND	ND
14 : 0	1.18	0.03	0.78	0.03	0.73	0.04	0.40	0.03
16 : 0	17.98	0.12	22.01	0.87	21.48	0.46	11.88	0.77
18 : 0	1.79	0.03	1.52	0.08	1.54	0.06	2.03	0.12
20 : 0	ND	ND	0.11	0.01	0.10	0.01	0.10	0.01
Total SFA	21.01	0.45	24.51	0.92	23.92	0.53	14.40	0.84
14 : 1*n*-5	ND	ND	0.02	0.01	0.01	0.02	ND	ND
16 : 1*n*-7	6.96	0.12	6.17	0.32	6.07	0.33	2.30	0.26
18 : 1*n*-9	45.70	0.88	52.00	0.83	51.59	0.46	34.13	0.27
20 : 1*n*-9	1.18	0.24	0.06	0.05	0.07	0.04	0.11	0.01
Total MUFA	53.84	0.83	58.26	0.84	57.75	0.59	36.57	0.32
18 : 2*n*-6	23.35	0.66	16.26	0.19	17.22	0.40	45.57	0.97
18 : 3*n*-3	1.78	0.21	0.68	0.02	0.79	0.03	2.92	0.20
20 : 2	0.02	0.01	0.03	0.03	0.01	0.02	0.15	0.04
20 : 3*n*-6	ND	ND	0.07	0.05	0.10	0.01	0.14	0.01
20 : 4	ND	ND	0.19	0.01	0.20	0.01	0.22	0.03
22 : 6*n*-3	ND	ND	ND	ND	ND	ND	0.04	0.03
Total PUFA	25.15	0.56	17.23	0.24	18.33	0.38	49.03	0.99

Notes:
POo, palm olein; IPOo, chemical interesterified palm olein; SOY, soybean; SFA, saturated fatty acids; MUFA, monounsaturated fatty acids; PUFA, polyunsaturated fatty acids; ND, not detected. Values expressed as mean and standard deviation, SD.

The positional distributions of fatty acids in the extracted lipids from subcutaneous and visceral adipose tissues were shown in Table 3.14. SFA at the *sn*-1,3 positions of triacylglycerols depreciated greatly from 70.8 mol% (in POo dietary group) to 38.9 mol% (subcutaneous adipose tissue) and 35.7 mol% (visceral adipose tissue), as well as from 49.6 mol% (in IPOo dietary group) to 21.7 mol% (subcutaneous adipose tissue) and 20.9 mol% (visceral adipose tissue). The decrement for soybean oil (SOY) fed group was the lowest (from 25.4 mol% to 22.1 mol% (subcutaneous adipose tissue) and

22.6 mol% (visceral adipose tissue)). These observations were associated with an increment of relative composition of MUFA.

Table 3.13 : Fatty acid composition of the extracted lipids from visceral adipose tissue of mice (*In vivo* study 1)

	Fatty acid composition as (% methyl esters)							
	Control		POo		IPOo		SOY	
Acyl chain	Mean	SD	Mean	SD	Mean	SD	Mean	SD
12 : 0	0.05	0.01	0.05	0.04	0.07	0.01	ND	ND
14 : 0	0.88	0.21	0.66	0.10	0.69	0.05	0.43	0.04
16 : 0	18.96	0.66	22.93	0.74	23.66	0.52	13.35	0.64
18 : 0	1.55	0.12	1.46	0.06	1.51	0.04	1.94	0.17
20 : 0	ND	ND	0.10	0.01	0.10	0.01	0.09	0.01
Total SFA	21.44	0.67	25.20	0.87	26.03	0.56	15.81	0.76
14 : 1*n*-5	ND	ND	0.01	0.02	0.01	0.02	ND	ND
16 : 1*n*-7	6.70	0.20	6.54	0.52	6.39	0.34	2.57	0.29
18 : 1*n*-9	45.90	0.59	50.50	0.86	49.56	0.56	32.76	0.52
20 : 1*n*-9	1.05	0.20	0.07	0.03	0.09	0.01	0.10	0.01
Total MUFA	53.65	0.78	57.12	0.71	56.05	0.50	35.43	0.51
18 : 2*n*-6	22.94	0.43	16.57	0.33	16.74	0.35	45.21	0.78
18 : 3*n*-3	1.92	0.12	0.75	0.04	0.81	0.04	2.98	0.28
20 : 2	0.05	0.01	0.03	0.03	0.06	0.01	0.14	0.01
20 : 3*n*-6	ND	ND	0.10	0.04	0.08	0.05	0.15	0.02
20 : 4	ND	ND	0.22	0.04	0.20	0.02	0.22	0.03
22 : 6*n*-3	ND	ND	ND	ND	0.02	0.02	0.06	0.01
Total PUFA	24.91	0.64	17.68	0.35	17.92	0.34	48.76	0.68

Notes:
POo, palm olein; IPOo, chemical interesterified palm olein; SOY, soybean; SFA, saturated fatty acids; MUFA, monounsaturated fatty acids; PUFA, polyunsaturated fatty acids; ND, not detected. Values expressed as mean and standard deviation, SD.

Moreover, the compositions of *cis*-11-monoene were elevated in all adipose tissues of mice from various dietary groups, except for the subcutaneous adipose tissue of mice from POo group. Similarly, the regiospecific data for subcutaneous and visceral adipose tissues did not differ significantly.

Table 3.14 : Positional fatty acid composition of the adipose tissues of mice (*In vivo* study 1)

Dietary group	Composition (mol%)								
	sn-position	SFA		MUFA				PUFA	
				cis-11-monoene		*cis*-9-monoene			
		Subcutaneous	Visceral	Subcutaneous	Visceral	Subcutaneous	Visceral	Subcutaneous	Visceral
Control	1, 3	35.2	30.9	10.5	6.8	41.6	46.4	12.7	15.8
	2	7.1	7.6	ND	ND	51.8	50.3	41.0	42.0
	1, 2, 3	25.3	23.2	6.8	4.5	45.2	47.7	22.6	24.6
POo	1, 3	38.9	35.7	ND	7.6	52.6	46.1	8.6	10.6
	2	9.2	9.0	ND	ND	58.5	62.0	32.3	29.0
	1, 2, 3	28.7	26.6	ND	5.0	54.6	51.5	16.7	16.9
IPOo	1, 3	21.7	20.9	2.6	5.5	53.6	51.9	22.1	21.7
	2	33.7	40.0	ND	ND	53.8	50.7	12.5	9.3
	1, 2, 3	25.5	26.2	1.8	4.0	53.7	51.6	19.0	18.3
SOY	1, 3	22.1	22.6	6.9	8.2	35.5	31.6	35.6	37.6
	2	ND	ND	ND	ND	33.4	33.0	66.6	67.1
	1, 2, 3	14.6	14.9	4.5	5.4	34.8	32.1	46.2	47.6

Notes:
SFA, saturated fatty acids; MUFA, monounsaturated fatty acids; PUFA, polyunsaturated fatty acids; POo, palm olein; IPOo, chemical interesterified palm olein; SOY, soybean oil; ND, not detected.

3.2.3 Discussion

In vivo study 1 shows that fatty acid composition (FAC) at the *sn*-1,3 position of triacylglycerol molecule affects the body fat deposition in C57BL/6 mice. In the event where the *sn*-1,3 positions are mainly occupied by long chain saturated fatty acids (SFA) (palmitic acid (C16:0) and above), the problem of fat deposition is lightened, while they have no effect if reside at the *sn*-2 position. During the 15 weeks, the differences between the three dietary groups and the control group were more pronounced than the differences among the three dietary groups in most of the nutritional parameters. This shows that the higher energy density in the test diets was accounted for the notable changes in body composition of mice. On the other hand, the total food consumption of mice in all dietary groups did not show any discrepancy proposing that all test oils exerted comparable effect on the appetite of mice. In

addition, mice body mass recorded the highest gain during Week 1 and subsequently remained similar from Week 2 until Week 15 in all dietary groups. It may due to the significantly higher food consumption during Week 1 as for the necessity of growth after weaning.

In the context of body mass gain, the differences were insignificant across all the dietary groups, even after normalisation with the total amount of food consumed (denoted as gain/feed) (Table 3.6, Section 3.2.2.2). Nonetheless, different dietary oils had resulted in different extent of fat deposition in the subcutaneous and visceral as well as total fat/feed (Table 3.8, Section 3.2.2.3). Henceforth, it demonstrates that the body mass gain and fat deposition are not necessarily occurred in tandem and this outdoes the previous studies which used body mass gain as the marker for obesity (Ikemoto *et al.*, 1996; Timmers *et al.*, 2011). As a consequence, the normalised data, denoted as fat/feed, should be given emphasis in the evaluation of diet-induced adipogenic effect of oils. Broadly, the present study showed that soybean oil (SOY) and chemical induced interesterified palm olein (IPOo)-enriched diets exhibit higher potential towards the risk of obesity if compared to palm olein (POo)-enriched diet.

The 15 weeks of SOY-enriched diet (17.5% of total saturation) feeding induced significantly higher fat deposition (30.9%, 12.1% and 18.2% of increments in subcutaneous fat/feed, visceral fat/feed and total fat/feed, respectively) if pair wise-compared with POo-enriched diet (50.3% total saturation). This is parallel with previous reports which are comparing between the both (Jen *et al.*, 2003; Stachon *et al.*, 2006). Nevertheless, a contradiction is found in the reports which made generalisation that any increase in fat deposition is correlated to the extent of total saturation in the oil; *i.e.* saturated oil triggered more fat deposition as compared to the lower saturated (or higher

unsaturated) oil, based on comparisons between beef tallow and sunflower oil (Shimomura *et al.*, 1990; Sanz *et al.*, 2000; Newman *et al.*, 2002; Matsuo *et al.*, 2002). In fact, this inconsistency can be elucidated by considering at the positional distribution of SFA in the oils being studied. Beef tallow contains about 33.6% and 79.4% of SFA at the *sn*-1,3 and *sn*-2 positions, respectively (Gunstone and Harwood, 2007), however POo on the contrary, contains 71.0% of SFA at the *sn*-1,3 positions, and 7.4% of SFA at the *sn*-2 position (Table 3.3, Section 3.2.1.1). Therefore, based on the current findings, if higher amount of long chain SFA occur at the *sn*-1,3 positions of triacylglycerols, they tend to lessen the accretion of fat. The aforementioned contradiction is cleared using the current postulation.

By exploring the types of fat, SOY-enriched diet caused 12.1% higher deposition of visceral fat per food consumed than POo-enriched diet. This significant difference may provide some prospective benefits to a healthier diet as deposited fat in the visceral cavity is well-known associated with several health problems, for instances cardiovascular disease, insulin resistance, breast cancer, endometrial cancer, hypertension and overall mortality (Emery *et al.*, 1993; Kim *et al.*, 2011). Hence, this warrants future clinical trials for further verification.

It was promising to note that the differences in fat deposition were remarkable between POo and SOY dietary groups, but not in pair wise comparison between IPOo and SOY dietary groups (Table 3.8, Section 3.2.2.3). Despite the identical total content of saturated and unsaturated fatty acids, the mice fed with IPOo-enriched diet were proven to trigger 14.3% more fat per food consumed as compared with POo-enriched diet. As depicted in Table 3.3 (Section 3.2.1.1), saturated content at the *sn*-1,3 positions in IPOo was 21.4 mol% lower than that in POo, thereby supports current hypothesis which states

that a lower SFA content at the *sn*-1,3 positions of triacylglycerols in IPOo was responsible for the higher fat absorption, re-synthesis of triacylglycerol in chylomicron and eventually the accretion of fat. While in POo, most SFA in free-form after deacylated from the *sn*-1,3 positions may suffer deferred absorption due to the formation of calcium salts, then subsequently excreted in the faeces. This is consistent with the statement suggested previously (Mattson *et al.*, 1979; Innis *et al.*, 1997). Further evidence is provided by the greater excretion index observed for palmitic (C16:0) and stearic acids (C18:0) in the faeces of mice receiving POo-enriched diet, which are 18.4% and 6.8%, respectively, higher than those in the faeces of mice fed with IPOo-enriched diet (Table 3.9, Section 3.2.2.4). Again, this is parallel with the trend observed by other investigators (Brink *et al.*, 1995). As a consequence, encouraging cutbacks of subcutaneous and total fat deposition in mice fed with POo-enriched diet as compared with those fed with IPOo-enriched diet are noted, despite their comparable total FAC. This retains the potential to surpass some prior studies which were investigating the obesogenic effect of oils merely based on their total SFA, monounsaturated fatty acid (MUFA) or polyunsaturated fatty acid (PUFA) contents.

According to reported data (Mattson *et al.*, 1979; Small, 1991; Brink *et al.*, 1995), long chain SFA originated from the *sn*-1,3 positions of glycerol backbone were observed to be poorly absorbed after cleavage by pancreatic lipase, and successively excreted in the form of magnesium or calcium salts. This was further validated in the present study. After the fatty acids in faeces were normalised with their corresponding composition in the ingested fats (denoted as excretion index), an interesting trend was observed for total SFA, MUFA and PUFA. All the excretion indices bear close resemblance regardless of the type of ingested fats. Major MUFA, namely, oleic acid (C18:1), were found to be least readily excreted in faeces, with the range of excretion index in 0.50 to 0.59 as they

were well-absorbed in the intestine. On the contrary, the relative composition of all types SFA in faeces were greater than those respective fatty acids present in dietary fats (excretion indices = 1.32-1.50).

For the effective absorption in intestine, micelles formed by the bile salts carry the nonpolar free fatty acids in order to allow their passage across the aqueous boundary layer of intestinal wall. Therefore, long chain SFA, which is relatively more non-polar than the unsaturated counterparts, is observed to be less susceptible towards intestinal absorption. The increasing susceptibility for fatty acid absorption in the intestine was followed by the sequence of SFA, PUFA and lastly the most absorbed MUFA.

Using the current postulation, a considerable number of previous contradicted reports can be further elucidated and clarified. Conventional saturated fats, namely, palm oil (Ikemoto *et al.*, 1996) and cocoa butter (Timmers *et al.*, 2011), as well as beef tallow (Shimomura *et al.*, 1990; Larson *et al.*, 1996; Sanz *et al.*, 2000; Newman *et al.*, 2002; Matsuo *et al.*, 2002) and lard (Catta-Preta *et al.*, 2012), had been observed to exert different adipogenic effects. Beef tallow and lard which were found to be more obesogenic, contain SFA mainly reside at the *sn*-2 positions, while major SFA are located at the *sn*-1,3 positions of triacylglycerol moiety in palm oil and cocoa butter (Gunstone and Harwood, 2007). In consequence, the positive correlation between total SFA composition and carcass fat content presented in previous study which employed beef tallow to represent the saturated fats (Matsuo *et al.*, 2002), might not be valid if similar investigation is being executed using cocoa butter as the saturated fat representative.

On the other hand, excessive intake of MUFA which had been reported to raise fat deposition (Catta-Preta *et al.*, 2012), can be interrelated to the higher rate of absorption (or lower rate of excretion) of MUFA observed in the current study. From the perspective of positional fatty acids at the *sn*-1,3 positions of triacylglycerol molecule, a negative relationship was found between fat/feed and the SFA content, whereas a positive relationship was noted between total fat/feed and unsaturated content at the similar *sn*-positions (Figure 3.3, Section 3.2.2.3). Besides, there was no correlation found between fat deposition and linoleic acid (C18:2*n*-6) composition in the current investigation (Figure 3.4, Section 3.2.2.3).

In addition, Ponnampalam *et al.* (2011) observed a slightly lower fat percentage (20.5 %) in piglets fed with native palm olein-enriched diet than those receiving lard-enriched (21.2%) and chemical-induced interesterified palm olein-enriched diets (21.5%). A recent study also reports that the dietary 1(3)-behenoyl-2,3(1)-dioleoylglycerol, which contains long chain saturated behenic acid (C22:0) at the *sn*-1 or *sn*-3 position, precludes the deposition of hepatic triacylglycerols and visceral fat (Kojima *et al.*, 2010). With no explicit reason had been disclosed beforehand, the present postulation is expected to provide more insights and understanding from the perspective of positional distribution of long chain SFA on fat accretion.

In the context of FAC of adipose tissue, the results show that there is a higher degree of deposition for MUFA, followed by PUFA and lastly by SFA. This is in accordance with the trend observed for the excretion index, as the greatest for SFA, then PUFA and lowest by MUFA. The deposited fatty acids are highly correlated to those absorbed through the intestine after the action of pancreatic lipase, which further elucidate the rate of absorption of different fatty acids, eventually the effect on fat deposition. Some

minor fatty acids, particularly myristic (C14:0) and palmitoleic acids (C16:1*n*-7), were found abundantly in both subcutaneous and visceral adipose tissues, suggesting *de novo* synthesis (Perona *et al.*, 2000).

In summary, instead of the total SFA content, *in vivo* study 1 evidenced that the positional distribution of long chain SFA exerted a more pronounce effect on body fat accretion. In other words, the problem of obesity will be alleviated in the event of long chain SFA (C16:0 and above) occur predominantly at the *sn*-1 and *sn*-3 positions of triacylglycerols.

3.3 *In Vivo* Study 2: Different Chain Length of Long Chain Saturated Fatty Acids at the *sn*-1,3 Positions of Triacylglycerols on Fat Deposition

3.3.1 Experimental

3.3.1.1 Diets

Autoclavable standard pellet feeds (digestible energy 14.0 MJ/kg) were purchased from Specialty Feeds, Glen Forrest, West Australia. The nutritional values of the autoclavable standard pellet feeds for mice are given in Table 3.1 (Section 3.2.1.1). Refined, bleached and deodorised (RBD) sal stearin (SAL), also known as *Shoria robusta*, was obtained from Mewah Oil Sdn. Bhd., Selangor, Malaysia. RBD cocoa butter (COB), palm mid fraction (PMF) and high-oleic sunflower oil (HOS) were provided by Intercontinental Specialty Fats Sdn. Bhd., Selangor, Malaysia. The total and positional fatty acid composition of the dietary oils were tabulated in Table 3.15 and Table 3.16, respectively.

Table 3.15 : Total fatty acid composition of dietary oils and fats for *in vivo* study 2

Acyl chain	Fatty acid composition (as % methyl esters)			
	COB	SAL	PMF	HOS
12 : 0	ND	ND	0.05	ND
14 : 0	0.10	0.02	0.84	0.04
16 : 0	25.55	4.55	58.24	3.84
18 : 0	36.61	51.83	5.46	2.88
20 : 0	1.17	8.00	0.37	ND
22 : 0	ND	0.50	ND	ND
Total SFA	63.43	64.90	64.96	6.76
16 : 1*n*-7	0.23	ND	0.06	0.10
18 : 1*n*-9	33.48	33.91	31.93	82.42
20 : 1*n*-9	0.05	0.08	0.05	0.26
Total MUFA	33.76	33.99	32.04	82.78
18 : 2*n*-6	2.62	0.95	2.96	10.37
18 : 3*n*-3	0.17	0.14	0.04	0.09
20 : 2*n*-6	0.02	0.02	ND	ND
Total PUFA	2.81	1.11	3.00	10.46

Notes:
COB, cocoa butter; SAL, sal stearin; PMF, palm mid fraction; HOS, high-oleic sunflower oil; SFA, saturated fatty acids; MUFA, monounsaturated fatty acids; PUFA, polyunsaturated fatty acids; ND, not detected.

The diets were prepared by fortifying the standard pellet feeds with test oils at an oil composition of 150g/kg diet, subsequently the mixtures were pelleted into original shape. Prior to feeding, these diets were left to dryness at 30℃ overnight. All test diets are isoenergetic (20 MJ/kg).

Table 3.16 : Positional fatty acid composition of dietary oils for *in vivo* study 2

Sample	Composition (mol%) *								
	sn-position	SFA		MUFA				PUFA	
				cis-11-monoene		*cis*-9-monoene			
		Mean	SD	Mean	SD	Mean	SD	Mean	SD
COB	1, 3	94.7	0.3	ND	ND	5.3	0.4	ND	ND
	2	5.0	0.5	ND	ND	88.9	0.8	6.1	0.2
	1, 2, 3	64.9	0.5	ND	ND	33.1	0.5	2.0	0.1
SAL	1, 3	93.7	0.6	ND	ND	4.6	0.7	1.7	0.6
	2	ND	ND	ND	ND	100.0	0.8	ND	ND
	1, 2, 3	62.4	0.8	ND	ND	36.5	0.7	1.1	0.4

Table 3.16, continued

Sample	Composition (mol%) *								
	sn-position	SFA		MUFA				PUFA	
				cis-11-monoene		*cis*-9-monoene			
		Mean	SD	Mean	SD	Mean	SD	Mean	SD
PMF	1, 3	92.3	0.4	ND	ND	6.5	0.8	1.2	0.2
	2	16.4	0.3	ND	ND	75.9	0.6	7.7	0.4
	1, 2, 3	68.3	0.3	ND	ND	28.5	0.6	3.3	0.3
HOS	1, 3	11.6	0.5	2.6	0.4	73.9	0.8	11.9	0.5
	2	ND	ND	ND	ND	86.5	0.5	13.5	0.5
	1, 2, 3	7.8	0.4	1.7	0.3	78.1	0.6	12.4	0.5

Notes:
SFA, saturated fatty acids; MUFA, monounsaturated fatty acids; PUFA, polyunsaturated fatty acids; COB, cocoa butter; SAL, sal stearin; PMF, palm mid fraction; HOS, high-oleic sunflower oil; ND, not detected. Values expressed as mean and standard deviation, SD.
* ^{13}C NMR results are mean of three (3) replicates.

3.3.1.2 Animal Experiment

40 weaned male C57BL/6 mice were obtained from Monash University, Selangor, Malaysia. The mice were acclimatised to the environmentally controlled laboratory environment (23 ± 2 ℃ and a relative humidity of 60%) with a 12:12 hours light:dark cycle. Subsequently, they were randomly divided into four dietary groups of 10 mice each and housed individually. The average body mass of mice for cocoa butter (COB), sal stearin (SAL), palm mid fraction (PMF) and high-oleic sunflower oil (HOS) dietary groups at the beginning of the study were not significantly differed after randomisation (P=0.088) and were 19.7 ± 0.7 g, 19.9 ± 0.8 g, 20.3 ± 0.5 g and 19.7 ± 0.6 g, respectively.

Throughout the 15 weeks of experimental duration, the mice were allowed free access to water and food. The food consumption was determined on daily basis, while the body mass was recorded on a weekly basis. Spilled food was separated from the mice faeces and then corrected for the data of food intake. Fresh faeces were collected daily, pooled

and stored at -20 ℃, starting from week 3 until week 15. At euthanasia, the mice were sacrificed by dislocation of the neck. The subcutaneous and visceral adipose tissues were removed from the carcass, weighed and kept frozen at -80 ℃. Data on the body mass gain and the mass of fat deposited were subjected to normalisation with total food consumption, denoted as gain/feed and fat/feed, respectively. All protocols for the mice experiment were approved by the Animal Care and Use Committee (ACUC), Faculty of Medicine, University of Malaya, Kuala Lumpur, Malaysia (ethic no: KIM/22/11/2011/GSW (R)).

3.3.1.3 Lipid Extraction

The extraction and isolation of lipid contents from adipose tissues and faeces were carried out in accordance to a modified method (Folch *et al.*, 1957), which has been explained in Section 3.2.1.3. The extracted lipids were stored at -20 ℃ prior to subsequent analyses.

3.3.1.4 Lipid Analysis

The analyses of total fatty acid compositions (FAC) of test oils, extracted lipids from faeces and adipose tissues, as well as the determination of the absolute amount of faecal fatty acids, were in accordance to Section 3.2.1.4. Regiospecific analyses of test oils and adipose tissues were performed using JEOL ECA-400MHz NMR spectrometer as described previously (Section 3.2.1.4).

3.3.1.5 Statistical Analysis

All statistical analyses were executed using IBM SPSS Statistic 20 (SPSS Inc. Chicago, IL, USA). One way analysis of variance (ANOVA) was used to assess the significance of the differences among the dietary groups, whereas Tukey's honestly significant

differences test was used for pair wise comparisons. *P* values < 0.05 were treated as significant.

3.3.2 Results

3.3.2.1 Food Consumption

All mice fed with dietary oils are showed comparable food consumption, as given in Table 3.17.

Table 3.17 : Total food consumption of C57BL/6 mice after 15 weeks (*In vivo* study 2)

	COB		SAL		PMF		HOS	
	Mean	SEM	Mean	SEM	Mean	SEM	Mean	SEM
Food consumption* (g)	438.15	10.22	423.18	6.68	416.78	9.19	421.01	10.44

Notes:
COB, cocoa butter; SAL, sal stearin; PMF, palm mid fraction; HOS, high-oleic sunflower oil. Values expressed as mean and standard error of the mean, SEM.
* Food consumption was calculated as the total food intake for each mouse in 15 weeks and then averaged for each group (n=10).

3.3.2.2 Body Mass Gain

Mice fed with high-oleic sunflower oil (HOS)-enriched diet gained significantly higher body mass as compared to those receiving cocoa butter (COB)-enriched (*P*=0.030) and sal stearin (SAL)-enriched diets (*P*=0.0002) (Table 3.18). Surprisingly, feeding with SAL-enriched diet gave significantly lower (*P*=0.023) body mass gain as compared to palm mid fraction (PMF) dietary group (Table 3.18).

Similar to findings from *in vivo* study 1, normalised data showed significantly lower body mass gain/feed in COB (*P*=0.002) and SAL fed groups (*P*=0.00002) compared with those in HOS dietary group. Mice fed with PMF-enriched diet remained having remarkable higher (*P*=0.003) body mass gain/feed compared with SAL fed group (Table

3.18). In the aspect of fat-free mass, the difference was only significant between pair wise comparison of SAL and HOS dietary groups (*P*=0.003).

Table 3.18 : Body mass of C57BL/6 mice over 15 weeks (*In vivo* study 2)

	COB		SAL		PMF		HOS	
	Mean	SEM	Mean	SEM	Mean	SEM	Mean	SEM
Body mass gain (g)	14.84^{ab}	0.92	12.12^{a}	0.86	16.77^{bc}	0.99	19.33^{c}	1.48
Body mass gain/feed ($x10^{-2}$ g/g)	3.37^{ab}	0.16	2.86^{a}	0.19	4.02^{bc}	0.22	4.55^{c}	0.27
Fat-free body mass (g)	31.76^{ab}	0.50	29.96^{a}	0.49	33.08^{ab}	0.49	34.79^{b}	0.75

Notes:
COB, cocoa butter; SAL, sal stearin; PMF, palm mid fraction; HOS, high-oleic sunflower oil. Values expressed as mean and standard error of the mean, SEM.
^{a,b,c}Mean values within a row with unlike superscript letters were significant different ($P<0.05$).

3.3.2.3 Fat Deposition

In Table 3.19, it is evidenced that the mice fed with high-oleic sunflower oil (HOS)-enriched diet gained significantly higher mass of subcutaneous fat compared with those fed to cocoa butter (COB)-enriched (*P*=0.004), sal stearin (SAL)-enriched (*P*=0.00008) and palm mid fraction (PMF)-enriched diets (*P*=0.029). Besides, visceral fat was found significantly lower in SAL dietary group than PMF (*P*=0.041) and HOS groups (*P*=0.010). HOS dietary group was associated with the significantly greater extent of total fat deposition as compared to those fed with COB-enriched (*P*=0.017) and SAL-enriched diets (*P*=0.001).

After normalised with total food consumed, significantly lower subcutaneous fat/feed in COB (*P*=0.001), SAL (*P*=0.00002) and PMF dietary groups (*P*=0.016) compared to those fed with HOS-enriched diet were noted (Table 3.19). While for the visceral fat/feed and total fat/feed, significantly lower values in SAL (*P*=0.007, *P*=0.0003,

respectively) and COB fed groups (P=0.043, P=0.006, respectively) in pair wise comparison to mice fed with HOS-enriched diet were observed. Mice receiving PMF-enriched diet exhibited significantly greater visceral fat/feed (P=0.029) compared with those fed with SAL-enriched diet (Table 3.19). In general, PMF-enriched diet was accounted for the significantly greater (P=0.037) total fat deposited per food consumed than that of the SAL-enriched diet. In contrast, COB dietary group exhibited non-significant difference (P>0.05) for all parameters while comparing to both SAL and PMF groups.

A poor linear correlation (Figure 3.5a) was noted between fat/feed and total saturated fatty acid (SFA) content at the *sn*-1,3 positions of triacylglycerols in dietary fats (r=0.6847-0.9195). All the correlation coefficients were insignificant as the resultant P values were greater than 0.05. However, when the data of fat/feed were plotted against the content of stearic acid at the similar positions, exceptional negative linear correlations were observed for subcutaneous, visceral and total fat/feed, in which the correlation coefficient were 0.9693, 0.9989, 0.9999, respectively (Figure 3.5b). Both correlation coefficients of total fat/feed and visceral fat/feed against the stearic acid content at the *sn*-1,3 positions were shown to be statistically significant at P values of 0.011 and 0.030, respectively. The data from the HOS dietary group was not included in Figure 3.5b as the factor affecting the fat deposition was predominantly attributed by the high monounsaturated fatty acid (MUFA) composition at the *sn*-1,3 positions of HOS.

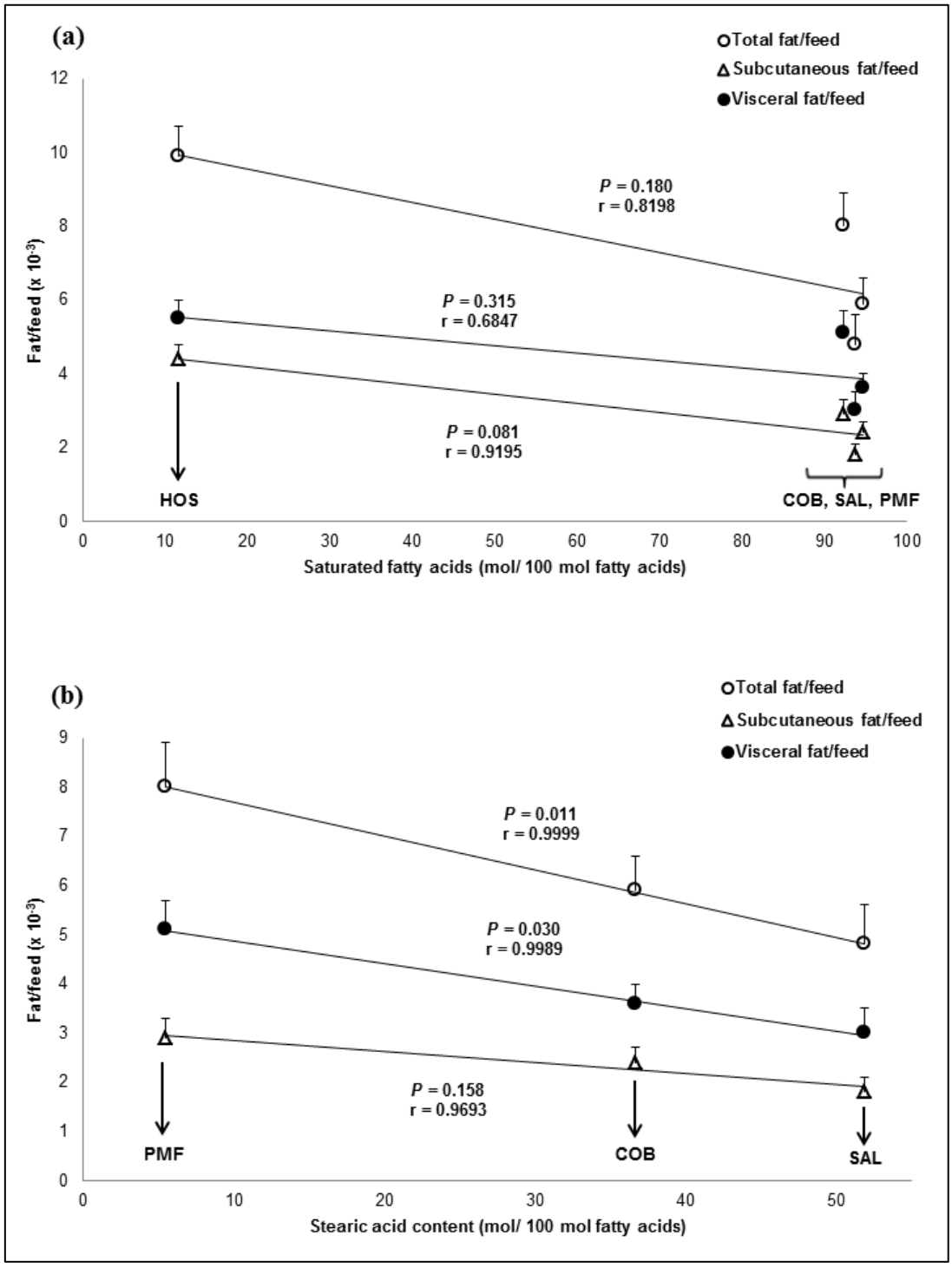

Notes:
The fat/feed ratios varied with (a) total saturated fatty acid (SFA) composition at *sn*-1,3 positions and (b) stearic acid composition at *sn*-1,3 positions. Values are mean with their standard error (SEM) represented by vertical bars. COB, cocoa butter; SAL, sal stearin; PMF, palm mid fraction; HOS, high-oleic sunflower oil. Correlation coefficients with *P* values < 0.05 were considered as significant.

Figure 3.5 : Effect of fatty acid composition at the *sn*-1,3 positions of triacylglycerols on fat deposition (mass of fat deposited/total feed consumed)

Table 3.19 : Fat deposition in C57BL/6 mice after 15 weeks (*In vivo* study 2)

	COB		SAL		PMF		HOS	
	Mean	SEM	Mean	SEM	Mean	SEM	Mean	SEM
Subcutaneous fat (g)	1.05^{a}	0.13	0.76^{a}	0.14	1.22^{a}	0.18	1.87^{b}	0.18
Visceral fat (g)	1.56^{ab}	0.18	1.29^{a}	0.22	2.15^{b}	0.26	2.32^{b}	0.21
Total fat (g)	2.60^{a}	0.30	2.04^{a}	0.35	3.37^{ab}	0.41	4.20^{b}	0.37
Subcutaneous fat/feed ($x10^{-3}$ g/g)	2.4^{a}	0.3	1.8^{a}	0.3	2.9^{a}	0.4	4.4^{b}	0.4
Visceral fat/feed ($x10^{-3}$ g/g)	3.6^{ab}	0.4	3.0^{a}	0.5	5.1^{bc}	0.6	5.5^{c}	0.5
Total fat/feed ($x10^{-3}$ g/g)	5.9^{ab}	0.7	4.8^{a}	0.8	8.0^{bc}	0.9	9.9^{c}	0.8

Notes:
COB, cocoa butter; SAL, sal stearin; PMF, palm mid fraction; HOS, high-oleic sunflower oil. Values expressed as mean and standard error of the mean, SEM.
^{a,b,c}Mean values within a row with unlike superscript letters were significant different (P<0.05).

3.3.2.4 Faecal Fatty Acids

From Table 3.20, cocoa butter (COB), sal stearin (SAL) and palm mid fraction (PMF) dietary groups showed no significant difference (P>0.05) in total saturated fatty acid (SFA) excretion. Similar observation was noted for the total excretion of polyunsaturated fatty acids (PUFA). Nonetheless, significant differences in the amount of monounsaturated fatty acids (MUFA) excreted in the faeces was found in the pair wise comparison of SAL group and PMF group (P=0.033). In addition, the content of faecal SFA, MUFA and PUFA from mice in high-oleic sunflower oil (HOS) dietary group were significantly differed compared to the other three groups.

Extracted lipid content in faeces of mice consisted of free fatty acids exclusively, while the triacylglycerols and other partial acylglycerols remained undetected (Table 3.21). In the absolute amount of faecal fatty acids, mice receiving SAL-enriched diet excreted significantly higher amount of free fatty acids than those from COB (P=0.038), PMF (P=0.031) and HOS (P=0.002) dietary groups (Table 3.21). Among all dietary groups,

it was important to note that the least amount of excreted fatty acids was found in the faeces of mice fed with HOS-enriched diet (Table 3.21).

Table 3.20 : Composition of free fatty acid in the faeces of mice from each test group (*In vivo* study 2)

Acyl chain	Faecal fatty acid composition (% as methyl esters)							
	COB		SAL		PMF		HOS	
	Mean	SD	Mean	SD	Mean	SD	Mean	SD
14 : 0	0.39^{ab}	0.07	0.21^{b}	0.04	1.01^{c}	0.12	0.86^{ac}	0.27
16 : 0	31.68^{a}	1.41	9.23^{b}	1.03	66.72^{c}	2.60	14.79^{d}	1.49
18 : 0	48.42^{a}	1.56	61.71^{b}	2.62	10.17^{c}	0.99	9.12^{c}	1.29
20 : 0	2.09^{a}	0.18	12.72^{b}	1.56	1.35^{a}	0.28	2.16^{a}	0.27
Total SFA	82.57^{a}	2.63	83.87^{a}	2.83	79.25^{a}	2.38	26.93^{b}	2.24
16 : 1*n*-7	0.18^{a}	0.09	0.02^{b}	0.01	0.11^{ab}	0.02	0.04^{ab}	0.01
18 : 1*n*-9	10.66^{ab}	2.05	9.35^{a}	1.47	12.50^{b}	1.55	49.83^{c}	1.99
20 : 1*n*-9	0.40^{ab}	0.04	0.49^{a}	0.13	0.35^{b}	0.05	0.97^{c}	0.14
Total MUFA	11.24^{ab}	1.13	9.86^{a}	1.55	12.97^{b}	1.67	50.84^{c}	2.01
18 : 2*n*-6	5.66^{a}	1.44	5.71^{a}	1.30	7.14^{a}	0.67	20.56^{b}	1.24
18 : 3*n*-3	0.53^{a}	0.12	0.53^{a}	0.13	0.65^{a}	0.06	1.61^{b}	0.13
20 : 2	ND	ND	0.04	0.01	ND	ND	ND	ND
Total PUFA	6.19^{a}	1.56	6.28^{a}	1.30	7.79^{a}	0.72	22.17^{b}	2.05

Notes:
COB, cocoa butter; SAL, sal stearin; PMF, palm mid fraction; HOS, high-oleic sunflower oil; SFA, saturated fatty acids; MUFA, monounsaturated fatty acids; PUFA, polyunsaturated fatty acids; ND, not detected. Values expressed as mean and standard deviation, SD.
[a,b,c,d] Mean values within a row with unlike superscript letters were significant different (P<0.05).

Table 3.21 : The absolute amount of free fatty acids in the faeces of mice from different dietary groups (*In vivo* study 2)

Fatty acid *	Absolute amount of free fatty acids (µg /1 g of faeces)			
	COB	SAL	PMF	HOS
16 : 0	2.39	0.53	4.06	0.55
18 : 0	4.00	8.02	0.91	0.67
18 : 1*n*-9	1.98	1.63	1.87	3.50
18 : 2*n*-6	0.39	0.69	0.44	1.45
20 : 0	0.88	1.55	0.09	0.15
Total	9.64^{a}	12.42^{b}	7.36^{c}	6.31^{d}

Notes:
COB, cocoa butter; SAL, sal stearin; PMF, palm mid fraction; HOS, high-oleic sunflower oil.
[a,b] Mean values within a row with unlike superscript letters were significant different (P<0.05)
* The analyses were done on major fatty acids (more than 5g/100 g total fatty acids in the composition).

Excretion index (Table 3.22) denotes the relationship between the contents of faecal fatty acids and their corresponding composition in the ingested fats. The most abundant MUFA, namely, oleic acid (C18:1), was the most susceptible to absorption as its excretion index was in the range of 0.28 to 0.60. As a whole, excretion indices for SFA and PUFA were noted to be greater than unity, whilst for MUFA, the excretion indices fell in the range of 0.29 to 0.61 (Table 3.22). From the perspective of major SFA, greater excretion index was observed for stearic acid (C18:0) compared with palmitic acid (C16:0) in all dietary groups.

Table 3.22 : The excretion index for each free fatty acid in the faeces of mice from different dietary groups (*In vivo* study 2)

	Excretion index			
Fatty acid	COB	SAL	PMF	HOS
14 : 0	3.81	13.91	1.19	21.84
16 : 0	1.24	1.19	1.15	3.33
18 : 0	1.32	1.33	1.86	3.87
20 : 0	1.78	1.59	3.63	ND
Total SFA	1.30	1.29	1.22	3.99
16 : 1*n*-7	0.79	ND	1.74	0.42
18 : 1*n*-9	0.32	0.28	0.39	0.60
20 : 1*n*-9	8.29	6.44	8.01	3.76
Total MUFA	0.33	0.29	0.40	0.61
18 : 2*n*-6	2.16	6.01	2.41	1.98
18 : 3*n*-3	3.13	3.82	17.15	17.27
20 : 2*n*-6	ND	1.85	ND	ND
Total PUFA	2.21	5.66	2.60	2.12

Notes:
COB, cocoa butter; SAL, sal stearin; PMF, palm mid fraction; HOS, high-oleic sunflower oil; SFA, saturated fatty acids; MUFA, monounsaturated fatty acids; PUFA, polyunsaturated fatty acids; ND, not detected.

3.3.2.5 Adipose Tissue

Fatty acid compositions (FAC) of the extracted lipids from subcutaneous and visceral adipose tissues were shown in Table 3.23 and Table 3.24, respectively.

Table 3.23 : Fatty acid composition of the extracted lipids from subcutaneous adipose tissue of mice (*In vivo* study 2)

Acyl chain	Adipose tissue fatty acid composition (as % methyl esters)							
	COB		SAL		PMF		HOS	
	Mean	SD	Mean	SD	Mean	SD	Mean	SD
12 : 0	ND	ND	ND	ND	0.02	0.02	ND	ND
14 : 0	0.57	0.06	0.62	0.07	0.75	0.05	0.34	0.05
16 : 0	16.30	0.95	10.77	0.63	26.47	0.64	8.83	0.49
18 : 0	5.05	0.41	7.18	1.35	1.37	0.07	1.36	0.15
20 : 0	0.19	0.03	0.91	0.22	0.12	0.01	0.08	0.01
Total SFA	22.11	1.15	19.48	1.93	28.73	0.70	10.61	0.60
14 : 1*n*-5	0.05	0.00	0.06	0.01	0.07	0.01	ND	ND
16 : 1*n*-7	5.60	0.34	3.84	0.57	10.74	0.49	2.02	0.33
18 : 1*n*-9	60.81	1.38	66.67	1.39	49.42	0.71	73.56	0.37
20 : 1*n*-9	0.51	0.06	0.58	0.05	0.46	0.02	0.55	0.04
Total MUFA	66.97	1.21	71.15	1.81	60.68	0.68	76.13	0.45
18 : 2*n*-6	9.83	0.25	8.35	0.32	9.68	0.10	12.41	0.17
20 : 2	0.06	0.01	0.07	0.01	0.04	0.02	0.05	0.02
20 : 3*n*-6	0.08	0.01	0.08	0.01	0.08	0.00	0.09	0.00
20 : 4	0.20	0.02	0.20	0.01	0.17	0.01	0.17	0.03
Total PUFA *n*-6	10.21	0.25	8.71	0.35	10.01	0.11	12.78	0.20
18 : 3*n*-3	0.62	0.05	0.58	0.07	0.51	0.01	0.43	0.04
22 : 6*n*-3	0.08	0.01	0.08	0.01	0.07	0.01	0.05	0.01
Total PUFA *n*-3	0.70	0.06	0.66	0.05	0.58	0.01	0.48	0.05

Notes:
COB, cocoa butter; SAL, sal stearin; PMF, palm mid fraction; HOS, high-oleic sunflower oil; SFA, saturated fatty acids; MUFA, monounsaturated fatty acids; PUFA, polyunsaturated fatty acids; ND, not detected. Values expressed as mean and standard deviation, SD.

For cocoa butter (COB), sal stearin (SAL) and palm mid fraction (PMF) fed groups, the amount of saturated fatty acids (SFA) decreased as compared with the corresponding content in ingested oils (Table 3.15, Section 3.3.1.1). Similar to findings from *in vivo* study 1, the content of minor fatty acids, namely, palmitoleic acid (C16:1) was increased much higher in adipose tissues compared to that in the diets. The highest increment was found in the adipose tissue of mice fed with PMF-enriched diet (166.55 and 169.35 fold for subcutaneous and visceral adipose tissues, respectively), associated with the greatest reduction of palmitic acid (C16:0). Moreover, several polyunsaturated fatty acids (PUFA) were found in adipose tissue, yet they were absent in the diets,

particularly for eicosatrienoic acid (C20:3*n*-6), arachidonic acid (C20:4*n*-6) and docosahexaenoic acid (C22:6*n*-3). After comparing the FAC between subcutaneous and visceral adipose tissues, no significant difference was noted.

Table 3.24 : Fatty acid composition of the extracted lipids from visceral adipose tissue of mice (*In vivo* study 2)

	Adipose tissue fatty acid composition (as % total methyl esters)							
	COB		SAL		PMF		HOS	
Acyl chain	Mean	SD	Mean	SD	Mean	SD	Mean	SD
12 : 0	0.02	0.02	ND	ND	0.03	0.02	ND	ND
14 : 0	0.61	0.06	0.59	0.06	0.67	0.24	0.37	0.02
16 : 0	18.93	1.24	12.03	0.50	29.49	1.01	10.13	0.30
18 : 0	4.57	0.45	6.18	0.83	1.42	0.09	1.36	0.08
20 : 0	0.14	0.01	0.71	0.12	0.11	0.01	0.08	0.00
Total SFA	24.27	1.58	19.51	1.19	31.73	1.09	11.93	0.32
14 : 1*n*-5	0.06	0.01	0.06	0.01	0.06	0.01	ND	ND
16 : 1*n*-7	6.57	0.41	4.81	0.66	10.56	0.48	2.24	0.33
18 : 1*n*-9	57.68	1.51	65.40	0.64	46.78	0.79	71.90	0.45
20 : 1*n*-9	0.43	0.03	0.53	0.04	0.46	0.04	0.56	0.02
Total MUFA	64.72	1.55	70.80	0.99	57.86	0.88	74.70	0.24
18 : 2*n*-6	9.81	0.25	8.43	0.26	9.47	0.19	12.45	0.22
20 : 2	0.07	0.01	0.10	0.02	0.06	0.01	0.05	0.03
20 : 3*n*-6	0.09	0.01	0.09	0.01	0.09	0.01	0.05	0.01
20 : 4	0.21	0.03	0.24	0.03	0.16	0.03	0.11	0.01
Total PUFA *n*-6	10.24	0.25	8.93	0.28	9.83	0.24	12.86	0.26
18 : 3*n*-3	0.68	0.05	0.66	0.03	0.52	0.03	0.45	0.06
22 : 6*n*-3	0.08	0.02	0.11	0.01	0.06	0.02	0.05	0.02
Total PUFA *n*-3	0.76	0.06	0.76	0.05	0.58	0.05	0.50	0.08

Notes:
COB, cocoa butter; SAL, sal stearin; PMF, palm mid fraction; HOS, high-oleic sunflower oil; SFA, saturated fatty acids; MUFA, monounsaturated fatty acids; PUFA, polyunsaturated fatty acids; ND, not detected. Values expressed as mean and standard deviation, SD.

Regiospecific data of subcutaneous and visceral adipose tissues were shown in Table 3.25. SFA at the *sn*-1,3 positions decreased greatly from 94.7 mol% (in COB group) to 35.2 mol% (subcutaneous adipose tissue) and 34.8 mol% (visceral adipose tissue), from 93.7 mol% (in SAL group) to 28.8 mol% (subcutaneous adipose tissue) and 28.1 mol% (visceral adipose tissue), as well as from 92.3 mol% (in PMF group) to 48.6 mol%

(subcutaneous adipose tissue) and 49.5 mol% (visceral adipose tissue). The decrement for SAL was the greatest and the least for PMF dietary group. These observations were associated with an increment of relative composition of monounsaturated fatty acids (MUFA). In COB group, MUFA increased from 5.3 mol% at the *sn*-1,3 positions of COB to 55.1 - 55.5 mol% at the similar positions of adipose tissues. Apart from that, in SAL group, it increased from 4.6 mol% at the *sn*-1,3 positions of SAL to 61.4 - 64.4 mol% at the similar positions of triacylglycerols in adipose tissues, while the increment was from 6.5 mol% at the *sn*-1,3 positions in PMF to 41.9 - 45.5 mol% in adipose tissues.

Table 3.25 : Positional fatty acid composition of the adipose tissues of mice (*In vivo* study 2)

Dietary group	Composition (mol%)								
	sn-position	SFA		MUFA				PUFA	
				cis-11-monoene		*cis*-9-monoene			
		Subcutaneous	Visceral	Subcutaneous	Visceral	Subcutaneous	Visceral	Subcutaneous	Visceral
COB	1, 3	35.2	34.8	3.6	4.5	55.5	55.1	5.7	5.6
	2	7.9	9.0	ND	ND	73.2	75.6	18.9	15.4
	1, 2, 3	25.9	26.7	2.4	2.6	61.5	62.8	10.2	7.9
SAL	1, 3	28.8	28.1	2.3	5.1	64.4	61.4	4.5	5.4
	2	3.3	6.2	ND	ND	81.0	77.3	15.7	16.5
	1, 2, 3	20.2	20.9	1.5	3.4	70.0	66.6	8.3	9.0
PMF	1, 3	48.6	49.5	2.0	3.5	45.5	41.9	3.9	5.2
	2	8.7	9.7	ND	ND	68.1	70.1	23.2	20.1
	1, 2, 3	38.0	36.6	1.6	2.3	47.9	51.0	12.5	10.0
HOS	1, 3	16.9	19.0	2.2	3.9	76.7	69.4	4.2	7.6
	2	2.5	2.8	ND	ND	74.3	74.6	23.2	22.7
	1, 2, 3	11.4	13.4	1.4	2.5	75.8	71.2	11.4	12.8

Notes:
SFA, saturated fatty acids; MUFA, monounsaturated fatty acids; PUFA, polyunsaturated fatty acids; COB, cocoa butter; SAL, sal stearin; PMF, palm mid fraction; HOS, high-oleic sunflower oil; ND, not detected.

The contents of *cis*-11-monoene were increased in all adipose tissues originated from COB, SAL and PMF fed groups, but not for those fed with HOS-enriched diet. These

fatty acids were originally absent in the diet, and eventually occurred at the *sn*-1,3 positions of triacylglycerols in adipose tissues. The regiospecific data for subcutaneous and visceral adipose tissues did not vary significantly.

3.3.3 Discussion

In the current *in vivo* study 2, the major triacylglycerol molecular species containing in the test oils, *viz.* cocoa butter (COB), sal stearin (SAL), palm mid fraction (PMF) and high-oleic sunflower oil (HOS), are 1-palmitoyl-2-oleoyl-3-stearoylglycerol (POSt), 1,3-distearoyl-2-oleoylglycerol (StOSt), 1,3-dipalmitoyl-2-oleoylglycerol (POP) and trioleoylglycerol (OOO), respectively (Gunstone and Harwood, 2007). In an effort to examine the obesity alleviating effect of saturated fatty acids (SFA) at the *sn*-1,3 positions of triacylglycerols, these positions were varied among palmitic (C16:0), stearic (C18:0) and oleic acids (C18:1), whilst the middle position was conserved with oleic acid.

In order to evaluate the diet-induced obesogenic effects of oils, the normalised data, namely, gain/feed and fat/feed, were emphasised, and the subcutaneous and visceral adiposity were used as the markers for obesity. Coherent with findings from *in vivo* study 1 (Section 3.2), HOS-enriched diet (monounsaturated fatty acids (MUFA) mainly reside at the *sn*-1,3 positions) was responsible for the higher fat deposition than those diets with long chain SFA at the similar positions, namely, COB, SAL and PMF. This is illustrated by the results on subcutaneous, visceral and total fat/feed in Table 3.19 (Section 3.3.2.3). It further affirms that when the long chain saturated palmitic (C16:0) and stearic acids (C18:0) reside predominantly at the *sn*-1,3 positions of triacylglycerol, the level of fat accretion will be reduced. Apart from that, greater excretion indices were observed for both fatty acids, indicating the lower fat deposition was correlated to the

higher excretion of long chain SFA originated from the *sn*-1,3 positions. Similar to *in vivo* study 1, major MUFA, namely, oleic acid (C18:1), was found least readily being excreted, in which the excretion indices < 1. They were well-absorbed in the intestine. No difference was found for total excretion of SFA and polyunsaturated fatty acids (PUFA) owing to the similar fatty acid profile (saturated-unsaturated-saturated (SUS)) of COB, SAL and PMF, whilst the major triacylglycerol molecular species in HOS is OOO.

The observed linear correlation between fat/feed and total SFA at the *sn*-1,3 positions in *in vivo* study 1 (Figure 3.3, Section 3.2.2.3) however diminished in the current study (Figure 3.5a, Section 3.3.2.3). Palmitic acid (C16:0) at the *sn*-1,3 positions was the sole major SFA in *in vivo* study 1, and subsequently was responsible for the promising linear correlation. Yet in the *in vivo* study 2, various amount of stearic (C18:0) and palmitic acids (C16:0) at the similar positions of triacylglycerols were employed in the investigation. Henceforth, linear correlation with exceptional correlation coefficients fell in the range of 0.9693 – 0.9999 (Figure 3.5b, Section 3.3.2.3) was noted between fat/feed and the amount of individual stearic acid (C18:0) at the *sn*-1,3 positions of triacylglycerol moiety. This suggests that both stearic and palmitic acids exert differential effects on the fat absorption and consequently their deposition in adipose tissues.

After cleavage by 1, 3-specific pancreatic lipase, micelles formed by the bile salts combine with the free fatty acids originated from the *sn*-1,3 positions of glycerol moiety to ease their transport through the aqueous boundary layer of intestinal mucosa (Small, 1991). The equilibrium between the apolar and polar phases, as well as the rate in which the free fatty acids establish the aforementioned equilibrium state, are critical in

determining the efficiency of fatty acid absorption (Freeman, 1969). Poor diffusion of fatty acid to aqueous phase may jeopardise the action of pancreatic lipase by blocking its interface. As a result, since stearic acid is relatively more apolar than palmitic acid, lower susceptibility towards intestinal absorption is expected. This is further confirmed by the excretion index of stearic acid which are 6.06% to 38.17% higher than that of palmitic acid (Table 3.22, Section 3.3.2.4). The reduction in fat absorption will successively affect the amount of re-synthesised triacylglycerols in chylomicron and finally their deposition in the adipose tissues. Henceforth, it contributes to the significant drops in gain/feed, visceral and total fat/feed in mice fed with SAL-enriched diet (StOSt as the major triacylglycerol molecular species) in pair wise comparison to those receiving PMF-enriched diet (POP as the major triacylglycerol species). Apart from the fat-reducing effect exerted by long chain SFA at the *sn*-1,3 positions of triacylglycerols proposed in *in vivo* study 1, an extended finding is found from *in vivo* study 2, in which stearic acid (C18:0) is more efficient in reducing fat deposition than palmitic acid (C16:0) at the aforementioned positions.

In addition, the differences in physiochemical properties of the calcium soaps of fatty acid may promote remarkable insights into their diverse extent of faecal excretion. As an example, Krafft point or Krafft temperature, is defined as the minimum temperature in which surfactants can form micelles. The Kraff point for a calcium soap formed with oleic acid is 31 ℃, while with palmitic acid is 65 ℃, and the Krafft point for calcium stearate is found to be 82 ℃ (Yamaguchi *et al.*, 1986). Hence, the latter is solid at the human body temperature (37 ℃) and there is no value for the critical micelle concentration (CMC). In other words, the formation of micelles is not feasible. In a broad sense, Krafft point of all fatty acids is elevated in the presence of calcium ions (Yamaguchi *et al.*, 1986). Apart from that, the solubility of calcium palmitate in water is

reported to be 0.012 mg/L, whilst a relatively lower extent of dissolution, *viz.* 0.0007 mg/L, is reported for calcium stearate at room temperature (Irani and Callis, 1960). Consequently, the intestinal absorption of free fatty acids originated from the *sn*-1,3 positions appears likely to be governed by both hydrophobicity as well as the Krafft point in aqueous environment.

Regiospecific analyses on adipose tissues show a tremendous reduction of SFA at the *sn*-1,3 positions of triacylglycerols, indicating the lower intestinal absorption of SFA and *de novo* synthesis by desaturation. The depreciation of SFA at above-mentioned positions are the greatest in mice from SAL group, followed by COB group, and the least for those fed with PMF-enriched diet. Interestingly, it matches the sequence of fat deposition, from the least fat deposited in mice fed with SAL-enriched diet, followed by COB-enriched diet and eventually the most fattening PMF-enriched diet.

As mentioned in the previous section, visceral adiposity was connected to diverse diseases and was detrimental to human subjects (Emery *et al.*, 1993). Yet in the *in vivo* study 2, SAL-enriched diet was observed to yield the lowest amount of deposited fats in the visceral cavity of mice. Consequently, similar favourable health benefit is envisaged on shea butter and mango fat, which exhibit comparable major triacylglycerol species (Gunstone and Harwood, 2007). Apart from that, the observation on cocoa butter (Timmers *et al.*, 2011) is better in preventing fat accretion compared with palm oil, has been successfully elucidated in the current study. It further advises that with StOSt and POSt as the major triacylglycerol molecular species present in the diet, the problem of obesity may be alleviated. Thus, with these chiefly found in cocoa butter equivalent for various food products, it gives a lower tendency towards the risks of obesity and visceral adiposity as compared with other highly unsaturated oil products. This is

parallel with prior literature observing that the cocoa butter equivalents in conjunction with high dietary calcium concentrations are used as confectionery fats with low energy content (Brink *et al.*, 1995).

3.4 Conclusion

Instead of the total saturated fatty acid (SFA) content, it is demonstrated in the *in vivo* study 1 that the positional distribution of long chain SFA exerted a more pronounce effect on body fat accretion. If the *sn*-1 and *sn*-3 positions of triacylglycerols predominantly occupied by long chain SFA (palmitic acid and above), they tend to reduce fat deposition. The amount of re-synthesised triacylglycerols is reduced, affecting their incorporation in chylomicrons and the successive metabolism and eventually the extent of fat deposition. On the other hand, it remains neutral if they occur at the *sn*-2 position. In addition to the malabsorption type effect, the reduced feed efficiency and adiposity observed may also be occurring as a result of increasing fat oxidation and energy expenditure.

Due to the greater faecal excretion attributed by a relatively longer chain stearic acid compared to the palmitic acid in free-form, there is a further alleviation of fat deposition if the longer chain of SFA reside mainly at the *sn*-1,3 positions of triacylglycerols. This has been validated in the *in vivo* study 2 using C57BL/6 mouse model. As a conclusion, the encouraging results from both studies warrant an interventional study on human subject, and subsequently the synthesis of prospective healthier structured lipids, for instance, 1,3-dibehenoyl-2-oleoylglycerol (BOB) and 1,3-dilignoceroyl-2-oleoylglycerol, in an effort to further investigate the prevalence of morbid obesity.

CHAPTER FOUR
SYNTHESIS OF PROSPECTIVE STRUCTURED LIPIDS FOR OBESITY ALLEVIATION

4.1 Background

4.1.1 Literature Review

Obesity is associated with some degenerative diseases, *viz.* diabetes, cardiovascular diseases, hypertension, high blood pressure and cancer. According to World Health Organisation (WHO) (2005), there were 400 million obese and 1.6 billion overweight adults around the globe. Even though family history and genetics play a crucial role in this context, yet the increase in worldwide obesity in such a short period of time cannot be fully attributed to genetics solely; there are several environmental and social issues such as diets and lifestyle.

The most energy-rich component of a diet is fat, providing 9 kcal/g compared with the 4 kcal/g of carbohydrate and protein. Therefore, dietary fat intake often has been claimed to be responsible for the increase of adiposity. In earlier *in vivo* studies, positive correlation was observed between the level of dietary fat and the body fat gain in both rat (Boozer *et al.*, 1995) and mouse models (Bourgeois *et al.*, 1983; Takahashi *et al.*, 1999). Meanwhile, human studies had shown that high-fat diets, namely, those fat content provided energy greater than 30%, could easily cause the prevalence of obesity (Bray and Popkin, 1998; Schrauwen and Westerterp, 2000; Hill *et al.*, 2000).

With increasing awareness of the risk linked with high fat intake, there is a market for reduced calorie fats. Due to the lower calorie value of carbohydrate and protein, they have been introduced into market as fat replacers. Nonetheless, their food applications

are more restricted as compared to fat, especially at the elevated temperatures during cooking and deep frying. Dietary fats also serve as a source of essential fatty acids, as well as play the role of carrier for fat-soluble vitamins and antioxidants. These benefits cannot be compensated by fat replacers made from carbohydrate and protein. As a result, only lipid-based fat substitutes can possibly mimic all the attributes of a natural fat.

Nagao *et al.* (2000) and Maki *et al.* (2002) conducted studies on the nutritional characteristics and dietary effects of diacylglycerols. They discovered that dietary diacylglycerols suppressed the accumulation of body fat more efficiently compared with triacylglycerol in a double-blind controlled trial. Diacylglycerol was also reported to be effective for fasting and postprandial hyperlipidemia and preventing excess adiposity by increasing postprandial energy expenditure (Maki *et al.*, 2002). However, this product has now been withdrawn from the market due to the concerns on high levels of potentially carcinogenic glycidol fatty acid esters in the oils and other diacylglycerol-enriched products, and more researches should be invested in searching other reduced calorie triacylglycerols.

In general, structured lipids are triacylglycerols that have been tailor-made by changing the fatty acid composition and the positional attachment of fatty acids on the glycerol backbone using chemicals, enzymatically catalysed reaction or genetic engineering. With these modified triacylglycerols, structured lipids are envisaged to provide improved nutritional or functional properties, particularly in food application. Specifically in the effort to reduce calorie, structured lipids are generally designed by taking the approaches of either the relatively low calorie density of medium chain fatty acids or the restricted absorption of long chain saturated fatty acids (SFA) in the

intestine. For instance, Akoh and Yee (1997) synthesised low calorie structured lipids through enzymatic interesterification between tricaprin and tristearin.

During the digestion and absorption of fat, the medium chain fatty acids (C8 - C12) and long chain fatty acids (C14 - C22) undergo different absorption pathways (Karupaiah and Sundram, 2007). Medium chain fatty acids are absorbed directly into the portal circulation and transported to liver for rapid oxidation, whilst long chain fatty acids are transported by chylomicrons into the lymphatic system allowing extensive uptake into adipose tissue (Karupaiah and Sundram, 2007). The higher rate of oxidation of medium chain fatty acids will aid the greater energy expenditure. In comparison with long chain fatty acids, several studies enclosed that the greater energy expenditure provided by the medium chain fatty acids would result in a lower body mass gain, as well as smaller fat depots in animal models (Geliebter *et al.*, 1983; Crozier *et al.*, 1987; St-Onge and Jones, 2002). Meanwhile, a recent clinical study had shown that the consumption of oil enriched in medium chain triacylglycerol would lead to significantly higher loss of fat mass and trunk fat mass, as compared with olive oil (St-Onge and Bosarge, 2008).

Nonetheless, Tholstrup *et al.* (2004) revealed that medium chain fatty acids exerted an unfavourable effect on blood lipid profiles in healthy young men by increasing plasma low-density-lipoprotein cholesterol (LDL-C) and blood triacylglycerols. In addition, with the deficiency in essential fatty acids, it is not recommended that medium chain triacylglycerol to be used as the sole lipid source in the diet. Therefore, structured medium and long chain saturated triacylglycerols were introduced and it was reported to deliver significantly lower intra-abdominal adipose tissues and carcass fat contents in rats compared with the long chain triacylglycerols (Matsuo and Takeuchi, 2004). This type of structured lipid serves as the basis for Caprenin^{TM} and SALATRIM^{TM}.

A unique dietary fat, Caprenin™, was introduced into the food supply as a potential cocoa butter substitute, as well as one of the reduced calorie fats (Webb and Sanders, 1991). It was a structured lipid produced by random interesterification of behenic acid (~45%) from fully hydrogenated high-erucic rapeseed oil and about 50% of capric (C10:0) and caprylic (C8:0) acids obtained from the coconut and palm kernel oils. As mentioned earlier, the advantages of the relatively lower calorie density of medium chain SFA, as well as the limited intestinal absorption of long chain SFA, were manifested in Caprenin™. Thus, the metabolisable energy in Caprenin™ had been found to be 5 kcal/g (Peters *et al.*, 1991). Notwithstanding the above, significant reduction in high-density-lipoprotein cholesterol (HDL-C) was observed in hypercholesterolemic men fed with Caprenin™ as compared with palm oil/palm kernel oil or butter diet, whereas total cholesterol, LDL-C, and serum triacylglycerols remained unchanged (Wardlaw *et al.*, 1995). As a result, it was postulated that one or more of capric, caprylic and behenic acids could contribute to hypercholesterolemia in men (Wardlaw *et al.*, 1995).

Another commercially available reduced calorie fats, SALATRIM™, was formulated with long chain stearic acid (C18:0) and short chain fatty acids, namely acetic (C2:0), propionic (C3:0) or butyric (C4:0) acids (Klemann *et al.*, 1994; Finley *et al.*, 1994). In contrast to Caprenin™, SALATRIM™ showed no adverse effect on blood lipids and lipoprotein metabolism (Auerbach *et al.*, 1998; Nestel *et al.*, 1998). In this context, Karupaiah and Sundram (2007) postulated that the differential biological effects exerted by both Caprenin™ and SALATRIM™ possibly caused by the variation in fatty acid composition, rather than the structural differences.

As mentioned earlier, long chain saturated behenic acid (C22:0) was selected as one of the substrates in design of Caprenin^{TM}, taking its advantage of limited intestinal absorption after hydrolysis by pancreatic lipase in the duodenum. On that account, several researchers concerted their efforts to synthesis structured lipids containing behenic acid at the *sn*-1 and/or *sn*-3 positions of triacylglycerols (Kanjilal *et al.*, 1999; Kojima *et al.*, 2010). Apart from the synthesis, Kojima *et al.* (2010) also found that the diet enriched with 1-behenoyl-2,3-dioleoylglycerol (BOO) prevented the deposition of visceral fat and hepatic triacylglycerols using the Wistar rat model.

In the market, conjugated linoleic acid (CLA) has been used extensively as food supplements with the benefit for reducing body fat mass. Its efficacy in alleviating fat mass was illustrated in numerous animal studies, ranging from mice (Park *et al.*, 1997; West *et al.*, 2000), hamsters (de Deckere *et al.*, 1999) to pigs (Dugan *et al.*, 2004). Whigham *et al.* (2007) observed that a 90 g of fat loss per week in human body could be triggered by the consumption of 3.2 g CLA daily. The positive health attributes of CLA prompted the investigations in designing structured lipids containing CLA, as well as medium chain fatty acids in the triacylglycerol molecule (Rocha-Uribe and Hernandez, 2004).

4.1.2 The Approach of Present Study

Apart from the fat-reducing effect of long chain saturated fatty acid (SFA) at the *sn*-1,3 positions of triacylglycerols proposed in the *in vivo* study 1 (Section 3.2), an extended finding is found in the *in vivo* study 2 (Section 3.3), in which the stearic acid (C18:0) is more efficient in reducing fat deposition than palmitic acid (C16:0) at the similar positions. Consequently, in designing the structured lipids which aims to associate with fat-alleviating effect, an even longer SFA, namely behenic acid (C22:0) is the candidate

for the substrate. Meanwhile, naturally occurring palm olein iodine valued (IV) 56 and high-oleic sunflower oil were selected as the base oils. Henceforth, the synthesised structured lipids are expected to contain natural antioxidants, phytonutrients and essential fatty acids originated from the base oils.

In the effort to achieve sustainable chemistry, immobilised lipases from the strain of *Rhizomucor miehei* (Lipozyme RM IM, Novozymes^{TM}) and *Thermomyces lanuginosa* (Lipozyme TL IM, Novozymes^{TM}) are employed in the current work. After selection of the substrates and enzyme, the most crucial justification will come upon the type of reaction for the synthesis. As mentioned in Section 1.4.2 (Chapter 1), two conventional approaches for the synthesis of structured lipids are acidolysis (reaction between fatty acids and oils) and interesterification (acyl chain exchange between ethyl esters and oils). Due to the higher melting point of behenic acid (80 ℃), therefore it is not a favourable substrate as a higher reaction temperature is required. Several studies disclosed that lower temperature was reported to be advantageous in terms of suppressing acyl migration (Xu *et al.*, 1998; Xu, 2000; Svensson and Adlercreutz, 2011). As a result, 1, 3-specific enzymatic interesterification between oils and ethyl behenate will be employed in the synthesis of obesity-alleviating structured lipids.

4.2 Enzymatic Interesterification between Palm Olein and Ethyl Behenate

4.2.1 Experimental

4.2.1.1 Materials

Refined, bleached and deodorised (RBD) palm olein iodine value (IV) 56 was provided by Intercontinental Specialty Fats Sdn. Bhd., Selangor, Malaysia. Behenic acid (95% purity) was obtained from Tokyo Chemical Industry, Tokyo, Japan. Absolute ethanol

(analytical grade) was purchased from Merck, Darmstadt, Germany. Immobilised lipases from the strain of *Rhizomucor miehei* (Lipozyme RM IM, Novozymes^{TM}) and *Thermomyces lanuginosa* (Lipozyme TL IM, Novozymes^{TM}) were supplied by Novozymes, Denmark. For peak identification in the analysis of triacylglycerol composition, standard triacylglycerols (purity ≥ 99%), namely, tripalmitoylglycerol (PPP), trioleoylglycerol (OOO), 1,3-dipalmitoyl-2-oleoylglycerol (POP), tristearoylglycerol (StStSt) and tribehenoylglycerol (BBB) were obtained from Sigma Chemical Company (St. Louis, Missouri).

4.2.1.2 Preparation of Ethyl Behenate

Esterification between behenic acid and ethanol was employed in the preparation of ethyl behenate. A 38 mL of ethanol and 22 g of behenic acid (molar ratio = 10:1) were placed in a round bottom flask. The reaction mixture was then refluxed for one hour in the presence of sulphuric acid (0.5 vol %) as catalyst. Upon the completion of the reaction, 50 mL of hexane was added into the reaction mixture and subsequently transferred into separating funnel. The hexane layer containing esters was washed with distilled water in order to remove the acidic catalyst. The final product can be obtained after removal of hexane under reduced pressure, and successively used as the starting material for the subsequent interesterification without further purification. The preparation of ethyl behenate was done in three replicates to examine the consistency and reproducibility.

4.2.1.3 Enzymatic Interesterification

Palm olein (5 g) was mixed with 6.43 g of ethyl behenate (molecular mass of 368.64 g/mol) at a molar ratio of 1:3 in a 100-mL Schott bottle with screw cap. The substrates were pre-heated at 65℃ to ensure their homogeneities in molten state. Thereafter,

immobilised lipase from Lipozyme RM IM or Lipozyme TL IM (10% of the total mass of substrates) was loaded in the reaction mixture. Solvent-free interesterification was performed in an orbital shaking water bath (Model SV1422, Memmert, Germany) at 150 rpm and 65 ℃. Individual samples were withdrawn at selected intervals (0.5, 1, 2, 3, 5, 10, 15, 20, 24 hours), filtered and subjected to further characterisation.

4.2.1.4 ^{13}C NMR Regiospecific Analysis

^{13}C NMR regiospecific analyses were conducted as established and described in Chapter 2. All structured lipids were diluted with deuterated chloroform to produce a 2:5 (m/v) sample/solvent ratio, degassed for 5 minutes and finally ultrasonicated for 1 minute. The volume of sample used in NMR analysis was set at 0.5 mL.

4.2.1.5 High Performance Liquid Chromatography (HPLC)

Analyses of triacylglycerol molecular species were carried out by reversed-phase high performance liquid chromatography (HPLC) on a Waters chromatographic system (Waters SFO, Milford, USA) equipped with an evaporative light scattering detector (ELSD) (Model 2424, Waters, USA). Separations were effected on a Purospher STAR RP-18 end capped column (250 x 4.6 mm) of 5-μm particle size (Merck, Darmstadt, Germany). Sample injection was carried out by a Sample Manager Waters 2757 injector with 20 μL loops (Waters, USA). The ELSD drift tube temperature was set at 60 ℃. Nitrogen gas was used as nebulising gas at the pressure of 40 psi.

Each oil sample (8 mg) was prepared in HPLC grade dichloromethane (10 mL) and subsequently vortexed for 1 minute to ensure sample homogeneity. Before injection into HPLC system, the samples were passed through a filter with pore size of 0.2 μm (Milipore, Bedford, USA). The mobile phase consisted of an isocratic elution of

acetonitrile/dichloromethane solvent system (40:60, by volume) for 25 minutes. The flow rate was set at 1 mL/minute. Data acquisition and processing were executed by MassLynx version 4.1 (Waters, USA). The order of elution of triacylglycerol molecular species was based on the corresponding equivalent carbon number (ECN). Peak identification was further confirmed on the plot of the logarithm of the retention volumes of triacylglycerols relative to trioleoylglycerol (OOO) versus the number of double bonds, as suggested by Stolyhwo *et al.* (1985).

4.2.2 Results and Discussion

4.2.2.1 Positional Distribution of Fatty Acids in Palm Olein and Structured Lipids Synthesised

Enzymatic interesterification between palm olein iodine value (IV) 56 and ethyl behenate was carried out using different enzymes, namely, immobilised lipases from the strain of *Rhizomucor miehei* (Lipozyme RM IM) and *Thermomyces lanuginose* (Lipozyme TL IM). The positional distributions of saturated (SFA), mono- (MUFA) and polyunsaturated fatty acids (PUFA) in the original palm olein IV 56 as well as the interesterified products catalysed by Lipozyme RM IM and Lipozyme TL IM are presented in Table 4.1 and Table 4.2, respectively. In contrast to analysis by gas chromatography (GC), fatty acid composition profile measured by ^{13}C NMR are stated in mole percentage.

As a consequence of the incorporation of saturated behenic acid into glycerol moiety, the overall SFA content of reaction intermediates were generally higher than that of the original palm olein IV 56, whilst the total MUFA contents depreciated (Table 4.1 and 4.2). In Lipozyme RM IM-catalysed interesterification, 78.0 - 87.7 mol% of SFA were observed at the *sn*-1,3 positions of triacylglycerols in various reaction products (Table 4.1). On the other hand, SFA composition found at similar positions in reaction products

catalysed by Lipozyme TL IM fell in the range of 73.1 - 83.5 mol% (Table 4.2). Greater incorporation of behenic acid into the *sn*-1,3 positions suggested that Lipozyme RM IM is more specific towards 1,3-interesterification as compared with Lipozyme TL IM.

Table 4.1 : Regiospecific data of the starting material (palm olein IV 56) and the interesterification reaction intermediates catalysed by Lipozyme RM IM with ethyl behenate

Duration	Composition (mol%)			
	sn-position	Saturated	Monounsaturated	Polyunsaturated
Palm olein IV 56	1,3	71.0 ± 0.4	26.1 ± 0.3	2.9 ± 0.3
	2	7.4 ± 0.9	74.3 ± 0.9	18.3 ± 0.2
	1,2,3	50.3 ± 0.4	41.8 ± 0.5	7.9 ± 0.2
0.5 hours	1,3	83.1 ± 0.6	13.3 ± 0.5	3.6 ± 0.1
	2	12.0 ± 0.1	62.8 ± 0.2	25.2 ± 0.3
	1,2,3	57.8 ± 1.1	30.9 ± 0.9	11.3 ± 0.2
1 hour	1,3	84.5 ± 0.8	12.5 ± 1.0	3.0 ± 1.8
	2	17.3 ± 0.6	61.1 ± 1.2	21.6 ± 0.9
	1,2,3	63.1 ± 0.4	28.0 ± 1.5	9.0 ± 1.2
2 hours	1,3	83.7 ± 1.1	12.8 ± 1.0	3.5 ± 0.9
	2	22.5 ± 0.5	60.9 ± 1.9	16.6 ± 2.4
	1,2,3	63.3 ± 1.5	28.8 ± 0.5	7.9 ± 1.2
3 hours	1,3	87.7 ± 0.9	9.3 ± 1.0	3.0 ± 0.1
	2	27.8 ± 0.0	58.5 ± 0.8	13.7 ± 0.8
	1,2,3	69.5 ± 0.5	24.3 ± 0.7	6.2 ± 0.3
5 hours	1,3	83.0 ± 0.3	13.7 ± 1.4	3.3 ± 1.1
	2	35.0 ± 0.1	50.7 ± 0.9	14.3 ± 1.0
	1,2,3	66.9 ± 0.3	26.1 ± 0.8	7.0 ± 0.7
10 hours	1,3	79.8 ± 1.5	16.3 ± 0.5	3.9 ± 2.1
	2	48.4 ± 0.4	44.7 ± 1.5	6.9 ± 1.8
	1,2,3	69.4 ± 0.9	25.8 ± 1.1	4.9 ± 1.9
15 hours	1,3	78.4 ± 0.6	16.9 ± 0.5	4.7 ± 0.2
	2	56.8 ± 0.7	35.6 ± 0.6	7.6 ± 1.3
	1,2,3	71.2 ± 0.1	23.1 ± 0.3	5.7 ± 0.4
20 hours	1,3	78.4 ± 0.8	17.1 ± 0.5	4.5 ± 0.4
	2	59.5 ± 1.6	30.8 ± 0.5	9.7 ± 1.1
	1,2,3	72.3 ± 1.2	21.5 ± 0.5	6.2 ± 0.6
24 hours	1,3	78.0 ± 0.2	17.1 ± 0.1	5.0 ± 0.1
	2	66.8 ± 0.7	26.1 ± 0.1	7.1 ± 0.6
	1,2,3	74.3 ± 0.2	20.0 ± 0.0	5.7 ± 0.2

Notes:
IV, iodine value. Values are mean of three replicates ± standard deviation.

Table 4.2 : Regiospecific data of the starting material (palm olein IV 56) and the interesterification reaction intermediates catalysed by Lipozyme TL IM with ethyl behenate

Duration	Composition (mol%)			
	sn-position	Saturated	Monounsaturated	Polyunsaturated
Palm olein IV 56	1,3	71.0 ± 0.4	26.1 ± 0.3	2.9 ± 0.3
	2	7.4 ± 0.9	74.3 ± 0.9	18.3 ± 0.2
	1,2,3	50.3 ± 0.4	41.8 ± 0.5	7.9 ± 0.2
0.5 hours	1,3	75.0 ± 0.4	18.7 ± 0.7	6.3 ± 0.4
	2	15.7 ± 0.8	58.7 ± 2.9	25.6 ± 3.6
	1,2,3	55.4 ± 0.8	31.9 ± 1.0	12.7 ± 1.7
1 hour	1,3	73.6 ± 3.5	20.1 ± 3.1	6.3 ± 0.5
	2	20.5 ± 1.0	61.8 ± 2.3	17.7 ± 3.3
	1,2,3	55.7 ± 0.8	34.1 ± 1.9	10.2 ± 1.1
2 hours	1,3	79.7 ± 0.0	16.4 ± 0.0	3.9 ± 0.0
	2	38.3 ± 1.5	48.9 ± 1.8	12.8 ± 0.4
	1,2,3	66.8 ± 0.8	26.5 ± 0.8	6.7 ± 0.0
3 hours	1,3	83.5 ± 0.5	14.4 ± 0.8	2.2 ± 0.4
	2	43.2 ± 0.8	43.3 ± 0.9	13.5 ± 0.1
	1,2,3	68.9 ± 0.7	24.9 ± 0.9	6.3 ± 0.3
5 hours	1,3	76.2 ± 0.6	19.3 ± 0.3	4.4 ± 0.3
	2	51.1 ± 0.6	33.0 ± 0.7	15.9 ± 0.7
	1,2,3	67.5 ± 0.6	24.1 ± 0.3	8.4 ± 0.4
10 hours	1,3	78.2 ± 1.7	17.8 ± 0.1	3.9 ± 1.6
	2	68.2 ± 2.4	27.1 ± 2.0	4.7 ± 0.4
	1,2,3	74.8 ± 2.0	21.0 ± 0.8	4.2 ± 1.2
15 hours	1,3	78.6 ± 0.0	18.5 ± 0.5	3.0 ± 0.1
	2	74.5 ± 0.3	22.9 ± 0.4	2.6 ± 0.1
	1,2,3	77.1 ± 0.2	20.0 ± 0.5	2.8 ± 0.1
20 hours	1,3	74.9 ± 0.4	20.5 ± 0.8	4.5 ± 0.4
	2	70.9 ± 0.5	23.1 ± 0.9	5.9 ± 0.5
	1,2,3	73.5 ± 0.4	21.5 ± 0.8	5.0 ± 0.4
24 hours	1,3	73.1 ± 0.2	20.3 ± 0.9	6.6 ± 0.8
	2	70.5 ± 0.6	21.5 ± 0.3	8.1 ± 0.6
	1,2,3	72.2 ± 0.4	20.7 ± 0.7	7.1 ± 0.7

Notes:
IV, iodine value. Values are mean of three replicates ± standard deviation.

In an effort to interpret the regiospecific data more explicitly, results in above tables are further illustrated in Figure 4.1 as the kinetic plot. As shown in the figure, SFA contents at the *sn*-1,3 positions reached the maximum after 3 hours of interesterification catalysed by both Lipozyme RM IM and TL IM (87.7 mol% and 83. 5 mol%, respectively). The successive decrement suggested that the ideal 1,3-specific

interesterification had gradually shifted to fatty acid randomisation. In a random interesterification process, there is a contingent distribution of triacylglycerols in which the fatty acids are rearranged randomly over the *sn*-1, *sn*-2 and *sn*-3 positions on the glycerol moiety. This randomisation might result from the acyl migration of fatty acids from the *sn*-2 position to *sn*-1 and *sn*-3, or possibly by a change in the specificity of the enzyme (Svensson and Adlercreutz, 2011).

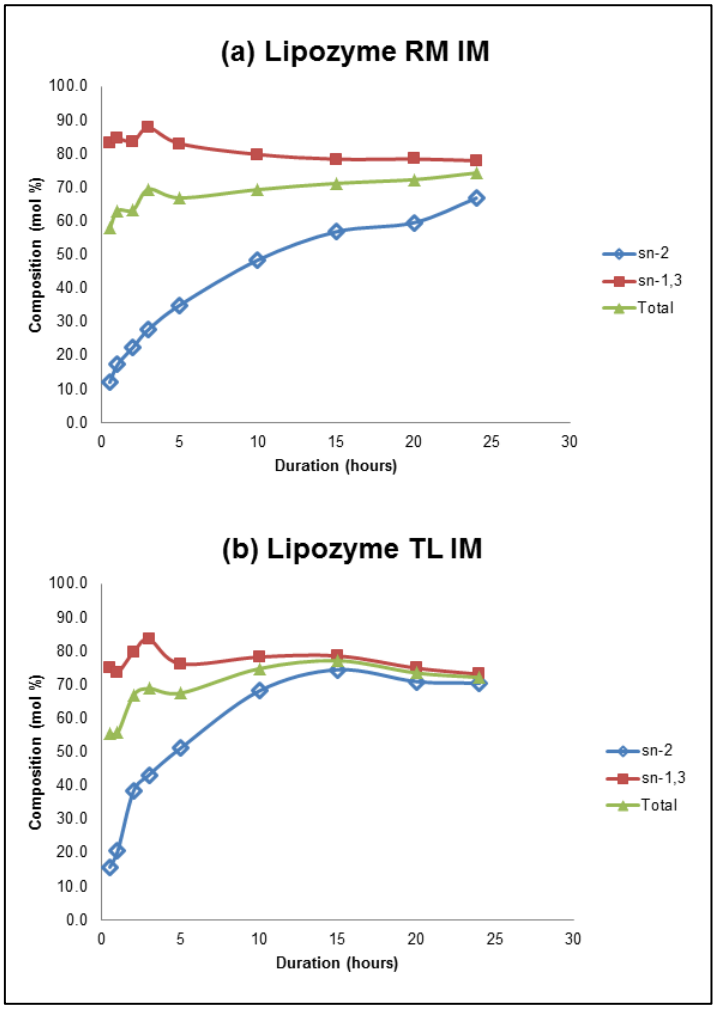

Notes:
Lipozyme RM IM, immobilised lipases from the strain of *Rhizomucor miehei*
Lipozyme TL IM, immobilised lipases from the strain of *Thermomyces lanuginose*

Figure 4.1 : Kinetics of the enzymatic interesterification between palm olein IV 56 and ethyl behenate catalysed by (a) Lipozyme RM IM (b) Lipozyme TL IM, measured by the positional distribution of saturated fatty acids (SFA) in triacylglycerol

In an ideal 1,3-specific lipase catalysed interesterification reaction, the fatty acid composition at the *sn*-2 position should be conserved. Yet in practice, changes were seen in the fatty acid composition in this position. Within 30 minutes, SFA content at the *sn*-2 position increased to 12.0 mol% (Table 4.1) and 15.7 mol% (Table 4.2) in reactions catalysed by Lipozyme RM IM and TL IM, respectively. In general, SFA content at the *sn*-2 position gradually increased with time for both reactions. Lipozyme TL IM produced relatively more saturation at the *sn*-2 position in all reaction products as compared with those produced by Lipozyme RM IM. Under current experimental conditions, 1,3-specific interesterification was preceded in the first three hours, while randomisation surpassed interesterification under prolonged reaction. Randomisation of fatty acids was kinetically slower than the 1,3-specific interesterification under current reaction conditions. Apart from the SFA composition, Figure 4.2 shows the variation of positional distribution of MUFA and PUFA contents with time.

Similar to earlier discussion, the highest SFA incorporation at the *sn*-1,3 positions (Figure 4.1) was concomitant with a minimum level of MUFA at the similar positions after 3 hours of reaction (Figure 4.2). The content of MUFA at the *sn*-2 position also depreciated tremendously from 74.3 mol% in original palm olein to 26.1 mol% (Table 4.1) and 21.5 mol% (Table 4.2) in structured lipids produced after 24 hours under action of Lipozyme RM IM and TL IM, respectively. During the interesterification, major MUFA, namely oleic acid, might migrate from the *sn*-2 position to *sn*-1,3, and was subjected to successive deacylation by 1,3-specific lipase. This postulation elucidates the reduction of MUFA content at the *sn*-2 position and also the slight increment in its composition at the outer positions of triacylglycerol. In contrast, minor fatty acids, *viz.* PUFA, did not show remarkable changes over the entire duration of study (Figure 4.2).

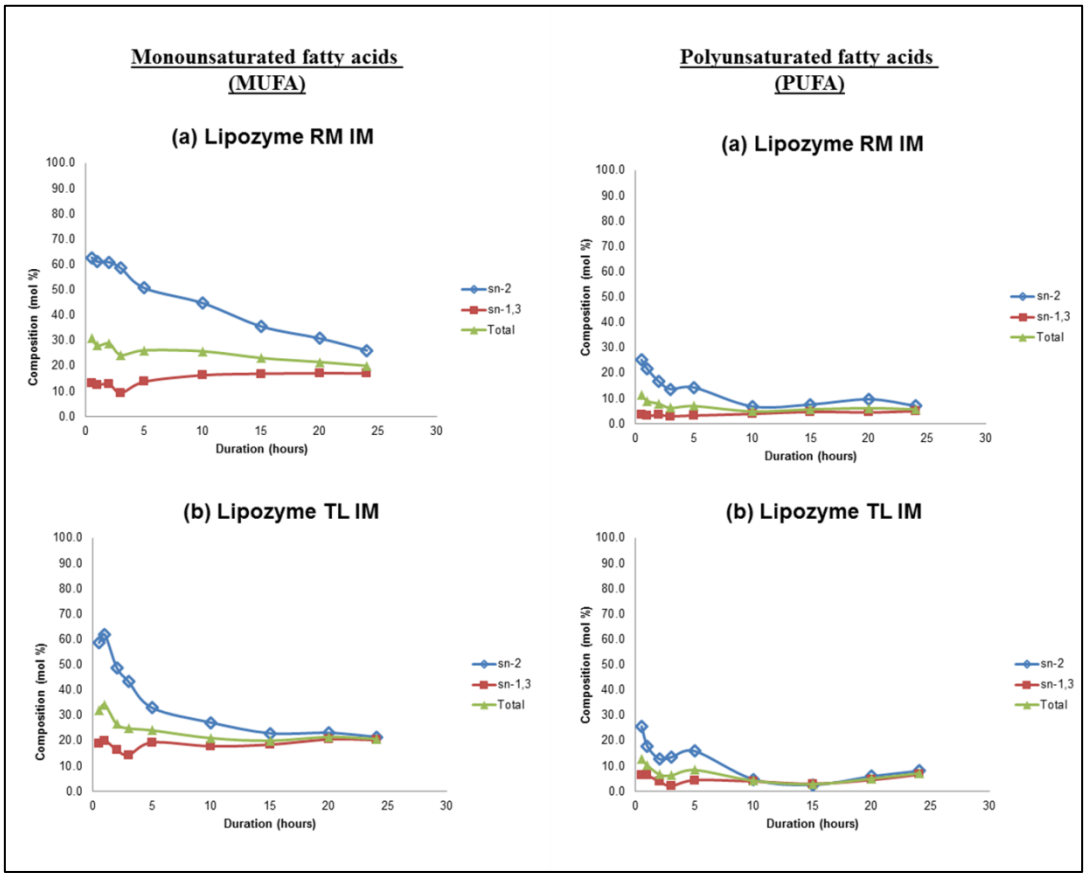

Notes:
Lipozyme RM IM, immobilised lipases from the strain of *Rhizomucor miehei*
Lipozyme TL IM, immobilised lipases from the strain of *Thermomyces lanuginose*

Figure 4.2 : Kinetics of the enzymatic interesterification between palm olein IV 56 and ethyl behenate catalysed by (a) Lipozyme RM IM (b) Lipozyme TL IM, measured by the positional distribution of mono- (MUFA) and polyunsaturated fatty acids (PUFA) in triacylglycerol

Another indication of randomisation reaction was the converging pattern of fatty acid compositions at the *sn*-1,3 and *sn*-2 positions, as observed in both SFA (Figure 4.1) and MUFA (Figure 4.2) variation with time. In order to achieve chemical equilibrium, randomisation will gradually equalise the fatty acid composition at three *sn*-positions, *i.e.* a complete randomised product will exhibit identical fatty acid composition at the *sn*-1, *sn*-2 and *sn*-3 positions of triacylglycerol. By comparing the plots of Lipozyme RM IM and TL IM in Figure 4.1 and Figure 4.2, the extent of converging pattern of

positional fatty acid composition was more prominent in the reaction catalysed by Lipozyme TL IM than those under catalytic action of Lipozyme RM IM. The contents of SFA, MUFA and PUFA at the *sn*-1, 3 positions bore a resemblance to those reside at the middle position after 24 hours of reaction (Table 4.2), suggesting that the Lipozyme TL IM had yielded a near-complete randomised product.

In conclusion, current work observes that Lipozyme RM IM is more regiospecific than Lipozyme TL IM. The former exhibits higher efficiency and specificity in 1,3-specific interesterification. Furthermore, extended interesterification will lead to complete randomisation owing to the acyl migration. This is in line with previous observation by Svensson and Adlercreutz (2011).

4.2.2.2 Identification of Triacylglycerol Molecular Species

Owing to the utilisation of reversed phase end capped column, the relatively more polar molecules are envisaged to be eluted with lower retention times, whilst those trisaturated triacylglycerols suffer delayed elution. The solubility of higher molecular mass triacylglycerols, *viz.* above tripalmitoylglycerol (PPP), have been reported to decrease dramatically in acetone/acetonitrile mixtures (Stolyhwo *et al.*, 1985). Thus, due to the incorporation of behenic acid into glycerol moiety, dichloromethane is used as the organic modifier in the mobile phase to ease the elution of relatively higher molecular mass triacylglycerols as well as to avoid precipitation during elution. In spite of the improvement in separation of the high performance liquid chromatography (HPLC) analysis, the problem of full identification of the chromatographic peaks still exists. As the purchase of standards for all species of triacylglycerols is almost impossible, therefore partition number (PN) and equivalent carbon number (ECN) are used for identification.

PN serves as a basis for the order of elution of various triacylglycerol molecular species (Barron *et al.*, 1990; Nájera *et al.*, 1998). It depends on the chain length as well as the number of double bonds of the constituting fatty acids (Equation 4.1). Nevertheless, with the enhanced resolution provided by the optimised mobile phase and with the aid of gradient elution, the separation of those triacylglycerols with the similar PN values becomes feasible (Perona *et al.*, 1998; Nájera *et al.*, 1999). In other words, the separation of triacylglycerols possessing similar PN values is following the different number of unsaturated fatty acids (NUFA), namely, those with higher NUFA are showing lower retention times. Henceforth, equivalent carbon number (ECN) is introduced and calculated according to the previous literature (Perona and Ruiz-Gutierrez, 2003). It is illustrated in Equation 4.2:

$$PN = CN - 2 \times DB \quad (4.1)$$

$$ECN = CN - 2 \times DB - 0.2 \times NUFA \quad (4.2)$$

where CN is the total carbon number of the three acyl chains, DB is the total number of double bonds and NUFA is the number of unsaturated fatty acids of the triacylglycerol molecules.

In the present characterisation of structured lipids, the order of elution is reaffirmed according to the corresponding ECN values of various triacylglycerol molecular species, as illustrated in Table 4.3. With increasing values of ECN, the relative retention time for the specific species will be lowered. As a result, current calculation of ECN has superseded those in prior study (Ibrahim *et al.*, 2008), which was grouping those with similar PN values and specifying as a group of triacylglycerols.

Table 4.3 : Equivalent carbon numbers (ECN) for various triacylglycerol molecular species

Molecular species	CN	DB	NUFA	PN = CN - 2 x DB	ECN = CN - 2 x DB - 0.2 x NUFA
LLL	54	6	3	42	41.4
OLL	54	5	3	44	43.4
PLL	52	4	2	44	43.6
OOL	54	4	3	46	45.4
POL	52	3	2	46	45.6
OOO	54	3	3	48	47.4
POO	52	2	2	48	47.6
POP	50	1	1	48	47.8
StOO	54	2	2	50	49.6
BLO	58	3	2	52	51.6
BLP	56	2	1	52	51.8
StOSt	54	1	1	52	51.8
BOO	58	2	2	54	53.6
BOP	56	1	1	54	53.8
BOSt	58	1	1	56	55.8
BLB	62	2	1	58	57.8
BOB	62	1	1	60	59.8
BBP	60	0	0	60	60.0
BBSt	62	0	0	62	62.0
BBB	66	0	0	66	66.0

Notes:
CN, total carbon number of the three acyl chains; DB, total number of double bonds; NUFA, the number of unsaturated fatty acids in the triacylglycerol molecule; PN, partition number; ECN, equivalent carbon number; P, palmitic; St, stearic; O, oleic; L, linoleic; B, behenic.

With the absence of unsaturated fatty acids, trisaturated species, *viz.* 1,2-dibehenoyl-3-palmitoylglycerol (BBP), 1,2-dibehenoyl-3-stearoylglycerol (BBSt) and tribehenoylglycerol (BBB), exhibit the highest ECN values. In other words, their affinities towards the stationary phase in reversed-phase column are the highest. On top of that, triacylglycerol molecular species of trioleoylglycerol (OOO), 1,2-dioleoyl-3-palmitoylglycerol (POO) and 1,3-dipalmitoyl-2-oleoylglycerol (POP) are sharing the resemblance in PN values (PN = 48). Yet, due to the different NUFA in these triacylglycerols, OOO is expected to be eluted prior to POO, and followed by POP. This

is in line with the trend observed in ECN values as well as in the actual chromatogram of palm olein iodine value (IV) 56 (Figure 4.3).

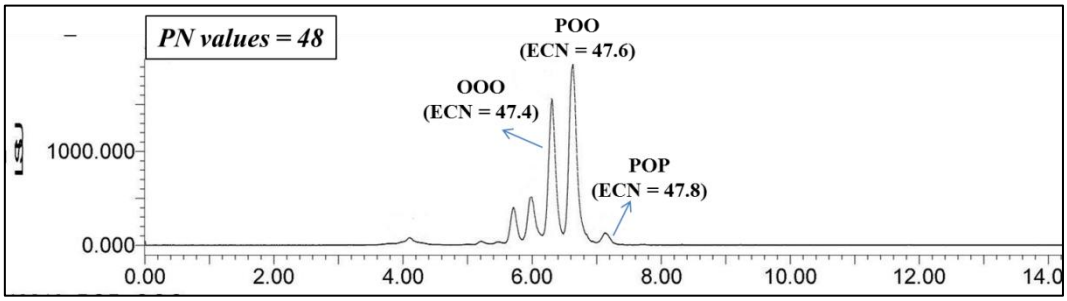

Notes:
PN, partition number; IV, iodine value; ECN, equivalent carbon number; P, palmitic acid; O, oleic acid.

Figure 4.3 : Separation of triacylglycerol molecular species with identical PN values in chromatogram of palm olein IV 56

Even though the information on the elution sequence of various molecular species is attainable, the exact chromatographic peak assignment is not feasible merely based on ECN values of triacylglycerols. As a consequence, the detailed chromatographic peak identification is accomplished by the approach of logarithms of retention volumes, as suggested in earlier studies (Goiffon *et al.*, 1981; Stolyhwo *et al.*, 1985; Fabien *et al.*, 1993).

A plot of the logarithm of the relative retention volume of saturated triacylglycerols (OOO as the reference triacylglycerol) against the total number of carbon atoms of the three acyl chain is shown in Figure 4.4. By employing the homogeneous standard saturated triacylglycerols, namely, PPP, tristearoylglycerol (StStSt) and BBB, an exceptional correlation coefficient equals to 0.9991, is obtained. As shown in Figure 4.4, the slope of the linear plot is 0.0194. This corresponds to an increase in the retention time by a factor of 1.23 when the chain of each acyl group increases by six

carbon atoms, *viz.* from PPP to BBB. In other words, it resembles an increment of 6.8% per additional carbon atom in retention time. This is in excellent agreement with previous observations on similar plots for homologous series. They reported a 7.2% increment in retention time for an additional carbon atom in the acyl chain (Stolyhwo *et al.*, 1985).

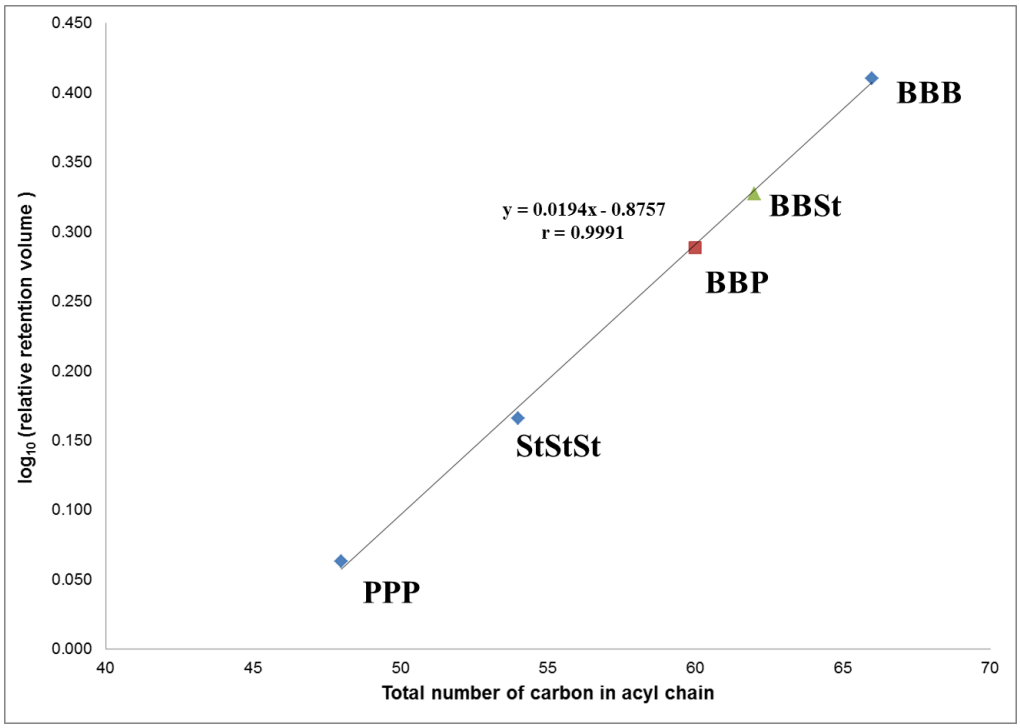

Notes:
P, palmitic acid; St, stearic acid; B, behenic acid.

Figure 4.4 : Graph of the logarithm of the retention volumes of saturated triacylglycerols, relative to trioleoylglycerol, against the total number of carbon atoms in the fatty acid acyl chains

In this plot, a mixed triacylglycerol made by two different fatty acids is represented by a point of the segment joining the points representing the two corresponding homogeneous triacylglycerols. Interestingly, the point denoting the mixed triacylglycerol is placed one-third of the way on the side of the dominant acid. This is

illustrated by the points corresponding BBSt and BBP in Figure 4.4. These two points are calculated and plotted using chromatographic data of structured lipids and they fit perfectly onto the graph made with standard homogeneous triacylglycerols.

Notwithstanding the excellent plot in Figure 4.4, it is not applicable to triacylglycerols containing unsaturated fatty acids as unsaturation gives significant influence on the order of elution and the retention time. Goiffon *et al.* (1981) has suggested a general scheme using the principle of the addition of solution free energies. The results are presented as a plot of logarithm of the relative retention volume against the number of double bonds contained in the triacylglycerol molecule. In the current study, a similar plot has been derived from the chromatographic data obtained by the analysis of synthetic mixtures of triacylglycerol standards, palm olein IV 56, high-oleic sunflower oil and the newly synthesised structured lipids, as depicted in Figure 4.5. Due to the presence of OOO in all samples, it remains the ideal reference in the identification of triacylglycerol molecular species.

In contrast with previous works applying a similar approach in the peak identification (Goiffon *et al.*, 1981; Stolyhwo *et al.*, 1985), our current analyses are focussing on the triacylglycerols containing behenic acid as this fatty acid is employed in the synthesis of prospective low-calorie structured lipids. As the retention time depends much on the column temperature, composition of mobile phase and other experimental conditions, Stolyhwo *et al.* (1985) suggested that such diagram must be established by measuring all the required data under similar experimental conditions so it will be engaged for successive qualitative analysis of oils and fats.

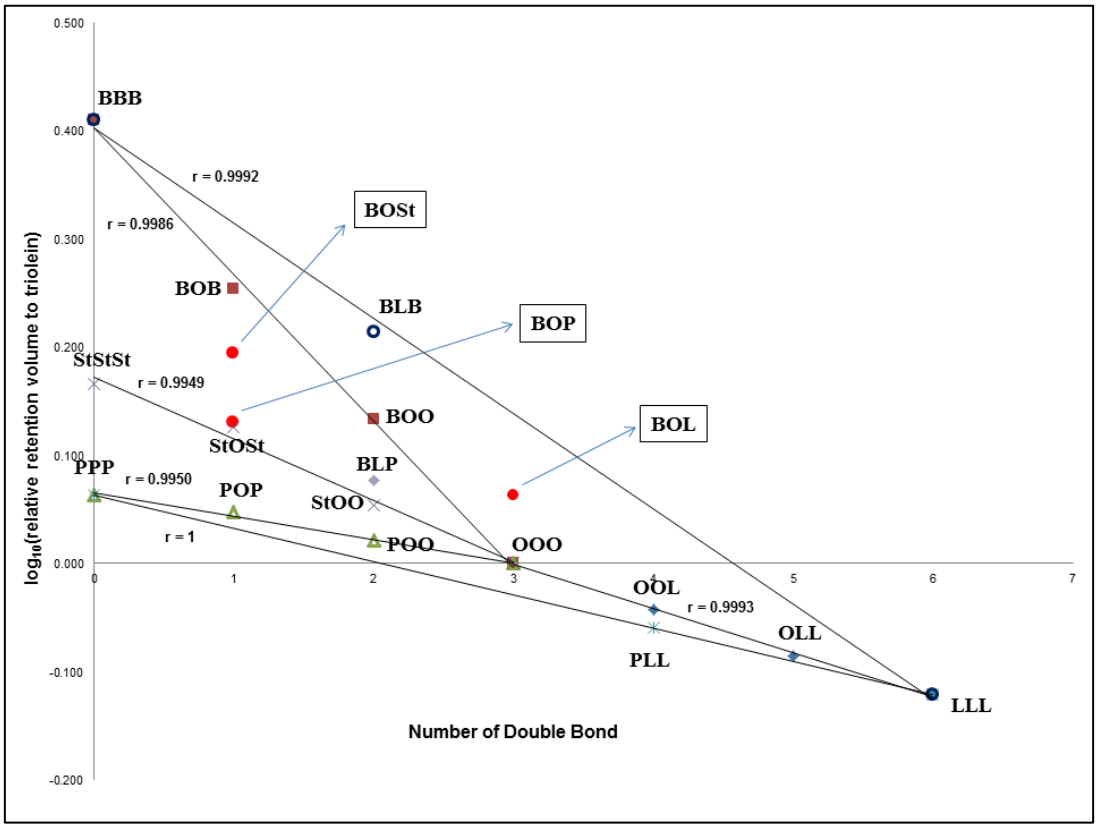

Notes:
P, palmitic acid; St, stearic acid; O, oleic acid; L, linoleic acid; B, behenic acid.

Figure 4.5 : Graph of the logarithm of the retention volumes of triacylglycerols, relative to trioleoylglycerol, against the total number of double bonds in the fatty acid acyl chains

Each triacylglycerol molecular species is represented by a point in Figure 4.5. Meanwhile, each plot is joining two points representing different homogenous triacylglycerols, whereas their corresponding mixed triacylglycerols are well-placed on the same plot. For instance, BOB and BOO are represented by two points on the plot connecting BBB and OOO, as well as they divide the plot into four equal segments. The point representing a mixed triacylglycerol made by three different acids (individual point as shown in Figure 4.5) is located at the mass centre of the triangle formed by the points of the three homogenous triacylglycerols. To illustrate, it can be seen in Figure 4.5 that the 1-behenoyl-2-oleoyl-3-stearoylglycerol (BOSt) is positioned at the centre of

the triangle formed by BBB, OOO and StStSt. Furthermore, the point representing BOSt remains equidistant from 1,3-dibehenoyl-2-oleoylglycerol (BOB) and 1,3-distearoyl-2-oleoylglycerol (StOSt). In other words, the logarithm of the relative retention volume of BOSt is equal to half of the sum of those of BOB and StOSt, and also one-third of the sum of those of BBB, OOO and StStSt.

At a constant number of double bonds, the logarithm of the retention volume is a linear function of the increasing number of carbon atoms and the ECN values of triacylglycerol molecular species (Table 4.3). Moreover, those triacylglycerol molecular species which are eluted prior to OOO, namely 1,2-dioleoyl-3-linoleoylglycerol (OOL), 1,2-dilinoleoyl-3-oleoylglycerol (OLL) and trilinoleoylglycerol (LLL), are showing negative values for their logarithm of the relative retention volume. All the criteria stated above will ease the identification of an unknown chromatographic peak with known relative retention volume.

Notwithstanding the varying slopes in different plots, all plots show exceptional correlation coefficients, r, which fall in the range of 0.9949 - 1.0000. This suggests that the current experimental condition of HPLC is robust and well-controlled throughout all analysis as the retention data in Figure 4.5 were derived from the analysis of various types of oils and fats. As a result, this diagram permits the recognition of a known triacylglycerol, as well as to identify an unknown triacylglycerol.

Figure 4.6 and Figure 4.7 illustrate some examples on the peak identification of various triacylglycerol molecular species in the chromatogram of the base oils, namely, palm olein IV 56 and high-oleic sunflower oil, respectively. The peak which is pertaining to OOO presents in both chromatograms, and consequently eases the identification of

remaining peaks. As depicted in Figure 4.5, triacylglycerol molecular species which are having negative values for the logarithm of the relative retention volume, are shown to elute prior to OOO (Figure 4.6 and 4.7). These molecular species are OOL, OLL and LLL. In general, the molecular structures of native triacylglycerol species are consisting of four common fatty acids, *viz.* palmitic acid, stearic acid, oleic acid and linoleic acid. On the contrary, interesterification with ethyl behenate introduces a variety of new triacylglycerol species, which makes the identification more challenging.

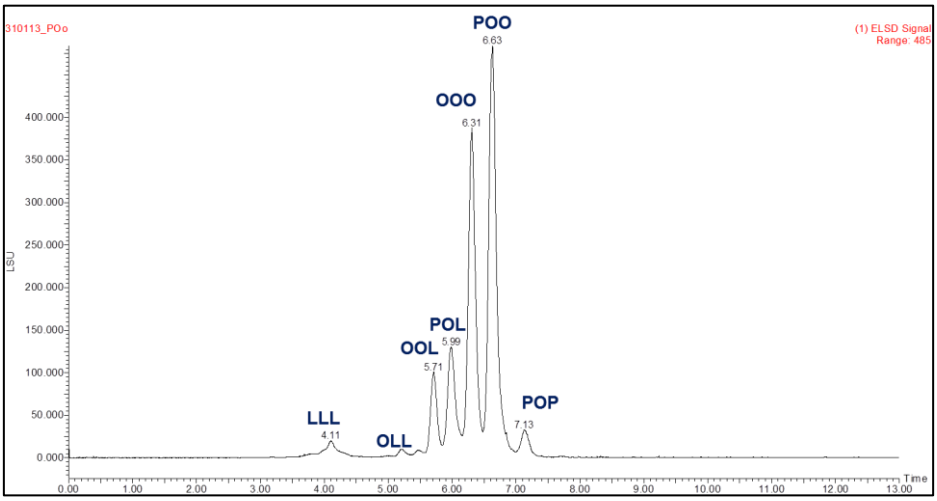

Notes:
L, linoleic acid; O, oleic acid; P, palmitic acid.

Figure 4.6 : Peak identification of various triacylglycerol molecular species in the chromatogram of palm olein IV 56

Figure 4.8 shows the chromatogram of structured lipids produced from the Lipozyme TL-catalysed interesterification between high-oleic sunflower oil and ethyl behenate in 24 hours. By incorporating the behenic acid into the native molecular species of high-oleic sunflower oil, various triacylglycerol species containing behenic acid at the *sn*-1,3 positions have been produced. It is noteworthy that the current identification method is capable to identify all the peaks present in the chromatogram. Despite the utilisation of dichloromethane as the organic modifier in the mobile phase, the relatively high

molecular mass trisaturated triacylglycerols, namely, BBP, BBSt and BBB, are still strongly retained in the column, giving broader peaks than those eluted beforehand.

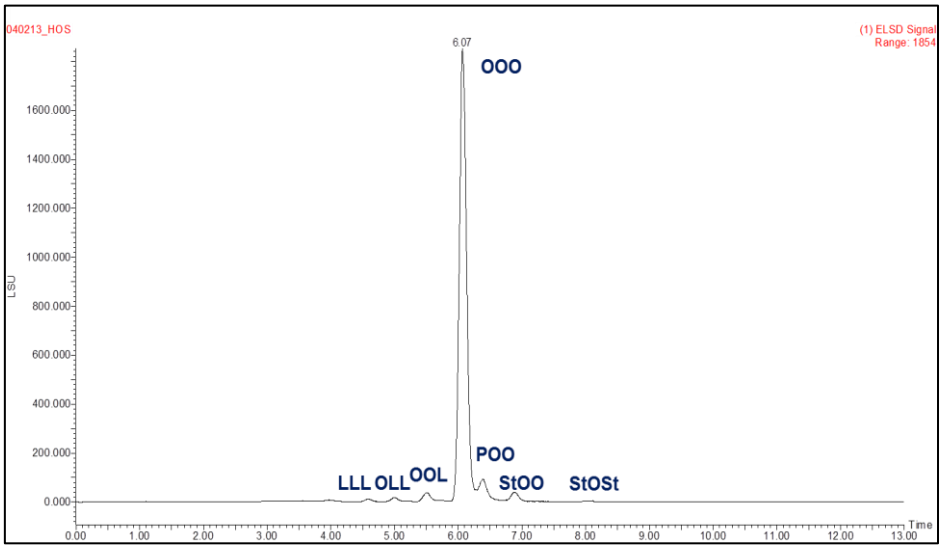

Notes:
L, linoleic acid; O, oleic acid; P, palmitic acid; St, stearic acid.

Figure 4.7 : Peak identification of various triacylglycerol molecular species in the chromatogram of high-oleic sunflower oil

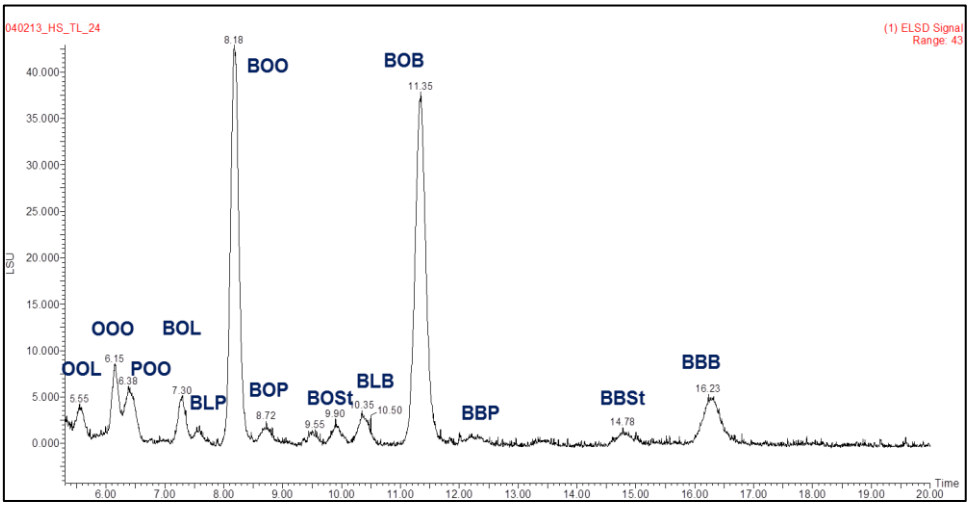

Notes:
O, oleic acid; L, linoleic acid; P, palmitic acid; B, behenic acid; St, stearic acid.

Figure 4.8 : Peak identification of various triacylglycerol molecular species in the chromatogram of structured lipids

As a conclusion, the present method in conjunction with ECN values of triacylglycerols, serves as a reliable means to predict and identify unknown chromatographic peaks, by using OOO as the reference.

4.2.2.3 Triacylglycerol Composition

The compositions of various triacylglycerol molecular species of palm olein iodine value (IV) 56 and its interesterified products in the presence of immobilised lipases from the strain of *Rhizomucor miehei* (Lipozyme RM IM) and *Thermomyces lanuginose* (Lipozyme TL IM) are given in Table 4.4 and Table 4.5, respectively.

Table 4.4 : Triacylglycerol composition of the starting material (palm olein IV 56) and the interesterification reaction intermediates catalysed by Lipozyme RM IM with ethyl behenate

Molecular species	Composition (% of total triacylglycerols)									Palm olein IV 56
	0.5 hours	1 hour	2 hours	3 hours	5 hours	10 hours	15 hours	20 hours	24 hours	
LLL	ND	ND	ND	ND	ND	ND	ND	ND	ND	2.2
OLL	ND	ND	ND	ND	ND	ND	ND	ND	ND	0.9
PLL	ND	ND	ND	ND	ND	ND	ND	ND	ND	0.7
OOL	3.3	1.2	1.8	2.3	1.3	2.7	2.0	4.7	1.6	7.4
POL	2.8	ND	ND	ND	ND	ND	ND	ND	ND	12.1
OOO	10.4	7.1	7.4	8.8	8.6	7.8	6.4	6.0	7.8	31.7
POO	9.9	3.7	3.1	3.1	3.3	3.5	2.1	2.5	2.4	42.9
POP	3.8	4.5	4.2	4.6	9.7	4.8	4.0	3.3	3.2	2.2
BLO	4.3	5.1	6.1	3.5	3.5	3.4	2.4	3.1	2.5	ND
BLP	8.4	10.9	10.7	10.3	10.5	8.4	6.9	6.8	6.9	ND
BOO	27.2	25.9	20.1	20.2	15.8	15.6	14.8	13.9	15.6	ND
BOP	2.6	3.3	3.1	4.2	5.4	5.9	6.7	8.4	6.7	ND
BOSt	3.9	4.5	4.4	4.6	4.7	3.7	4.6	5.2	3.1	ND
BLB	2.6	2.8	2.6	3.1	5.3	2.7	3.9	2.8	3.2	ND
BOB	18.3	26.7	26.4	25.9	19.3	21.4	21.8	19.8	20.0	ND
BBP	2.4	4.2	6.9	6.5	8.5	12.1	13.4	13.2	15.8	ND
BBSt	ND	ND	ND	ND	ND	2.1	2.9	2.1	2.6	ND
BBB	ND	ND	3.2	2.8	4.1	6.0	8.1	8.4	8.5	ND

Notes:
IV, iodine value; ND, not detected; P, palmitic; St, stearic; O, oleic; L, linoleic; B, behenic.

With reference to both tables, the composition of polyunsaturated species containing linoleic acid, such as trilinoleoylglycerol (LLL) and 1,2-dilinoleoyl-3-oleoylglycerol (OLL), diminished during the interesterification reactions. Under 24-hour catalytic action of Lipozyme RM IM, depreciations in the composition of the major native triacylglycerol species in the precursor starting material, namely, 1,2-dioleoyl-3-palmitoylglycerol (POO) and trioleoylglycerol (OOO), were about 40.5% and 23.9%, respectively (Table 4.4). The corresponding reductions under action of Lipozyme TL IM were 27.5% and 15.9%, respectively (Table 4.5). Meanwhile, the predominant ideal structured triacylglycerols produced throughout the interesterification were 1,3-dibehenoyl-2-oleoylglycerol (BOB) and 1-behenoyl-2,3-dioleoylglycerol (BOO) which constituted more than 30% and 40% of total triacylglycerols in the structured lipids obtained with Lipozyme TL IM and RM IM, respectively. The interesterification reaction scheme for the production of major products (BOB and BOO) from the predominant triacylglycerol species in palm olein (POO) and ethyl behenate is shown in Figure 4.9.

Among all the undesirable co-products, 1,2-dibehenoyl-3-palmitoylglycerol (BBP) was the highest composition due to the relatively high concentration of palmitic acid in the starting material as well as the occurrence of acyl migration under the current reaction conditions. On the other hand, tribehenoylglycerol (BBB) was found relatively more abundant with Lipozyme TL IM compared with Lipozyme RM IM as the former was observed to be less regiospecific and subsequently produced more undesirable co-products. This was parallel with the discussion in Section 4.3.2.1.

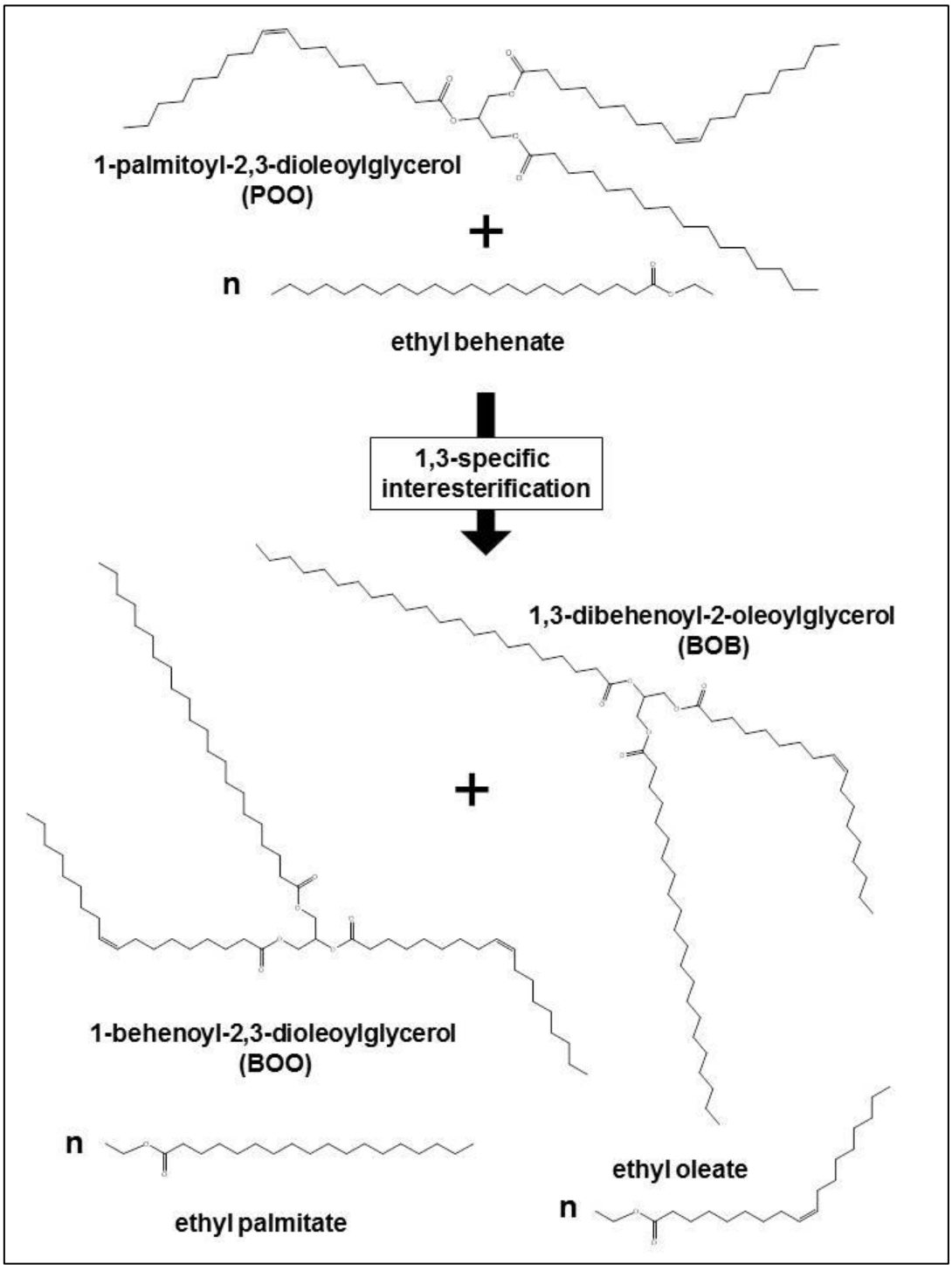

Figure 4.9 : Enzymatic interesterification reaction scheme between ethyl behenate and 1-palmitoyl-2,3-dioleoylglycerol (POO) in palm olein IV 56

Table 4.5 : Triacylglycerol composition of the starting material (palm olein IV 56) and the interesterification reaction intermediates catalysed by Lipozyme TL IM with ethyl behenate

Molecular species	Composition (% of total triacylglycerols)									Palm olein IV 56
	0.5 hours	1 hour	2 hours	3 hours	5 hours	10 hours	15 hours	20 hours	24 hours	
LLL	ND	ND	ND	ND	ND	ND	ND	ND	ND	2.2
OLL	ND	ND	ND	ND	ND	ND	ND	ND	ND	0.9
PLL	2.1	1.1	1.3	ND	ND	ND	ND	ND	ND	0.7
OOL	4.4	1.8	2.2	2.4	1.9	1.2	ND	ND	ND	7.4
POL	4.2	1.6	1.1	ND	ND	ND	ND	ND	ND	12.1
OOO	15.8	7.4	7.9	9.2	9.6	9.2	9.1	8.5	8.5	31.7
POO	15.4	4.1	2.8	2.8	2.5	2.2	2.0	1.9	2.1	42.9
POP	5.0	3.9	4.6	4.6	4.2	4.1	2.5	3.2	3.2	2.2
BLO	3.3	3.6	3.2	3.4	2.7	2.1	2.0	2.6	2.7	ND
BLP	8.8	11.2	9.9	8.9	8.4	6.6	6.3	6.1	5.7	ND
BOO	21.0	22.1	17.4	16.6	15.4	13.7	14.3	13.5	13.0	ND
BOP	3.1	10.2	6.2	7.5	5.9	7.0	6.8	5.9	7.4	ND
BOSt	1.8	8.1	4.9	4.2	3.8	4.4	2.7	4.1	3.7	ND
BLB	1.3	5.2	3.6	3.0	2.6	2.8	3.8	3.0	2.6	ND
BOB	11.4	15.3	19.9	19.0	20.2	18.8	18.7	18.1	19.3	ND
BBP	2.2	4.3	8.8	10.3	13.4	15.6	16.4	15.6	16.1	ND
BBSt	ND	ND	1.9	2.1	2.5	1.9	2.9	4.5	3.0	ND
BBB	ND	ND	4.4	6.1	6.9	10.5	12.4	13.2	12.8	ND

Notes:
IV, iodine value; ND, not detected; P, palmitic; St, stearic; O, oleic; L, linoleic; B, behenic.

For ease of discussion, the triacylglycerol molecular species in the above tables are grouped into several categories, namely, targeted structured lipids, co-products as well as the reactant triacylglycerols. In the presence of 1,3-specific enzymes, the targeted products will be triacylglycerols with behenic acid incorporated at the *sn*-1,3 positions, in which BOB and BOO make up the predominant compositions. Meanwhile, the reactants represent triacylglycerols which are natively obtainable in palm olein IV 56, whereas the co-products referred to the trisaturated species. The evolution of these molecular species are tabulated in Table 4.6 and subsequently illustrated in Figure 4.10 for those obtained under catalytic action of Lipozyme RM IM.

Table 4.6 : Evolution of targeted structured lipids, co-products and reactant triacylglycerols as a function of time in interesterification of palm olein IV 56 catalysed by Lipozyme RM IM

Duration (hours)	Compositions (% of total triacylglycerols)				Ratio of Targeted SL / reactant	Ratio of Targeted SL / co-product
	Targeted SL	BOB + BOO	Co-Product	Reactant		
0.5	67.4	45.5	2.4	30.2	2.23	28.50
1	79.3	52.6	4.2	16.5	4.81	18.75
2	73.4	46.5	10.0	16.5	4.44	7.32
3	71.7	46.1	9.4	18.9	3.80	7.64
5	64.5	35.0	12.6	22.9	2.81	5.11
10	61.1	37.0	20.2	18.8	3.26	3.03
15	61.0	36.6	24.5	14.5	4.20	2.49
20	59.8	33.7	23.6	16.5	3.63	2.53
24	58.1	35.6	26.9	15.0	3.87	2.16

Notes:
Targeted SL = Targeted structured lipids (sum of the compositions of BLO, BLP, BOO, BOP, BOS, BLB and BOB); BOB + BOO = the compositions of major targeted structured triacylglycerol species; co-product = sum of the compositions of BBP, BBS and BBB; reactant = the compositions of triacylglycerol species present in the base oil.

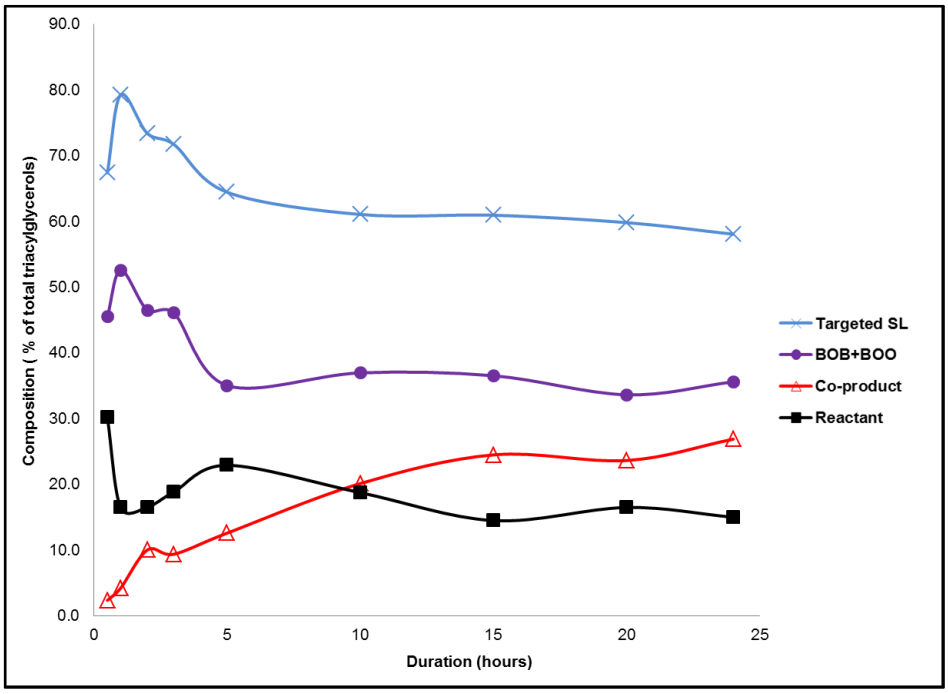

Notes:
IV, iodine value; SL, structured lipids; B, behenic acid; O, oleic acid.

Figure 4.10 : Interesterification reaction between palm olein IV 56 and ethyl behenate catalysed by Lipozyme RM IM

In Table 4.6, the ratio of targeted structured lipids to reactants illustrates the evolution of native triacylglycerols to the desired products. Conversely, the ratio of targeted structured lipids to co-products represents the development of unfavourable trisaturated species during the course of reaction. The highest ratio of targeted structured lipids to reactants was found in 1-hour reaction product (4.81, Table 4.6), whilst its ratio to the co-products remained highest in the structured lipids produced after 30 minutes of reaction (28.50, Table 4.6). Nevertheless, the main concern is still on the elevated trisaturated species as these species are expected to exert detrimental effects on human health (Berry, 2009).

Figure 4.10 exhibits that the desired triacylglycerol molecular species generally decreased once reaching maximum after 1 hour of reaction (79.3%, Table 4.6). These phenomenon could be attributed to the gradual shifting of the reaction from initially 1,3-specific interesterification to the fatty acid randomisation among the three *sn*-positions. Under prolonged reaction, the newly synthesised structured lipids, for instance the BOB and BOO might be subjected to successive acyl migration and enzymatic hydrolysis. As a result, the decrement was accompanied by the elevating composition of the undesired co-products. For reaction after 5 hours, no major changes in the composition of BOO and BOB were observed. Similar interpretation is done on structured lipids obtained with Lipozyme TL IM, as depicted in Table 4.7 and Figure 4.11.

Similar to those obtained with Lipozyme RM IM, the ratio of targeted structured lipids to the co-products remained the highest in the 0.5-hour-reaction product catalysed by Lipozyme TL IM (22.74, Table 4.7). Nevertheless, lower amount of the targeted triacylglycerols (50.8%, Table 4.7) produced by Lipozyme TL IM was relatively lower than those obtained with Lipozyme RM IM. The latter was again being validated to be

more efficient compared with the former in 1,3-specific interesterification. This is also in line with the discussion in Section 4.3.2.1.

Table 4.7 : Evolution of targeted structured lipids, co-products and reactant triacylglycerols as a function of time in interesterification of palm olein IV 56 catalysed by Lipozyme TL IM

Duration (hours)	Compositions (% of total triacylglycerols)				Ratio of Targeted SL / reactant	Ratio of Targeted SL / co-product
	Targeted SL	BOB + BOO	Co-Product	Reactant		
0.5	50.8	32.4	2.2	47.0	1.08	22.74
1	75.7	37.4	4.3	20.0	3.79	17.58
2	65.1	37.3	15.0	19.8	3.28	4.33
3	62.6	35.6	18.5	19.0	3.30	3.39
5	59.1	35.6	22.8	18.1	3.26	2.59
10	55.4	32.5	27.9	16.7	3.32	1.98
15	54.6	33.1	31.7	13.7	4.00	1.72
20	53.2	31.5	33.3	13.5	3.94	1.60
24	54.3	32.2	31.9	13.8	3.93	1.70

Notes:
Targeted SL = Targeted structured lipids (sum of the compositions of BLO, BLP, BOO, BOP, BOS, BLB and BOB); BOB + BOO = the compositions of major targeted structured triacylglycerol species; co-product = sum of the compositions of BBP, BBS and BBB; reactant = the compositions of triacylglycerol species present in the base oil.

With reference to the Figure 4.11, interesterification proceeded rapidly at the beginning, and then was surpassed gradually by randomisation after 1 hour. The composition of reactant triacylglycerols (mainly 1,2-dioleoyl-3-palmitoylglycerol (POO) and 1,3-dipalmitoyl-2-oleoylglycerol (POP)) did not experience significant changes after 1 hour. Furthermore, the composition of targeted triacylglycerol species reached the maximum in one-hour interesterification product (75.7%, Table 4.7), and subsequently depreciated and attained a near-equilibrium state after 10 hours. This variation was associated with the increment of co-products as a function of time, which suggests that more BBP and BBB were formed at the expenses of BOB and BOO. In the context of their highest amount of co-products, Lipozyme RM IM produced 26.9% (Table 4.6) in the 24-hour structured lipids whereas Lipozyme TL IM yielded 33.3% of total triacylglycerols as the

undesirable trisaturated species (Table 4.7). A major shift from enzymatic interesterification to complete and non-specific hydrolysis was therefore observed.

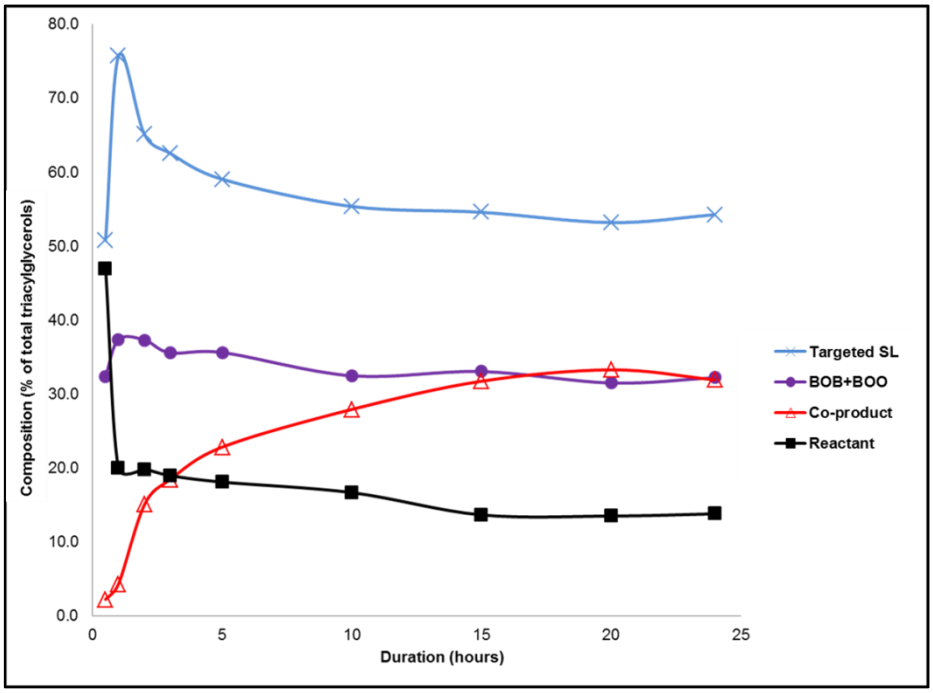

Notes:
IV, iodine value; SL, structured lipids; B, behenic acid; O, oleic acid.

Figure 4.11 : Interesterification reaction between palm olein IV 56 and ethyl behenate catalysed by Lipozyme TL IM

As a result, by varying the reaction time and choosing suitable enzymes, different triacylglycerol mixtures can be produced, *i.e.* products originating from 1,3-specific interesterification, as well as partially or fully randomised products. Both Lipozyme RM IM and TL IM serve as the choices available for the synthesis of structured lipids for diverse triacylglycerol composition.

4.3 Enzymatic Interesterification between High-Oleic Sunflower Oil and Ethyl Behenate

4.3.1 Experimental

4.3.1.1 Materials

Refined, bleached and deodorised (RBD) high-oleic sunflower oil was a generous gift from Intercontinental Specialty Fats Sdn. Bhd., Selangor, Malaysia. The sources of behenic acid, immobilised lipases and solvents are as described in Section 4.2.1.1.

4.3.1.2 Preparation of Ethyl Behenate

Esterification between behenic acid and ethanol was employed in the preparation of ethyl behenate, following the protocols established in Section 4.2.1.2.

4.3.1.3 Enzymatic Interesterification

5 g of high-oleic sunflower oil (average molecular mass of 885.43 g/mol) was mixed with 6.25 g of ethyl behenate (molecular mass of 368.64 g/mol) at a molar ratio of 1:3 in a 100-mL Schott bottle with screw cap. Enzymatic interesterification between high-oleic sunflower oil and ethyl behenate was carried out following the methods described in Section 4.2.1.3.

4.3.1.4 ^{13}C NMR Regiospecific Analysis

The protocols for ^{13}C NMR regiospecific analysis of the present batch of structured lipids were similar as reported in the previous section (Section 4.2.1.4).

4.3.1.5 High Performance Liquid Chromatography (HPLC)

Triacylglycerol molecular species of structured lipids were determined using high performance liquid chromatography (HPLC) equipped with evaporative light-scattering

detector (ELSD). The protocols used were similar as reported in the previous section (Section 4.2.1.5).

4.3.2 Results and Discussion

4.3.2.1 Positional Distribution of Fatty Acids in High-Oleic Sunflower Oil and Structured Lipids Synthesised

Regiospecific analysis of structured lipids was executed by the ^{13}C NMR approach, as described in Chapter 2. Table 4.8 and Table 4.9 present the positional distribution of saturated (SFA), mono- (MUFA) and polyunsaturated fatty acids (PUFA) in the precursor starting material, *viz.* high-oleic sunflower oil, as well as the interesterified products catalysed by immobilised lipases from the strain of *Rhizomucor miehei* (Lipozyme RM IM) and *Thermomyces lanuginose* (Lipozyme TL IM), respectively.

Under the catalytic action of Lipozyme RM IM, 55.1 - 64.0 mol% of SFA (Table 4.8) were found at the *sn*-1,3 positions of triacylglycerols in various reaction products. On the contrary, poorer incorporation of behenic acid had resulted relatively lower saturation (43.3 - 61.5 mol%, Table 4.9) at the similar positions of triacylglycerols in the reaction catalysed by Lipozyme TL IM. This again suggested that Lipozyme RM IM possessed a higher efficiency and activity compared with Lipozyme TL IM under the current reaction conditions. Oppositely, the SFA contents at the *sn*-2 position fell in the range of 0.0 - 45.8 mol% (Table 4.8) and 6.1 - 58.7 mol% (Table 4.9) for the reaction products produced by the Lipozyme RM IM and Lipozyme TL IM, respectively. Apart from being relatively more efficient, Lipozyme RM IM was also shown to be more regiospecific than the Lipozyme TL IM. Moreover, it was noteworthy that the saturation level at the *sn*-2 position of structured lipids was still remained undetectable after 1 hour of Lipozyme RM IM-catalysed interesterification (Table 4.8). In order to interpret the

regiospecific data more explicitly, results in the above tables are further demonstrated in Figure 4.12 as the kinetic plot on the changes of the positional SFA composition with time.

Table 4.8 : Regiospecific data of the starting material (high-oleic sunflower oil) and the interesterification reaction intermediates catalysed by Lipozyme RM IM with ethyl behenate

Duration	Composition (mol%)			
	sn-position	Saturated	Monounsaturated	Polyunsaturated
High-oleic sunflower oil	1,3	11.6 ±0.3	76.5 ±0.2	11.9 ±0.5
	2	ND	86.5 ±0.4	13.5 ±0.7
	1,2,3	7.8 ±0.3	79.8 ±0.3	12.4 ±0.7
0.5 hours	1,3	58.5 ±2.0	35.9 ±1.6	5.5 ±0.6
	2	ND	85.0 ±0.9	15.0 ±0.9
	1,2,3	38.6 ±1.3	52.6 ±1.2	8.8 ±0.4
1 hour	1,3	60.4 ±0.8	34.1 ±0.6	5.5 ±0.1
	2	ND	81.5 ±0.2	18.5 ±0.2
	1,2,3	40.1 ±0.3	50.0 ±0.2	9.9 ±0.1
2 hours	1,3	62.1 ±0.1	31.2 ±0.4	6.8 ±0.5
	2	5.6 ±0.1	75.4 ±0.4	19.0 ±0.5
	1,2,3	40.8 ±0.1	47.9 ±0.4	11.4 ±0.2
3 hours	1,3	60.7 ±0.3	34.0 ±0.5	5.4 ±0.4
	2	9.1 ±1.3	74.4 ±2.7	16.5 ±1.7
	1,2,3	41.9 ±0.3	48.7 ±0.8	9.4 ±1.0
5 hours	1,3	64.0 ±0.4	30.7 ±0.2	5.4 ±0.6
	2	11.4 ±1.2	72.0 ±0.4	16.6 ±0.8
	1,2,3	45.4 ±0.5	45.3 ±0.1	9.3 ±0.6
10 hours	1,3	62.4 ±0.6	32.4 ±0.5	5.1 ±0.2
	2	26.2 ±0.3	59.4 ±0.7	14.4 ±1.1
	1,2,3	50.3 ±0.5	41.4 ±0.7	8.2 ±0.4
15 hours	1,3	60.8 ±0.3	32.5 ±0.2	6.8 ±0.4
	2	32.5 ±1.2	57.4 ±0.9	10.1 ±0.3
	1,2,3	50.7 ±0.4	41.3 ±0.1	7.9 ±0.4
20 hours	1,3	55.9 ±0.3	39.4 ±1.1	4.7 ±1.4
	2	37.1 ±1.3	52.4 ±0.9	10.5 ±2.0
	1,2,3	49.6 ±0.6	43.8 ±0.9	6.6 ±1.6
24 hours	1,3	55.1 ±0.5	39.0 ±0.4	5.9 ±0.9
	2	45.8 ±0.4	44.1 ±1.2	10.2 ±0.8
	1,2,3	52.0 ±0.4	40.7 ±0.1	7.3 ±0.3

Notes:
ND, not detected. Values are mean of three replicates ± standard deviation.

Table 4.9 : Regiospecific data of the starting material (high-oleic sunflower oil) and the interesterification reaction intermediates catalysed by Lipozyme TL IM with ethyl behenate

Duration	Composition (mol%)			
	sn-position	Saturated	Monounsaturated	Polyunsaturated
High-oleic sunflower oil	1,3	11.6 ±0.3	76.5 ±0.2	11.9 ±0.5
	2	ND	86.5 ±0.4	13.5 ±0.7
	1,2,3	7.8 ±0.3	79.8 ±0.3	12.4 ±0.7
0.5 hours	1,3	43.3 ±1.3	45.9 ±1.7	10.8 ±0.5
	2	6.1 ±0.3	74.0 ±0.4	19.9 ±0.2
	1,2,3	29.9 ±0.7	56.0 ±0.8	14.1 ±0.3
1 hour	1,3	53.6 ±0.8	39.5 ±0.4	6.9 ±0.6
	2	10.0 ±0.3	78.8 ±0.4	11.2 ±0.3
	1,2,3	39.5 ±0.2	52.2 ±0.3	8.3 ±0.3
2 hours	1,3	58.6 ±1.0	34.3 ±1.7	7.1 ±2.2
	2	24.7 ±0.5	65.4 ±1.7	9.9 ±1.8
	1,2,3	46.8 ±0.6	45.1 ±1.3	8.1 ±1.9
3 hours	1,3	61.5 ±1.7	35.3 ±0.9	3.2 ±1.6
	2	26.7 ±0.7	64.4 ±0.1	8.9 ±0.6
	1,2,3	49.9 ±1.3	45.0 ±0.7	5.1 ±1.3
5 hours	1,3	60.2 ±0.2	35.6 ±0.2	4.2 ±0.0
	2	39.8 ±0.0	53.4 ±0.0	6.8 ±0.0
	1,2,3	52.0 ±0.4	40.3 ±0.2	7.7 ±0.2
10 hours	1,3	59.4 ±0.0	37.7 ±0.0	2.9 ±0.0
	2	50.4 ±1.0	42.8 ±0.9	6.8 ±1.9
	1,2,3	56.2 ±0.4	39.5 ±0.3	4.3 ±0.7
15 hours	1,3	56.9 ±1.5	37.0 ±0.3	6.1 ±1.8
	2	53.7 ±2.0	40.0 ±0.0	6.4 ±1.9
	1,2,3	55.8 ±1.7	38.0 ±0.2	6.2 ±1.8
20 hours	1,3	50.9 ±1.3	41.4 ±0.7	7.8 ±0.7
	2	55.9 ±0.3	37.2 ±0.2	6.9 ±0.4
	1,2,3	52.5 ±0.8	40.0 ±0.4	7.5 ±0.5
24 hours	1,3	53.4 ±0.9	40.5 ±0.7	6.2 ±0.7
	2	58.7 ±1.1	33.5 ±2.0	7.9 ±1.9
	1,2,3	55.0 ±0.4	38.2 ±0.7	6.7 ±1.1

Notes:
ND, not detected. Values are mean of three replicates ± standard deviation.

As a consequence of the incorporation of saturated behenic acid into glycerol moiety, the total SFA contents increased readily over the entire experimental duration. Specifically to the *sn*-1,3 positions of triacylglycerols, SFA compositions reached the maximum after 3 and 5 hours of interesterification under catalytic actions of Lipozyme TL IM (61.5 mol%) and Lipozyme RM IM (64.0 mol%), respectively (Figure 4.12).

The drop thereafter indicated that the randomisation had surpassed the ideal 1,3-specific interesterification reaction. The key reason behind the shifting of the types of reaction might due to the occurrence of acyl migration.

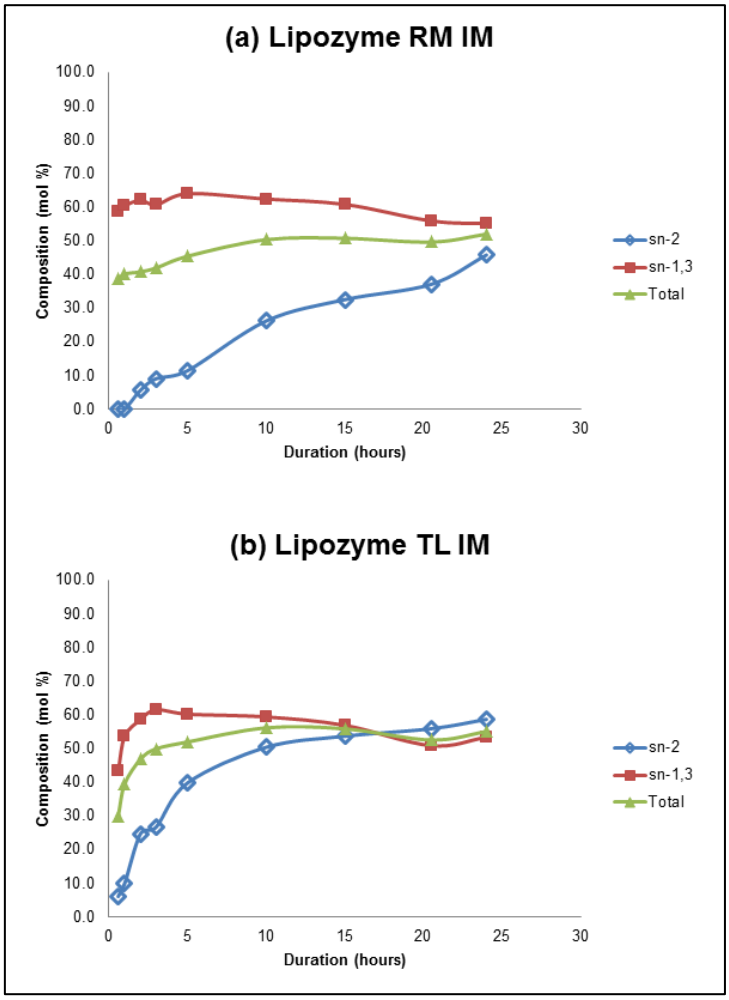

Notes:
Lipozyme RM IM, immobilised lipases from the strain of *Rhizomucor miehei*
Lipozyme TL IM, immobilised lipases from the strain of *Thermomyces lanuginose*

Figure 4.12 : Kinetics of the enzymatic interesterification between high-oleic sunflower oil and ethyl behenate catalysed by (a) Lipozyme RM IM (b) Lipozyme TL IM, measured by the positional distribution of saturated fatty acids (SFA) in triacylglycerol

Under the action of the 1,3-specific enzyme, the acyl chain at the middle position of triacylglycerol was postulated to migrate to the outer positions by virtue of the relatively higher stability of the secondary hydroxyl group compared with the primary kinds.

Consequently, this was followed by the incorporation of saturated behenic acid into the *sn*-2 position. Nevertheless, the build-up of saturation levels at the *sn*-2 position of triacylglycerol in high-oleic sunflower oil-based structured lipids was relatively slower than those based on palm olein IV 56 (Figure 4.1, Section 4.2.2.1). Generally speaking, fatty acid compositions at the different stereospecific positions seemed to converge as a function of time (Figure 4.12).

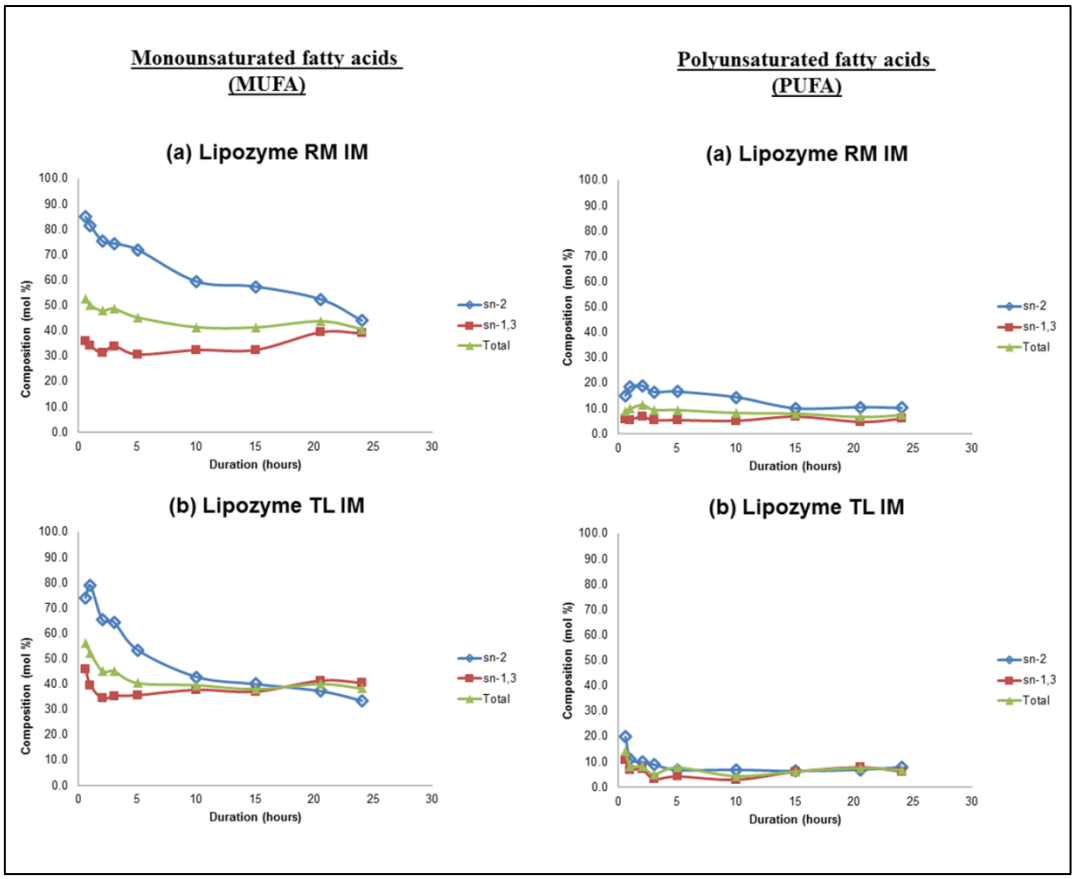

Notes:
Lipozyme RM IM, immobilised lipases from the strain of *Rhizomucor miehei*
Lipozyme TL IM, immobilised lipases from the strain of *Thermomyces lanuginose*

Figure 4.13 : Kinetics of the enzymatic interesterification between high-oleic sunflower oil and ethyl behenate catalysed by (a) Lipozyme RM IM (b) Lipozyme TL IM, measured by the positional distribution of mono- (MUFA) and polyunsaturated fatty acids (PUFA) in triacylglycerol

By comparing the differential effects of both enzymes, Lipozyme TL IM was observed to be less regiospecific than Lipozyme RM IM. After 15 hours of reaction catalysed by Lipozyme TL IM, the SFA content at the *sn*-2 position was elevated at a higher extent than those reside at the *sn*-1,3 positions. Conversely, reaction products with Lipozyme RM IM were still exhibiting greater SFA compositions at the *sn*-1,3 positions compared with the inner position over duration of 24 hours, despite the converging pattern of the fatty acid composition at all three *sn*-positions.

Apart from the SFA composition, Figure 4.13 depicts the variation of positional MUFA and PUFA contents as a function of time under the actions of Lipozyme RM IM and Lipozyme TL IM. Similar to the trends observed in Figure 4.12, the variation of MUFA was following the SFA composition in the reserve order. In an ideal 1,3-specific interesterification, the fatty acid composition at the *sn*-2 position should be conserved or altered at a minimum level. However, the current MUFA contents at the *sn*-2 position, mainly consist of the oleic acid, were depreciated greatly over the time. Meanwhile, the PUFA, which is the minority, did not experience significant changes in composition throughout the whole experimental duration. In conclusion, different structured lipids could be produced by varying the reaction time, *i.e.* products originating from the 1,3-specific interesterification, as well as the partially or completely randomised products, as suggested in the published work by Svensson and Adlercreutz (2011).

4.3.2.2 Triacylglycerol Composition

Triacylglycerol molecular species of the structured lipids were identified using the similar approach as described in Section 4.2.2.2. The molecular structures of the triacylglycerol species present in high-oleic sunflower oil and its interesterified products catalysed by the immobilised lipases from the strain of *Rhizomucor miehei* (Lipozyme

RM IM) and *Thermomyces lanuginose* (Lipozyme TL IM) are given in Table 4.10 and Table 4.11, respectively.

Table 4.10 : Triacylglycerol compositions of the starting material (high-oleic sunflower oil) and the interesterification reaction intermediates catalysed by Lipozyme RM IM with ethyl behenate

Molecular species	Composition (% of total triacylglycerols)									High-oleic sunflower oil
	0.5 hours	1 hour	2 hours	3 hours	5 hours	10 hours	15 hours	20 hours	24 hours	
LLL	ND	ND	ND	ND	ND	ND	ND	ND	ND	0.5
OLL	ND	ND	ND	ND	ND	ND	ND	ND	ND	0.7
OOL	2.3	2.1	2.0	2.6	3.1	1.8	2.8	2.0	2.4	1.8
OOO	12.9	9.6	8.3	8.9	6.9	6.3	6.7	6.8	5.0	90.0
POO	3.6	2.6	2.4	2.6	3.3	3.4	3.1	3.1	3.2	4.7
POP	ND	ND	ND	ND	ND	ND	ND	ND	ND	2.0
StOSt	ND	ND	ND	ND	ND	ND	ND	ND	ND	0.3
BLO	3.4	3.8	4.2	4.5	3.6	3.5	4.6	4.0	3.8	ND
BLP	1.6	1.2	1.2	1.5	0.7	1.2	1.7	1.5	2.1	ND
BOO	45.8	45.8	46.0	42.4	42.9	40.0	34.0	34.4	33.9	ND
BOP	2.7	1.6	1.6	1.7	1.0	1.5	1.7	2.0	2.3	ND
BOSt	1.5	1.3	1.3	1.9	1.8	1.5	2.1	1.6	2.3	ND
BLB	2.6	2.9	2.5	2.8	3.4	2.6	3.3	3.1	3.6	ND
BOB	23.6	29.1	30.4	31.3	31.6	32.2	33.3	33.5	32.7	ND
BBP	ND	ND	ND	ND	ND	2.2	1.4	1.3	1.8	ND
BBB	ND	ND	ND	ND	1.6	3.9	5.3	6.7	7.0	ND

Notes:
ND, not detected; P, palmitic; St, stearic; O, oleic; L, linoleic; B, behenic.

The enzyme catalysed interesterification between high-oleic sunflower oil and ethyl behenate produced a complex mixture of triacylglycerol molecular species. Some of the triacylglycerols were species that were absent in the precursor starting materials. The most prominent triacylglycerol species that had been built-up during the course of reaction were 1-behenoyl-2,3-dioleoylglycerol (BOO) and 1,3-dibehenoyl-2-oleoylglycerol (BOB). Under the action of Lipozyme RM IM, the composition of BOO

and BOB fell in the range of 33.9% - 45.8% and 23.6% - 33.5%, respectively (Table 4.10). Meanwhile, Lipozyme TL IM produced 31.2% - 45.3% of BOO and 12.7% - 35.5% of BOB in various reaction products (Table 4.11) at the expense of trioleoylglycerol (OOO).

Accompanying with the targeted structured triacylglycerol species, the undesirable fully saturated species, namely tribehenoylglycerol (BBB) and 1,2-dibehenoyl-3-palmitoylglycerol (BBP) were also being introduced during the interesterification. The aforementioned species were produced after two-hour reaction under Lipozyme TL IM (Table 4.11), while the similar contents were only developed gradually after 5 hours of reaction catalysed by Lipozyme RM IM (Table 4.10). Hence, Lipozyme RM IM was again appearing to be more regiospecific than Lipozyme TL IM, that is, the forming of the co-products in the former was relatively slower than the latter. This is parallel with the discussion on the triacylglycerol compositions of palm olein-based structured lipids produced under both enzymes (Section 4.2.2.3). Furthermore, the polyunsaturated species, namely trilinoleoylglycerol (LLL) and 1,2-dilinoleoyl-3-oleoylglycerol (OLL), as well as the symmetrical triacylglycerols, for instance 1,3-dipalmitoyl-2-oleoylglycerol (POP) and 1,3-distearoyl-2-oleoylglycerol (StOSt), were diminished after the enzymatic interesterification.

Similar to Section 4.2.2.3, all molecular species are classified into three categories, *viz.* the targeted structured lipids, co-products and reactant triacylglycerols. Owing to the specificity of the enzymes, the targeted products will be referred to those with the behenic acid being incorporated at the *sn*-1,3 positions, as well as the middle position remained unaltered. Therefore, the BOB and BOO were accounted for the chief constituents. On the other hand, the reactant triacylglycerols are defined as the

triacylglycerol species which are natively attainable in high-oleic sunflower oil and mainly consisted of OOO (90.0% of total triacylglycerols, Table 4.10), while the co-products are referred to the fully saturated species. The evolution of these molecular species is tabulated in Table 4.12 and successively illustrated in Figure 4.14 for those obtained under action of Lipozyme RM IM.

Table 4.11 : Triacylglycerol compositions of the starting material (high-oleic sunflower oil) and the interesterification reaction intermediates catalysed by Lipozyme TL IM with ethyl behenate

Molecular species	Composition (% of total triacylglycerols)									High-oleic sunflower oil
	0.5 hours	1 hour	2 hours	3 hours	5 hours	10 hours	15 hours	20 hours	24 hours	
LLL	ND	ND	ND	ND	ND	ND	ND	ND	ND	0.5
OLL	ND	ND	ND	ND	ND	ND	ND	ND	ND	0.7
OOL	4.8	3.2	2.6	3.4	2.8	2.1	2.1	2.4	2.2	1.8
OOO	28.8	15.7	8.7	6.6	5.9	5.3	4.8	4.0	4.6	90.0
POO	4.1	3.1	4.4	4.5	4.5	4.4	4.5	5.6	4.7	4.7
POP	ND	ND	ND	ND	ND	ND	ND	ND	ND	2.0
StOSt	ND	ND	ND	ND	ND	ND	ND	ND	ND	0.3
BLO	3.7	4.7	4.5	4.0	3.8	3.6	3.2	3.5	3.8	ND
BLP	1.4	2.2	1.2	1.0	1.6	1.5	0.9	1.4	1.2	ND
BOO	41.2	45.3	42.5	35.6	33.0	32.5	31.2	31.8	32.1	ND
BOP	1.2	2.4	1.9	1.3	1.3	2.0	1.8	1.6	2.0	ND
BOSt	0.7	0.8	1.4	2.0	1.6	2.1	1.9	1.9	1.8	ND
BLB	1.3	2.1	2.4	3.6	3.2	3.0	3.5	3.6	3.2	ND
BOB	12.7	20.6	27.4	29.9	32.4	33.1	34.4	35.1	35.5	ND
BBP	ND	ND	ND	2.2	1.5	1.8	2.4	1.8	1.1	ND
BBB	ND	ND	2.9	5.7	8.4	8.5	9.2	7.5	7.9	ND

Notes:
ND, not detected; P, palmitic; St, stearic; O, oleic; L, linoleic; B, behenic.

Table 4.12 : Evolution of targeted structured lipids, co-products and reactant triacylglycerols as a function of time in interesterification of high-oleic sunflower oil catalysed by Lipozyme RM IM

Duration (hours)	Compositions (% of total triacylglycerols)				Ratio of Targeted SL / reactant	Ratio of Targeted SL / co-product
	Targeted SL	BOB + BOO	Co-Product	Reactant		
0.5	81.3	69.4	ND	18.7	4.35	NA
1	85.8	74.9	ND	14.2	6.02	NA
2	87.3	76.9	ND	12.7	6.86	NA
3	86.0	73.7	ND	14.0	6.14	NA
5	85.1	74.5	1.6	13.3	6.41	51.94
10	82.4	72.1	6.1	11.5	7.19	13.44
15	80.7	67.3	6.7	12.5	6.45	11.99
20	80.1	67.9	8.0	11.9	6.73	10.06
24	80.7	66.6	8.7	10.6	7.59	9.25

Notes:
Targeted SL = Targeted structured lipids (sum of the compositions of BLO, BLP, BOO, BOP, BOS, BLB and BOB); BOB + BOO = the compositions of major targeted structured triacylglycerol species; co-product = sum of the compositions of BBP, BBS and BBB; reactant = the compositions of triacylglycerol species present in the base oil; ND, not detected; NA, not applicable.

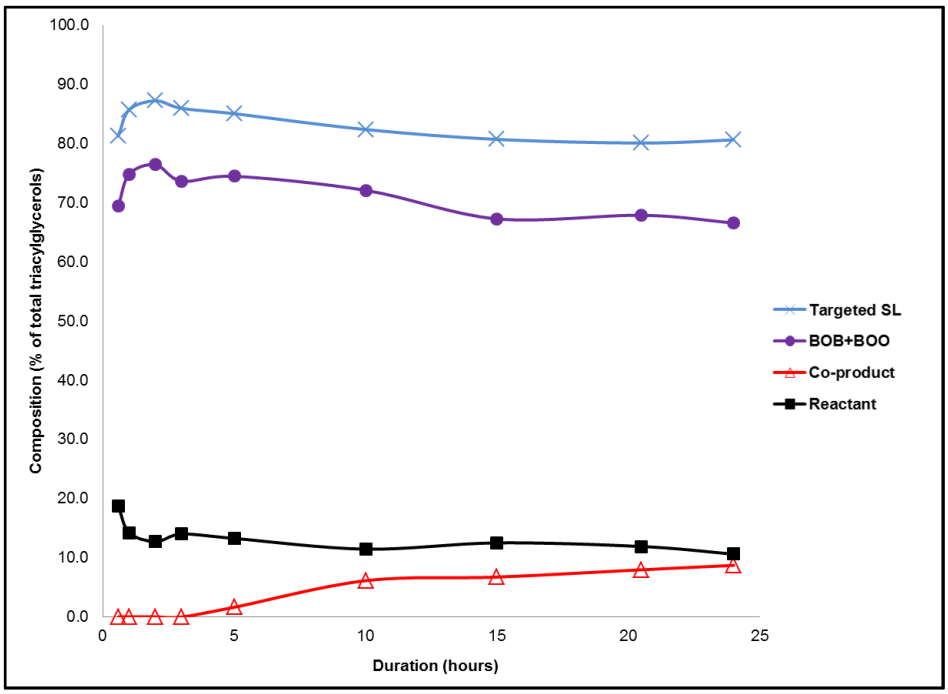

Notes:
SL, structured lipids; B, behenic acid; O, oleic acid.

Figure 4.14 : Interesterification reaction between high-oleic sunflower oil and ethyl behenate catalysed by Lipozyme RM IM

As can be observed in Table 4.12, the ideal triacylglycerol species constituted more than 80% of total triacylglycerols in all intermediates, and with the principal constituents, namely BOB and BOO accounted for 67.3 - 76.9% of total triacylglycerols. These reflected a promising yield achieved in the current synthesis of structured triacylglycerols for obesity alleviation, with the highest yield was being found in the 2-hour reaction product. The total amount of the targeted species was about 87.3% of total triacylglycerols (Table 4.12). Apart from that, another encouraging observation would be the evolution of the undesirable fully saturated species during the course of the reaction. The amounts of these co-products were only detectable after 5 hours of enzymatic interesterification. These remained as an additional benefit as those fully saturated triacylglycerol species may jeopardise the nutritional attributes of the structured lipids. As a whole, there were no remarkable changes in all triacylglycerol categories throughout the 24 hours of enzymatic interesterification (Figure 4.14).

By definition, the ratio of targeted structured lipids to reactants illustrates the evolution of native triacylglycerols to the desired products. This ratio did not experience significant variations after 1 hour of interesterification (Table 4.12), suggesting that the Lipozyme RM IM was efficient in catalysing the reaction under current conditions. On the other hand, the ratio of targeted structured lipids to co-products describes the progression of the unfavourable trisaturated species during the course of reaction. As the reaction performed from 5 hours to 24 hours, the aforementioned ratio decreased with time (Table 4.12). The proposed randomisation of the fatty acids was taken place which corresponded with an increase in the co-product compositions at the expense of preferred BOB and BOO. The interesterification reaction scheme for the production of major products (BOB and BOO) from the predominant triacylglycerol species in high-oleic sunflower oil, namely OOO, and ethyl behenate is shown in Figure 4.15.

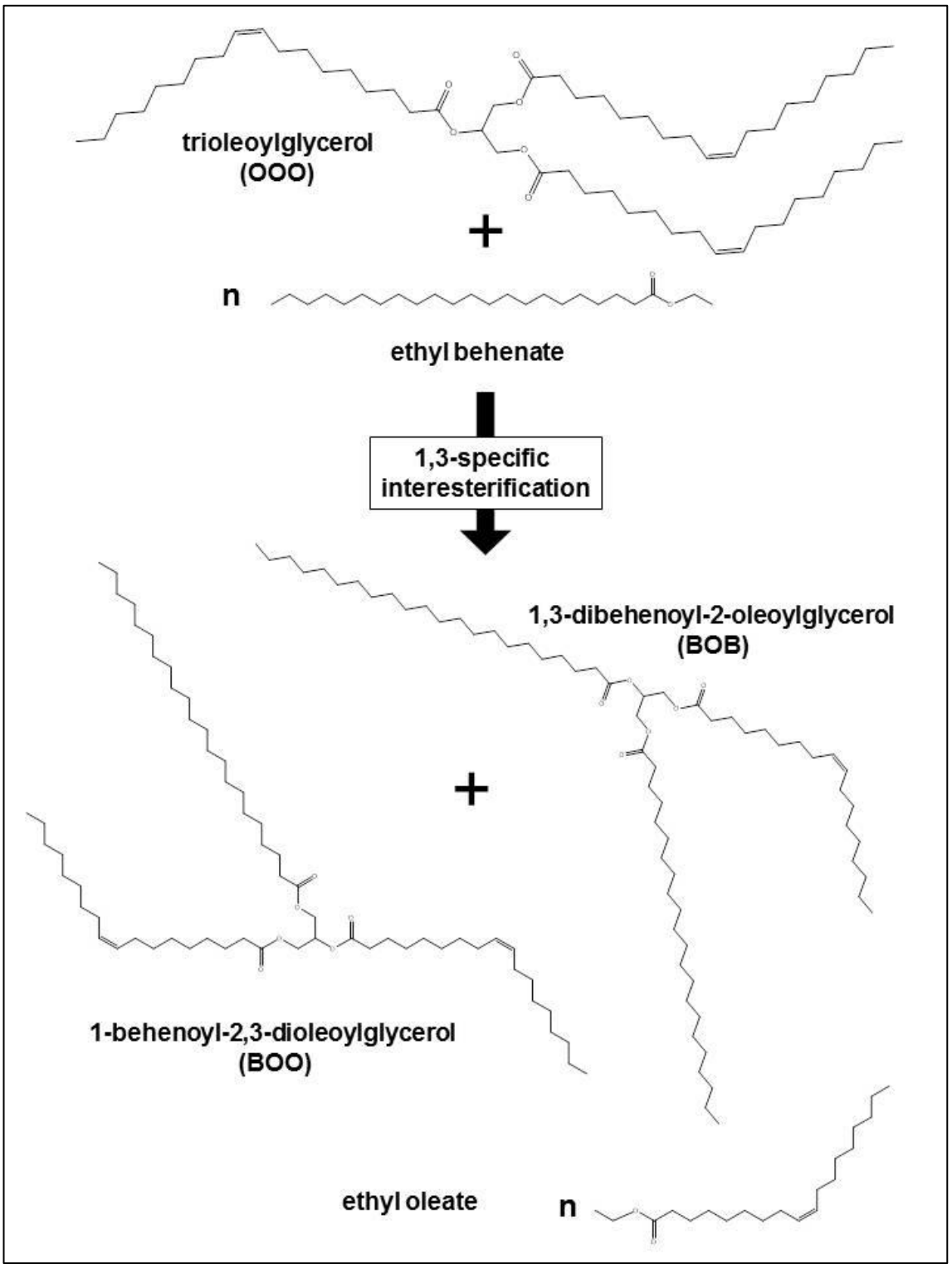

Figure 4.15 : Enzymatic interesterification reaction scheme between ethyl behenate and trioleoylglycerol (OOO) in high-oleic sunflower oil

Table 4.13 : Evolution of targeted structured lipids, co-products and reactant triacylglycerols as a function of time in interesterification of high-oleic sunflower oil catalysed by Lipozyme TL IM

Duration (hours)	Compositions (% of total				Ratio of Targeted SL / reactant	Ratio of Targeted SL / co-product
	Targeted SL	BOB + BOO	Co-Product	Reactant		
0.5	62.4	54.0	ND	37.6	1.66	NA
1	78.0	65.9	ND	22.0	3.55	NA
2	81.4	69.9	2.9	15.7	5.18	28.32
3	77.4	65.5	7.9	14.6	5.30	9.74
5	76.9	65.4	9.9	13.2	5.85	7.77
10	77.8	65.6	10.3	11.9	6.56	7.52
15	76.9	65.6	11.7	11.4	6.74	6.59
20	78.8	66.9	9.2	11.9	6.60	8.55
24	79.5	67.6	9.0	11.5	6.93	8.87

Notes:
Targeted SL = Targeted structured lipids (sum of the compositions of BLO, BLP, BOO, BOP, BOS, BLB and BOB); BOB + BOO = the compositions of major targeted structured triacylglycerol species; co-product = sum of the compositions of BBP, BBS and BBB; reactant = the compositions of triacylglycerol species present in the base oil; ND, not detected; NA, not applicable.

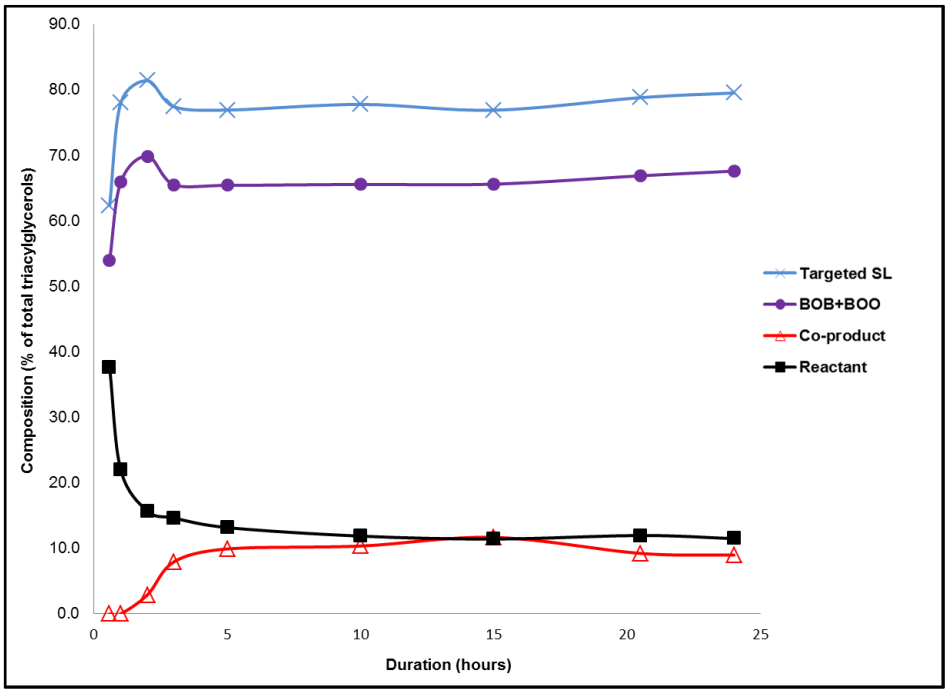

Notes:
SL, structured lipids; B, behenic acid; O, oleic acid.

Figure 4.16 : Interesterification reaction between high-oleic sunflower oil and ethyl behenate catalysed by Lipozyme TL IM

For the reaction catalysed by Lipozyme TL IM, the evolution of the above-mentioned categories is given in Table 4.13 and successively illustrated in Figure 4.16. The composition of the ideal triacylglycerol species produced by Lipozyme TL IM fell in the range of 62.4 - 81.4% (Table 4.13), which remained significantly lower than those obtained with Lipozyme RM (Table 4.12). Similar observations were noted for the major constituents, namely BOB and BOO which accounted for 54.0% - 69.9% of total triacylglycerols in the various reaction intermediates produced by Lipozyme TL IM (Table 4.13). Henceforth, Lipozyme RM IM was again being proven its relatively higher specificity towards *sn*-1,3 positions compared with Lipozyme TL IM under current reaction conditions.

Apart from being higher specificity, Lipozyme RM IM exhibited greater efficiency in catalysing the enzymatic interesterification than Lipozyme TL IM. This could be seen in the relative compositions of the remaining reactant triacylglycerol species after 30 minutes of reaction, which showed the values of 37.6% (Table 4.13) and 18.7% (Table 4.12) for Lipozyme TL IM and Lipozyme RM IM, respectively. Besides, the unfavourable trisaturated species were starting to evolve after 2 hours of reaction catalysed by Lipozyme TL IM (Table 4.13). In general, Figure 4.16 demonstrates the insignificant variations for all the categories after 5 hours of interesterification, suggesting a near-equilibrium state was achieved.

By observing the ratio of targeted to reactant triacylglycerol species, a progressively increment with time was noted (Table 4.13). Nonetheless, prolonged interesterification would lead to the boost of significant amounts of undesirable trisaturated species by virtue of the occurrence of acyl migration. As a consequence, a compromise is achieved

during the selection of the most ideal structured lipids for obesity alleviation among all reaction intermediates.

4.4 Purification and Characterisation of Structured Lipids for Obesity Alleviation

4.4.1 Experimental

4.4.1.1 Purification and Isolation of Structured Triacylglycerols

Silicic acid column chromatography is employed to isolate and purify the structured triacylglycerols from unreacted ethyl behenate, free fatty acids and other partial acylglycerols. 2.5 g of the reaction products was subjected to open column separation using silica gel G (50 g, Kieselgel 60-200 mesh, Merck Art. No 7731, Darmstadt, Germany). Solvent system of 1% ethyl acetate in hexane was used to elute ethyl behenate, while 5% ethyl acetate for the elution of structured triacylglycerols. The elution was monitored using silica gel G thin layer chromatography plate (Kieselgel 60, Merck, Darmstadt, Germany) and developed in 5% ethyl acetate in hexane. The retention factor for ethyl behenate was 0.57, while for the triacylglycerols was 0.32. The unreacted free fatty acids and other partial acylglycerols remained undeveloped. Fractions containing triacylglycerols as the sole component were combined. The purification steps were repeated to accumulate sufficient amount of purified structured lipids for further analysis.

4.4.1.2 Determination of Acidity and Iodine Values

Free acidity and iodine value (IV) were determined using American Oil Chemists' Society (AOCS) official methods Ca 5a-40 and Ja 14-91, respectively.

4.4.1.3 Gas Chromatography (GC)

Total fatty acid composition (FAC) was determined using gas chromatography (GC). The purified structured lipids were derivatised to fatty acid methyl esters by sodium methoxide-catalysed transesterification (Christie, 1989). The GC protocol was the same as described in Section 2.4.1.4 (Chapter 2).

4.4.1.4 Differential Scanning Calorimetry (DSC)

Thermal properties of structured lipids were determined by a Mettler Toledo differential scanning calorimetry (DSC) Model DSC823e (Greifensee, Switzerland). A lipid sample of 4-5 mg was hermetically sealed in an aluminium pan, with an empty pan serving as a reference. Analysis was performed according to the American Oil Chemists' Society (AOCS) official DSC method Cj 1-94 (MC-CJ194). The sample was first heated rapidly (200 ℃/minute) from 25 ℃ to 80 ℃ and held at this temperature for 10 minutes to destroy crystallisation history. Then, the sample was cooled to -40 ℃ at 10 ℃/minute and kept isothermally for 30 minutes. Melting profiles of structured lipids were recorded from -40 ℃ to 80 ℃ at a heating rate of 5 ℃/minute. Normal standardisation of the instrument was performed with *n*-decane (melting point = -30 ℃) and indium (melting point = 176 ℃) as reference standards. Liquid nitrogen was used as the coolant.

4.4.2 Results and Discussion

4.4.2.1 Selection of Ideal Structured Lipids

It is predominantly essential to keep the degree of saturation at the *sn*-2 position of triacylglycerol at a minimum level, as the dietary fats with high saturation at the aforementioned position has shown to be atherogenic and cholesterolemic (Kritchevsky *et al.*, 1982; Renaud *et al.*, 1995; Berry, 2009). Commercially available palm olein iodine value (IV) 56 which contains 7.4 mol% saturated content at the *sn*-2 position

(Table 4.1, Section 4.2.2.1) is reported to give similar nutritional attributes as compared with highly unsaturated vegetable oils, namely, olive oil (Ng *et al.*, 1992; Choudhury *et al.*, 1995) and canola oil (Sundram *et al.*, 1995). Moreover, there are 24.5% of palmitic and 2.5% of stearic acids found at the middle position of triacylglycerols in crude palm oil (Gunstone and Harwood, 2007). Therefore, we postulate that the saturation levels of 10.0 - 15.0 mol% at the *sn*-2 position may not exert significant detrimental effects on human health.

Current justification on the ideal products among all interesterified intermediates is based on the saturation level at the *sn*-2 position, as well as the composition of targeted structured triacylglycerol species. Among all structured lipids produced from the palm olein IV 56 by Lipozyme RM IM, the amount of the targeted triacylglycerol species, *i.e.* incorporation of behenic acid at the *sn*-1,3 positions of triacylglycerol, reached the maximum after 1 hour of reaction (Figure 4.6, Section 4.2.2.3). Nevertheless, saturation level at the *sn*-2 position of the above-mentioned intermediate was 17.3 mol% (Table 4.1, Section 4.2.2.1). A compromise between the saturation level at the *sn*-2 position and the amount of targeted structured lipids must be reached. Consequently, the reaction product after 0.5 hours of interesterification catalysed by Lipozyme RM IM (12.0 mol% saturation at the *sn*-2 position) is chosen as the ideal product from the whole batch. A similar phenomenon was observed for the structured triacylglycerols produced from palm olein IV 56 and high-oleic sunflower oil with Lipozyme TL IM, in which the selected structured lipids are the 0.5-hour and 1-hour reaction products, respectively.

On the other hand, the highest amount of desired structured triacylglycerols in concomitant with the negligible co-products was found at 2-hour reaction intermediate produced from the high-oleic sunflower oil using Lipozyme RM IM (Figure 4.13,

Section 4.3.2.2). It was noteworthy that its saturation level at the *sn*-2 position of triacylglycerol was only 5.6 mol% (Table 4.8, Section 4.3.2.1). Therefore, from the standpoints of both nutrition and reaction kinetics, this is the ideal structured lipid produced from the Lipozyme RM IM-catalysed interesterification between high-oleic sunflower oil and ethyl behenate.

In order to avoid confusion, PO_RM is thereafter denotes as the selected structured lipid produced from palm olein IV 56 under the action of Lipozyme RM IM, whereas HS_RM represents the selected structured lipid produced from high-oleic sunflower oil. The similar form of nomenclature is also applied for PO_TL and HS_TL structured lipids. The triacylglycerol composition and regiospecific data of the four selected structured lipids are presented in Table 4.14 and Table 4.15, respectively.

Table 4.14 : Triacylglycerol compositions of the selected structured lipids from different batches

Triacylglycerol Species	Composition (% of total triacylglycerols)			
	PO_RM (0.5 hours)	PO_TL (0.5 hours)	HS_RM (2 hours)	HS_TL (1 hour)
Targeted structured triacylglycerol	67.4	50.8	87.3	78.0
BOB + BOO	45.5	32.4	76.4	65.9
Co-product	2.4	2.2	ND	ND
Reactant	30.2	47.0	12.7	22.0

Notes:
Targeted structured triacylglycerol = sum of the compositions of BLO, BLP, BOO, BOP, BOS, BLB and BOB; BOB + BOO = the compositions of major targeted structured triacylglycerol species; co-product = sum of the compositions of BBP, BBS and BBB; reactant = the compositions of triacylglycerol species present in the base oil; ND, not detected.

Under the reaction conditions applied in the current study, the structured lipids which were produced from high-oleic sunflower oil (HS_RM and HS_TL), were having significantly higher amount of targeted triacylglycerol species compared to those produced from palm olein IV 56 (Table 4.14). On top of that, the absence of co-product

signified an additional advantage for the structured lipids based on high-oleic sunflower oil. Under prolonged reaction in the synthesis of HS_RM (2 hours) and HS_TL (1 hour) compared with those based on palm olein IV 56 (0.5 hours), the amounts of reactant triacylglycerols were depreciated more readily in the former.

Table 4.15 : Regiospecific data of the selected structured lipids

Duration	Composition (mol%)			
	sn-position	Saturated	Monounsaturated	Polyunsaturated
PO_RM (0.5 hours)	1,3	83.1 ± 0.6	13.3 ± 0.5	3.6 ± 0.1
	2	12.0 ± 0.1	62.8 ± 0.2	25.2 ± 0.3
	1,2,3	57.8 ± 1.1	30.9 ± 0.9	11.3 ± 0.2
PO_TL (0.5 hours)	1,3	75.0 ± 0.4	18.7 ± 0.7	6.3 ± 0.4
	2	15.7 ± 0.8	58.7 ± 2.9	25.6 ± 3.6
	1,2,3	55.4 ± 0.8	31.9 ± 1.0	12.7 ± 1.7
HS_RM (2 hours)	1,3	62.1 ± 0.1	31.2 ± 0.4	6.8 ± 0.5
	2	5.6 ± 0.1	75.4 ± 0.4	19.0 ± 0.5
	1,2,3	40.8 ± 0.1	47.9 ± 0.4	11.4 ± 0.2
HS_TL (1 hour)	1,3	54.3 ± 0.8	39.5 ± 0.4	6.3 ± 0.6
	2	9.7 ± 0.3	78.9 ± 0.4	11.4 ± 0.3
	1,2,3	39.4 ± 0.2	52.6 ± 0.3	8.0 ± 0.3

Notes:
Values are mean of three replicates ± standard deviation.

In the context of positional fatty acids within the glycerol moiety, HS_RM and HS_TL were having saturation levels of 5.6 mol% and 9.7 mol% at the *sn*-2 position, respectively (Table 4.15). These were significantly lower compared to PO_RM and PO_TL (12.0 mol% and 15.7 mol%, respectively). Nonetheless, due to the presence of native triacylglycerols in palm olein IV 56, PO_RM and PO_TL exhibited significantly greater amount of saturated fatty acids (SFA) at the *sn*-1,3 positions of triacylglycerol compared to those produced from high-oleic sunflower oil (Table 4.15). This is one of the essential criteria for obesity alleviation.

4.4.2.2 Acidity and Iodine Values

The physicochemical properties of the starting materials (palm olein and high-oleic sunflower oil) and the selected structured lipids are summarised in Table 4.16. The acidity for the structured lipids was analysed only after purification by column chromatography, as described in Section 4.4.1.1. In general, low free acidity (0.56 - 0.61 mg KOH/g oil, Table 4.16) was observed for all structured lipids after purification, which fell within the limit established by Codex Alimentarius (2011) stating the maximum level of 0.6 mg KOH/g oil for refined oils. This is critical as highly acidic oils exert deleterious effects on humans.

Table 4.16 : Physicochemical properties of the starting materials and the selected structured lipids

Sample	Acidity (mg KOH/g oil)	Iodine values (g iodine/100 g oil)
Palm olein (base oil)	0.38 ± 0.02	56.8 ± 0.6
PO_RM	0.56 ± 0.02	42.5 ± 0.3
PO_TL	0.61 ± 0.01	45.8 ± 0.5
High-oleic sunflower oil (base oil)	0.26 ± 0.01	94.1 ± 0.8
HS_RM	0.58 ± 0.02	53.6 ± 0.4
HS_TL	0.56 ± 0.02	55.9 ± 0.3

Notes:
Values are mean of three replicates ± standard deviation. PO_RM and PO_TL, structured lipids produced from palm olein IV 56 under action of Lipozyme RM IM and Lipozyme TL IM, respectively; HS_RM and HS_TL, structured lipids produced from high-oleic sunflower oil under action of Lipozyme RM IM and Lipozyme TL IM, respectively.

Iodine value (IV) is a measure of the degree of unsaturation in oils and fats. By definition, high IV oil contains a greater number of double bonds in its fatty acid chains than the low IV oil. As expected, high-oleic sunflower oil exhibited the highest IV (94.1 g iodine/100 g oil) among all the samples (Table 4.16) as it contained high amount of oleic acid (83.15 % of total fatty acids, Table 4.18, Section 4.2.2.3). The incorporation of behenic acid was associated with a decrement of IV in the resultant structured lipids.

Palm olein-based structured lipids exhibited a 19.4 - 25.2 % of IV decrement, while those produced from high-oleic sunflower oil was 53.6 - 55.9 % (Table 4.16). On the other hand, structured lipids produced using Lipozyme RM IM were showing lower IV than those produced from Lipozyme TL IM. This is owing to the better and faster incorporation of behenic acid as a result of the relatively higher efficiency of the former in catalysing 1,3-specific interesterification.

4.4.2.3 Total Fatty Acid Composition

Total fatty acid composition (FAC) of the selected structured lipids produced from palm olein IV 56 is listed in Table 4.17. The most abundant fatty acid in PO_RM structured lipid was behenic acid (36.52% of total fatty acids) whereas for PO_TL was the oleic acid (34.61% of total fatty acids). Within 0.5 hours of interesterification, Lipozyme RM IM introduced significantly higher amount of behenic acid into the glycerol moiety compared to Lipozyme TL IM. Therefore, the former was claimed to be more efficient in catalysing the enzymatic interesterification. Moreover, the incorporation of saturated behenic acid was also reflected in the concomitant increase of the total saturation levels for both structured lipids (63.71 and 58.71% of total fatty acids), compared to the base oil, namely, palm olein IV 56 (45.70% of total fatty acids). In general, the palm olein based structured lipids were primarily composed of three major fatty acids, namely, palmitic, oleic and behenic acids.

Data given in Table 4.18 refer to the total FAC of high-oleic sunflower oil, as well as the structured lipids synthesised under the actions of the Lipozyme RM IM and Lipozyme TL IM. Owing to the extreme high content of the oleic acid in the base oil (83.15% of total fatty acids), this fatty acid still remained the most abundant in HS_RM and HS_TL structured lipids. In addition, 35.71% of behenic acid was introduced into

high-oleic sunflower triacylglycerols by Lipozyme RM IM. The composition of behenic acid found in HS_TL was relatively lower (30.62% of total fatty acids). The higher efficiency of Lipozyme RM IM was again recognised and it was independent of the types of the base oil. After interesterification, the increment of total saturation was found to be 35.7% and 29.5% in HS_RM and HS_TL structured lipids, respectively. For the sunflower oil based structured lipids, the oleic and behenic acids were the predominant fatty acids and constituted 85% of total fatty acids.

Table 4.17 : Fatty acid composition of palm olein IV 56 and the selected structured lipids produced by Lipozymes RM IM and TL IM

Acyl chain	Composition (% of total fatty acids)		
	Palm olein	PO_RM	PO_TL
12 : 0	0.27	0.13	0.10
14 : 0	0.96	0.47	0.51
16 : 0	39.98	19.97	25.44
18 : 0	4.04	2.57	2.97
20 : 0	0.33	3.55	2.49
22 : 0	0.06	36.52	26.68
24 : 0	0.06	0.51	0.51
Total SFA	45.70	63.71	58.71
16 : 1	0.17	0.06	0.08
18 : 1	43.48	31.00	34.61
20 : 1	0.15	0.05	0.10
22 : 1	ND	0.06	0.24
Total MUFA	43.80	31.17	35.03
18 : 2	10.27	5.00	6.14
18 : 3	0.23	ND	ND
20 : 2	ND	0.06	0.05
22 : 2	ND	0.07	0.07
Total PUFA	10.50	5.12	6.26

Notes:
PO_RM, structured lipid produced from palm olein IV56 under action of Lipozyme RM IM; PO_TL, structured lipid produced from palm olein IV56 under action of Lipozyme TL IM; SFA, saturated fatty acids; MUFA, monounsaturated fatty acids; PUFA, polyunsaturated fatty acids; ND, not detected.

Table 4.18 : Fatty acid composition of high-oleic sunflower oil and the selected structured lipids produced by Lipozymes RM IM and TL IM

Acyl chain	Composition (% of total fatty acids)		
	Sunflower oil	HS_RM	HS_TL
12 : 0	ND	ND	ND
14 : 0	0.04	0.05	0.04
16 : 0	3.78	2.86	2.27
18 : 0	2.92	1.56	1.35
20 : 0	0.25	3.13	3.09
22 : 0	1.21	35.71	30.62
24 : 0	0.25	0.76	0.53
Total SFA	8.44	44.07	37.91
16 : 1	ND	0.12	0.12
18 : 1	83.15	50.15	53.94
20 : 1	0.28	0.15	0.18
22 : 1	ND	0.07	0.31
Total MUFA	83.43	50.78	55.06
18 : 2	8.17	4.99	6.56
18 : 3	ND	ND	ND
20 : 2	ND	0.07	0.31
22 : 2	ND	0.08	0.17
Total PUFA	8.17	5.14	7.04

Notes:
HS_RM, structured lipid produced from high-oleic sunflower oil under action of Lipozyme RM IM; HS_TL, structured lipid produced from high-oleic sunflower oil under action of Lipozyme TL IM; SFA, saturated fatty acids; MUFA, monounsaturated fatty acids; PUFA, polyunsaturated fatty acids; ND, not detected.

4.4.2.4 Thermal Properties

Differential scanning calorimetry (DSC) is the most common thermoanalytical technique in oils and fats. It is being used in the investigation of various heat-related phenomena in materials by monitoring the associated changes in enthalpy. This technique can provide valuable information on melting and crystallisation temperatures as well as heats of fusion and crystallisation (Sessa, 1996), phase behaviour of triacylglycerol mixtures (Rossell, 1967), evaluation of the effect of minor components in the crystallisation behaviour of lipids (Cebula and Smith, 1992) and many more. The basic thermal behaviour of edible fats is characterised by two physical events, namely, melting and crystallisation. Due to the complexity of the recorded thermograms, all melting and crystallisation points are detected at the local maximum or minimum point

of either endotherm or exotherm curve. These transition temperatures for melting and crystallisation curves of starting materials and selected structured lipids are given in Table 4.19.

Table 4.19 : Comparison of the transition temperatures for melting and crystallisation curves of starting materials and selected structured lipids

Curve	Sample	Transition temperature (℃)						
		1	2	3	4	5	6	7
Melting	Palm olein IV 56	2.82	5.99	7.66	9.74	16.17		
	PO_RM	18.83	33.30	41.17	49.19			
	PO_TL	16.68	27.83	31.67	43.01			
	High-oleic sunflower oil	-7.73						
	HS_RM	-15.98	4.42	13.49	21.16	24.82	30.93	38.18
	HS_TL	12.51	22.15	31.15	41.18			
Crystallisation	Palm olein IV 56	-5.76	1.71					
	PO_RM	16.50	30.73	34.30				
	PO_TL	13.82	26.51	33.15				
	High-oleic sunflower oil	-17.88						
	HS_RM	1.33	19.02	23.02	29.22			
	HS_TL	1.31	19.85	25.51	28.53	33.84		

Notes:
PO_RM and PO_TL, structured lipids produced from palm olein IV 56 under action of Lipozyme RM IM and Lipozyme TL IM, respectively; HS_RM and HS_TL, structured lipids produced from high-oleic sunflower oil under action of Lipozyme RM IM and Lipozyme TL IM, respectively.

Figure 4.17 shows the DSC melting curves for the palm olein iodine value (IV) 56 and its selected structured lipids produced by Lipozyme RM IM and Lipozyme TL IM. The melting curve of palm olein IV 56 consisted of a broad endothermic peak made up of various triacylglycerols, ranging from relatively more saturated species, namely, 1,3-dipalmitoyl-2-oleoylglycerol (POP) to highly unsaturated trilinoleoylglycerol (LLL) in the transition temperature range of 2.82 ℃ - 16.17 ℃ (Table 4.19). Figure 4.17 shows

that the melting profile shifted to the higher temperature region in the structured lipid samples owing to the incorporation of saturated behenic acid (literature melting point = 80 ℃) into the glycerol moiety. The melting curve of PO_RM depicted four distinct endothermic peaks which corresponded to the transition temperatures of 18.83 ℃, 33.39 ℃, 41.17 ℃, and 49.19 ℃. The two endothermic peaks at a lower temperature were the major features of the sample. This could be due to the targeted triacylglycerol species, *viz.* 1-behenoyl-2,3-dioleoylglycerol (BOO) and 1,3-dibehenoyl-2-oleoylglycerol (BOB) as the principal constituents in the sample (27.2% and 18.3% of total triacylglycerol, respectively, Table 4.4, Section 4.2.2.3). Conversely, the melting curve for PO_TL shows only two major endothermic regions. The overlapping peaks in the low-temperature region may due to the presence of high composition of the unreacted reactant triacylglycerol species in the sample (40.7% of total triacylglycerols, Table 4.7, Section 4.2.2.3).

The DSC melting curves for the high-oleic sunflower oil and its corresponding structured lipids are illustrated in Figure 4.18. The base oil for the interesterification reaction, high-oleic sunflower oil, showed a single distinct tall endothermic peak at -7.73 ℃ (Table 4.19). This was most likely due to the presence of high content of trioleoylglycerol (OOO) in the sample (90% of total triacylglycerols, Table 4.10, Section 4.3.2.2). During the enzymatic interesterification, the alteration of the triacylglycerol composition exerted concomitant effects on the melting behaviour of the reaction products. A wider melting range was observed in the endotherm of HS_RM (Figure 4.18) illustrated the occurrence of great variety of triacylglycerols at the expense of OOO originated from the precursor starting material. In contrast, HS_TL displayed less complex features on its melting curve compared to that of HS_RM. The former had only three major endothermic regions, in which the medium-temperature region was

apparently the major component (transition temperature = 22.15 - 33.15 ℃, Table 4.19). Meanwhile, the minor species which were responsible for the high melting point (transition temperature = 41.18 ℃) might be caused by the presence of undesirable saturated triacylglycerol species produced during the course of interesterification.

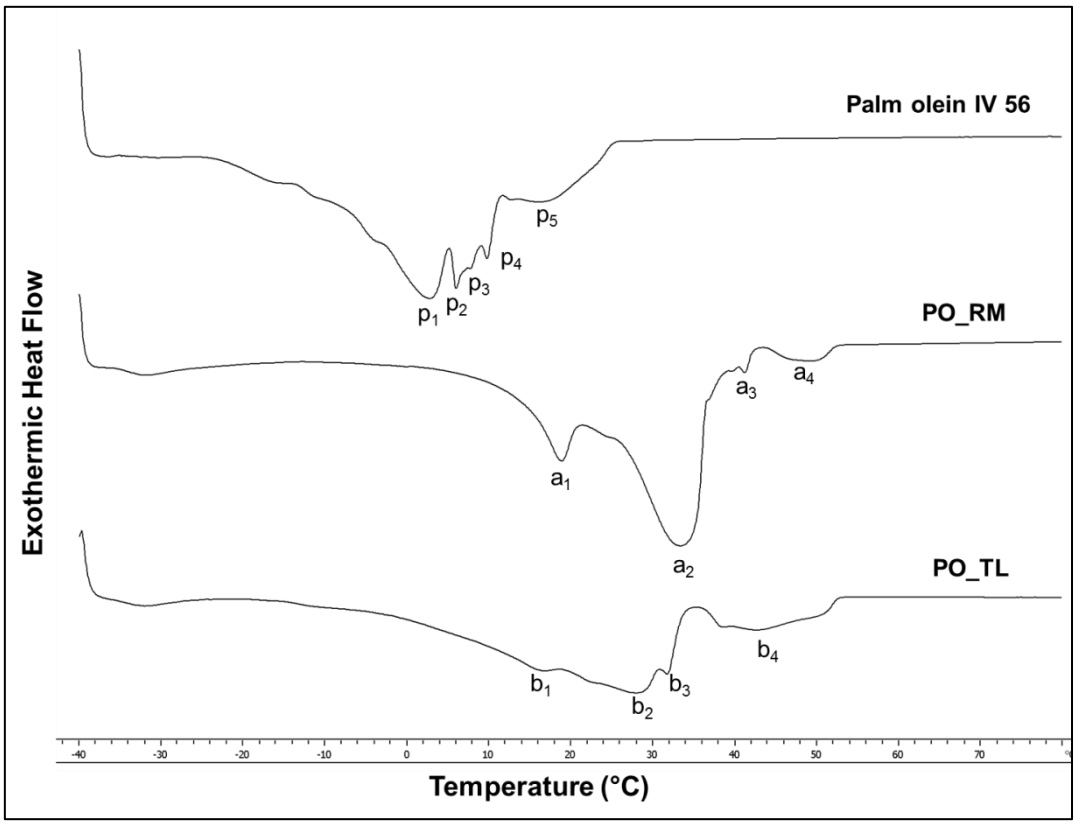

Notes:
IV, iodine value; PO_RM, structured lipid produced from palm olein IV 56 under action of Lipozyme RM IM; PO_TL, structured lipid produced from palm olein IV 56 under action of Lipozyme TL IM. Refer to Table 4.19 for the transition temperatures.

Figure 4.17 : Differential scanning calorimetry melting curves of palm olein IV 56 and its selected interesterified products

In the DSC melting curves of oils and fats, complex features were not effortlessly interpretable. This is a consequence of the known phenomenon of polymorphism of oils and fats that is strongly dependent on the thermal history of the sample. On the other hand, the crystallisation profile, which is influenced only by the chemical composition

of the sample, and not by the initial crystalline state, is much simpler than the melting curve (Tan and Che Man, 1999).

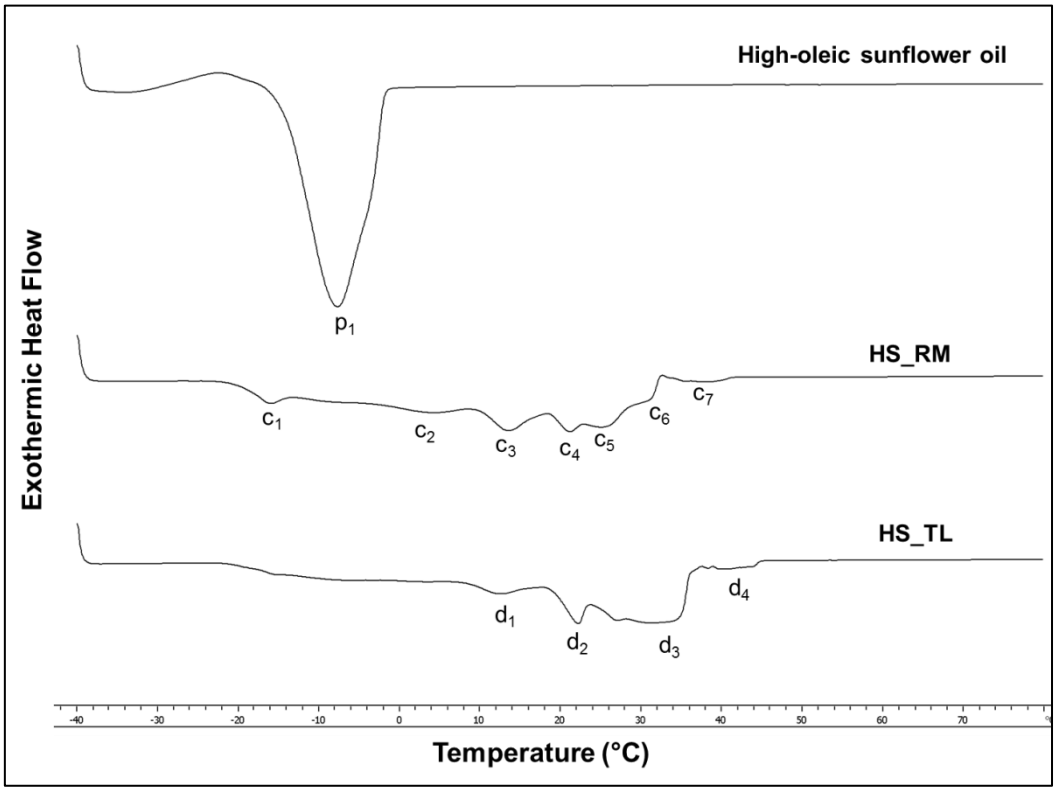

Notes:
HS_RM, structured lipid produced from high-oleic sunflower oil under action of Lipozyme RM IM; HS_TL, structured lipid produced from high-oleic sunflower oil under action of Lipozyme TL IM. Refer to Table 4.19 for the transition temperatures.

Figure 4.18 : Differential scanning calorimetry melting curves of high-oleic sunflower oil and its selected interesterified products

The examples of the DSC crystallisation curves of palm olein IV 56 and its corresponding structured lipids are demonstrated in Figure 4.19. In the starting material of the interesterification, namely, palm olein IV 56, a major exothermic peak (transition temperature = -5.76 ℃) with a shoulder peak (transition temperature = 1.71 ℃) was noted. A remarkable shift to the higher temperature region was observed in the exotherms of the structured lipids compared with that of palm olein IV 56. In PO_RM structured lipid, a major exothermic plateau consisting of three merging peaks was

observed, in which the temperature shift observed was about 30 ℃. Moreover, PO_TL showed both exothermic regions (Figure 4.19); the high-temperature region was distinguished by a small distinct exothermic peak at the transition temperature of 33.15 ℃ (Table 4.19) preceding the low-temperature region which consisted of two fusion peaks (transition temperature = 13.82 and 26.51 ℃, Table 4.19).

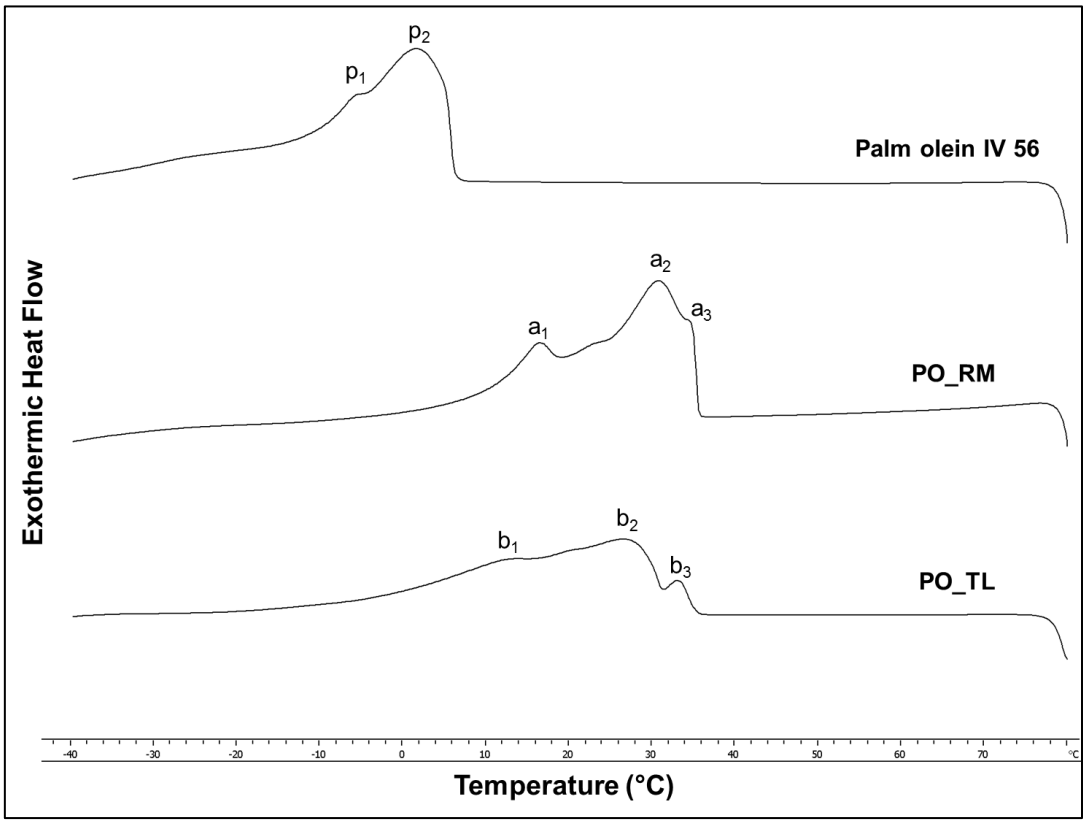

Notes:
IV, iodine value; PO_RM, structured lipid produced from palm olein IV 56 under action of Lipozyme RM IM; PO_TL, structured lipid produced from palm olein IV 56 under action of Lipozyme TL IM. Refer to Table 4.19 for the transition temperatures.

Figure 4.19 : Differential scanning calorimetry crystallisation curves of palm olein IV 56 and its selected interesterified products

Owing to the high degree of unsaturation, the exotherm of high-oleic sunflower oil (Figure 4.20) displayed a crystallisation profile below the cooling temperature programme exercised in the present study. The lowest cooling temperature employed was -40.0 ℃ limited by the present DSC instrumentation. Consequently, the detailed

information on the crystallisation profile of base oil was unable to establish. Nonetheless, the crystallisation curve of HS_RM displayed two major exothermic regions (Figure 4.20). The exothermic region at higher temperature defined crystallisation of the behenin fraction, while the lower-temperature region pertained to the crystallisation of the olein fraction. A similar pattern was observed for the exotherm of HS_TL, despite the HS_RM exhibited a higher unsaturated fraction compared with HS_TL. On top of that, the major exothermic region at a higher temperature (the behenin fraction) in the crystallisation curves of structured lipids showed a plateau consisting of three and four merging peaks for HS_RM and HS_TL, respectively.

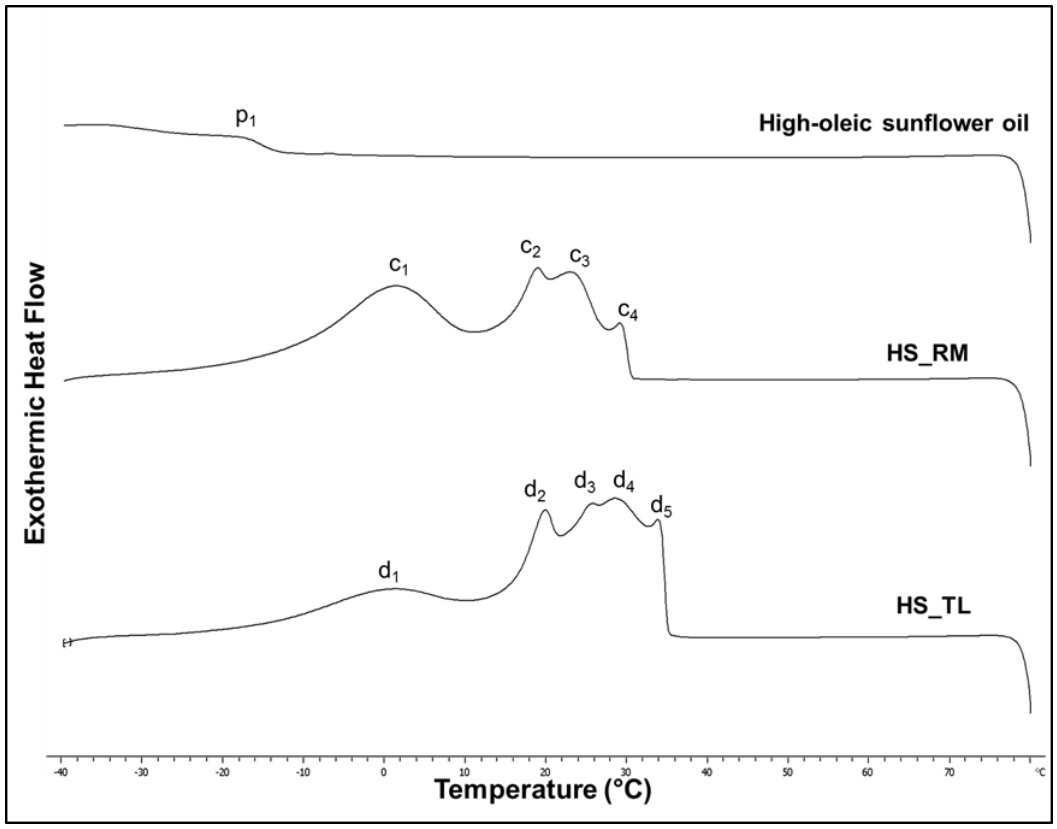

Notes:
HS_RM, structured lipid produced from high-oleic sunflower oil under action of Lipozyme RM IM; HS_TL, structured lipid produced from high-oleic sunflower oil under action of Lipozyme TL IM. Refer to Table 4.19 for the transition temperatures.

Figure 4.20 : Differential scanning calorimetry crystallisation curves of high-oleic sunflower oil and its selected interesterified products

In general, the thermal properties of various oils and fats from the DSC melting and crystallisation curves can be characterised by various transition temperature, as depicted in Table 4.19. Nonetheless, the comparison of aforementioned temperatures can be sophisticated and obscure by virtue of their complex features. A more systematic way to characterise the thermal properties of the various structured lipids reflected in DSC melting and crystallisation curves has been employed in the present study. Three DSC parameters, *viz.* the onset temperature (T_o), offset temperature (T_f) and the temperature range, *i.e.* the temperature difference between T_o and T_f. A complete comparison of these three DSC parameters is summarised in Table 4.20. On top of that, the melting and crystallisation curves of the selected structured lipids are presented in Figure 4.21 and Figure 4.22, respectively.

Table 4.20 : Comparison of the onset, offset and range of temperatures for thermograms of the starting materials and selected structured lipids

Thermogram	Sample	Temperature (℃)		
		T_o	T_f	Range $\|(T_f - T_o)\|$
Melting	Palm olein IV 56	-35.14	25.78	60.92
	PO_RM	-24.80	52.19	76.99
	PO_TL	-22.72	53.52	76.24
	High-oleic sunflower oil	-22.47	-0.44	22.03
	HS_RM	-26.64	42.01	68.65
	HS_TL	-23.49	45.26	68.75
Crystallisation	Palm olein IV 56	7.60	-39.55	47.15
	PO_RM	36.62	-22.89	59.51
	PO_TL	35.98	-20.50	56.48
	High-oleic sunflower oil	-4.82	NA	NA
	HS_RM	30.57	-29.39	59.96
	HS_TL	35.16	-24.89	60.05

Notes:
T_o, onset temperature; T_f, offset temperature; PO_RM and PO_TL, structured lipids produced from palm olein IV 56 under action of Lipozyme RM IM and Lipozyme TL IM, respectively; HS_RM and HS_TL, structured lipids produced from high-oleic sunflower oil under action of Lipozyme RM IM and Lipozyme TL IM, respectively; NA, not available.

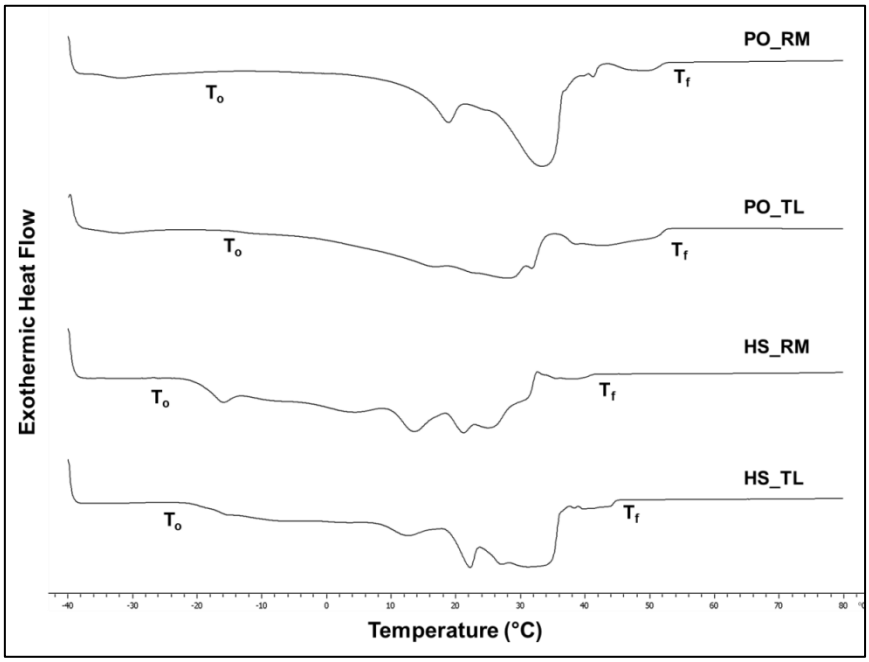

Notes:
PO_RM and PO_TL, structured lipids produced from palm olein IV 56 under action of Lipozyme RM IM and Lipozyme TL IM, respectively; HS_RM and HS_TL, structured lipids produced from high-oleic sunflower oil under action of Lipozyme RM IM and Lipozyme TL IM, respectively; T_o, onset temperature; T_f, offset temperature. Refer to Table 4.20 for the temperature parameters.

Figure 4.21 : Differential scanning calorimetry melting curves of the selected structured lipids produced from the enzymatic interesterification between oil and ethyl behenate

The comparison among these parameters showed significant differences between T_o of the crystallisation curves and T_f of the melting curves of the oil samples. The latter appeared to be 1.3 to 3.4 times greater than the former (Table 4.20). Nevertheless, there was no general trend observed in the comparison between T_o of the melting curves and T_f of the crystallisation curves (Table 4.20). In addition, the structured lipids were generally melted at a broader range (Figure 4.21) than their crystallisation (Figure 4.22). The aforementioned observations could be due to the complex phenomenon of polymorphism of oil samples, which was strongly dependent on their thermal history. A longer duration for melting process was needed and finally a relatively higher temperature than that of crystallisation upon complete melting was reached. Crystallisation was presumed to be influenced only by the chemical composition of the

sample, and not by the initial crystalline state (Tan and Che Man, 2000), was much simpler than the melting curve.

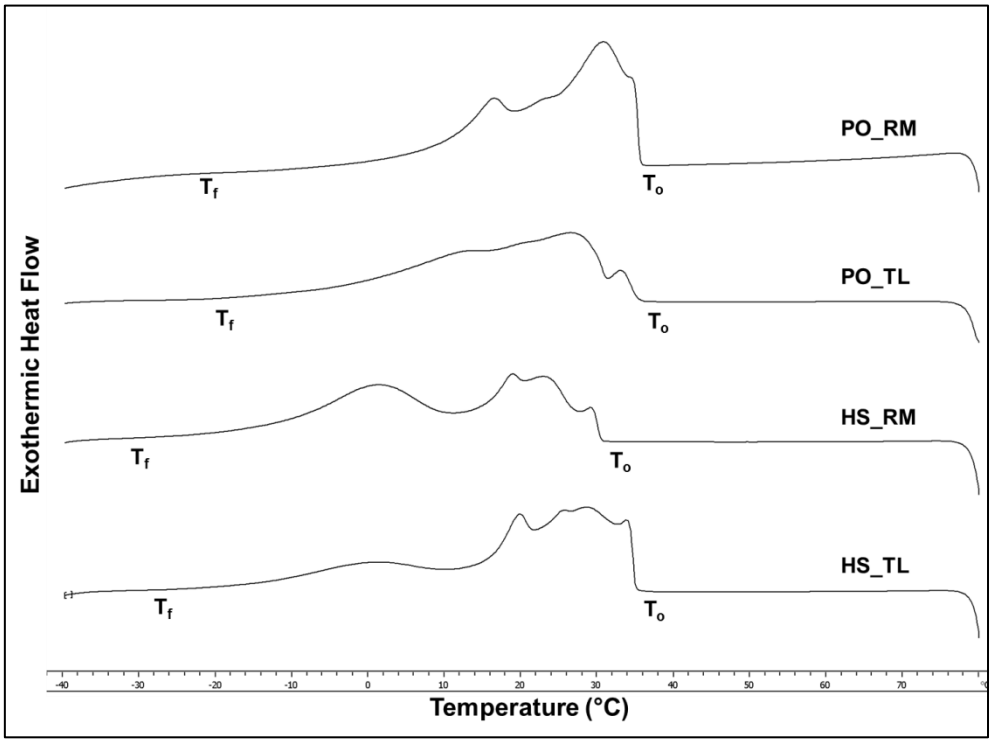

Notes:
PO_RM and PO_TL, structured lipids produced from palm olein IV 56 under action of Lipozyme RM IM and Lipozyme TL IM, respectively; HS_RM and HS_TL, structured lipids produced from high-oleic sunflower oil under action of Lipozyme RM IM and Lipozyme TL IM, respectively; T_o, onset temperature; T_f, offset temperature. Refer to Table 4.20 for the temperature parameters.

Figure 4.22 : Differential scanning calorimetry crystallisation curves of the selected structured lipids produced from the enzymatic interesterification between oil and ethyl behenate

As discussed previously, the exotherm of high-oleic sunflower oil (Figure 4.20) displayed a crystallisation profile lied beyond the cooling temperature used in the present instrumentation. Consequently, the T_f of the crystallisation curve of high-oleic sunflower oil was not attainable. On the other hand, enzymatic interesterification promoted a variety of new triacylglycerol species, which could be seen in the greater temperature ranges, *i.e.* differences between T_o and T_f (Table 4.20), in the thermograms

of structured lipids compared with their corresponding starting materials. Furthermore, in the study of the differential effects of 1,3-specific enzymes, structured lipids produced under the catalytic action of Lipozyme TL IM exhibited higher T_f in their melting profile compared to those obtained with Lipozyme RM IM. This mirrors a greater amount of undesirable high-melting-point saturated species had been produced by Lipozyme TL IM compared to Lipozyme RM IM. However, no significant difference was noticed for the temperature ranges ($|(T_f - T_o)|$) of melting, as well as the crystallisation curves for the structured lipids from the similar base oil, but were produced by different enzymes (Table 4.20).

Structured lipids based on palm olein IV 56, namely, PO_RM and PO_TL, showed greater differences between T_o and T_f in their melting curves (76.99 ℃ and 76.24 ℃, respectively, Table 4.20) compared to those produced from high-oleic sunflower oil (68.65 ℃ - 68.75 ℃, Table 4.20). The presence of a greater variety of triacylglycerol molecular species was therefore noted in the palm olein-based structured lipids. In addition, the melting T_f of both PO_RM and PO_TL were significantly higher than the melting T_f of HS_RM and HS_TL. The endothermic peaks in the high-temperature region (above 37 ℃) were also significantly broader in the melting curves of PO_RM and PO_TL compared to those produced from high-oleic sunflower oil (Figure 4.21). This reflects the triacylglycerol species present in palm olein-based structured lipids were relatively more saturated than those contained in sunflower oil-based structured lipids. Therefore, the latter displayed a lower T_o than the former in their melting profiles, on account of the high contents of oleic acid (Table 4.20). As a consequence, the structured lipids were envisaged to experience poor absorption in human partially due to their moderately higher melting temperature compared with the human body temperature (37 ℃).

In the context of crystallisation, both T_o and T_f of palm olein-based structured lipids were significantly higher than sunflower oil-based products (Figure 4.22). The latter contained more unsaturated species, for instance OOO, which crystallised at a lower temperature range. In summary, thermal properties of the structured lipids produced are crucial in determining its absorption.

4.4.2.5 Prospective Applications

In the current synthesis work, structured lipids which contain high amounts of 1-behenoyl-2,3-dioleoylglycerol (BOO) and 1,3-dibehenoyl-2-oleoylglycerol (BOB) molecular species have been successfully synthesised through enzyme-catalysed interesterification. These newly modified oils are envisaged to reduce the risk of obesity by taking the advantage of poor absorption of long chain saturated fatty acids (SFA) originated from the *sn*-1,3 positions of triacylglycerols.

Due to their physical properties at room temperature, these structured lipids may confer desirable rheological properties to bakery and confectionery products. The melting behaviour of the structured lipids can be easily modified by adjusting the extent of the behenic acid incorporation. On top of that, the current structured lipids may also serve as the hard stock for the physical blending with other softer oils, namely, canola, sunflower oil as well as soybean oil. A wide variety of suitable blending formulations for food products can be tailor-made along with the structured lipids. Thus, the plasticity of the blended oils widens the application scope of the current synthesised structured lipids. They may find applications in regular cooking and deep-frying as well as a bakery shortening or as a base for *trans*-fat-free products, *viz.* margarine, shortening and vanaspati. These products will display characteristics and melting behaviour

comparable to those of the hydrogenated counterparts, with an additional advantage of lowering the problem of fat deposition.

In standpoints of high contents of symmetrical triacylglycerols, namely, BOB, the structured lipids can also be used as cocoa butter equivalent for chocolate and confectionery coatings. The BOB species possesses a similar fatty acid profile, that is, saturated-unsaturated-saturated (SUS) compared with the major triacylglycerol species present in the typical cocoa butter equivalents, namely, palm mid fractions, illipe fat, shea butter, sal fat and mango fat.

4.5 Conclusion

In the current work, structured lipids containing high amount of 1-behenoyl-2,3-dioleoylglycerol (BOO) and 1,3-dibehenoyl-2-oleoylglycerol (BOB) have been successfully synthesised through lipase-catalysed interesterification of palm olein and high-oleic sunflower oils with ethyl behenate. They may serve as functional and healthy fats due to their benefits in alleviating the extent of fat accretion through the poor absorption of long chain behenic acids originated from the *sn*-1,3 positions of triacylglycerols. The effectiveness in lowering fat deposition are depending on their melting behaviour, triacylglycerol composition as well as the composition of behenic acid at the *sn*-1,3 positions. In summary, the structured lipids are still exhibiting fat properties, with potential and additional advantage in lowering risk factor towards excessive fat deposition.

REFERENCES

Abildgaard, F., Gesmar, H., & Led, J. J. (1988). Quantitative analysis of complicated nonideal Fourier Transform NMR spectra. *Journal of Magnetic Resonance, 79*, 78-89.

Abumrad, N. A., Park, J. H., & Park, C. R. (1984). Permeation of long-chain fatty acids in adipocyte. *Journal of Biological Chemistry, 259*, 8945-8953.

Adlof, R. O., & List, G. R. (2007). Synthesis and physical properties of EOE and EEO, triacylglycerols containing elaidic and oleic fatty acids. *Journal of the American Oil Chemists' Society, 84*, 427-431.

Agren, J. J., & Kuksis, A. (2002). Analysis of diastereomeric DAG naphthylethylurethanes by normal-phase HPLC with on-line electrospray MS. *Lipids, 37*, 613-619.

Akoh, C. C. (1995). Structured lipids—Enzymatic approach. *Inform, 6*, 1055–1061.

Akoh, C. C., & Yee, L. N. (1997). Enzymatic synthesis of position-specific low-calorie structured lipids. *Journal of the American Oil Chemists' Society,74*, 1409-1413.

Angers, P., & Arul, J. (1999). A simple method for regiospecific analysis of triacylglycerols by gas chromatography. *Journal of the American Oil Chemists' Society, 76*, 481-484.

AOCS Official Method Cj 1-94 (1988) and Ja 14-91 (1998). Official methods and recommended practices of the American Oil Chemists' Society (3rd ed.). In D. Firestone (Ed.), Champaign, Illinois: American Oil Chemists' Society.

Arcos, J. A., Garcia, H. S., & Hill, C. G. (2000). Regioselective analysis of the fatty acid composition of triacylglycerols with conventional high-performance liquid chromatography. *Journal of the American Oil Chemists' Society, 77*, 507-512.

Auerbach, M. H., Chang, P. W., Kosmark, R., O'Neill, J. J., & Philips, J. C. (1998). Salatrim: A family of reduced-calorie structured lipids. In A. B. Christophe (Ed), *Structurally modified food fats: synthesis, biochemistry, and use* (pp. 89-116). Champagne, Illinois: AOCS Press.

Aursand, M., Jørgesen, L., & Grasdalen, H. (1995). Positional distribution of ω3 fatty acids in marine lipid triacylglycerols by high-resolution ^{13}C nuclear magnetic resonance spectroscopy. *Journal of the American Oil Chemists' Society, 72*, 293-297.

Aursand, M., Standal, I. B., & Axelson, D. E. (2007). High-resolution ^{13}C nuclear magnetic resonance spectroscopy pattern recognition of fish oil capsules. *Journal of Agricultural and Food Chemistry, 55*, 38-47.

Babayan, V. K. (1987). Medium-chain triglycerides and structured lipids. *Lipids, 22*, 417-420.

Baliga, B. P., & Shitole, A. D. (1981). Cocoa butter substitutes from mango fat. *Journal of the American Oil Chemists' Society, 58*, 110-114.

Barron, L. J. R., Hierro, M. T. G., & Santa-Maria, G. (1990). HPLC and GLC analysis of the triglyceride composition of bovine, ovine and caprine milk fat. *Journal of Dairy Research, 57*, 517-526.

Becker, C. C., Rosenquist, A., & Hølmer, G. (1993). Regiospecific analysis of triacylglycerols using allyl magnesium bromide. *Lipids, 28*, 147-149.

Bergana, M. M., & Lee T. W. (1996). Structure determination of long-chain polyunsaturated triacylglycerols by high resolution ^{13}C Nuclear magnetic resonance. *Journal of the American Oil Chemists' Society, 73*, 551-556.

Berger, K. G. (1981). Food uses of palm oil. *PORIM Occasional Paper, 2*, 1-27.

Berger, M., & Schneider, M. P. (1991). Regioselectivity of lipases in organic solvents. *Biotechnology Letters, 13*, 333–338.

Berry, S. E. (2009). Triacylglycerol structure and interesterification of palmitic and stearic acid-rich fats: An overview and implications for cardiovascular disease. *Nutrition Research Reviews, 22*, 3-17.

Boozer, C. N., Schoenbach G., & Atkinson, R. L. (1995). Dietary fat and adiposity: a dose-response relationship in adult male rats fed isocalorically. *American Journal of Physiology: Endocrinology and Metabolism, 268*, E546-E550.

Bottino, N. R., Vandenburg, G. A., & Reiser, R. (1967). Resistance of certain long-chain polyunsaturated fatty acids of marine oils to pancreatic lipase hydrolysis. *Lipids, 2*, 489-493.

Bourgeois, F., Alexiu, A., & Lemonnier, D. (1983). Dietary-induced obesity: effect of dietary fats on adipose tissue cellularity in mice. *British Journal of Nutrition, 49*, 17-26.

Bray, G. A., & Popkin B. M. (1998). Dietary fat intake does affect obesity. *The American Journal of Clinical Nutrition, 68*, 1157-1173.

Brink, E. J., Haddeman, E., de Fouw, N. J., & Weststrate, J. A. (1995). Positional distribution of stearic acid and oleic acid in a triacylglycerol and dietary calcium concentration determines the apparent absorption of these fatty acids in rats. *Journal of Nutrition, 125*, 2379-2387.

Brockerhoff, H. (1965). A stereospecific analysis of triglycerides. *Journal of Lipid Research, 6*, 10-15.

Brockerhoff, H. (1967). Stereospecific analysis of triglycerides: An alternative method. *Journal of Lipid Researsh, 8*, 167-169.

Catta-Preta, M., Martins, M. A., Brunini, T. M. C., Mendes-Ribeiro, A. C., Mandarim-de-Lacerda, C. A., & Aguila, M. B. (2012). Modulation of cytokines, resistin, and distribution of adipose tissue in C57BL/6 mice by different high-fat diets. *Nutrition, 28*, 212-219.

Cebula, D. J., & Smith K. W. (1992). Differential scanning calorimetry of confectionery fats. Part II- Effects of blends and minor components. *Journal of the American Oil Chemists' Society, 69*, 992-998.

Chan, S., McCowen, K. C., & Bistrian, B. (1998). Medium-chain triglyceride and *n*-3 polyunsaturated fatty acid-containing emulsions in intravenous nutrition. *Current Opinion in Clinical Nutrition and Metabolic Care, 1*, 163-169.

Chandler, I. C., Quinlan, P. T., & McNeill. G. P. (1998). Lipase-catalysed synthesis of chiral triglycerides. *Journal of the American Oil Chemists' Society, 75*, 1513-1518.

Choudhury, N., Tan, L., & Truswell, A. S. (1995). Comparison of palmolein and olive oil: Effects on plasma lipids and vitamin E in young adults. *The American Journal of Clinical Nutrition, 61*, 1043-1051.

Christie, W. W. (1989). *Gas Chromatography and Lipids : A Practical Guide*. Ayr: The Oily Press Ltd.

Christie, W. W., Nikolova-Damyanova, B., Laakso, P., & Herslof, B. (1991). Stereospecific analysis of triacyl-*sn*-glycerols *via* resolution of diastereomeric diacylglycerol derivatives by high-performance liquid chromatography on silica. *Journal of the American Oil Chemists' Society, 68*, 695-701.

Claridge, T. D. (1999). *High-resolution NMR Techniques in Organic Chemistry*. New York, NY: Pergamon.

Codex Alimentarius Commission (2011). Codex standards for named vegetable oils, CODEX STAN 210 (revisions 2011) FAO/WHO. Rome, Italy.

Crozier, G., Bois-Joyeux, B., Chanez, M., Girald, J., & Peret, J. (1987). Metabolic effects induced by long-term feeding of medium-chain triglycerides in the rat. *Metabolism, 36*, 807-814.

Czernichow, S., Thomas, D., & Bruckert, E. (2010). *n*-6 Fatty acids and cardiovascular health: a review of the evidence for dietary intake recommendations. *British Journal of Nutrition, 104*, 788-796.

de Deckere, E. A., van Amelsvoort, J. M., McNeill, G. P., & Jones, P. (1999). Effects of conjugated linoleic acid (CLA) isomers on lipid levels and peroxisome proliferation in the hamster. *British Journal of Nutrition, 82*, 309-317.

Derome, A. E. (1987). *Modern NMR Techniques for Chemistry Research*. New York, NY: Pergamon.

Dourtoglou, T., Stefanou, E., Lalas, S., Dourtoglou, V., & Poulos, C. (2001). Quick regiospecific analysis of fatty acids in triaclyglycerols with GC using 1, 3-specific lipase in butanol. *Analyst, 126*, 1032-1036.

Dugan, M. E., Aalhus, J. L., & Kramer, J. K. (2004). Conjugated linoleic acid pork research. *The American Journal of Clinical Nutrition, 79*, 1212S-1216S.

Dutta, J., Das, A. K., & Saha, S. (1978). Enzymatic reactions on thin-layer chromatographic plates: I. Lipolysis of triglycerides and separation of products on a single plate. *Journal of Chromatography A, 154*, 33-37.

Dutta, J., Das, A. K., & Biswas, A. (1979). Enzymatic reactions on thin-layer chromatographic plates. II. Phospholipase A_2 hydrolysis of phosphatidylcholine and separation of the products on a single plate. *Journal of Chromatography, 173*, 379-387.

Eckey, E. W. (1956). Esterification and interesterification. *Journal of the American Oil Chemists' Society, 33*, 575-579.

Emery, E. M., Schmid, T. L., Kahn, H. S., & Filozof, P. P. (1993). A review of the association between abdominal fat distribution, health outcome measures, and modifiable risk factors. *American Journal of Health Promotion, 7*, 342-353.

Fabien, R., Craske, J. D., & Wootton M. (1993). Quantitative analysis of synthetic mixtures of triacylglycerols with fatty acids from caprylic to stearic. *Journal of the American Oil Chemists' Society, 70*, 551-554.

Farquhar, J. W., Insull Jr., W., Rosen, P., Stoffel, W., & Ahrens Jr., E. H. (1959). The analysis of fatty acid mixtures by gas-liquid chromatography; construction and operation of an ionization chamber instrument. *Nutrition Reviews, 17*, 1–30.

Finley, J. W., Klemann, L. P., Leveille, G. A., Otterburn, M. S., & Walchak, C. G. (1994). Caloric availability of SALATRIM in rats and humans. *Journal of Agricultural and Food Chemistry, 42*, 495-499.

Foglia, T. A., Petruso, K., & Feairheller, S. H. (1993). Enzymatic interesterification of tallow-sunflower oil mixtures. *Journal of the American Oil Chemists' Society, 70*, 281-285.

Foglia, T. A., Conkerton, E. J., & Sonnet, P. E. (1995). Regioselective analysis of triacylglycerols by lipase hydrolysis. *Journal of the American Oil Chemists' Society, 72*, 1275-1279.

Folch, J., Leens, M., & Sloane-Stanley, G. H. (1957). A simple method for the isolation and purification of total lipids from animal tissue. *Journal of Biological Chemistry, 226*, 497-509.

Fomuso, L. B., & Akoh, C. C. (1998). Structured lipids: Lipase-catalyzed interesterification of tricaproin and trilinolein. *Journal of the American Oil Chemists' Society, 75*, 405-410.

Fomuso, L. B., & Akoh, C. C. (2001). Enzymatic modification of high-laurate canola to produce margarine fat. *Journal of Agricultural and Food Chemistry, 49*, 4482-4487.

Foresti, M. L., & Ferreira, M. L. (2010). Lipase-catalyzed acidolysis of tripalmitin with capric acid in organic solvent medium: Analysis of the effect of experimental conditions through factorial design and analysis of multiple responses. *Enzyme and Microbial Technology, 46*, 419-429.

Forsythe, C. E., French, M. A., Goh, Y. K., & Clandinin, M. T. (2007). Cholesterolaemic influence of palmitic acid in the *sn*-1, 3 v. the *sn*-2 position with high or low dietary linoleic acid in healthy young men. *British Journal of Nutrition, 98*, 337-344.

Freeman, C. P. (1969). Properties of fatty acids in dispersion of emulsified lipid and bile salt and the significance of these properties in fat absorption in the pig and the sheep. *British Journal of Nutrition, 23*, 249-263.

Garcia, H. S., Stockson, J. M., Pariza, M. W., & Hill Jr., C. G. (1998). Enrichment of butteroil with conjugated linoleic acid *via* enzymatic interesterification (acidolysis) reacitons. *Biotechnology Letters, 20*, 393-395.

Geliebter, A., Torbay, N., Bracco, E. F., Hashim, S. A., & Van Itallie, T. B. (1983). Overfeeding with medium-chain triglyceride diet results in diminished deposition of fat. *The American Journal of Clinical Nutrition, 37*, 1-4.

Goiffon, J. P., Reminiac, C., & Furon, D. (1981). Application de la chromatographie haute performance à l'analyse des triglycérides des corps gras, ll: Grandeurs de retention de triglycerides. *Rev. Fran. Corps Gras, 28*, 199-208.

Goli, S. A. H., Sahri, M. M., & Kadivar, M. (2008). Enzymatic interesterification of structured lipids containing conjugated linoleic acid with palm stearin for possible margarine production. *European Journal of Lipid Science and Technology, 110*, 1102-1108.

Gunstone, F. D. (1967). *An Introduction to the Chemistry and Biochemistry of Fatty Acids and Their* Glycerides (2nd ed.). London, England: Chapman and Hall Limited.

Gunstone, F. D. and Harwood J. L. (2007). Occurrence and Characterisation of Oils and Fats. In F. D. Gunstone, J. L. Harwood & A. J. Dijkstra (Eds.), *The Lipid Handbook* (3rd ed.) (pp. 37-142). Boca Raton: CRC Press.

Gupta, R., Rathi, P., & Bradoo, S. (2003). Lipase mediated upgradation of dietary fats and oils. *Critical Reviews in Food Science and Nutrition, 43*, 635-644.

Gurr, M. I. (1999). *Lipids in Nutrition & Health: A Reappraisal*. Bridgwater: The Oily Press.

Hamam, F., & Shahidi, F. (2004). Synthesis of structured lipids *via* acidolysis of docosahexaenoic acid single cell oil (DHASCO) with capric acid. *Journal of Agricultural and Food Chemistry, 52*, 2900-2906.

Hamam, F., & Shahidi, F. (2004). Enzymatic acidolysis of an arachidonic acid single-cell oil with capric acid. *Journal of the American Oil Chemists' Society, 81*, 887-892.

Hariri, N., Gougeon, R., & Thibault, L. (2010). A highly saturated fat-rich diet is more obesogenic than diets with lower saturated fat content. *Nutrition Research, 30*, 632-643.

Harwood, J. L. (2007). Lipid Metabolism. In F. D. Gunstone, J. L. Harwood & A. J. Dijkstra (Eds.), *The Lipid Handbook* (3rd ed.) (pp. 637-702). Boca Raton: CRC Press.

Hill, J. O., Melanson, E. L., & Wyatt, H. T. (2000). Dietary fat intake and regulation of energy balance: implications for obesity. *Journal of Nutrition, 130*, 284S-288S.

Huang, K. H., & Akoh, C. C. (1996). Enzymatic synthesis of structured lipids: transesterification of triolein and caprylic acid ethyl ester. *Journal of the American Oil Chemists' Society, 73*, 245-250.

Ibrahim, N. A., Guo, Z., & Xu, X. (2008). Enzymatic interesterification of palm stearin and coconut oil by a dual lipase system. *Journal of the American Oil Chemists' Society, 85*, 37-45.

Igarashi, T., Aursand, M., Hirata, Y., Gribbestad, I. S., Wada, S., & Nonaka, M. (2000). Nondestructive quantitative determination of docosahexaenoic acid and *n*-3 fatty acids in fish oils by high-resolution ^{1}H Nuclear Magnetic Resonance spectroscopy. *Journal of the American Oil Chemists' Society, 77*, 737-748.

Ikeda, I., Tomari, Y., Sugano, M., Watanabe, S., & Nagata, J. (1991). Lymphatic absorption of structured glycerolipids containing medium-chain fatty acids and linoleic acid, and their effect on cholesterol absorption in rats. *Lipids, 26*, 369-373.

Ikemoto, S., Takahashi, M., Tsunoda, N., Maruyama, K., Itakura, H., & Ezaki, O. (1996). High-fat diet-induced hyperglycemia and obesity in mice: differential effects of dietary oils. *Metabolism, 45*, 1539-1546.

Innis, S. M., Dyer, R. A., & Lien, E. L. (1997). Formula containing randomized fats with palmitic acid (16:0) in the 2-position increases 16:0 in the 2-position of plasma and chylomicron triglycerides in formula-fed piglets to levels approaching those of piglets fed sow's milk. *Journal of Nutrition, 127*, 1362-1370.

Irani, R. R., & Callis, C. F. (1960). Metal complexing by phosphorus compounds II. Solubility of calcium soaps of linear carboxylic acids. *Journal of Physical Chemistry, 64*, 1741-1743.

Irimescu, R., Yasui, M., Iwasaki, Y., Shimidzu, N., & Yamane, T. (2000). Enzymatic synthesis of 1, 3–dicapryloyl-2-eicosapentaenoylglycerol. *Journal of the American Oil Chemists' Society, 77*, 501-506.

Irimescu, R., Furihata, K., Hata, K., Iwasaki, Y., & Yamane, T. (2001). Two-step enzymatic synthesis of docosahexaenoic acid-rich symmetrically structured triacylglycerols *via* 2-monoacylglycerols. *Journal of the American Oil Chemists' Society, 78*, 743-748.

Iwasaki, Y., & Yamane, T. (2000). Enzymatic synthesis of structured lipids. *Journal of Molecular Catalysis B: Enzymatic, 10*, 129-140.

Jandacek, R. J., Whiteside, J. A., Holcombe, B. N., Volpenhein, R. A., & Taulbee, J. D. (1987). The rapid hydrolysis and efficient absorption of triglycerides with octanoic acid in the 1 and 3 positions and long chain fatty acid in the 2 position. *The American Journal of Clinical Nutrition, 45*, 940-945.

Jen, K. L. C., Buison, A., Pellizzon, M., Ordiz Jr, F., Santa Ana, L., & Brown, J. (2003). Differential effects of fatty acids and exercise on body weight regulation and metabolism in female Wistar rats. *Experimental Biology and Medicine, 228*, 843-849.

Jensen, G. L., McGarvey, N., Taraszewski, R., Wixson, S. K., Seidner, D. L., Pai, T., Yeh, Y. Y., Lee, T. W., & DeMichele, S. J. (1994). Lymphatic absorption of enterally fed structured triacylglycerol vs physical mix in a canine model. *The American Journal of Clinical Nutrition, 60*, 518-524.

Kanjilal, S., Prasad, R. B. N., Kaimal, T. N. B., Ghafoorunissa, & Rao, S. H. (1999). Synthesis and estimation of calorific value of a structured lipid-potential reduced calorie fat. *Lipids, 34*, 1045-1055.

Karupaiah T., & Sundram K. (2007). Effects of stereospecific positioning of fatty acids in triacylglycerol structures in native and randomized fats: a review of their nutritional implications. *Nutrition and Metabolism, 4*, 16.

Katan, M. B., Zock, P. L., & Mensink, R. P. (1994). Effects of fats and fatty acids on blood lipids in humans: An overview. *The American Journal of Clinical Nutrition, 60*, 1017S-1022S.

Kaunitz, H. (1986). Medium chain triglycerides (MCT) in aging and arteriosclerosis. *Journal of Environmental Pathology, Toxicology and Oncology, 6*, 115-121.

Kayden, H. J., Senior, J. R., & Mattson, F. H. (1967). The monoglyceride pathway of fat absorption in man. *Journal of Clinical Investigation, 46*, 1695-1703.

Kim, M. K., Jang, E. H., Son, J. W., Kwon, H. S., Baek, K. H., Lee, K. W., & Song, K. H. (2011). Visceral obesity is a better predictor than generalized obesity for basal insulin requirement at the initiation of insulin therapy in patients with type 2 diabetes. *Diabetes Research and Clinical Practice, 93*, 174-178.

Klemann, L. P., Aji, K., Chrysam, M., D'Amelia, R. P., Henderson, J. J., Huang, A., Otterburn, M. S., Yarger, R. G., Boldt, G., & Roden, A. (1994). Random nature of triacylglycerols produced by the catalyzed interesterification of short- and long-chain fatty acid triglycerides. *Journal of Agricultural and Food Chemistry, 42*, 442-446.

Koçak, D., Keskin, H., Fadiloglu, S., Kowalski, B., & Göğüş, F. (2011). Characterization of terebinth fruit oil and optimization of acidolysis reaction with caprylic and stearic acids. *Journal of the American Oil Chemists' Society, 88*, 1531-1538.

Kojima, M., Tachibana, N., Yamahira, T., Seino, S., Izumisawa, A., Sagi, N., Arishima, T., Kohno, M., Takamatsu, K., Hirotsuka, M., & Ikeda, I. (2010). Structured triacylglycerol containing behenic and oleic acids suppresses triacylglycerol absorption and prevents obesity in rats. *Lipids in Health and Disease, 9*, 77-82.

Kosugi, Y., Oshima, A., Koike, S., Fukatsu, M., Minami, K., Miyake, Y., & Masui, K. (2002). Determination of fatty acid composition at *sn*-2 acyl position in triacylglycerol by capillary gas chromatography with lipase from *Rhizopus delemar*. *Journal of Oleo Science, 51*, 599-605.

Kritchevsky, D., Davidson, L. M., Weight, M., Kriek, N. P., & du Plessis, J. P. (1982). Influence of native and randomized peanut oil on lipid metabolism and aortic sudanophilia in the vervet monkey. *Atherosclerosis, 42*, 53-58.

Kritchevsky, D. (1988). Effects of triglyceride structure on lipid metabolism. *Nutrition Reviews, 46*, 177-181.

Kuksis, A., & Itabashi, Y. (2005). Regio- and stereospecific analysis of glycerolipids. *Methods, 36*, 172-185.

Lands, W. E., Pieringer, R. A., Slakey, S. P., & Zschocke, A. (1966). A micromethod for the stereospecific determination of triglyceride structure. *Lipids, 1*, 444-448.

Laning, S. J. (1985). Chemical interesterification of palm, palm kernel and coconut oils. *Journal of the American Oil Chemists' Society, 62*, 400-407.

Larson, D. E., Hunter, G. R., Williams, M. J., Kekes-Szabo, T., Nyikos, I., & Goran, M. I. (1996). Dietary fat in relation to body fat and intraabdominal adipose tissue: a cross-sectional analysis. *The American Journal of Clinical Nutrition, 64*, 677-684.

Lee, K. T., & Akoh, C. C. (1997). Effects of selected substrate forms on the synthesis of structured lipids by two immobilized lipases. *Journal of the American Oil Chemists' Society, 74*, 579-584.

Lee, K. T., & Akoh, C. C. (1998). Characterization of enzymatically synthesized structured lipids containing eicosapentaenoic, docosahexaenoic and caprylic acids. *Journal of the American Oil Chemists' Society, 75*, 495-499.

Lee, K. T., & Foglia, T. A. (2000). Synthesis, purification, and characterization of structured lipids produced from chicken fat. *Journal of the American Oil Chemists' Society, 77*, 1027-1034.

Lichtenstein, A. H., Ausman, L. M., Carrasco, W., Gualtieri, L. J., Jenner, J. L., Ordovas, J. M., Nicolosi, R. J., Goldin, B. R., & Schaefer, E. J. (1994). Rice bran oil consumption and plasma lipid levels in moderately hypercholesterolemic humans. *Arteriosclerosis, Thrombosis, and Vascular Biology, 14*, 549-556.

Lien, E. L., Yuhas, R. J., Boyle, F. G., & Tomarelli, R. M. (1993). Corandomization of fats improves absorption in rats. *Journal of Nutrition, 123*, 1859-1867.

Lin, S. W. (2002). Palm Oil. In F. D. Gunstone (Ed.), *Vegetable Oils in Food Technology: Composition, Properties and Uses* (pp. 59-97). Boca Raton: CRC Press.

Liu, L. (2004). How is chemical interesterification initiated: Nucleophilic substitution or α-proton abstraction? *Journal of the American Oil Chemists' Society, 81*, 331-337.

Lo, Y. C., & Handel, A. P. (1983). Physical and chemical properties of randomly interesterified blends of soybean oil and tallow for use as margarine oils. *Journal of the American Oil Chemists' Society, 60*, 815-818.

Luddy, F. E., Barford, R. A., Herb, S. F., Magidman, P., & Riemenschneider, R. W. (1964). Pancreatic lipase hydrolysis of triglycerides by a semimicro technique. *Journal of the American Oil Chemists' Society, 41*, 693-696.

Maki, K. C. Davidson, M. H., Tsushima, R., Matsuo, N., Tokimitsu, I., Umporowicz, D. M., Dicklin, M. R., Foster, G. S., Ingram, K. A., Anderson, B. D., Frost, S. D., & Bell, M. (2002). Consumption of diacylglycerol oil as part of a reduced-energy diet enhances loss of body weight and fat in comparison with consumption of a triacylglycerol control oil. *The American Journal of Clinical Nutrition, 76*, 1230-1236.

Manganaro, F., Myher, J. J., Kuksis, A., & Kritchevsky, D. (1981). Acylglycerol structure of genetic varieties of peanut oils of varying atherogenic potential. *Lipids, 16*, 508-517.

Mangos, T. J., Jones, K. C., & Foglia, T. A. (1999). Lipase-catalyzed synthesis of structured low-calorie triacylglycerols. *Journal of the American Oil Chemists' Society, 76*, 1127-1132.

Martinez-Victoria, E., & Yago, M. D. (2012). Omega 3 polyunsaturated fatty acids and body weight. *British Journal of Nutrition, 107*, S107-S116.

Matsuo, T., Takeuchi, H., Suzuki, H., & Suzuki, M. (2002). Body fat accumulation is greater in rats fed a beef tallow diet than in rats fed a safflower or soybean oil diet. *Asia Pacific Journal of Clinical Nutrition, 11*, 302-308.

Matsuo, T., & Takeuchi, H. (2004). Effects of structured medium- and long-chain triacylglycerols in diets with various levels of fat on body fat accumulation in rats. *British Journal of Nutrition, 91*, 219-225.

Mattson, F. H., & Volpenhein, R. A. (1961). The use of pancreatic lipase for determining the distribution of fatty acids in partial and complete glycerides. *Journal of Lipid Research, 2*, 58-62.

Mattson, F. H., Nolen, G. A., & Webb, M. R. (1979). The absorbability by rats of various triglycerides of stearic and oleic acid and the effect of dietary calcium and magnesium. *Journal of Nutrition, 109*, 1682-1687.

Mcleod, K., & Comisarow, M. B. (1989). Systematic errors in the discrete integration of FT NMR spectra. *Journal of Magnetic Resonance, 84*, 490-500.

Micallef, M., Munro, I., Phang, M., & Garg, M. (2009). Plasma *n*-3 polyunsaturated fatty acids are negatively associated with obesity. *British Journal of Nutrition, 102*, 1370-1374.

Mu, H., & Høy C. E. (2004). The digestion of dietary triacylglycerols. *Progress in Lipid Research, 43*, 105-133.

Muñío, M. M., Esteban, L., Robles, A., Hita, E., Jiménez, M. J., González, P. A., Camacho, B., & Molina, E. (2008). Synthesis of 2-monoacylglycerols rich in polyunsaturated fatty acids by ethanolysis of fish oil catalyzed by 1, 3 specific lipases. *Process Biochemistry, 43*, 1033-1039.

Muñío, M. M., Robles, A., Esteban, L., González, P. A., & Molina, E. (2009). Synthesis of structured lipids by two enzymatic steps: Ethanolysis of fish oils and esterification of 2-monoacylglycerols. *Process Biochemistry, 44*, 723-730.

Myher, J. J., Marai, L., & Kuksis, A. (1977). Acylglycerol structure of peanut oils of different atherogenic potential. *Lipids, 12*, 775-785.

Nadjari, R., & Grivet, J. P. (1991). Precision of integrals in quantitative NMR. *Journal of Magnetic Resonance, 91*, 353-361.

Nagao, T., Watanabe, H., Goto, N., Onizawa, K., Taguchi, H., Matsuo, N., Yasukawa, T., Tsushima, R., Shimasaki, H., & Itakura, H. (2000). Dietary diacylglycerol suppresses accumulation of body fat compared to triacylglycerol in men in a double-blind controlled trial. *Journal of Nutrition, 130*, 792-797.

Nájera, A. I., Barcina, Y., de Renobales, M., & Barron, L. J. R. (1998). Changes in triacylglycerols during the ripening of idiazabal cheese. *Journal of Agricultural and Food Chemistry, 46*, 322-3256.

Nájera, A. I., Perea, S., Barcina, Y., de Renobales, M., & Barron L. J. R. (1999). A reverse-phase high-performance liquid chromatographic method for analyzing complex mixtures of triglycerides. Application to the fat fraction of an aged cheese. *Journal of the American Oil Chemists' Society, 76*, 399-407.

Neff, W. E., & List, G. R. (1999). Oxidative stability of natural and randomized high-palmitic- and high-stearic-acid oils from genetically modified soybean varieties. *Journal of the American Oil Chemists' Society, 76*, 825-831.

Nenzonana, G., & Desnuelle, P. (1968). Action of some effectors on the hydrolysis of long chain triglycerides by pancreatic lipase. *Biochimica et Biophysica Acta, 165*, 47-58.

Nestel, P. J., Pomeroy, S., Kay, S., Sasahara, T., & Yamashita, T. (1998). Effect of a stearic acid-rich, structured triacylglycerol on plasma lipid concentrations. *The American Journal of Clinical Nutrition, 68*, 1196-1201.

Newman, R. E., Bryden, W. L., Fleck, E., Ashes, J. R., Buttemer, W. A., Storlien, L. H., & Downing, J. A. (2002). Dietary *n*-3 and *n*-6 fatty acids alter avian metabolism: metabolism and abdominal fat deposition. *British Journal of Nutrition, 88*, 11-18.

Ng, S. (1985). Analysis of positional distribution of fatty acids in palm oil by ^{13}C NMR spectroscopy. *Lipids, 20*, 778-782.

Ng, S., & Koh, H. F. (1988). Detection of *cis*-vaccenic acid in palm oil by ^{13}C NMR spectroscopy. *Lipids, 23*, 140-143.

Ng, T. K., Hayes, K. C., DeWitt, G. F., Jegathesan, M., Satgunasingam, N., Ong, A. S., & Tan, D. (1992). Dietary palmitic and oleic acids exert similar effects on serum cholesterol and lipoprotein profiles in normocholesterolemic men and women. *Journal of the American College of Nutrition, 11*, 383-390.

Noor Lida, H. M. D., Sundram, K., Siew, W. L., Aminah, A., & Mamot, S. (2002). TAG composition and solid fat content of palm oil, sunflower oil, and palm kernel olein blends before and after chemical interesterification. *Journal of the American Oil Chemists' Society, 79*, 1137-1144.

Nunes, P. A., Pires-Cabral, P., Guillén, M., Valero, F., & Ferreira-Dias, S. (2012). Optimized production of MLM triacylglycerols catalyzed by immobilized heterologous *Rhizopus oryzae* lipase. *Journal of the American Oil Chemists' Society, 89*, 1287-1295.

Oil World Annual (2012). Hamburg: ISTA Mielke GmBH.

Okuno, M., Kajiwara, K., Imai, S., Kobayashi, T., Honma, N., Maki, T., Suruga, K., Goda, T., Takase, S., Muto, Y., & Moriwaki, H. (1997). Perilla oil prevents the excessive growth of visceral adipose tissue in rats by down-regulating adipocyte differentiation. *Journal of Nutrition, 127*, 1752-1757.

Ong, A. S. H., & Goh, S. H. (2002). Palm oil: A healthful and cost-effective dietary component. *Food and Nutrition Bulletin, 23*, 11-22.

Osborn, H. T., & Akoh, C. C. (2002). Structured lipids-novel fats with medical, nutraceutical, and food applications. *Comprehensive Reviews in Food Science and Food Safety, 1*, 110-120.

Pantzaris, T. P., & Basiron, Y. (2002). The Lauric (Coconut and Palmkernel) Oils. In F. D. Gunstone (Ed.), *Vegetable Oils in Food Technology: Composition, Properties and Uses* (pp. 157-202). Boca Raton: CRC Press.

Park, Y., Albright, K. J., Liu, W., Storkson, J. M., Cook, M. E., & Pariza, M. W. (1997). Effect of conjugated linoleic acid on body composition in mice. *Lipids, 32*, 853-858.

Pauli, G. F., Jaki, B. U., & Lankin, D. C. (2005). Quantitative ^{1}H NMR: Development and potential of a method for natural products analysis. *Journal of Natural Product, 68*, 133-149.

Pauli, G. F., Jaki, B. U., & Lankin, D. C. (2007). A routine experimental protocol for qHNMR illustrated with taxol. *Journal of Natural Product, 70*, 589-595.

Pehowich, D. J., Gomes, A. V., & Barnes, J. A. (2000). Fatty acid composition and possible health effects of coconut constituents. *West Indian Medical Journal, 49*, 128-133.

Perona, J. S., Barron, L. J. R., & Ruiz-Gutiérrez, V. (1998). Determination of rat liver triglycerides by gas-liquid chromatography and reversed-phase high performance liquid chromatography. *Journal of Chromatography B, 706*, 173-179.

Perona, J. S., Portillo, M. P., Macarulla, M. T., Tueros A. I., & Ruiz-Gutiérrez, V. (2000). Influence of different dietary fats on triacylglycerol deposition in rat adipose tissue. *British Journal of Nutrition, 84*, 765-774.

Perona, J. S., & Ruiz-Gutierrez, V. (2003). Simultaneous determination of molecular species of monoacylglycerols, diacylglycerols and triacylglycerols in human very-low-density lipoproteins by reversed-phase liquid chromatography. *Journal of Chromatography B, 785*, 89-99.

Peters, J. C., Holcombe, B. N., Hiller, L. K., & Webb, D. R. (1991). Caprenin 3. Absorption and calorie value in adult humans. *Journal of American College of Toxicology, 10*, 357-367.

Petrosino, T., Riccieri, R., Blasi, F., Brutti, M., D'arco, G., Bosi, A., Maurelli, S., Cossignani, L., Simonetti, M. S., & Damiani, P. (2007). Original normal-phase high-performance liquid chromatographic separation of monoacylglycerol classes from extra virgin olive oil triacylglycerols for their stereospecific analysis. *Journal of AOAC International, 90*, 1647-1654.

Ponnampalam, E. N., Lewandowski, P., Nesaratnam, K., Dunshea, F. R., & Gill, H. (2011). Differential effects of natural palm oil, chemically- and enzymatically-modified palm oil on weight gain, blood lipid metabolites and fat deposition in a pediatric pig model. *Nutrition Journal, 10*, 53.

Renaud, S. C., Ruf, J. C., & Petithory, D. (1995). The positional distribution of fatty acids in palm oil and lard influences their biologic effects in rats. *Journal of Nutrition, 125*, 229-237.

Rocha-Uribe, A., & Hernandez, E. (2004). Solvent-free enzymatic synthesis of structured lipids containing CLA from coconut oil and tricaprylin. *Journal of the American Oil Chemists' Society, 81*, 685-689.

Rossell, J. B. (1967). Phase diagrams of triglyceride systems. *Advance in Lipid Research, 5*, 353-408.

Rousseau, D., Forestière, K., Hill, A. R., & Marangoni, A. G. (1996). Restructuring butterfat through blending and chemical interesterification: 1. Melting behaviour and triacyglycerol modifications. *Journal of the American Oil Chemists' Society, 73*, 963-972.

Rukmini, C., & Raghuram, T. C. (1991). Nutritional and biochemical aspects of the hypolipidemic action of rice bran oil: A review. *Journal of American College of Nutrition, 10*, 593-601.

Sanz, M., Lopez-Bote, C. J., Menoyo, D., & Bautista, J. M. (2000). Abdominal fat deposition and fatty acid synthesis are lower and β-oxidation is higher in broiler chickens fed diets containing unsaturated rather than saturated fat. *Journal of Nutrition, 130*, 3034-3037.

Scano, P., Casu, M., Lai, A., Saba, G., Dessi, M. A., Deiana, M., Corongiu, F. P., & Bandino, G. (1999). Recognition and quantitation of *cis*-vaccenic and eicosenoic fatty acids in olive oils by ^{13}C nuclear magnetic resonance spectroscopy. *Lipids, 34*, 757-759.

Schmid, U., Bornscheuer, U. T., Soumanou, M. M., McNeill, G. P., & Schmid, R. D. (1998). Optimization of the reaction conditions in the lipase-catalyzed synthesis of structured triglycerides. *Journal of the American Oil Chemists' Society, 75*, 1527-1531.

Schrauwen, P., & Westerterp, K. R. (2000). The role of high-fat diets and physical activity in the regulation of body weight. *British Journal of Nutrition, 84*, 417-427.

Schuchardt, U., Sercheli, R., & Vargas, R. M. (1998). Transesterification of vegetable oils: A review. *Journal of the Brazilian Chemical Society, 9*, 199-210.

Schulthess, G., Lipka, G., Compassi, S., Boffelli, D., Weber, F. E., Paltauf, F., & Hauser, H. (1994). Absorption of monoacylglycerols by small intestinal brush border membrane. *Biochemistry, 33*, 4500-4508.

Scrimgeour, C. M., & Harwood, J. L. (2007). Fatty Acid and Lipid Structure. In F. D. Gunstone, J. L. Harwood & A. J. Dijkstra (Eds.), *The Lipid Handbook* (3rd ed.) (pp. 1-36). Boca Raton: CRC Press.

Sellappan, S., & Akoh, C. C. (2001). Synthesis of structured lipids by transesterification of trilinolein catalyzed by Lipozyme IM60. *Journal of Agricultural and Food Chemistry, 49*, 2071-2076.

Seriburi, V., & Akoh, C. C. (1998). Enzymatic transesterification of triolein and stearic acid and solid fat content of their products. *Journal of the American Oil Chemists' Society, 75*, 511-516.

Seriburi, V., & Akoh, C. C. (1998). Enzymatic interesterification of triolein and tristearin: Chemical structure and differential scanning calorimetric analysis of the products. *Journal of the American Oil Chemists' Society, 75*, 711-716.

Sessa, D. J. (1996). Derivation of a cocoa butter equivalent from jojoba transesterified ester *via* a differential scanning calorimetry index. *Journal of the Science of Food and Agriculture, 72*, 295-298.

Shetty, U. S., Reddy, Y. R. S., & Khatoon, S. (2011). Plastic fats from sal, mango and palm oil by lipase catalysed interesterification. *Journal of Food Science and Technology*, DOI: 10.1007/s13197-011-0492-z.

Shimomura, Y., Tamura, T., & Suzuki, M. (1990). Less body fat accumulation in rats fed a sunflower oil diet than in rats fed a beef tallow diet. *Journal of Nutrition, 120*, 1291-1296.

Simova, S., Ivanova, G., & Spassov, S. L. (2003). Alternative NMR method for quantitative determination of acyl positional distribution in triacylglycerols and related compounds. *Chemistry and Physics of Lipids, 126*, 167-176.

Small, D. M. (1991). The effects of glyceride structure on absorption and metabolism. *Annual Review of Nutrition, 11*, 413-434.

Sotak, C. H., Dumoulin, C. L., & Levy, G. C. (1984). High Accuracy Quantitative Analysis by ^{13}C Fourier Transform NMR Spectroscopy. In G. C. Levy (Ed.), *Topics in Carbon-13 NMR Spectroscopy* (pp. 97). New York, NY: Wiley.

Soumanou, M. M., Bornscheuer, U. T., Menge, U., & Schmid, R. D. (1997). Synthesis of structured triglycerides from peanut oil with immobilized lipase. *Journal of the American Oil Chemists' Society, 74*, 427-433.

Soumanou, M. M., Bornscheuer, U. T., & Schmid, R. D. (1998). Two-step enzymatic reaction for the synthesis of pure structured triacylglycerides. *Journal of the American Oil Chemists' Society, 75*, 703-710.

Stachon, M., Furstenberg, E., & Gromadzka-Ostrowska, J. (2006). Effects of high-fat diets on body composition, hypothalamus NPY, and plasma leptin and corticosterone levels in rats. *Endocrine, 30*, 69-74.

Standal, I. B., Axelson, D. E., & Aursand, M. (2009). Differentiation of fish oils according to species by ^{13}C NMR regiospecific analyses of triacylglycerols. *Journal of the American Oil Chemists' Society, 86*, 401-407.

Stolyhwo, A., Colin, H., & Guiochon, G. (1985). Analysis of triglycerides in oils and fats by liquid chromatography with the laser light scattering detector. *Analytical Chemistry, 57*, 1342-1354.

St-Onge, M. P., & Jones, P. J. (2002). Physiological effects of medium-chain triglycerides: potential agents in the prevention of obesity. *Journal of Nutrition, 132*, 329-332.

St-Onge, M. P., & Bosarge, A. (2008). Weight-loss diet that includes consumption of medium-chain triacylglycerol oil leads to a greater rate of weight and fat mass loss than does olive oil. *The American Journal of Clinical Nutrition, 87*, 621-626.

Stremmel, W. (1988). Uptake of fatty acids by jejunal mucosal cells is mediated by a fatty acid binding membrane protein. *Journal of Clinical Investigation, 82*, 2001-2010.

Suárez, E. R., Mugford, P. F., Rolle, A. J., Burton, I. W., Walter J. A., & Kralovec J. A. (2010). ^{13}C-NMR regioisomeric analysis of EPA and DHA in fish oil derived triacylglycerol concentrates. *Journal of the American Oil Chemists' Society, 87*, 1425-1433.

Sundram, K., Hassan, A. H., Siru, O. H., & Hayes, K. C. (1991). Dietary palmitate lowers cholesterol relative to laurate and myristate in humans. *Arteriosclerosis, Thrombosis, and Vascular Biology*, *11*, 1614 (abs.).

Sundram, K., Hayes, K. C., & Siru, O. H. (1995). Both dietary 18:2 and 16:0 may be required to improve the serum LDL/HDL cholesterol ratio in normocholesterolemic men. *Journal of Nutritional Biochemistry, 6*, 179-187.

Surwit, R. S., Kuhn, C. M., Cochrane, C., McCubbin, J. A., & Feinglos, M. N. (1988). Diet-induced type II diabetes in C57BL/6J mice. *Diabetes, 37*, 1163-1167.

Surwit, R. S., Feinglos, M. N., Rodin, J., Sutherland, A., Petro, A. E., Opara, E. C., Kuhn, C. M., & Rebuffé-Scrive, M. (1995). Differential effects of fat and sucrose on the development of obesity and diabetes in C57BL/6J and A/J mice. *Metabolism, 44*, 645-651.

Svensson, J., & Adlercreutz, P. (2011). Effect of acyl migration in Lipozyme TL IM-catalyzed interesterification using a triacylglycerol model system. *European Journal of Lipid Science and Technology, 113*, 1258-1265.

Takagi, T., & Ando, Y. (1990). Stereospecific analysis of acyl group distribution in triacylglycerols by HPLC with chiral column. *Journal of Japan Oil Chemists' Society (Yukagaku), 39*, 622-628.

Takahashi, M., Ikemoto, S., & Ezaki, O. (1999). Effect of the fat/carbohydrate ratio in the diet on obesity and oral glucose tolerance in C57BL/6J mice. *Journal of Nutritional Science and Vitaminology (Tokyo), 45*, 583-593.

Tan, C. P., & Che Man, Y. B. (1999). Quantitative differential scanning calorimetric analysis for determining total polar compounds in heated oils. *Ibid, 76*, 1047-1057.

Tan, C. P., & Che Man Y. B. (2000). Differential scanning calorimetric analysis of edible oils: comparison of thermal properties and chemical composition. *Journal of the American Oil Chemists' Society, 77*, 143-155.

Tholstrup, T., Ehnholm, C., Jauhiainen, M., Petersen, M., Høy, C. E., Lund, P., & Sandström, B. (2004). Effects of medium-chain fatty acids and oleic acid on blood lipids, lipoproteins, glucose, insulin, and lipid transfer protein activities. *The American Journal of Clinical Nutrition, 79*, 564-569.

Tholstrup, T., & Samman, S. (2004). Postprandial lipoprotein (a) is affected differently by specific individual dietary fatty acids in healthy young men. *Journal of Nutrition, 134*, 2550-2555.

Timmers, S., de Vogel-van den Bosch, J., de Wit, N., Schaart, G., van Beurden, D., Hesselink, M., van der Meer, R., & Schrauwen, P. (2011). Differential effects of saturated versus unsaturated dietary fatty acids on weight gain and myocellular lipid profiles in mice. *Nutrition and Diabetes, 1*, e11.

Torres, C. F., Barrios, E., & Hill Jr., C. G. (2002). Lipase-catalyzed acidolysis of menhaden oil with CLA: Optimization by factorial design. *Journal of the American Oil Chemists' Society, 79*, 457-466.

Truswell, A. S., Choudhury, N., & Roberts, D. C. K. (1992). Double blind comparison of plasma lipids in healthy subjects eating potato crisps fried in palmolein or canola oil. *Nutrition Research, 12*, S43-S52.

Vlahov, G. (1998). Regiospecific analysis of natural mixtures of triglycerides using quantitative ^{13}C nuclear magnetic resonance of acyl chain carbonyl carbons. *Magnetic Resonance in Chemistry, 36*, 359-362.

Vlahov, G., Giuliani, A. A., & Del Re, P. (2010). ^{13}C NMR spectroscopy for determining the acylglycerol positional composition of lampante olive oils. Chemical shift assignments and their dependence on sample concentration. *Analytical Methods, 2*, 916-923.

Wardlaw, G. M., Snook, J. T., Park, S., Patel, P. K., Pendley, F. C., Lee, M. S., & Jandacek, R. J. (1995). Relative effects on serum lipids and apolipoproteins of a caprenin-rich diet compared with diets rich in palm oil/palm-kernel oil or butter. *The American Journal of Clinical Nutrition, 61*, 535-542.

Watts, G. F., Ahmed, W., Quing, J., Houlston, R., Jackson, P., Iles, C., & Lewis, B. (1988). Effective lipid lowering diets including lean meat. *British Medical Journal, 296*, 235-237.

Webb, D. R., & Sanders, R. A. (1991). Caprenin I. Digestion, absorption, and rearrangement in thoracic duct-cannulated rats. *Journal of the American College of Toxicology, 10*, 325-340.

Weiss, G. H., & Ferretti, J. A. (1983). Accuracy and precision in the estimation of peak areas and NOE factors. *Journal of Magnetic Resonance, 55,* 397-407.

Weiss, T. J., Jacobson, G. A., & Wiedermann, L. H. (1961). Reaction mechanism of sodium methoxide treatment of lard. *Journal of the American Oil Chemists' Society, 38*, 396-399.

West, D. B., Blohm, F. Y., Truett, A. A., & Delany, J. P. (2000). Conjugated linoleic acid persistently increases total energy expenditure in AKR/J mice without increasing uncoupling protein gene expression. *Journal of Nutrition, 130*, 2471-2477.

Whigham, L. D., Watras, A. C., & Schoeller, D. A. (2007). Efficacy of conjugated linoleic acid for reducing fat mass: a meta-analysis in humans. *The American Journal of Clinical Nutrition, 85,* 1203-1211.

Winzell, M. S., & Ahrén, B. (2004). The high-fat diet-fed mouse: A model for studying mechanisms and treatment of impaired glucose tolerance and type 2 diabetes. *Diabetes, 53,* S215-S219.

Wollenberg, K. F. (1990). Quantitative high resolution ^{13}C nuclear magnetic resonance of the olefinic and carbonyl carbons of edible vegetable oils. *Journal of the American Oil Chemists' Society, 67,* 487-494.

World Health Organisation (2005). Obesity and overweight. Retrieved from http://www.who.int/mediacentre/factsheets/fs311/en/index.html on 1 September 2013.

Xu, X., Skands, A. R. H., Høy, C. E., Mu, H., Balchen, S., & Adler-Nissen, J. (1998). Production of specific-structured lipids by enzymatic interesterification: Elucidation of acyl migration by response surface design. *Journal of the American Oil Chemists' Society, 75,* 1179-1186.

Xu, X. (2000). Enzymatic production of structured lipids: Process reactions and acyl migration. *Inform, 11,* 1121-1131.

Xu, X., Fomuso, L. B and Akoh, C. C. (2000). Modification of menhaden oil by enzymatic acidolysis to produce structured lipids: Optimization by response surface design in a packed bed reactor. *Journal of the American Oil Chemists' Society, 77,* 171-176.

Yamaguchi, T., Kaneda, M. and Kakinuma, K. (1986). Effect of saturated and unsaturated fatty acids on the oxidative metabolism of human neutrophils. The role of calcium ion in the extracellular medium. *Biochimica et Biophysica Acta, 861*, 440-446.

Yang, T., Fruekilde, M. B. and Xu, X. (2003). Applications of immobilized *Thermomyces lanuginosa* lipase in interesterification. *Journal of the American Oil Chemists' Society, 80*, 881-887.

LIST OF PUBLICATIONS AND PAPERS PRESENTED

Refereed Journal Paper

1. **Gouk, S. W.**, Cheng, S. F., Ong, A. S. H., & Chuah, C. H. (2012). Rapid and direct quantitative analysis of positional fatty acids in triacylglycerols using ^{13}C NMR. *European Journal of Lipid Science and Technology, 114*, 510 – 519.

2. **Gouk, S. W.**, Cheng, S. F., Malon, M., Ong, A. S. H., & Chuah, C. H. (2013). Critical considerations for fast and accurate regiospecific analysis of triacylglycerols using quantitative ^{13}C NMR. *Analytical Methods, 5*, 2064 – 2073.

3. **Gouk, S. W.**, Cheng, S. F., Mok, J. S. L., Ong, A. S. H., & Chuah, C. H. (2013). Long-chain SFA at the *sn*-1, 3 positions of TAG reduce body fat deposition in C57BL/6 mice. *British Journal of Nutrition, 110*, 1987-1995.

4. **Gouk, S. W.**, Cheng, S. F., Ong, A. S. H., & Chuah, C. H. (2014). Stearic acids at *sn*-1, 3 positions of triacylglycerols are more efficient in limiting adiposity than palmitic and oleic acids in C57BL/6 mice. *British Journal of Nutrition, 111*, 1174-1180.

Proceeding Papers

1. **Gouk, S. W.**, Cheng, S. F., Ong, A. S. H., & Chuah, C. H. (2009). Regiospecific analysis of natural occurring triacylglycerols using ^{13}C NMR spectroscopy. Poster presented at Sokendai Asian Winter School, 1-4 December, Okazaki, Japan.

2. **Gouk, S. W.**, Cheng, S. F., Ong, A. S. H., & Chuah, C. H. (2010). Regiospecific analysis of triacylglycerols by using ^{13}C NMR spectroscopy. Oral presentation in 16th Malaysian Chemical Congress 2010 (16th MCC), 12-14 October, Putra World Trade Centre, Kuala Lumpur.

3. **Gouk, S. W.**, Cheng, S. F., Ong, A. S. H., & Chuah, C. H. (2010). Quantitative analysis of positional fatty acids in triacylglycerols of edible oil and fats using ^{13}C NMR. Poster presented at Oil and Fats International Congress (OFIC) 2010, 20-22 October, Kuala Lumpur Convention Centre, Kuala Lumpur.

4. **Gouk, S. W.**, Cheng, S. F., Ong, A. S. H., & Chuah, C. H. (2010). Quantitative Analysis of positional fatty acids in triacylglycerols of edible oil and fats using ^{13}C NMR. Poster presented at Bilateral Symposium "Emerging Trends in Chemistry" between University of Malaya and University of Hyderabad. 26-28 October, Department of Chemistry, Faculty of Science, University of Malaya. Kuala Lumpur, Malaysia.

5. **Gouk, S. W.**, Cheng, S. F., Ong, A. S. H., & Chuah, C. H. (2011). Rapid and direct quantitative analysis of positional fatty acids in triacylglycerols of natural occurring oils and fats. Oral presentation in 102nd American Oil Chemists' Society (AOCS) Annual Meeting and Expo, 1-4 May, Duke Energy Convention Center, Cincinnati, Ohio, USA.

6. Cheng, S. F., **Gouk, S. W.**, Ong, A. S. H., & Chuah, C. H. (2011). Regiospecific analysis of triacylglycerols in various oils and fats by ^{13}C NMR. Oral presentation in 9th Euro Fed Lipid, 18-21 September, Rotterdam, The Netherlands.

7. **Gouk, S. W.**, Cheng, S. F., Ong, A. S. H., & Chuah, C. H. (2012). Positional distribution of long chain saturated fatty acids in a triacylglycerol determines the body fat deposition in C57BL/6 mice. Poster presented at Oil and Fats

International Congress (OFIC) 2012, 12-14 September, Kuala Lumpur Convention Centre, Kuala Lumpur, Malaysia.

8. **Gouk, S. W.**, Cheng, S. F., Ong, A. S. H., & Chuah, C. H. (2012). Differential effect of long chain saturated and unsaturated fatty acids at *sn*-1, 3 positions of triacylglycerols on fat accretion in C57BL/6 mice. Oral presentation in World Congress of Oleo Science & 29th ISF Congress (WCOS), 30 September – 4 October, Arkas Sasebo, Nagasaki, Japan.

9. **Gouk, S. W.**, Cheng, S. F., Ong, A. S. H., & Chuah, C. H. (2014). Fatty acids at the *sn*-1,3 positions of triacylglycerols are crucial in alleviating fat accretion illustrated in C57BL/6 mice. Oral presentation in 105th American Oil Chemists' Society (AOCS) Annual Meeting and Expo, 4-7 May, Henry B. Gonzalez Convention Center, San Antonio, Texas, USA.